DIPL.-MATH. THOMAS GÜNTHER

MATCHING OF

LOCAL AND GLOBAL GEOMETRY

IN OUR UNIVERSE

2013

Theoretische Physik

Dissertationsthema

Matching of local and global geometry in our universe

Inaugural-Dissertation
zur Erlangung des Doktorgrades
der Naturwissenschaften im Fachbereich Physik
der Mathematisch-Naturwissenschaftlichen Fakultät
der Westfälischen Wilhelms-Universität Münster

vorgelegt von

Dipl.-Math. Thomas Günther
aus Saarbrücken

- 2013 -

Dekan:	Prof. Dr. T. Kuhn
Erster Gutachter:	Prof. Dr. P. Boschan
Zweiter Gutachter:	Prof. Dr. G. Münster
Tag der mündlichen Prüfung:	21.06.13
Tag der Promotion:	21.06.13

Zusammenfassung der Dissertation in deutscher Sprache
(§ 8 Abs. 1 der Promotionsordnung)

Obwohl unser Universum als Ganzes (global) expandiert, gibt es (lokale) gravitationsgebundene Systeme, wie etwa Galaxienhaufen, welche selbst nicht expandieren. Innerhalb solcher Systeme dominiert die Gravitation über den Einfluss der allgemeinen Expansion des Universums. Die vorliegende Dissertation befasst sich hauptsächlich mit der Frage, wie die lokale Geometrie an die globale Geometrie des Universums im Modell angepasst werden kann.

Saul Perlmutter, Brian Schmidt und Adam Riess haben entdeckt, dass unser Universum heute sogar beschleunigt expandiert. Dafür erhielten sie 2011 den Nobelpreis für Physik. Um der beschleunigten Expansion im Modell Rechnung zu tragen, bilden Einstein's Gleichungen mit kosmologischer Konstante Λ die Grundlage der vorliegenden Dissertation. Die vier Schwerpunkte dieser Arbeit sind:

(1) Die Schwarzschild-de Sitter-Metrik soll durch Transformation der radialen Koordinate in isotrope Form gebracht werden. Auf Grundlage von numerischen Berechnungen wird eine neue Metrik (in expliziter Form) präsentiert, welche eine sehr gute Näherungslösung von Einstein's Gleichungen mit Λ für den leeren Raum darstellt. Die Komponenten der neuen Metrik setzten sich aus einer Art Produkt der entsprechenden Komponenten von de Sitter- und Schwarzschild-Metrik zusammen. Aufgrund dieser Struktur wird die neue Metrik im Folgenden als 'Produkt-Metrik' bezeichnet. Aus den Feldgleichungen mit kosmologischer Konstante wird ein Energie-Impuls Tensor hergeleitet, mit dem zusammen die Produkt-Metrik eine exakte Lösung bildet. Basierend auf der Produkt-Metrik wird bestimmt, an welcher Stelle sich die Effekte von Expansion und Gravitation aufheben.

(2) In der vorliegenden Dissertation wird der Übergang zwischen lokaler und globaler Geometrie bei einem räumlich flachen 'ΛCDM-Swiss-Cheese'[1] Modell untersucht. Aus einem Friedmann–Lemaître–Robertson–Walker (FLRW) Universum wird das Material eines kugelförmigen Bereichs entfernt und durch eine entsprechende Punktmasse im Zentrum der Kugel ersetzt. Diese Punktmasse ist von Vakuum umgeben. Es wird gezeigt, dass das ΛCDM-Swiss-Cheese Modell eine Teillösung des McVittie-Problems darstellt: Die Begrenzung des kugelförmigen Bereichs expandiert zusammen mit dem FLRW Hintergrund, falls ihr Radius größer als der Gravitationsradius (Schwarzschildradius) der Punktmasse ist. Der Ereignishorizont selbst expandiert nicht.

(3) Ein ähnliches 'Swiss-Cheese' Modell erhält man durch Einbettung einer Schwarzschild-Sphäre in ein Lemaître-Tolman-Bondi (LTB) Universum. Aus den Anpassungsbedingungen für lokale und globale Geometrie wird ein Zusammenhang für die Zeitkoordinaten beider Koordinatensysteme am Rand der Sphäre hergeleitet.

(4) Eine neue Lösung der Einstein'schen Gleichungen mit Λ wird vorgestellt. Diese Lösung wurde durch Zufall gefunden, sie basiert auf einer Erweiterung der isotropen de Sitter-Metrik. Die Existenz der neuen Lösung wird bewiesen. Die geodätischen Gleichungen werden aufgestellt, ein Spezialfall wird numerisch gelöst.

---

[1] Das 'ΛCDM-Swiss-Cheese' Modell ist ein FLRW Universum, welches (mindestens) einen kugelförmigen Bereich enthält, dessen Gravitationsfeld durch die Schwarzschild-de Sitter Lösung beschrieben wird. Ein solches Universum (mit vielen kugelförmigen Löchern) sieht aus wie ein Schweizer Käse. In der Literatur wird der Name 'Swiss-Cheese universe' für solche Modelle verwendet.

Acknowledgment

I would like to express my deep gratitude to Prof. Dr. Peter Boschan for his excellent guidance, advice and support during the development of this work, for helping me to develop my background in physics and mathematics and for many interesting discussions. His encouragement, guidance and support made this thesis possible. Another thanks goes to Prof. Dr. Gernot Münster for his valuable and constructive suggestions.

Thomas Günther

Declaration

I declare that this dissertation is my own work, and that all the sources I have used or quoted have been indicated or acknowledged by means of completed references.

Thomas Günther

Date

Contents

Abstract

Although our universe expands in its entirety, gravitationally bound systems like galaxy clusters don't take part in this expansion. At sufficiently small scales the influence of gravitational attraction prevails over the influence of cosmic expansion. Matter clumps together and these formations do not individually expand. The current work is mainly concerned with the compatibility of the local (static) geometry and the global (expanding) geometry of spacetime. Saul Perlmutter, Brian Schmidt and Adam Riess shared the Nobel Prize in Physics 2011 "*for the discovery of the accelerating expansion of the Universe through observations of distant supernovae*" [115]. In order to take into account the observed acceleration of the expansion rate, our investigations are based on Einstein's field equations, including a non-zero cosmological constant Λ. The four main topics of this paper are:

(1) We work on isotropic coordinates for the Schwarzschild-de Sitter metric. A new isotropic metric, which represents a high-precision approximation of Einstein's empty-space equations including a cosmological constant, is presented. Due to the fact that this solution resembles some kind of product of de-Sitter and Schwarzschild case, it is called 'Product-metric'. We determine the remainder stress–energy tensor, based on the assumption that the Product-metric is an exact solution of Einstein's equations. Based on the Product-metric, we propose a new method to determine the zero-gravity[1] radius for a given mass.

(2) We study the matching of local and global geometry in a spatially flat 'ΛCDM Swiss-Cheese model[2]'. The matter content of a comoving homogeneous sphere in FLRW cosmology is removed and replaced by a point mass condensation at its center. It is shown that the ΛCDM Swiss-Cheese model may represent a (partial) solution of the McVittie-problem: The boundary of the spherical cavity, which is surrounding the mass condensation, expands with the FLRW background, if the radius of the sphere exceeds the gravitational radius, which is associated to the point mass. But the model predicts, that the gravitational sphere itself does not take part in this expansion.

[1] A Newton-based estimation for the zero-gravity sphere was proposed by Chenin et al.

[2] The ΛCDM Swiss-Cheese model is a FLRW universe which contains at least one spherical Schwarzschild-de Sitter cavity, see for example [23, 24].

(3) We study the matching of local and global geometry in a similar Swiss-Cheese model, a Schwarzschild cavity in an expanding, dust-dominated Lemaitre-Tolman-Bondi background. A relation between the observer time and the world time at the edge of the cavity is derived.

(4) Fortuitously, we found a new spacetime model while working on coordinate transformations in the De Sitter case. The proof that the corresponding metric is an exact solution of Einstein's field equations is given. Furthermore, we establish the geodesic equations and solve a special case numerically.

1. Introduction

"*We have believable evidence that the universe is expanding, the space between the galaxies opening up, and that this expansion traces back to a hot dense phase, the big bang.*" Phillip James Edwin Peebles, [91]

Up to roughly a century ago, astronomy and physics could be regarded as separate sciences. Cosmology / Astrophysics arose when Albert Einstein published his final version of General Relativity [35] in 1916. The content of space-time can be described by the stress-energy-momentum tensor T_{ik}, which is related to the Ricci tensor R_{ik}, the scalar curvature R and the metric tensor g_{ik} by Einstein's field equations[3]:

$$R_{ik} - \frac{1}{2}Rg_{ik} = \frac{8\pi\gamma}{c^4}T_{ik}$$

At the same time David Hilbert also found the gravitational field equations. Some authors suggest that they should be called "Einstein-Hilbert equations", cf. [94].

Einstein's equations do not involve derivatives of the metric higher than the second and replace the Poisson equation[4] of Newtons theory. Einstein's field equations represent one of three postulates of General Relativity. The remaining two postulates are local causality[5] and local energy conservation. Local conservation of energy and momentum is complied by the existence of a symmetric, divergence-free stress-energy-momentum tensor, which is zero on an open set $\mathcal{U}$ if and only if all the matter fields vanish on $\mathcal{U}$. Hence, Einstein's tensor $G_{ik} = R_{ik} - \frac{1}{2}Rg_{ik}$ has to be divergence-free too.

In the same year (1916) Karl Schwarzschild discovered an exact static, spherically symmetric solution, which represents the gravitational field outside a single point mass. The local geometry of our solar system or the gravitational field of a black hole can be described to a good approximation by Schwarzschild's solution. On the other hand, Einstein's equations have solutions that describe the global geometry of the universe. At that time there was no observational evidence to

---

[3] where $\gamma \approx 6,67 \cdot 10^{-11} \frac{\mathrm{Nm}^2}{\mathrm{kg}^2}$ is the gravitational constant and $c \approx 3 \cdot 10^8 \frac{\mathrm{m}}{\mathrm{s}}$ the speed of light.

[4] $\triangle\phi = 4\pi\gamma\rho$

[5] We adopt the definition from [56]: "*The equations governing the matter fields must be such that if $\mathcal{U}$ is a convex normal neighborhood and p and q are points in $\mathcal{U}$ then a signal can be sent in $\mathcal{U}$ between p and q if and only if p and q can be joined by a C^1 curve lying entirely in $\mathcal{U}$, whose tangent vector is everywhere non-zero and is either time-like or null.*" A paradox like someone travels into it's own past is precluded.

suppose that the universe is not static. But Einstein's equations contradict this assumption. So Einstein added a cosmological constant Λ to allow a static solution for the global universe, see [36]. Adding or subtracting a constant is the only possibility to extend Einstein's equations by conserving the above mentioned conditions. De Sitter found an empty space solution[6] of the modified field equations in 1917: "D*e Sitter pointed out that one can find another solution to Einstein's field equations for a universe that is homogeneous, isotropic and static. De Sitter's solution has negligibly small values for the mass density and pressure in ordinary matter.*" [91]. In the spatially flat case, the standard form of this solution is $ds^2 = c^2dt^2 - \exp\left[2\sqrt{\Omega_\Lambda}\cdot H_0 t\right]\left\{dr^2 + r^2d\theta^2 + r^2\sin^2\theta\, d\phi^2\right\}$, which is not static but can be transformed into a static line element, see subsection 2.4. De Sitter's metric is the first line element given in a comoving system of coordinates. "*This form will reappear as the line element for the steady-state cosmology, and as a close approximation to the line element in some versions of the inflation scenario.*" [91].

The global geometry of our expanding universe can be appropriately described by the homogeneous and isotropic Friedmann–Lemaître–Robertson–Walker (FLRW) solution. But this model is inadequate for describing the gravitational effects by which a galaxy is held together. On the other hand, there exists an non-isotropic empty-space-solution of Einstein's equations with nonzero cosmological constant, the Schwarzschild-de Sitter metric, which represents the spherically symmetric gravitational field outside a single point mass. McVittie was the first to consider the gravitational field of a point singularity in the presence of an expanding cosmological background (McVittie problem), cf. [79]. From Birkhoff's theorem it is known that any spherically symmetric empty-space-solution of Einstein's equations must be stationary, but what we need is a solution which presents the field of a single point mass embedded in an expanding (time-dependent) cosmological background. George McVittie found a new solution of Einstein's equations, which is of Schwarzschild-type in the neighborhood of the central mass-point and which turns into the spatially flat FLRW metric for increasing distance. Another approach was given by Einstein and Straus in [37]. They proposed an expanding FLRW cosmological model which contains a static Schwarzschild field. Einstein and Straus presuppose that there is no cosmological constant. Current observations contradict the assumption of a $\Lambda = 0$ universe. WMAP data [63] of 2010 indicates that our universe is made up of over 70% dark energy, which can be modeled with a nonzero cosmological constant.

[6] In general the n dimensional de Sitter solution dS_n can be considered as a n dimensional hyperboloid embedded in a $n+1$ dimensional flat Minkowski space time. Here we deal with $n = 4$. The de Sitter space has constant positive curvature $R > 0$, the analog space with constant negative curvature $R < 0$ is called anti-de Sitter space, see [56].

Main topics of the present work:
We study the matching of local and global geometry of spacetime, based on Einstein's field equations with cosmological constant:

$$R_{ik} - \frac{1}{2}Rg_{ik} - \Lambda g_{ik} = \frac{8\pi\gamma}{c^4}T_{ik} \tag{1.1}$$

Section 4 contains a reconsideration of McVittie's metric. We deduce a McVittie class solution from a simple coordinate transformation and proof that this metric is an exact solution of (1.1).

Section 5 deals with the question whether there are isotropic coordinates for the Schwarzschild-de Sitter solution. Motivated by the numerical result, we introduce a metric which resembles some kind of product of de-Sitter and Schwarzschild case: The 'Product-metric'. It is shown that this line element is a high-accuracy approximation of Einstein's empty-space equations including a cosmological constant.

In section 6 we analyze the Schwarzschild-de Sitter field and the Product-metric concerning the effects of expansion and gravitation. Based on the Product-metric, we determine the zero-gravity radius for our Local Group and the Virgo Cluster.

Section 7 is concerned with another approach to the McVittie problem including a cosmological constant: The 'ΛCDM Swiss-Cheese model' is a FLRW universe, which contains at least one spherical Schwarzschild-de Sitter cavity[7]. We study the expansion of a sphere surrounding the mass condensation in a spatially flat ΛCDM Swiss-Cheese model, and show that the sphere expands with the FLRW background if its radius exceeds the gravitational radius associated to the point mass. The gravitational sphere itself does not take part in the general expansion.

Section 8 deals with a similar Swiss-Cheese model, a Schwarzschild cavity in an expanding, dust-dominated Lemaitre-Tolman-Bondi background. We establish a relation between the observer time and the world time at the edge of the cavity.

In section 9, a new solution of Einstein's equations (1.1) is introduced. Fortuitously, we found this spacetime model while working on coordinate transformations in the De Sitter case. We proof that the new metric is an exact solution of (1.1), and we establish the geodesic equations. The path of a radial moving particle is determined numerically. Further studies may decide about the astrophysical relevance of the new spacetime.

[7] see for example [23, 24].

1.1. **An expanding universe without cosmological constant.**

At about 1917 Slipher finished his measurements of 25 galaxy spectra. He discovered that almost all of them were receding from Earth. But since all observed galaxies are concentrated in one direction, this was not unusual. Slipher thought that Galaxies in the opposite direction may be approaching. In 1922 Alexander Friedmann found a non-static isotropic solution of Einstein's original field equations (where $\Lambda = 0$) for a homogeneous distribution of matter. His model predicts an expanding (or contracting) universe. After nearly a decade of observations Edwin Hubble published in 1929 his sensational discovery that distant galaxies are moving away from us, see [59]. The result is what we now call Hubble's law: The radial velocities v of the galaxies are proportional to their distance d, i.e. $v = H_0 d$ where H_0 is the Hubble constant[8]. Hubble interpreted his data in the framework of de Sitter's universe: "*The outstanding feature, however, is the possibility that the velocity-distance relation may represent the de Sitter effect,...*", see [59]. In consequence of Hubble's work, Einstein abandoned the cosmological constant in 1931.

1.1.1. ***The big bang theory.***

Since the universe is expanding today, it stands to reason that in the past everything was much closer together. The Big Bang theory refers to the idea that the universe has expanded from a primordial hot, dense state. The idea was formulated first by Georges Lemaître. He had already published a model of an expanding space-time in 1927 [75] to explain the redshifts of spiral nebulae observed by Slipher. Hubble's observations confirmed that the universe was expanding. The current standard cosmological model contains three[9] cosmological parameters: The mass density ρ of the universe, the Hubble constant H_0 and the cosmological constant Λ. The dimension free parameters are the mass density parameter $\Omega_M = \frac{8\pi\gamma}{3H_0^2}\rho$ and the dark energy parameter $\Omega_\Lambda = \frac{c^2\Lambda}{3H_0^2}$. In 1932, the accepted parameters for the universe are $\Omega_M = 1$ and $\Omega_\Lambda = 0$ (i.e. there is no cosmological constant), see [15]. The corresponding mathematical model, which predicts that the universe expanded from a highly condensed state, is the Einstein-de Sitter model: A spatially flat Friedmann–Lemaître–Robertson–Walker spacetime with $\Omega_M = 1$ and $\Omega_\Lambda = 0$. But the first measurements of Hubble's parameter[10] in the velocity-distance relation resulted in $H_0 = 500\frac{\text{km}}{\text{s}\cdot\text{Mpc}} \approx 0.51\frac{1}{\text{Gyr}}$. Thus H_0^{-1}, the Hubble time, would be less than 2 Gyr, i.e. if the expansion rate was constant, the Big Bang occurred less than

[8] In the original paper Hubble calls it the "*K term*" .

[9] Observational evidence indicates that the universe is spatially flat, see [63]. Hence, an additional parameter which represents the curvature of the universe can be neglected, i.e. it is $K = 0$ in Friedmann's equations (2.4) and (2.5).

[10] Since 1Mpc is about $3.086 \cdot 10^{19}$km we obtain $1\frac{\text{km}}{\text{s}\cdot\text{Mpc}} \approx 0.001\frac{1}{\text{Gyr}}$.

$2 \cdot 10^9$ years ago. This contradicts the geologists' predicted age of the earth[11], which is more than 2 billion years. Since matter slows down the expansion, it depends on the content of the universe how much time is needed to reach the current state of the universe. Consequently, a model which contains more matter was revived. The universe is spatially positive curved in this case, and it's age can exceed H_0^{-1}. As an alternative to spatially positive curved models, a nonzero cosmological constant affects the age of the universe. Actually, in an extreme case where $\Omega_M = 0$ and $\Omega_\Lambda > 0$ the universe is infinitely old[12], it has no beginning and no end.

The value of the Hubble constant was a matter of discussion for a long time. A dimensionless Hubble parameter h was commonly used to relegate the uncertainty of the Hubble constant: $H_0 = h \cdot 100 \frac{\text{km}}{\text{s} \cdot \text{Mpc}}$. Some physicists supposed that the dimensionless Hubble parameter had to be in the range of $h = 0.5$ while others thought about $h = 1$. Since about five years, the Hubble constant is very well determined, see (1.2). The dimensionless Hubble parameter is $h \approx 0.7$.

Besides Hubble's discovery that the universe is expanding, the Big Bang theory is supported by other important observations. The theory predicts the fusion of ^{2}H (deuterium, an isotope of hydrogen), He (helium) and ^{7}Li (an isotope of lithium) shortly after the Big Bang. The formation of light elements in the early universe, particularly during the first three minutes, is called Big Bang nucleosynthesis. Deuterium and the lithium isotope ^{7}Li could be produced almost exclusively during the Big Bang nucleosynthesis. Helium is formed in stars, but the abundance of helium in our universe can not be explained by stellar nucleosynthesis. Big Bang theory predicts that about 24% of the ordinary matter in the universe should be helium, this is in very good agreement with measurements of the WMAP satellite [58, 63].

1.1.2. ***Cosmic microwave background radiation.***

A further very strong proof of the Big Bang theory comes from the observation of the cosmic microwave background radiation (CMB). The existence of this radiation was proposed by Gamow, Herman and Alpher as early as 1948, see [4, 44, 45]. The volume of the expanding universe is increasing as $a(t)^3$, where $a(t)$ is the scale factor. During the expansion, the energy density of the non-relativistic matter is decreasing with time as $a(t)^{-3}$ and the radiation energy density as $a(t)^{-4}$. "*Alpher and Gamow noted that at the temperatures of interest for element formation,* [...] *the*

[11]The (accepted) age of the Earth 4.54 Gyr was determined by Claire Patterson, see [89].

[12]Partly motivated by the age problem, Thomas Gold, Hermann Bondi and Fred Hoyle developed the Steady-State model in 1948, see [11]. Later, the Steady-State model was abandoned since it does not fit observations. Especially the CMB contradicts to the Steady State cosmology.

universe would be filled with blackbody radiation (the CBR)" [91]. Gamow studied the relation between baryon number density n and temperature[13] T. He found $n \sim 10^{18}\text{cm}^{-3}$ at the epoch of deuterium formation, $T = 10^9\text{K}$. Alpher and Herman used Gamow's results to compute the first numerical estimate of the present CBR temperature, $T_0 \sim 5\text{K}$.

In 1965 Arno Penzias and Robert Wilson detected a persistent noise of microwaves while working with a large antenna, which was part of an early satellite transmission system. They earned the 1978 Nobel prize for the discovery of this radiation, the CMB, in 1965. The thermal emission spectrum corresponds to a temperature of 2.725K, cf. [58, 63]. Intensity of this radiation peaks at 160.2GHz, the corresponding wavelength is $\lambda = c/f \approx 1.87\text{mm}$. This isotropic cosmic background "*is a sea of radiation that uniformly fills space. This would mean an observer in any other galaxy would see the same intensity of radiation, equally bright in all directions, consistent with the cosmological principle.*" [91]. CMB intensity is extremely uniform all over the sky. Nevertheless, there are tiny fluctuations at the part per million level, see figure 1.1. Big Bang theory appropriately explains the CMB as

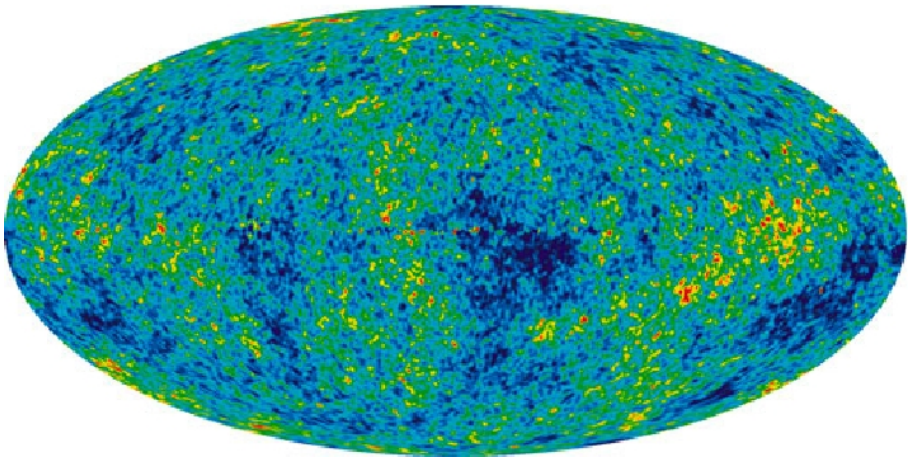

FIGURE 1.1. Cosmic microwave background radiation. The CMB reaches us from all directions with almost exactly the same intensity. Tiny temperature fluctuations are shown as color differences. "Seven Year Microwave Sky" Credit: NASA / WMAP Science Team
http://wmap.gsfc.nasa.gov/media/101080/index.html

the heat leftover from the Big Bang. The early universe was very hot and as it expands, the content within it cools. Accordingly, Big Bang theory predicts that the

[13] T and $n^{1/3}$ are inversely proportional to the cosmic scale factor $a(t)$.

universe should be filled with radiation. The discovery of the CMB is of particular importance for cosmology: For the first time cosmology has important predictive power.

1.1.3. ***Revival of the cosmological constant.***

The cosmological constant was originally introduced by Einstein in 1918 to admit static solutions of Einstein's equations, see [36]. With the discovery that our universe is expanding, the cosmological constant seemed to become redundant. Roughly half a century later, the cosmological constant was reintroduced in order to model the accelerated expansion of the universe. Quasi-stellar objects with measured redshifts at about $z = 2$ were discovered in the 1960s. The light of distant objects is shifted toward the red, due to the expansion of the universe. The dimensionless quantity z, representing the redshift, is defined as $z = \frac{\lambda_b}{\lambda_e} - 1$ where λ_b is the observed wavelength and λ_e the emitted wavelength of the light. Petrosian, Salpeter and Szekeres remarked in their article [93] of 1967: "[...] *interpretation of the redshift seems to lead to discrepancies with the observations if the more usual cosmologies with a zero value of the cosmological constant* Λ *are used: First, the observed apparent optical magnitude*[14] M_v *does not increase rapidly enough with increasing* z*. Second, a preponderance of sources with* z *near* 2.0 *has been observed.*" It was the first hint to a nonzero cosmological constant.

An interesting question is: What is the nature of the cosmological constant? The omnipresence of its influence suggests that Λ has geometric nature. On the other hand, as it was proposed by Zeldovich 1968, it is possible that Λ is related to the zero-point energy of the vacuum and the resulting gravitational effects. This interpretation was earlier considered by Nernst[15] in 1916 and Pauli in the 1920s, but the majority of the scientific community first took notice in 1968, see [15]. Contradictions, concerning the order of magnitude of vacuum energy density, arise at the intersection between general relativity and quantum field theory[16] (QFT). On the one hand there are global measurements (cosmological constant), on the other hand there are local measurements (e.g. Casimir effect) of vacuum energy. The results indicate that local vacuum energy differs from Einstein's cosmological constant.

[14]Commonly, the apparent optical magnitude is denoted with a small letter m instead of M_v. In the majority of cases the capital letter M denotes the absolute optical magnitude.

[15]Nernst' investigations about the energy content of the vacuum concerned chemical research. He purposed to put forward a model for the water molecule.

[16]Quantum field theory appeared in the 1920s. Max Born, Pascual Jordan, and Werner Heisenberg constructed a quantum mechanical theory of the electromagnetic field in 1926. Abdus Salam, Sheldon Glashow and Steven Weinberg shared the 1979 Nobel Prize in Physics for presenting a quantum field theory which unifies two of the four fundamental interactions, the electromagnetism and the weak interaction.

Rugh and Zinkernagel wrote in [101]: "*Solar system and galactic observations already put an upper bound on the* $\Lambda-$*term, but the tightest bound come from large scale cosmology* [...] *By contrast, theoretical estimates of various contributions to the vacuum energy density in QFT exceed the observational bound by at least 40 orders of magnitude.*" Most frequently mentioned is a discrepancy of even 120 orders of magnitude, see for example [47]: "*The corresponding vacuum energy density is* $\rho_V \sim M_p^4$*, which is some 120 orders of magnitude greater than the observational bounds.*"

1.1.4. ***Cosmic inflation***.

The classical Big Bang theory had several problems, we mention here the 'Flatness Problem', the 'Horizon Problem' and the 'Monopole Problem'. Corresponding to the classical model, one would expect an inhomogeneous and most likely highly (spatially) curved universe as a result of the Big Bang. $\Omega \sim 1$ requires an unbelievable extreme fine-tuning of initial conditions[17]. The CMB is uniform throughout the cosmos, even in distant regions, which could never have been in causal contact. The Big Bang cosmology predicts the existence of magnetic monopoles, which have never been observed yet.

Alan Guth noticed in 1981 that some problems can be explained by the concept of cosmic inflation, see [55]. According to the theory of cosmic inflation, the early universe passed through a period of huge exponential growth shortly after the Big Bang. Cosmic inflation is in accordance with current astronomical observations of a homogeneous, isotropic and flat universe. In 1984 Peebles shows that "*the inflationary scenario requires that the universe have negligible curvature along constant-density surfaces*" [90], i.e. cosmic inflation implies flattening of the universe. Further "[...] *the observed universe is accurately homogeneous because the large expansion in the quasi-de Sitter phase stretched the coherence length of fluctuations in the fields to a value much larger than our horizon*" [90]. Distant regions could have been causally connected prior to Inflation and so attained the same temperature. As a further result of Inflation, the abundance of magnetic monopoles, which were produced in the early universe, conceivably dropped to undetectable levels. The model of cosmic inflation was quickly accepted by the scientific community.

[17]The initial value of Hubble's constant and the density must be fine tuned to extraordinary accuracy to produce a spatially flat universe.

1.1.5. ***Cold dark matter.***

In the middle 1980s it became increasingly clear that the mass density of the Einstein - de Sitter model[18] is essentially larger than the observed luminous matter density. Consequently, the major part of matter in our universe was supposed to be invisible. This 'cold dark matter' (CDM) is gravitationally attractive but does not emit nor absorb light or electromagnetic radiation. Further the cold dark matter has a negligible thermal velocity. George Blumenthal, Sandra Moore Faber, Joel Primack and Martin Rees originally published the theory of cold dark matter in 1984, see [10]. Cold dark matter together with baryonic matter[19] constitute the gravitationally attractive content of our universe. The overall mass is more smoothly distributed than the visible matter. Due to the CDM theory, structures in our universe grow hierarchically. Dust particles clump together and form more and more massive objects up to galaxies and their clusters. "*In a universe dominated by CDM, galaxy formation presumably occurs at peaks of the matter-density field*" [31]. Astronomers can determine the total mass of a spiral galaxy, measuring the orbital speed of stars and gas inside the galaxy as well as the orbital velocity of satellite dwarf galaxies. The rotation curve of a galaxy shows the orbital velocity at different distances from the center of rotation and relates the orbital velocity of stars or gas to the total mass inside their orbits. Measurements from rotation curves

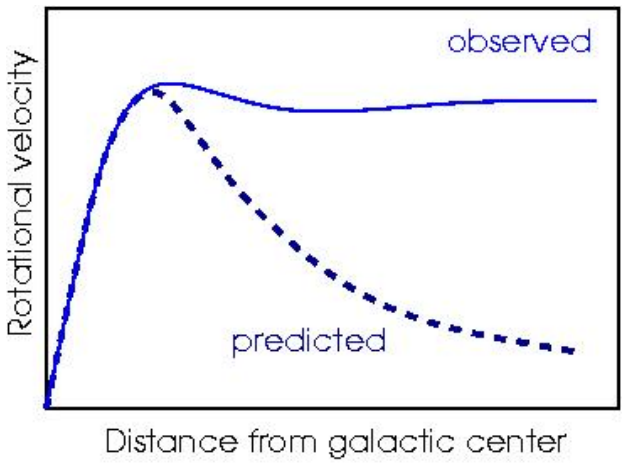

FIGURE 1.2. Rough, self made draft of a rotation curve for a spiral galaxy. Most rotation curves are not decreasing at large distance from the galactic center as predicted. Several measured rotation curves are given in [100] for example.

[18]The Einstein - de Sitter model is a spatially flat FLRW spacetime with $\Omega_M = 1$ and $\Omega_\Lambda = 0$.
[19]Baryonic matter includes all the material made up of protons, neutrons and electrons, e.g. stars, gas and dust.

in spiral galaxies do not coincide with the theoretical predictions, based on the visible matter. Rubin, Ford and Thonnard noticed in 1980: "*Most rotation curves are rising slowly even at the farthest measured point. Neither high nor low luminosity Sc galaxies have falling rotation curves. Sc galaxies of all luminosities must have significant mass located beyond the optical image.*" [100]. From the evaluation of the observed data of NASA's Wilkinson Microwave Anisotropy Probe (WMAP) mission it is known that the amount of dark matter in a galaxy is roughly ten times larger than the mass of baryonic matter. Concerning the nature of cold dark matter there are only speculations. Non-baryonic material like 'weakly interacting massive particles' (WIMP's) are new forms of particles, produced shortly after the Big Bang. It is hoped that supercolliders may reproduce these particles. Based on numerical simulations of nonlinear gravitational clustering, Davis, Efstathiou, Frenk and White proposed in 1985 that the evolution of large scale structure in our universe is substantially governed by the influence of cold dark matter, see [31]. Their numerical simulations[20] predicted the formation of filaments, superclusters and voids, resembling the observed structures in our universe. Owing to the rapid progress in computer technology, simulations become more and more complex. In 2012, the current status of galaxy formation was reviewed by Silk and Mamon: "*Numerical simulations of large-scale structure have met with great success. However these same simulations fail to account for several of the observed properties of galaxies. On large scales,* $\sim 0.01 - 100$Mpc*, the ansatz of cold, weakly interacting dark matter has led to realistic maps of the galaxy distribution* [...]", cf. [108].

1.1.6. ***Mixed dark matter***.

In the early 1990s, the standard cold dark matter theory was extended to the 'mixed dark matter" (MDM) model, which represents a composition of cold dark matter and 'hot dark matter', most likely massive neutrinos. Results of the 'Cosmic Microwave Explorer' (COBE) satellite indicated that predictions of pure CDM theory did not agree entirely with observations on intermediate scales. Andrew Liddle and David Lyth published in [76]: "*the standard CDM model is specified by a single parameter, the amplitude of the power spectrum* [...] *the required amplitude as inferred on small scales by pairwise velocities or cluster abundances appears to differ by a factor of around two from that required by COBE, and the pattern of clustering in the galaxy distribution on intermediate scales appears to indicate that the standard CDM spectrum has an incorrect shape on these scales.*"

[20]Among others, they run a simulation of a spatially flat universe with positive cosmological constant.

1.1.7. ***The anthropic cosmological principle.***

J. Barrow and F. Tipler defined the (weak) anthropic cosmological principle in [6]: "*The observed values of all physical and cosmological quantities are not equally probable but take on values restricted by the requirement that there exist sites where carbon-based life can evolve and by the requirement that the Universe be old enough for it to have already done so.*" They state that the anthropic principle confines the initial conditions of our universe to values that admit the formation of planets, stars and galaxies: "*In universes that are expanding much more slowly than the rate which allows them to lie close to the critical,* $\Omega_0 = 1$*, state, the universe will evolve to a second singularity too soon for stars to form and evolve (*$\gtrsim 10^9 yr$*) or even for conditions to cool off sufficiently for non-equilibrium structures like atoms to form (*$\gtrsim 10^6 yr$*). If the expansion is much faster than the critical rate, material will recede with so high a velocity that gravitational condensations like stars and galaxies will not form. Only for a range of initial conditions lying close to* $\Omega_0 = 1$ *will conditions be conducive to the evolution of life in the universe after billions of years.*" Due to the same idea, the value of the cosmological constant Λ is strictly limited. It should not be so large as to prevent the formation of gravitationally bound states. "*However this limit and its equivalent* [...] *have great significance for the possibility of life evolving in the Universe*" [6]. Likewise, Steven Weinberg pointed out in 1987 that the vacuum energy density (and thus the cosmological constant) should not be so large as to prevent the formation of galaxies. Otherwise living observers would not be able to exist, and hence, observe the universe. The parameters of the universe are limited by the anthropic cosmological principle.

1.2. **The ΛCDM model.**

Research in 1990 indicated that the standard cold dark matter cosmology fails to predict the proper amount of large-scale structure in our universe. Efstathiou, Sutherland and Maddox published in [33]: "*recent work suggests that there is more cosmological structure on very large scales ($l > h^{-1}Mpc$, where h is the Hubble constant H_0 in units of $100km\,s^{-1}Mpc^{-1}$) than simple versions of the CDM theory predict.*" A remedy is to relaunch the cosmological constant. The modified model is a spatially flat universe (which contains cold dark matter), largely dominated by a positive cosmological constant: "*the successes of the CDM theory can be retained and the new observations accommodated in a spatially flat cosmology in which as much as 80% of the critical density is provided by a positive cosmological constant, which is dynamically equivalent to endowing the vacuum with a non-zero energy density. In such a universe, expansion was dominated by CDM until a recent epoch, but is now governed by the cosmological constant.*" [33]. This concept is commonly referred to as the 'Lambda-Cold Dark Matter' (ΛCDM) model.

Alternatively, a spatially open universe with negative curvature (hyperbolic geometry), small Ω_M and $\Lambda = 0$ might explain the large-scale structure. However, the observation of far and near standard candles as Type Ia supernovae shows that the ΛCDM model is the simplest model that is in general agreement with current observations. The spatially open, $\Lambda = 0$ case does not fit the observational data of prospective research, see for example [95]. Research in the early and middle 1990s enhanced the indispensability of adding a nonzero cosmological constant Λ. Ostriker and Steinhardt published 1995 in [88]: "*Observations are providing progressively tighter constraints on cosmological models advanced to explain the formation of large-scale structure in the Universe. These include recent determinations of the Hubble constant* [...] *and measurements of the anisotropy of the cosmic microwave background.* [...] *a Universe having the critical energy density and a large cosmological constant appears to be favored.*" Several investigations concerning the age of the universe, the baryon content in galaxy clusters and the nature of large scale structure independently point to a mass density parameter Ω_M in between 0.2 and 0.3. Correspondingly, in a spatially flat universe where $\Omega_{tot} := \Omega_M + \Omega_\Lambda = 1$, there is a dark energy parameter Ω_Λ in between 0.7 and 0.8.

1.2.1. ***Accelerating cosmic expansion.***

Riess et al (1998) used a set of 16 high-redshift supernovae (including 10 new high-redshift Type Ia supernovae) and a set of 34 nearby supernovae to determine or place constraints on the Hubble constant, the mass density Ω_M, the vacuum energy

density Ω_Λ (correspondingly the cosmological constant Λ), the deceleration parameter q_0 and the age of the universe. The analysis of observational data affirmed that the expansion of our universe currently accelerates at high confidence levels: "*Different light curve fitting methods, SN Ia subsamples and prior constraints unanimously favor eternally expanding models with positive cosmological constant (i.e.,* $\Omega_\Lambda > 0$*) and a current acceleration of the expansion (i.e.,* $q_0 < 0$*).*", see [98]. In the following year, Perlmutter et al (1999) presented further evidence for a spatially flat universe with nonzero cosmological constant Λ: "*the data indicate that the cosmological constant is non-zero and positive, with a confidence of* $P(\Lambda > 0) = 99\%$", see [95]. They yielded a mass density parameter of $\Omega_M \approx 0.28$ and a vacuum energy density parameter of $\Omega_\Lambda \approx 0.72$, corresponding to a spatially flat model where $\Omega_M + \Omega_\Lambda = 1$. Consequently, the content of repulsive 'dark energy' in our universe is about 2.5 times larger than the content of gravitationally attractive baryonic and dark matter. This mix ratio is in accordance with accelerating cosmic expansion, caused by dark energy that manifests itself as cosmological constant $\Lambda > 0$ in Einstein's field equations. Michael Turner established the term 'dark energy' in 1999: "*Distance measurements to type Ia supernovae (SNe Ia) indicate that the Universe is accelerating and that two-thirds of the critical energy density exists in a dark-energy component with negative pressure.*" [60]. Finally in 2011, Saul Perlmutter, Brian Schmidt and Adam Riess shared the Nobel Prize "*for the discovery of the accelerating expansion of the Universe through observations of distant supernovae*" [115].

Cosmological constant problems[21], like the discrepancy between the observed value of dark energy density and the large values suggested by quantum field theory, still remained unsolved. Dark energy is considered to be one of the most fundamental theoretical problems of the current century. There are certain models of modified gravity and alternative ideas for the dark energy concept, like quintessence models, String- or M-theory, see for example [47, 28, 84, 114]. However, recent observations of the WMAP mission confirmed the ΛCDM model.

[21] see e.g. [122]

1.3. **Parameters of the universe.**
According to the results of NASA's Wilkinson Microwave Anisotropy Probe (WMAP) satellite mission, we admit a nonzero cosmological constant Λ in Einstein's field equations, and our work in this paper is based on a spatially flat ΛCDM model. We acknowledge the use of the Legacy Archive for Microwave Background Data Analysis (LAMBDA). Support for LAMBDA is provided by the NASA Office of Space Science. The WMAP mission started to map the cosmic microwave background radiation in August 2001. The WMAP 7-year results, released in January 2010 [63], strongly provide a spatially flat ΛCDM universe: "*The seven year data set is well fit by a minimal six-parameter flat ΛCDM model.*" Following WMAP [63], these six parameters of the ΛCDM universe are physical baryon density $\Omega_b h^2$, physical dark matter density $\Omega_c h^2$, dark energy density Ω_Λ, scalar spectral index n_s, reionization optical depth τ and the fluctuation amplitude σ_8 at $8\mathrm{h}^{-1}$Mpc. *"The parameters for this model, using the WMAP data in conjunction with baryon acoustic oscillation data from the Sloan Digital Sky Survey*[22] *and priors on H_0 from Hubble Space Telescope observations, are:* $\Omega_b h^2 = 0.02260 \pm 0.00053$, $\Omega_c h^2 = 0.1123 \pm 0.0035$, $\Omega_\Lambda = 0.728^{+0.015}_{-0.016}$, $n_s = 0.963 \pm 0.012$, $\tau = 0.087 \pm 0.014$ and $\sigma_8 = 0.809 \pm 0.024$ *(68% CL uncertainties).*" see [63]. The dimensionless Hubble parameter h is related to the Hubble constant by $H_0 = h \cdot 100 \frac{\mathrm{km}}{\mathrm{s\ Mpc}}$. Measurements of the Hubble constant H_0 yielded the value

$$H_0 = 70.4^{+1.3}_{-1.4} \frac{\mathrm{km}}{\mathrm{s\ Mpc}} \approx 0.07 \frac{1}{\mathrm{Gyr}} \tag{1.2}$$

where we have used $1\mathrm{Mpc} \approx 3.09 \cdot 10^{19}\mathrm{km}$. Resultant from the combined WMAP data $WMPA + BAO + H_0$ the age of the universe is $t_0 = 13.75 \pm 0.11\mathrm{Gyr}$, see [63]. Since $1\mathrm{Gyr} = 3.1536 \cdot 10^{16}\mathrm{s}$ the age is roughly $t_0 \approx 4.34 \cdot 10^{17}\mathrm{s}$.

1.3.1. ***Content of the universe.***
Measurements of the baryon density, dark matter density and dark energy density tell us about the composition of our universe. In cosmology, the ordinary matter which consists of atoms is called baryonic matter. For example, a planet is baryonic matter. Dark matter is a mysterious form of matter which acts gravitational attractive. Dark energy is an even more mysterious form of energy, it accelerates the expansion of the universe. Resultant from WMAP data combined with additional data sets (Sloan Digital Sky Survey and priors on H_0 from Hubble Space Telescope observations $WMPA + BAO + H_0$ see [63]), the values for Baryon density parameter Ω_b, dark matter density parameter Ω_c and dark energy density parameter Ω_Λ

[22]Sloan Digital Sky Survey: http://www.sdss.org/. The 2011 data release is given in [2].

are:

$$\Omega_b = 0.0456 \pm 0.0016, \quad \Omega_c = 0.227 \pm 0.014, \quad \Omega_\Lambda = 0.728^{+0.015}_{-0.016} \tag{1.3}$$

The mass density parameter Ω_M which includes baryonic and dark matter is roughly

$$\Omega_M = \Omega_b + \Omega_c \approx 0.273$$

and the measured value for the total density of the universe is $\Omega_{tot} = 1.0023^{+0.0056}_{-0.0054}$. Mostly, we will use $\Omega_M \approx 0.27$ and $\Omega_\Lambda \approx 0.73$ for our calculations. The huge contingent of dark matter and dark energy governs the universe. Only about five percent consists of 'normal' (baryonic) matter, the major content of our universe is a mystery to us. Today's composition of our universe is illustrated in figure 1.3.

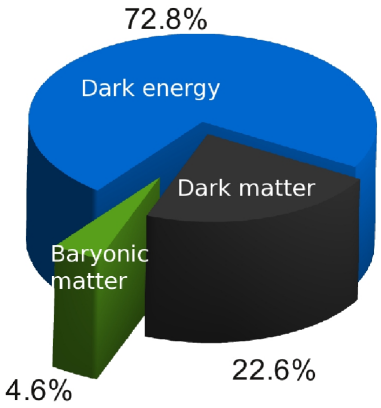

FIGURE 1.3. Content of the universe in accordance to recent data. Roughly five percent consists of baryonic matter. Dark matter and baryonic matter both have an attractive gravitational effect. Dark energy, which accounts for the largest share, has a repulsive effect.

1.3.2. *The evolution of the early universe after the Big Bang.*

According to our current understanding of physics, space and time didn't exist prior to the Big Bang. Therefore it is meaningless to ask what happened before the Big Bang, because time itself came into existence. The earliest period after the Big Bang, up to approximately 10^{-43}s, is called 'Planck epoch'. Since there is no theory of quantum gravity[23] so far, we are not able to describe events occurring over intervals shorter than the Planck time[24]. Most theories suggest that the four

[23]Quantum gravity is a theory unifying quantum mechanics and relativistic gravity.

[24]The Planck time $t_p = \sqrt{\frac{\hbar\gamma}{c^5}} \approx 5.39 \cdot 10^{-44}$s is a (unique) combination of reduced Planck constant $\hbar$, gravitational constant γ and speed of light c, so that t_p has units of time. Usually, the Planck time is approximately referred to as $t_p \approx 10^{-43}$s.

fundamental forces (gravity force, electromagnetic force and the strong and weak nuclear forces) were combined into one unified force during the Planck epoch. At the era around one Planck time ($\approx 10^{-43}$s) after the Big Bang, it is believed that the gravity force begins to differentiate from the other three fundamental forces. The following phase, during which electromagnetic force and the strong and weak nuclear forces remained unified into one universal interaction, is called 'grand unification epoch'. As the universe expanded and its temperature decreased to roughly 10^{28}K, the strong nuclear force separated from the other forces. Electromagnetic force and weak nuclear force still combined into one 'electroweak force'. This era, subsequent to the grand unification epoch, is called 'electroweak epoch'. As already mentioned, our universe passed through a phase of huge exponential expansion. It is believed that this 'inflationary epoch' occurred at the beginning of the electroweak epoch and ended at about 10^{-32}s after the Big Bang. Inflation increased the volume of the universe by a gigantic factor. Nevertheless, the temperature of the universe was still extremely high after the inflationary epoch, the universe was filled with free quarks and gluons (quark-gluon plasma). The universe continued to expand, but at a much slower rate. The final symmetry breaking occurred subsequent to the electroweak epoch, roughly 10^{-12}s after the Big Bang, resulting in the four separate forces[25] we know today. One second after the Big Bang, the universe contained protons, neutrons, positrons, electrons, photons and neutrinos. Helium was produced during the first few minutes. Meanwhile, the early Universe was dominated by photons. The radiation dominated era lasted for roughly ten thousand years. Atoms[26] formed when the universe was roughly 380 000 years old, and its temperature dropped below 2967°K. In cosmology this epoch usually is referred to as 'recombination'. Shortly after, photons separated from the now electrically neutral atoms and radiation decoupled[27] from matter. Hydrogen gas is almost completely transparent to cosmic background radiation. The last moment at which the universe was opaque to cosmic background radiation formed the 'surface of last scattering'. "*At this epoch of recombination, the CMB* [cosmic background radiation] *filled the universe with a red, uniformly bright glow of blackbody radiation, but later the temperature dropped and the CMB shifted to the infrared. To human eyes, the universe would then have appeared as a completely dark place.*" [80]. The ensuing 'dark age' lasted until stars and galaxies were formed by gravitational effects.

---

[25]Gravitation, electromagnetic force and the strong and weak nuclear forces

[26]Neutral hydrogen formed as the temperature dropped below 2967°K. Previously most of the hydrogen in the early universe was ionized.

[27]Due to the WMAP mission the redshift of decoupling is $z_* = 1090.89^{+0.69}_{-0.68}$ corresponding to an age of 377730^{+3205}_{-3200} years after the big bang, see [63].

1.3.3. ***Structure formation in the universe.***

"*A long period of time had to pass until the first objects collapsed, forming the first stars that shone in the universe with the first light ever emitted that was not part of the CMB* [cosmic background radiation]." [80]. Recent research indicates that halos of dark matter were the first structures to form in the universe, and they were the gravitational glue that attracted ordinary (baryonic) matter. Following Jordi Miralda-Escude's article [80], our Milky Way galaxy likely formed from the collapse of a $10^{12} M_\odot$ halo, where $M_\odot \approx 1.99 \cdot 10^{33}$g is the mass of the Sun. The origin of the first galaxies and quasars[28], roughly 400 million years after the Big Bang, marked the beginning of an epoch called 'reionization'. Astronomers speculate that an early generation of massive stars or super-massive black holes (re)ionized the gas in the universe. According to the WMAP data, the redshift of reionization is $z_{reion} = 10.4 \pm 1.2$, see [63]. At about one billion years after the Big Bang reionization was complete, and the universe became fully transparent once again. In 2010 Gobat et. al. "report evidence of a fully established galaxy cluster at $z = 2.07$" [49]. This cluster formed roughly three billion years[29] after the big bang. Our solar system formed as the universe was roughly 9 billion years old. The influence of cold dark matter and baryonic matter had slowed down the expansion of our universe for some billion years, but the speed of expansion has started to accelerate again. Over the last few billion years, the universe passed through a phase, largely dominated by the influence of the cosmological constant.

[28] Quasars are believed to be super-massive black holes

[29] Based on the ΛCDM model and $z = \frac{1}{a(t)} - 1$ we get $t = \frac{2}{3H_0\sqrt{\Omega_\Lambda}} \text{Arsinh} \sqrt{\frac{\Omega_\Lambda}{\Omega_M} \left(\frac{1}{1+z}\right)^3}$.

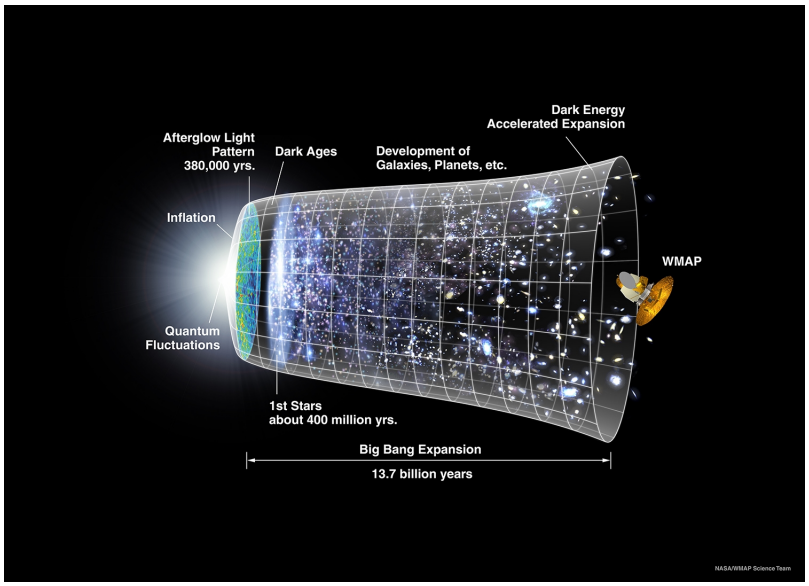

FIGURE 1.4. Credit: NASA / WMAP Science Team
http://wmap.gsfc.nasa.gov/media/060915/index.html

1.4. **Gravitationally bound systems.**

Matter in the universe usually clumps together by gravitational attraction. A gravitationally bound system comprises objects orbiting each other, such as planets and their moons, planetary systems, galaxies or galaxy clusters.

1.4.1. ***Planets and planetary systems.***

A planet is spherically shaped by its own gravity, but it is not massive enough to cause thermonuclear fusion. Usually planets are orbiting a star or stellar remnant. For example, our Earth is a planet with a mass of roughly $5.97 \cdot 10^{27}$g and an equatorial radius of about $6.39 \cdot 10^{6}$m. Frequently, there are one or more moons orbiting a planet. The Earth-Moon has an equatorial radius of $1.74 \cdot 10^{6}$m and a mass of $7.35 \cdot 10^{25}$g. Earth and Moon constitute a gravitationally bound system, which is again contained in the gravitationally bound 'solar system'. The biggest planet in our solar system is Jupiter, composed largely of hydrogen and helium. Jupiter has an equatorial radius of about $7.15 \cdot 10^{7}$m and its mass is more than 317 times the mass of the earth. Figure 1.5 compares all planets sizes: The planets outward from the Sun (left to right) are: Mercury, Venus, Earth, Mars, Jupiter, Saturn, Uranus, Neptune, and Pluto. The 'terrestrial' planets Mercury, Venus, Earth and Mars are primarily composed of rock and metal. The four planets in the outer region Jupiter, Saturn, Uranus, and Neptune are 'gas giants'. The center of a planetary system is a star like our Sun or a stellar remnant. Due to [112],

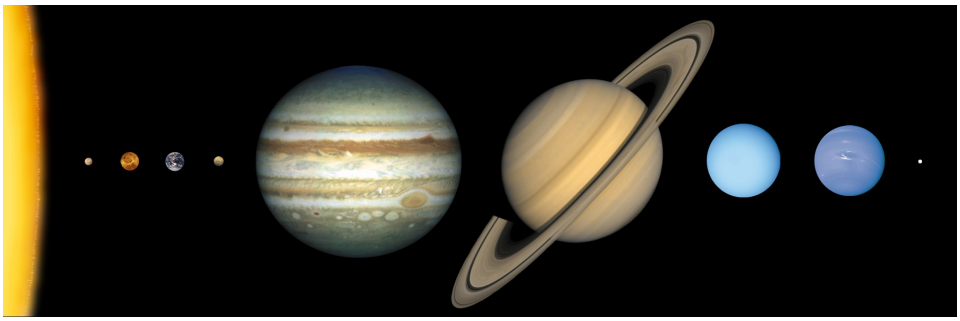

FIGURE 1.5. "All Planet Sizes"
Credit: NASA / Lunar and Planetary Institute
http://sse.jpl.nasa.gov/multimedia/display.cfm?IM_ID=178

our Sun has a mass of $M_\odot = 1.99 \cdot 10^{33}$g and a radius of $6.96 \cdot 10^8$m. The sun contains nearly 99.9% of the solar system's known mass. 'Main sequence stars' fuse hydrogen atoms together to make helium atoms in their cores. When the limited supply of hydrogen is exhausted, a low mass star like our Sun evolves into a red giant that finally ends as white dwarf. An upper bound on the mass of non-rotating white dwarfs is given by the Chandrasekhar limit[30]. The collapse of a massive star, for example around ten times more massive than the Sun, comes to an extremely luminous stellar explosion that is called supernova. The remnant of a supernova explosion is a hot neutron core, whose final fate depends upon the mass of the progenitor star. It will form a neutron star, if nuclear forces can resist the pull of gravity. Otherwise, the core collapses to form a black hole. It is believed that a black hole forms if the progenitor mass exceeds $10M_\odot$.

1.4.2. *Galaxies.*

A galaxy represents a huge gravitationally bound system which contains a large number of stars, stellar remnants, planetary systems, gas, dust and dark matter. A small galaxy contains less than a billion (10^9) stars, but the number of stars can easily exceed a trillion (10^{12}) in large galaxies. The visible part of a galaxy ranges in diameter from a few thousand to $5 \cdot 10^5$ light-years. Figure 1.6 shows the spiral galaxy $M101$ which is estimated to contain at least one trillion stars. The diameter of luminous matter in $M101$ is roughly $1.7 \cdot 10^5$ light-years ($\approx 52\,\text{kpc}$). Moreover, a galaxy contains non-luminous baryonic matter (e.g. gas, planets or stellar remnants) and a huge amount of dark matter. A dark matter halo is surrounding every galaxy. Our luminous Milky Way has a diameter of about 10^5 light-years ($\approx 30\,\text{kpc}$)

[30]If a mass of a non-rotating star exceeds the Chandrasekhar limit, degenerate electron pressure is not able to prevent further gravitationally collapse.

FIGURE 1.6. "Pinwheel Galaxy (Messier 101)"
Credit: European Space Agency & NASA
http://www.spacetelescope.org/images/heic0602a/

and includes some 200 billion[31] stars, but the diameter of its dark matter halo is at least three or four times larger[32] ($\sim 100\,\mathrm{kpc}$). "*We can estimate the mass of the Galaxy from the distribution of the stellar light and the mean mass-to-light ration of the stellar population, since gas and dust represent less than* $\sim 10\%$ *of the mass of the stars.*" [104]. Since dark matter outweighs baryonic matter by around a factor of five ($\Omega_c/\Omega_b \approx 5$ see (1.3) or [63]), a rough estimate of the total mass of our Milky Way galaxy is $M_{Gal} \approx 5 \cdot 2 \cdot 10^{11} M_\odot = 2 \cdot 10^{45}$g. Within a galaxy there are smaller gravitationally bound systems like star clusters. The number of stars in a cluster range from less than a few hundred (open cluster) to several million (globular cluster). The galaxies themselves are classified into elliptical galaxies, spiral galaxies, barred spiral galaxies and irregular ones. Elliptical galaxies are subdivided concerning their ellipticity, ranging from $E0$ (nearly spherically symmetric) to $E7$ (highly elongated). Spiral galaxies are labeled with the capital letter S followed by a, b or c which categorizes the compactness of their spiral arms. Barred spiral galaxies are characterized by their bar of stars through the central bulge. They are labeled by SB (instead of S) and a succeeding letter a, b or c. Galaxies in the

[31]Following [70], the Milky Way contains 200 to 400 billion stars.
[32]Koupelis and Kuhn estimated the "*total radius of the halo*" to 200,000 light years in [70].

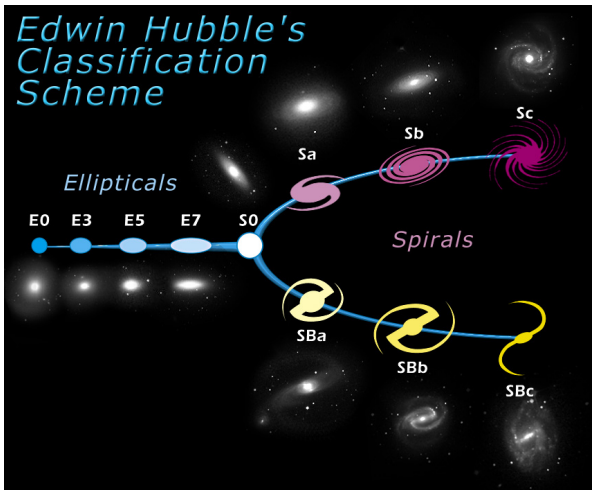

FIGURE 1.7. "Hubble Galaxy Classification"
Credit: ESA / ESO
http://www.spacetelescope.org/images/heic9902o/

transition zone between elliptical and spiral galaxies are called lenticular galaxies, denoted by $S0$.

It is believed that galaxies contain super massive black holes at their centers. Observations by the European Southern Observatory (ESO) in Chile yielded strong evidence for the existence of a gigantic black hole[33] at the center of the Milky Way. Ghez et. al. estimated its mass to be $2.6 \cdot 10^6 M_\odot$, see [48]. The binary black hole system OJ287 contains an object of $1.84 \cdot 10^{10} M_\odot$, which is the largest super massive black hole known so far. Valtonen et al. determined its mass in 2010, [119].

1.4.3. ***Galaxy groups and galaxy clusters.***
Gravitation can keep many individual galaxies bound together. A conglomeration up to about fifty galaxies is called galaxy group. At a rough estimate the mass of a typical galaxy group lies in the range $10^{12} M_\odot$ to $10^{13} M_\odot$. Karachentsev and Kashibadze estimated $(1.29 \pm 0.14) \cdot 10^{12} M_\odot$ for the mass of our Local Group, whose brightest members are the Milky Way and the Andromeda galaxy, cf. [67, 66]. Galaxy clusters typically have total masses of $10^{14} M_\odot$ to $10^{15} M_\odot$ and contain from a few dozen to several thousand galaxies. A galaxy cluster's diameter may exceed 10^7 light-years ($\approx 3\,\mathrm{Mpc}$). The nearest galaxy cluster to Earth, at a distance of $5.4 \cdot 10^7$ light-years, is the Virgo Cluster. Virgo is a large cluster, comprised of over 2000 galaxies. Another galaxy cluster in our neighborhood is the Fornax Cluster,

[33]The astronomical radio source at the center of the Milky Way is called Sagittarius A*

FIGURE 1.8. "The Fornax Galaxy Cluster"
Credit: ESO / J. Emerson / VISTA.
http://www.eso.org/public/images/eso0949c/

located about $6 \cdot 10^7$ light-years away. Figure 1.8 shows a picture of the Fornax Cluster. It is apparent from the analysis of galaxy velocities that clusters contain a large amount of dark matter. The velocities of the galaxies are too large to remain gravitationally bound by their mutual attractions.

1.4.4. ***Superclusters, filaments and voids***.

Galaxy clusters are grouped in larger structures called superclusters. Our Local Supercluster is spread over roughly 10^8 light-years (more than 30 Mpc) and the order of magnitude for its mass is estimated as $10^{15} M_\odot$. Fornax and Virgo are the two largest galaxy clusters, which are contained in our Local Supercluster. Actually, it is centered on the Virgo Cluster of galaxies, which represents its largest member. Due to this reason our Local Supercluster sometimes is called 'Virgo Supercluster'. The Local Supercluster then again "*seems to be appended to a very large agglomeration that includes the Coma/A1367, Hydra-Centaurus, Perseus-Pisces, and Pisces-Cetus Superclusters. The whole entity includes 48 known Abell-class clusters,* $10^{17} - 10^{18} M_\odot$*, and extends across a diameter of* $360 h_{75}^{-1}$ *Mpc* [...]" [118]. These agglomerations of Superclusters, sometimes called filaments or hyperclusters, are the largest known structures in the universe. They form the boundaries between huge areas of (nearly) empty space, called voids. At this scale our universe has a cellular structure resembling honeycombs. Up to present day, the Sloan Great

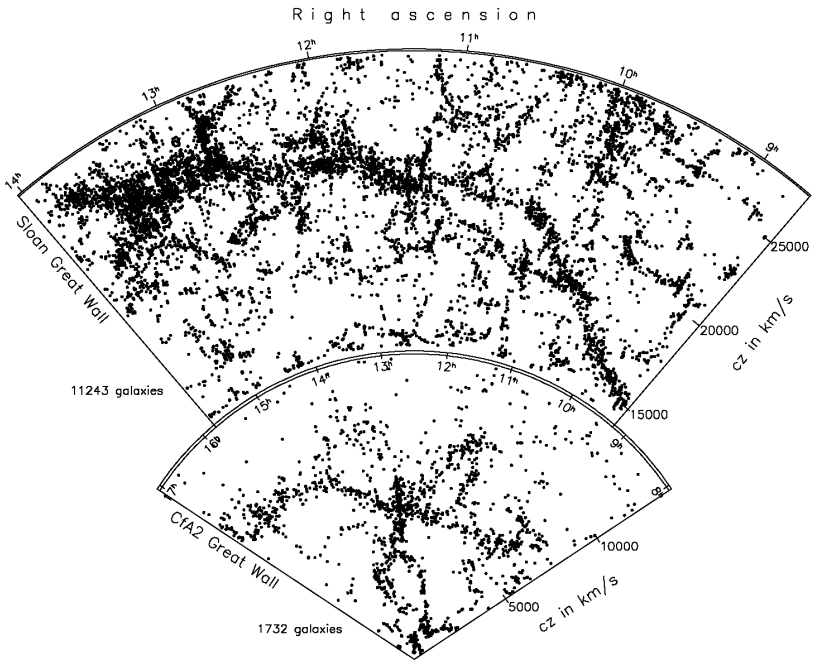

FIGURE 1.9. The Sloan Great Wall and the CfA Great Wall, [51]

Wall is the largest known filament, see figure 1.9. Filaments spread over billions (10^9) of light-years (more that 300 Mpc) and likely contain components that are not, and might never become, gravitationally bound together. Hence, a filament technically is not a gravitationally bound system. Filaments and voids form the largest scale structure of our universe. Generally, it can be assumed that our universe is homogeneous and isotropic at this scales "[...] *cosmology begins at distances that are larger than the size of the cell of uniformity which is* $100 - 150$ *Mpc or more*." [25].

1.4.5. ***Structure in our universe at different orders of magnitude.*** Structure in the universe occurs at different scales. The table gives a rough overview. It should be noticed that there is no clear cut-off point. For example, the diameter of large galaxy group may easily exceed 10^6 light-years.

Diameter	**Structure**	**Typical mass**
10^{-3} light-years	Solar system	$M_\odot$
$\vdots$	$\vdots$	$\vdots$
10^{1} light-years	Open star clusters	$10M_\odot - 10^4 M_\odot$
10^{2} light-years	Globular star clusters	$10^4 M_\odot - 10^6 M_\odot$
$\vdots$	$\vdots$	$\vdots$
10^{5} light-years	Galaxies	$10^{12} M_\odot$
10^{6} light-years	Groups of galaxies	$10^{13} M_\odot$
10^{7} light-years	Clusters of galaxies	$10^{14} M_\odot - 10^{15} M_\odot$
10^{8} light-years	Superclusters	$10^{15} M_\odot - 10^{16} M_\odot$
10^{9} light-years	Filaments	$10^{17} M_\odot - 10^{18} M_\odot$
10^{10} light-years	Universe	$\sim 10^{22} M_\odot$

2. Model solutions in general relativity

2.1. **Friedmann equations.**

It is supposed that the dynamics of the expanding universe are described by Einstein's general relativity theory. An important model for the geometry of the global universe is based on the Friedmann–Lemaître–Robertson–Walker (FLRW) metric:

$$ds^2 = c^2dt^2 - a^2(t)\left(\frac{dr^2}{1-Kr^2} + r^2d\theta^2 + r^2\sin^2\theta\, d\phi^2\right) \tag{2.1}$$

$K \in \mathbb{R}$ represents the spatial curvature of the spacetime. Appendix B.1 contains the calculations for the Einstein tensor, whose nonzero components are:

$$G_t^t = \frac{3}{c^2}\left(\frac{\dot{a}}{a}\right)^2 + \frac{3K}{a^2} - \Lambda, \quad G_r^r = G_\theta^\theta = G_\phi^\phi = \frac{K}{a^2} + \frac{1}{c^2}\left[2\frac{\ddot{a}}{a} + \left(\frac{\dot{a}}{a}\right)^2\right] - \Lambda \tag{2.2}$$

The cosmological principle states that matter is homogeneously distributed in our universe at very large scales. Friedmann's equations result from Einstein's field equations, where the Einstein tensor is given by (2.2), and the corresponding stress-energy tensor represents the content of the universe as a perfect fluid with a given mass density ρ and pressure p. Einstein's field equations are $G_k^i = \frac{8\pi\gamma}{c^4}T_k^i$ and the physical unit of the G_k^i is m^{-2}. The component of the stress-energy tensor which represents the mass density is $T_t^t = c^2\rho$. The unit of $\frac{8\pi\gamma}{c^4}T_t^t = \frac{8\pi\gamma}{c^2}\rho$ is m^{-2}, since ρ is measured in $\frac{\mathrm{kg}}{\mathrm{m}^3}$ and $\gamma \approx 6,67\cdot 10^{-11}\,\frac{\mathrm{m}^3}{\mathrm{s}^2\mathrm{kg}}$. The component $T_r^r = -p$ of the stress-energy tensor represents the pressure p, which is measured in $\frac{\mathrm{kg}}{\mathrm{s}^2\mathrm{m}}$. The unit of $\frac{8\pi\gamma}{c^4}T_r^r = -\frac{8\pi\gamma}{c^4}p$ is m^{-2} and the algebraic sign implies that a cosmological constant $\Lambda > 0$ is the antagonist to a pressure $p > 0$ since $R_k^i - \frac{1}{2}R\delta_k^i - \Lambda\delta_k^i = \frac{8\pi\gamma}{c^4}T_k^i$. Finally, the structure of Einstein's tensor (2.2) requires $T_r^r = T_\theta^\theta = T_\phi^\phi$ and $T_k^i = 0$ for $i \neq k$, hence the stress-energy tensor of the 'cosmic fluid' is given by:

$$T_t^t = c^2\rho; \quad T_r^r = T_\theta^\theta = T_\phi^\phi = -p; \quad \text{and} \quad T_k^i = 0 \text{ for } i \neq k \tag{2.3}$$

Einstein's field equations yield:

$$\frac{3}{c^2}\left(\frac{\dot{a}}{a}\right)^2 + \frac{3K}{a^2} - \Lambda \quad = \quad \frac{8\pi\gamma}{c^2}\rho \tag{2.4}$$

$$\frac{K}{a^2} + \frac{1}{c^2}\left[2\frac{\ddot{a}}{a} + \left(\frac{\dot{a}}{a}\right)^2\right] - \Lambda \quad = - \quad \frac{8\pi\gamma}{c^4}p \tag{2.5}$$

The Friedmann equations are usually given by (2.4) and

$$\frac{\ddot{a}}{a} - \frac{c^2\Lambda}{3} = -\frac{4\pi\gamma}{3}\left(\rho + \frac{3}{c^2}p\right) \tag{2.6}$$

which results from a combination of (2.4) and (2.5).

2.2. **Spatial curvature and critical density of the universe.**
Consider the Friedmann equation (2.4). We plug in the function $H = H(t) := \frac{\dot{a}}{a}$ and the equation reads:

$$\frac{3K}{a^2} = \frac{8\pi\gamma}{c^2}\rho + \Lambda - \frac{3}{c^2}H^2 \tag{2.7}$$

The spacetime is spatially flat if $K = 0$. In this case we obtain $\frac{8\pi\gamma}{c^2}\rho + \Lambda - \frac{3}{c^2}H^2 = 0$ and thus the condition:

$$\frac{8\pi\gamma}{3H^2}\rho + \frac{c^2\Lambda}{3H^2} = 1 \tag{2.8}$$

Obviously, if the average density ρ of a $\Lambda = 0$ universe reaches $\rho = \frac{3H^2}{8\pi\gamma}$, the spacetime is spatially flat. The value of $\rho_c = \frac{3H^2}{8\pi\gamma}$ is called critical density.

Mass density parameter and dark energy parameter
Currently, the average density of our universe is given by $\rho = \rho_0$, and the Hubble parameter H_0 is the current value of $H(t)$. The mass density parameter Ω_M is defined as the ratio $\Omega_M = \rho_0/\rho_c$. The dark energy parameter Ω_Λ represents the remaining part on the left side of equation (2.8). One has

$$\Omega_M = \frac{8\pi\gamma}{3H_0^2}\rho_0 \qquad \text{and} \qquad \Omega_\Lambda = \frac{c^2\Lambda}{3H_0^2} \tag{2.9}$$

see [91]. Usually, the total density parameter is $\Omega_{tot} = \Omega_\Lambda + \Omega_M$. Together with (2.9) the Friedmann equation (2.7) reads:

$$K = \frac{H_0^2 a^2}{c^2}\{\Omega_M + \Omega_\Lambda - 1\} \tag{2.10}$$

Consequently, there are three categories for the possible spatial geometry of the universe:

(1) $\Omega_M + \Omega_\Lambda = 1$, the universe is spatially flat since from (2.10) follows $K = 0$
(2) $\Omega_M + \Omega_\Lambda < 1$, negative curvature: (2.10) yields $K < 0$ (hyperbolic geometry)
(3) $\Omega_M + \Omega_\Lambda > 1$, positive curvature: (2.10) yields $K > 0$ (spherical geometry)

The mass density parameter Ω_M can be divided into the baryon density parameter Ω_b and the dark matter density parameter Ω_c, i.e. it is $\Omega_M = \Omega_b + \Omega_c$. Measurements of the NASA Explorer mission WMAP in conjunction with data from the Sloan Digital Sky Survey and the Hubble Space Telescope yielded

$$\Omega_b = 0.0456 \pm 0.0016,\ \Omega_c = 0.227 \pm 0.014,\ \Omega_\Lambda = 0.728^{+0.015}_{-0.016}$$

and for the total density parameter $\Omega_{tot} := \Omega_b + \Omega_c + \Omega_\Lambda = 1.0023^{+0.0056}_{-0.0054}$, see [63].

2.3. **Solutions of Friedmann's equations.**
According to the cosmological principle, the universe is homogeneous and isotropic on sufficiently large scales. Hence, it can be modeled with a FLRW metric. Our Universe expanded from an extremely dense state and the density decreases with time, consequently ρ is time dependent. Additionally, the density ρ may depend on the radial coordinate r, but we only deal with the case $\rho = \rho(t)$. Consider an expanding, dust-dominated model universe, which is increasing as $a(t)^3$. Accordingly, its density is decreasing with time as $a(t)^{-3}$. A suitable ansatz for the density in a dust dominated model universe is

$$\rho(t) = \frac{\rho_0}{a^3(t)} \tag{2.11}$$

where ρ_0 is the average density of the universe today. Obviously, $a(0) = 0$ implies an infinite density at $t = 0$. With the above ansatz, the first Friedmann equation (2.4) reads:

$$\frac{3}{c^2}\left(\frac{\dot{a}}{a}\right)^2 = \frac{8\pi\gamma\rho_0}{c^2a^3} - \frac{3K}{a^2} + \Lambda \tag{2.12}$$

In order to plug in the mass density parameter Ω_M and dark energy parameter Ω_Λ from (2.9) and introduce the curvature parameter $\Omega_K = \frac{c^2K}{3H_0^2}$, we rearrange (2.12):

$$\left(\frac{\dot{a}}{a}\right)^2 = H_0^2\left(\frac{8\pi\gamma\rho_0}{3H_0^2a^3} - \frac{c^2K}{3H_0^2a^2} + \frac{c^2\Lambda}{3H_0^2}\right) = H_0^2\left(\frac{\Omega_M}{a^3} - \frac{\Omega_K}{a^2} + \Omega_\Lambda\right) \tag{2.13}$$

We can rewrite this equation to

$$\frac{da}{a\,dt} = \pm H_0\sqrt{\frac{\Omega_M}{a^3} - \frac{\Omega_K}{a^2} + \Omega_\Lambda} \tag{2.14}$$

and the corresponding integral equation reads

$$\int_{a_1}^{a} \frac{dx}{x\sqrt{\frac{\Omega_M}{x^3} - \frac{\Omega_K}{x^2} + \Omega_\Lambda}} = \pm H_0(t - t_1) \tag{2.15}$$

where a_1 and t_1 are constants of integration. Equation (2.15) contains an elliptic integral. In general, elliptic integrals cannot be expressed in terms of elementary functions. By measurements of the NASA Explorer mission WMAP we know today that the universe is spatially flat with only a 2% margin of error. Thus we assume $\Omega_K = 0$ and $\Omega_M + \Omega_\Lambda = 1$ during our investigations. Further, the following considerations are restricted to the "+" branch of (2.15).

Using (2.11), the mass density parameter Ω_M and dark energy parameter Ω_Λ, Friedmann's second equation (2.6) is related to the pressure function p:

$$p = \frac{c^2}{4\pi\gamma}\left(\frac{c^2\Lambda}{3} - \frac{\ddot{a}}{a} - \frac{4\pi\gamma\rho_0}{3a^3}\right) = \frac{c^2}{4\pi\gamma}\left(H_0^2\Omega_\Lambda - \frac{\ddot{a}}{a} - \frac{H_0^2\Omega_M}{2a^3}\right) \tag{2.16}$$

In the following it is generally proofed that there is zero pressure if the density is given by (2.11). In case of de Sitter, Einstein-de Sitter and ΛCDM model we later reconfirm this fact by using equation (2.16).

2.3.1. ***Density and pressure in Friedmann's equations.***
We can rewrite the above equations (2.4) and (2.5) to give a relationship between density ρ and pressure p in Friedmann's model.

Lemma 1. *Density and pressure in Friedmann's equations.*
Density ρ, pressure p and the scale factor a in Friedmann's model are related by:

$$c^2 \frac{d}{dt}\left[\rho a^3\right] + p\frac{d}{dt}\left[a^3\right] = 0 \tag{2.17}$$

Proof. Equation (2.4) gives

$$c^2\rho a^3 = \frac{c^4}{8\pi\gamma}\left(\frac{3}{c^2}\dot{a}^2 a + 3Ka - \Lambda a^3\right)$$

and thus

$$c^2 \frac{d}{dt}\left[\rho a^3\right] = \frac{c^4}{8\pi\gamma}\left(\frac{3}{c^2}\left[2\ddot{a}\dot{a}a + \dot{a}^3\right] + 3K\dot{a} - 3\Lambda a^2\dot{a}\right). \tag{2.18}$$

Equation (2.5) gives

$$p = -\frac{c^4}{8\pi\gamma}\left(\frac{K}{a^2} + \frac{1}{c^2}\left[2\frac{\ddot{a}}{a} + \left(\frac{\dot{a}}{a}\right)^2\right] - \Lambda\right)$$

and together with $\frac{d}{dt}\left[a^3\right] = 3a^2\dot{a}$ we get:

$$p\frac{d}{dt}\left[a^3\right] = -\frac{c^4}{8\pi\gamma}\left(3K\dot{a} + \frac{3}{c^2}\left[2\ddot{a}\dot{a}a + \dot{a}^3\right] - 3\Lambda a^2\dot{a}\right) \tag{2.19}$$

From (2.18) and (2.19) we directly obtain (2.17). □

If the density is given by (2.11), equation (2.17) in lemma 1 reduces to $p\frac{d}{dt}\left[a^3\right] = 0$. Consequently, there is zero pressure in a dust dominated model universe.

2.4. **De Sitter universe.** $(\Omega_\Lambda = 1,\ \Omega_M = 0,\ \Omega_K = 0)$
At the time when Einstein published his General Relativity (1916), there was no observational evidence that our universe is expanding. Originally, Einstein added the cosmological constant to his equations in order to allow a static solution. Based on the modified field equations, de Sitter found his cosmological model in 1917. "*De Sitter's solution has negligibly small values for the mass density and pressure in ordinary matter*" [91], but a nonzero cosmological constant. Today, a considerable number of observations indicate that our universe is expanding, even with accelerating speed. A nonzero cosmological constant, which acts as a negative pressure and counteracts the effect of gravitation at large scale, is used to model the accelerating expansion of the universe. De Sitter's solution is inappropriate to describe the real universe, since it contains no matter. But the model reappears "*as a close approximation to the line element in some versions of the inflation scenario.*" [91].

Consider equation (2.13) for $\Omega_M = 0$ (and $\Omega_K = 0$):

$$\left(\frac{\dot{a}}{a}\right)^2 = H_0^2 \Omega_\Lambda$$

The integral equation (2.15) reduces to

$$\int_{a_1}^{a} \frac{dx}{x} = H_0 \sqrt{\Omega_\Lambda} \int_{t_1}^{t} dz.$$

From

$$\ln a = H_0 \sqrt{\Omega_\Lambda}\,(t - t_1) + \ln a_1$$

we finally obtain

$$a\,(t) = a_0 \exp\left[\sqrt{\Omega_\Lambda} \cdot H_0 t\right] \tag{2.20}$$

where $a_0 = a_1 \exp\left(-\sqrt{\Omega_\Lambda} \cdot H_0 t_1\right)$ contains the constants of integration. (2.20) is the scale factor of de Sitter's space-time. Current measurements yielded $\Omega_\Lambda \approx 0.7$, but the real universe contains matter. Here we have $\Omega_M + \Omega_\Lambda = 1$ but $\Omega_M = 0$, thus it is plausible to use $\Omega_\Lambda = 1$ in de Sitter's cosmological model.

Pressure in de Sitter's universe
Obviously, we have

$$\ddot{a} = \Omega_\Lambda H_0^2 a_0 \exp\left[\sqrt{\Omega_\Lambda} \cdot H_0 t\right] = \Omega_\Lambda H_0^2 a$$

and since $\Omega_M = 0$ the pressure equation (2.16) yields:

$$p = \frac{c^2}{4\pi\gamma}\left(H_0^2 \Omega_\Lambda - \Omega_\Lambda H_0^2\right) \equiv 0$$

2.4.1. ***Transformation into the static form.***
De Sitter's solution represents a special case of the FLRW metric (2.1): It is $K = 0$ and the scale factor is given by (2.20). In the following we show that de Sitter's metric can be transformed into a static line element. Let us now use the coordinates $\{\bar{t}, \bar{r}, \bar{\theta}, \bar{\phi}\}$ for the comoving system. Further we introduce the parameter

$$r_\Lambda := \sqrt{\frac{3}{\Lambda}}.$$

Together with $\Omega_\Lambda = \frac{c^2\Lambda}{3H_0^2}$ it is $\sqrt{\Omega_\Lambda} \cdot H_0 = c/r_\Lambda$ and de Sitter's metric reads

$$ds^2 = c^2 d\bar{t}^2 - a_0^2 \exp\left[\frac{2c\bar{t}}{r_\Lambda}\right] \left(d\bar{r}^2 + \bar{r}^2 d\bar{\theta}^2 + \bar{r}^2 \sin\bar{\theta}\, d\bar{\phi}^2\right) \tag{2.21}$$

where a_0 is a constant of integration.

Lemma 2.
De Sitter's metric (2.21) can be transformed into the static line element

$$ds^2 = \left[1 - \left(\frac{r}{r_\Lambda}\right)^2\right] c^2 dt^2 - \frac{1}{1 - \left(\frac{r}{r_\Lambda}\right)^2} dr^2 - r^2 d\theta^2 - r^2 \sin^2\theta\, d\phi^2 \tag{2.22}$$

by using the $\{t, r, \theta, \phi\}$ coordinates :

$$\bar{t} = t + \frac{r_\Lambda}{2c} \ln\left[1 - \left(\frac{r}{r_\Lambda}\right)^2\right], \quad \bar{r} = \frac{r \exp\left(-\frac{c}{r_\Lambda} t\right)}{a_0 \sqrt{1 - \left(\frac{r}{r_\Lambda}\right)^2}}, \quad \bar{\theta} = \theta, \quad \bar{\phi} = \phi \tag{2.23}$$

Proof. The coordinate transformation (2.23) gives

$$d\bar{t} = dt - \frac{r\, dr}{c r_\Lambda \left[1 - \left(\frac{r}{r_\Lambda}\right)^2\right]}, \quad d\bar{r} = \frac{\exp\left(-\frac{c}{r_\Lambda} t\right)}{a_0 \sqrt{1 - \left(\frac{r}{r_\Lambda}\right)^2}} \left[\frac{dr}{1 - \left(\frac{r}{r_\Lambda}\right)^2} - \frac{cr}{r_\Lambda} dt\right]$$

and therewith

$$\begin{aligned} c^2 d\bar{t}^2 &= c^2 dt^2 - \frac{2cr\, dt\, dr}{r_\Lambda \left[1 - \left(\frac{r}{r_\Lambda}\right)^2\right]} + \frac{r^2 dr^2}{r_\Lambda^2 \left[1 - \left(\frac{r}{r_\Lambda}\right)^2\right]^2} \\ d\bar{r}^2 &= \frac{\exp\left(-\frac{2c}{r_\Lambda} t\right)}{a_0^2 \left[1 - \left(\frac{r}{r_\Lambda}\right)^2\right]} \left\{ \frac{dr^2}{\left[1 - \left(\frac{r}{r_\Lambda}\right)^2\right]^2} - \frac{2cr\, dt\, dr}{r_\Lambda \left[1 - \left(\frac{r}{r_\Lambda}\right)^2\right]} + \frac{c^2 r^2}{r_\Lambda^2} dt^2 \right\}. \end{aligned}$$

With (2.23), the scale factor $a_0^2 \exp\left[\frac{2c\bar{t}}{r_\Lambda}\right]$ in (2.21) transformes into

$$a_0^2 \exp\left[\frac{2c\bar{t}}{r_\Lambda}\right] = a_0^2 \left[1 - \left(\frac{r}{r_\Lambda}\right)^2\right] \exp\left[\frac{2ct}{r_\Lambda}\right].$$

Together with

$$\bar{r}^2 = \frac{r^2}{a_0^2 \left[1 - \left(\frac{r}{r_\Lambda}\right)^2\right] \exp\left(\frac{2c}{r_\Lambda} t\right)}$$

we finally obtain:

$$\begin{aligned} ds^2 &= c^2 d\bar{t}^2 - a_0^2 \exp\left[\frac{2c\bar{t}}{r_\Lambda}\right] d\bar{r}^2 - a_0^2 \exp\left[\frac{2c\bar{t}}{r_\Lambda}\right] \bar{r}^2 \left(d\bar{\theta}^2 + \sin\bar{\theta}\, d\bar{\phi}^2\right) \\ &= \left[1 - \left(\frac{r}{r_\Lambda}\right)^2\right] c^2 dt^2 - \frac{1}{1 - \left(\frac{r}{r_\Lambda}\right)^2} dr^2 - r^2 \left(d\theta^2 + \sin^2\theta\, d\phi^2\right) \end{aligned}$$

This is the static de Sitter metric (2.22). □

2.5. **Einstein-de Sitter model.** $(\Omega_\Lambda = 0,\ \Omega_M = 1,\ \Omega_K = 0)$

The first expanding matter-filled world model was discovered independently by Friedmann in 1922 and Lemaitre in 1927. They adopted Einstein's assumption of spatial homogeneity and isotropy (cosmological principle). Einstein dropped the cosmological constant from his equations as a consequence of Hubble's observations. De Sitter and Einstein proposed "*it would be best to concentrate on the simplest reasonable case.*" [91]. In this model, the mass density parameter Ω_M is the only source term of the expansion rate. Space curvature and cosmological constant are neglected. For $\Omega_\Lambda = 0$ (as mentioned before it is additionally assumed that $\Omega_K = 0$) we are left with

$$\left(\frac{\dot{a}}{a}\right)^2 = H_0^2 \frac{\Omega_M}{a^3}$$

see (2.13), and equation (2.15) reduces to

$$\int_{a_1}^{a} \sqrt{x} dx = \pm H_0 \sqrt{\Omega_M} \int_{t_1}^{t} dz.$$

The solution is

$$\frac{2}{3} a^{\frac{3}{2}} = H_0 \sqrt{\Omega_M}\,(t - t_1) + \frac{2}{3} a_1^{\frac{3}{2}}$$

and we finally get

$$a\,(t) = \left[\frac{3}{2} H_0 \sqrt{\Omega_M}\,(t - t_0)\right]^{\frac{2}{3}} \tag{2.24}$$

where $t_0 = 2a_1^{\frac{3}{2}} \left(3H_0\sqrt{\Omega_M}\right)^{-1} - t_1$ contains the constants of integration. Expansion of the model universe proceeds but is decelerating, see figure 2.1. Current measurements yielded $\Omega_M \approx 0.3$, but today it is supposed that there exists a huge amount of dark energy. For the Einstein-de Sitter model we assume $\Omega_M + \Omega_\Lambda = 1$ but $\Omega_\Lambda = 0$. Thus, it is plausible to use $\Omega_M = 1$ here.

Pressure in the Einstein-de Sitter model

Since $\Omega_\Lambda = 0$, the pressure equation (2.16) reduces to

$$p = -\frac{c^2}{4\pi\gamma} \left(\frac{\ddot{a}}{a} + \frac{H_0^2 \Omega_M}{2a^3}\right).$$

For the dust dominated Einstein-de Sitter universe we get

$$\dot{a} = \frac{2}{3} \left(\frac{3}{2} H_0 \sqrt{\Omega_M}\right)^{\frac{2}{3}} (t - t_0)^{-\frac{1}{3}} \quad \text{and} \quad \ddot{a} = -\frac{2}{9} \left(\frac{3}{2} H_0 \sqrt{\Omega_M}\right)^{\frac{2}{3}} (t - t_0)^{-\frac{4}{3}}$$

so that $\ddot{a}/a = -\frac{2}{9}\,(t - t_0)^{-2}$. We yield zero pressure:

$$p = -\frac{c^2}{4\pi\gamma} \left(-\frac{2}{9\,(t - t_0)^2} + \frac{H_0^2 \Omega_M}{2\left[\frac{3}{2} H_0 \sqrt{\Omega_M}\,(t - t_0)\right]^2}\right) \equiv 0$$

2.6. **Spatially flat ΛCDM cosmological model.** $(\Omega_\Lambda + \Omega_M = 1,\ \Omega_K = 0)$
Results from the observations of distant supernovae indicate that the expansion of the universe is not decelerating, but in fact accelerates. The ΛCDM (Lambda Cold Dark Matter) model is the simplest known cosmological model which is in agreement with observed phenomena. The universe contains dust ($\Omega_M \neq 0$), and there is a nonzero cosmological constant ($\Omega_\Lambda \neq 0$). Based on the WMAP data [63], we assume that the universe is spatially flat ($K = 0$), and that it can be modeled with a FLRW metric[34]. The corresponding Friedmann equation (2.13) reads:

$$\left(\frac{\dot{a}}{a}\right)^2 = H_0^2\left(\frac{\Omega_M}{a^3} + \Omega_\Lambda\right) \tag{2.25}$$

Lemma 3 will help to solve the latter differential equation:

Lemma 3. *Let $l, m \in \mathbb{R}$ with $l \neq 0$ and $m \neq 0$.*

$$\int \frac{dx}{x\sqrt{\frac{m}{x^3} + l}} \quad = \quad \frac{2}{3\sqrt{l}}\mathrm{Arsinh}\left(\sqrt{\frac{l}{m}x^3}\right) + c_0 \tag{2.26}$$

where c_0 is the constant of integration.

Proof. Since $m \neq 0$, the integral can be rewritten as

$$\int \frac{dx}{x\sqrt{\frac{m}{x^3} + l}} = \frac{1}{\sqrt{m}}\int \frac{\sqrt{x}}{\sqrt{1 + \frac{l}{m}x^3}}dx.$$

Substitution of $z^2 = \frac{l}{m}x^3$ (remember $l \neq 0$) gives:

$$\frac{1}{\sqrt{m}}\int \frac{\sqrt{x}dx}{\sqrt{1 + \frac{l}{m}x^3}} = \frac{2}{3\sqrt{l}}\int \frac{dz}{\sqrt{1 + z^2}} = \frac{2}{3\sqrt{l}}\mathrm{Arsinh}\,(z) + c_0$$

With $z = \sqrt{lx^3/m}$ we obtain (2.26). □

Now it is easy to solve (2.25). The corresponding integral equation reads[35]

$$\int_{a_1}^{a} \frac{dx}{x\sqrt{\frac{\Omega_M}{x^3} + \Omega_\Lambda}} = \int_{t_1}^{t} H_0 dz \tag{2.27}$$

[34]The interval (2.1) reduces to $ds^2 = c^2dt^2 - a^2(t)\left\{dr^2 + r^2d\theta^2 + r^2\sin^2\theta\, d\phi^2\right\}$ in case of $K = 0$. If we use the Cartesian coordinate system, the flat FLRW metric has the most simple form $ds^2 = c^2dt^2 - a^2(t)\left\{dx^2 + dy^2 + dz^3\right\}$

[35]Since $\Omega_\Lambda + \Omega_M = 1$ we might replace Ω_M by $\Omega_M = 1 - \Omega_\Lambda$ alternatively.

see (2.15) for $\Omega_K = 0$. The integral is solved by lemma 3 with $m = \Omega_M$ and $l = \Omega_\Lambda$. Equation (2.27) yields

$$\frac{2}{3\sqrt{\Omega_\Lambda}}\mathrm{Arsinh}\left(\sqrt{\frac{\Omega_\Lambda}{\Omega_M}a^3}\right) = H_0\,(t - t_0)$$

where t_0 contains all constants of integration. Finally, we rearrange the equation:

$$a(t) \;=\; \sqrt[3]{\frac{\Omega_M}{\Omega_\Lambda}}\,\sinh^{\frac{2}{3}}\left[\frac{3}{2}\sqrt{\Omega_\Lambda}H_0\,(t - t_0)\right] \tag{2.28}$$

This is the scale factor for the standard cosmological model (ΛCDM).

Pressure in the ΛCDM model

In order to determine the pressure p we use

$$U := \frac{3\sqrt{\Omega_\Lambda}}{2}H_0\,(t - t_0)$$

in the following. With $\frac{dU}{dt} = \frac{3\sqrt{\Omega_\Lambda}}{2}H_0$ we get

$$\dot{a} = \sqrt{\Omega_\Lambda}H_0\sqrt[3]{\frac{\Omega_M}{\Omega_\Lambda}}\,\sinh^{-\frac{1}{3}}[U]\cosh[U]$$

and

$$\begin{aligned}\ddot{a} &= \sqrt{\Omega_\Lambda}H_0\sqrt[3]{\frac{\Omega_M}{\Omega_\Lambda}}\left(-\frac{\sqrt{\Omega_\Lambda}}{2}H_0\sinh^{-\frac{4}{3}}[U]\cosh^2[U] + \frac{3\sqrt{\Omega_\Lambda}}{2}H_0\sinh^{\frac{2}{3}}[U]\right)\\ &= \frac{\Omega_\Lambda H_0^2}{2}\sqrt[3]{\frac{\Omega_M}{\Omega_\Lambda}}\,\sinh^{-\frac{4}{3}}[U]\left(-\cosh^2[U] + 3\sinh^2[U]\right)\end{aligned}$$

from (2.28). Hence it is

$$\begin{aligned}\frac{\ddot{a}}{a} &= \frac{\Omega_\Lambda H_0^2}{2}\sinh^{-2}[U]\left(-\cosh^2[U] + 3\sinh^2[U]\right)\\ &= \frac{\Omega_\Lambda H_0^2}{2}\left(3 - \frac{\cosh^2[U]}{\sinh^2[U]}\right) = \Omega_\Lambda H_0^2 - \frac{\Omega_\Lambda H_0^2}{2\sinh^2[U]}\end{aligned}$$

where we have used the identity $\cosh^2[U] - \sinh^2[U] = 1$. Equation (2.16) yields zero pressure:

$$p = \frac{c^2}{4\pi\gamma}\left\{H_0^2\Omega_\Lambda - \Omega_\Lambda H_0^2 + \frac{\Omega_\Lambda H_0^2}{2\sinh^2[U]} - \frac{H_0^2\Omega_M}{2\frac{\Omega_M}{\Omega_\Lambda}\sinh^2[U]}\right\} \equiv 0$$

2.6.1. ***Comparison of the spatially flat solutions.*** $(\Omega_K = 0)$
Einstein-de Sitter model ($\Omega_M \neq 0$, $\Omega_\Lambda = 0$) and ΛCDM model ($\Omega_M \neq 0$, $\Omega_\Lambda \neq 0$) expand from a singularity at $t = t_0$. We may choose $t_0 = 0$ in (2.24) and (2.28), in order that this singularity is located at the coordinate origin. Whereas in the de Sitter case ($\Omega_M = 0$, $\Omega_\Lambda \neq 0$) it is $a > 0$ for all $a_0 \neq 0$, see equation (2.20). Let us choose $a_0 = 1$. As reasoned before, we use $\Omega_\Lambda = 1$ in De Sitter's model and $\Omega_M = 1$ for the Einstein-de Sitter universe. According to the WMAP [63] data, it is $H_0 \approx 0.07 \frac{1}{\text{Gyr}}$, and the values for the ΛCDM model are $\Omega_M \approx 0.27$ and $\Omega_\Lambda \approx 0.73$. Figure 2.1 shows the scale factors in comparison:

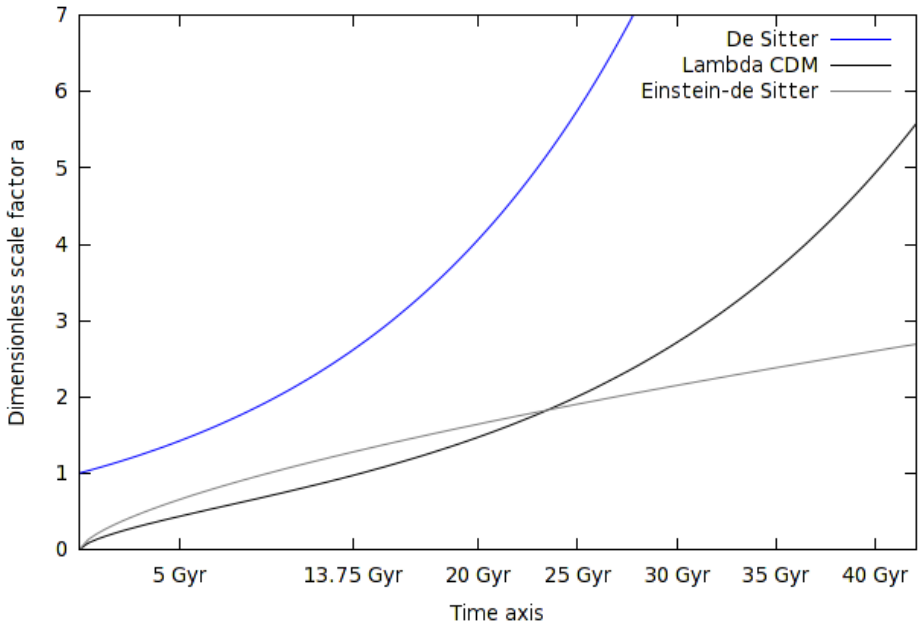

FIGURE 2.1. Scale factors

De Sitter model: $a(t) = \exp(H_0 t)$

ΛCDM model: $a(t) = \sqrt[3]{\frac{\Omega_M}{\Omega_\Lambda}} \sinh^{\frac{2}{3}}\left(\frac{3\sqrt{\Omega_\Lambda}}{2} H_0 t\right)$

Einstein-de Sitter model: $a(t) = \left(\frac{3}{2} H_0\right)^{\frac{2}{3}} t^{\frac{2}{3}}$

Remark 4. In consequence of the assumptions in lemma 3, $\Omega_M \neq 0$ and $\Omega_\Lambda \neq 0$ are necessary conditions for the ΛCDM solution. Hence, we can not expect to get back the de Sitter (2.20) or Einstein-de Sitter (2.24) scale factor as limiting case of the ΛCDM scale factor (2.28).

2.7. **Schwarzschild-de Sitter or Kottler metric.**

Schwarzschild's spherically symmetric, static and asymptotically flat solution of Einstein's equations for the empty space represents the gravitational field outside a single point mass[36]. Kottler's solution, also known as Schwarzschild-de Sitter metric, generalizes the Schwarzschild solution by including a cosmological constant term, cf. [69]. Let us first draw attention to the $\Lambda = 0$ case and Schwarzschild's solution.

2.7.1. ***Schwarzschild solution.***

In 1916, Karl Schwarzschild discovered this spherically symmetric solution of Einstein's vacuum field equations with $\Lambda = 0$. Schwarzschild's metric describes the gravitational field outside an uncharged and non-rotating point mass, for example the field of a static black hole[37]. In 1969, Debney, Kerr and Schild found a solution which could represent the axisymmetric field outside a rotating massive object, cf. [?]. The latter solution is commonly called Kerr metric[38]. Since our Sun is only slowly rotating, the Schwarzschild metric represents a good approximation for the local geometry of our solar system. In Schwarzschild coordinates $\{t, r, \theta, \phi\}$, where t is the time coordinate measured at infinity, r is the radial coordinate[39], θ is the colatitude and ϕ the longitude, the metric takes the form:

$$ds^2 = \left[1 - \frac{r_g}{r}\right] c^2 dt^2 - \frac{1}{1 - \frac{r_g}{r}} dr^2 - r^2 d\theta^2 - r^2 \sin^2\theta \, d\phi^2 \tag{2.29}$$

There is a curvature singularity at $r = 0$, which is covered by an event horizon at $r = r_g$. The radius r_g of this spherical event horizon (or gravitational sphere) is called gravitational radius or Schwarzschild radius. It is related to the mass M of the central body by

$$r_g := \frac{2M\gamma}{c^2} \tag{2.30}$$

where γ is the constant of gravitation and c the speed of light. An observer who enters the gravitational sphere cannot cross the event horizon again. The event horizon at $r = r_g$ "*acts as a one-way membrane, letting future-directed timelike and null curves cross only from the outside* $[r > r_g]$ *to the inside* $[r < r_g]$." [56]. The Schwarzschild spacetime is asymptotically flat as the metric (2.29) approximates $ds^2 = c^2 dt^2 - dr^2 - r^2 d\theta^2 - r^2 \sin^2\theta \, d\phi^2$, the Minkowski metric, for large r.

---

[36]For example, one can describe the local geometry of space time in the solar system to a good approximation by Schwarzschild's solution.

[37]The gravitational field of a charged non-rotating black hole is given by the Reissner–Nordström solution, cf. [56].

[38]The Kerr metric can be modified in order to describe the field of a charged rotating black hole. This solution is called Kerr–Newman metric.

[39]corresponds to the circumference of a circle (centered on the coordinate origin) divided by 2π

2.7.2. ***The Schwarzschild-de Sitter solution and Einstein's equations.***
In the following, we consider the general case, i.e. we assume the existence of a nonzero cosmological constant. The Schwarzschild-de Sitter (Kottler) metric, as well as Schwarzschild's metric in case of $\Lambda = 0$, results from a stationary, spherically symmetric ansatz:

$$ds^2 = \alpha(r)\, c^2 dt^2 - \beta(r)\, dr^2 - r^2 d\theta^2 - r^2 \sin^2\theta\, d\phi^2 \tag{2.31}$$

In the following we establish the Schwarzschild-de Sitter metric by solving Einstein's vacuum field equations for the interval (2.31). Appendix B.2 contains the calculations of Einstein's tensor for (2.31). The empty space equations $G^i_k = 0$ are:

$$0 = \frac{\beta'}{\beta^2 r} - \frac{1}{\beta r^2} + \frac{1}{r^2} - \Lambda \tag{2.32}$$

$$0 = -\frac{\alpha'}{\alpha\beta r} - \frac{1}{\beta r^2} + \frac{1}{r^2} - \Lambda \tag{2.33}$$

$$0 = -\frac{\alpha'}{2\alpha\beta r} + \frac{\beta'}{2\beta^2 r} - \frac{\alpha''}{2\alpha\beta} + \frac{\alpha'^2}{4\alpha^2\beta} + \frac{\alpha'\beta'}{4\alpha\beta^2} - \Lambda \tag{2.34}$$

From (2.32) together with (2.33) we get $\frac{\beta'}{\beta} = -\frac{\alpha'}{\alpha}$. Both sides can be rewritten by using the natural logarithm: $\frac{d}{dr}[\ln\beta] = \frac{d}{dr}\left[\ln\alpha^{-1}\right]$. Obviously, it is

$$\beta(r) = \frac{k_0}{\alpha(r)}$$

where k_0 is a constant of integration. We may choose $k_0 = 1$ and (2.31) reduces to:

$$ds^2 = \alpha(r)\, c^2 dt^2 - \alpha^{-1}(r)\, dr^2 - r^2 d\theta^2 - r^2 \sin^2\theta\, d\phi^2 \tag{2.35}$$

Further it is $\beta' = -\frac{\alpha'}{\alpha^2}$, so we are left with the empty space equations:

$$\alpha' + \frac{1}{r}\alpha - \frac{1}{r} + r\Lambda = 0 \tag{2.36}$$

$$\alpha'' + \frac{2}{r}\alpha' + 2\Lambda = 0 \tag{2.37}$$

Equation (2.36) is an inhomogeneous linear differential equation. The solution of the homogeneous equation $\alpha' + \frac{1}{r}\alpha = 0$ is $\alpha_h = \frac{k_0}{r}$ where k_0 is a constant of integration. From the ansatz $\alpha = \frac{k(r)}{r}$ and (2.36) we get $k' = 1 - \Lambda r^2$ so that $k = r - \frac{\Lambda}{3}r^3 - r_g$ where r_g is a constant of integration. Finally we obtain:

$$\alpha(r) = 1 - \frac{r_g}{r} - \frac{\Lambda}{3}r^2 \tag{2.38}$$

Equation (2.37) is fulfilled since $\alpha' = \frac{r_g}{r^2} - \frac{2}{3}\Lambda r$, $\alpha'' = -\frac{2r_g}{r^3} - \frac{2}{3}\Lambda$ and

$$\alpha'' + \frac{2}{r}\alpha' + 2\Lambda = -\frac{2r_g}{r^3} - \frac{2}{3}\Lambda + \frac{2}{r}\left(\frac{r_g}{r^2} - \frac{2}{3}\Lambda r\right) + 2\Lambda \equiv 0.$$

2.8. **Analysis of the Schwarzschild-de Sitter model.**
For our purpose, the Schwarzschild-de Sitter model is probably the most important solution including a cosmological constant. Let us introduce the parameter[40]

$$r_\Lambda := \sqrt{\frac{3}{\Lambda}}. \tag{2.39}$$

From the above calculations together with (2.39) we obtain the Schwarzschild-de Sitter interval:

$$ds^2 = \left[1 - \frac{r_g}{r} - \left(\frac{r}{r_\Lambda}\right)^2\right] c^2 dt^2 - \frac{1}{1 - \frac{r_g}{r} - \left(\frac{r}{r_\Lambda}\right)^2} dr^2 - r^2 d\theta^2 - r^2 \sin^2\theta \, d\phi^2 \tag{2.40}$$

This non-isotropic solution of Einstein's field equations describes the gravitational field outside a spherically symmetric point mass, contained in a universe with nonzero cosmological constant Λ. In the following we analyze $\alpha(r) = 1 - \frac{r_g}{r} - \left(\frac{r}{r_\Lambda}\right)^2$. Since $r_\Lambda \approx 5\,\mathrm{Gpc}$, the term $(r/r_\Lambda)^2$ is negligible if r is in the range of r_g. In this region the Schwarzschild-de Sitter α reduces to the Schwarzschild case. Now consider the region far out from r_g. The term r_g/r is negligibly small for $r \gg r_g$ and α reduces to the de Sitter case. We have:

$$\alpha(r) = 1 - \frac{r_g}{r} - \left(\frac{r}{r_\Lambda}\right)^2 \approx \begin{cases} 1 - \frac{r_g}{r} & \text{for } r \approx r_g \quad \text{(Schwarzschild case)} \\ 1 - \left(\frac{r}{r_\Lambda}\right)^2 & \text{for } r \gg r_g \quad \text{(De Sitter case)} \end{cases}$$

This behavior is important for the choice of initial conditions while dealing with numerical calculations later.

2.8.1. ***Roots of*** $\alpha(r)$.
In the Schwarzschild case $\Lambda = 0$ there is a boundary in spacetime beyond which particles cannot escape the gravitational pull. This so-called event horizon is located at $\alpha(r) = 0$. From $1 - \frac{r_g}{r} = 0$ we get $r = r_g$. The corresponding Schwarzschild-de Sitter equation $1 - \frac{r_g}{r} - \left(\frac{r}{r_\Lambda}\right)^2 = 0$ can be transformed into

$$r^3 - r_\Lambda^2 r + r_\Lambda^2 r_g = 0. \tag{2.41}$$

Equation (2.41) is a depressed cubic, which generally has the form $y^3 + py + q = 0$. Its discriminant $D = \frac{q^2}{4} + \frac{p^3}{27}$ tells us about the number of real- and complex-valued solutions, see for example [14]. Equation (2.41) yields $D = r_\Lambda^4 \left(\frac{r_g^2}{4} - \frac{r_\Lambda^2}{27}\right)$, which remains negative as long as $r_g < \frac{2}{3\sqrt{3}} r_\Lambda \approx 1.9\,\mathrm{Gpc}$. This upper boundary for the gravitational radius corresponds to a central object with a mass of roughly $2 \cdot 10^{22} M_\odot$. But the largest known structure in the universe are filaments with a

[40] $\Lambda \approx 1.3 \cdot 10^{-52}\mathrm{m}^{-2}$

typical mass in range of $10^{17}-10^{18}M_\odot$. Thus we can assume $D<0$. Consequently, there are always three real roots for r given by[41]:

$$r_1 = \frac{2}{\sqrt{3}}r_\Lambda \cos\left\{\frac{1}{3}\arccos\left(-\frac{3\sqrt{3}}{2}\cdot\frac{r_g}{r_\Lambda}\right)\right\} \tag{2.43}$$

$$r_{2,3} = -\frac{2}{\sqrt{3}}r_\Lambda \cos\left\{\frac{1}{3}\arccos\left(-\frac{3\sqrt{3}}{2}\cdot\frac{r_g}{r_\Lambda}\right)\mp\frac{\pi}{3}\right\}$$

Taylor approximation[42] of (2.43) gives $r_1\approx r_\Lambda-\frac{1}{2}r_g$, $r_2\approx -r_\Lambda-\frac{1}{2}r_g$ and $r_3\approx r_g$. Since $r_\Lambda\approx 5\,\mathrm{Gpc}$ and $r_g\ll r_\Lambda$, the solution r_1 is of no relevance. Based on the assumption that our universe is $13.7\cdot 10^9$ years old, the radius of the observable universe is about $4.2\,\mathrm{Gpc}$. The solution r_2 is also unimportant because $r_2<0$. The solution $r_3\approx r_g$ corresponds roughly to the Schwarzschild case, where the equation reduces to $1-\frac{r_g}{r}=0$. Evaluation of (2.43) at $r_g\approx 3.9\cdot 10^{15}\mathrm{m}$ (which corresponds to the mass of the Local Group) with the computer algebra system Maple confirmed these results[43]: There is one solution in the range of $5\,\mathrm{Gpc}$, a negative one, and a solution in the range of r_g. The solutions $r_1\approx 5\,\mathrm{Gpc}$ and $r_2<0$ are highly stable against the change of the central mass M within realistic range. For example if we replace $M=1.3\cdot 10^{12}M_\odot$ (Local Group) by the mass of our Sun $M=M_\odot$, the solution $r_1\approx 5\,\mathrm{Gpc}$ increases less that $1\,\mathrm{pc}$. The third root r_3 changes like r_g does, but the relation $r_3\approx r_g$ remains unaffected.

2.8.2. *Extrema and inflection points of* α.

There is a local maximum of $\alpha(r)=1-\frac{r_g}{r}-\left(\frac{r}{r_\Lambda}\right)^2$ at

$$r_* := \left(\frac{1}{2}r_g r_\Lambda^2\right)^{\frac{1}{3}} \tag{2.44}$$

since the necessary condition for a local extremum

$$0=\alpha'(r)=\frac{d}{dr}\left[1-\frac{r_g}{r}-\left(\frac{r}{r_\Lambda}\right)^2\right]=\frac{r_g}{r^2}-\frac{2r}{r_\Lambda^2}$$

---

[41] If $p<0$ and $D=\frac{q^2}{4}+\frac{p^3}{27}\le 0$ the cubic equation $y^3+py+q=0$ is solved by

$$y_1 = 2\sqrt{-\frac{p}{3}}\cos\left\{\frac{1}{3}\arccos\left(-\frac{q}{2\sqrt{-\frac{p^3}{27}}}\right)\right\} \tag{2.42}$$

$$y_{2,3} = -2\sqrt{-\frac{p}{3}}\cos\left\{\frac{1}{3}\arccos\left(-\frac{q}{2\sqrt{-\frac{p^3}{27}}}\right)\mp\frac{\pi}{3}\right\}$$

[42] We used $\arccos(x)=\frac{\pi}{2}-x+\mathcal{O}(x^3)$, $\cos(x)=1+\mathcal{O}(x^2)$ and $\sin(x)=x+\mathcal{O}(x^3)$. Terms with $(r_g/r_\Lambda)^n$ are neglected for $n\ge 2$.

[43] Since r_g/r_Λ is very small, a high precision is required. Especially for the evaluation of r_3 it is recommended to use Maple with the command evalf[50](...) for example.

is fulfilled only at r_* and it is:

$$\alpha''(r_*) = -\frac{2r_g}{r_*^3} - \frac{2}{r_\Lambda^2} = -\frac{6}{r_\Lambda^2} < 0.$$

Interestingly, the location r_* of the local extremum corresponds with the radius of the 'zero-gravity surface' proposed by Chernin et. al. in [26]. Section 6 contains a detailed discussion concerning the interaction of expansion and gravitation in the Schwarzschild-de Sitter model.

Finally, we determine the inflection points of α. We assume $\Lambda > 0$. Hence, the necessary condition $0 = \alpha''(r) = -\frac{2r_g}{r^3} - \frac{2}{r_\Lambda^2}$ for an inflection point is only fulfilled at $r = -\sqrt[3]{r_\Lambda^2 r_g} < 0$. Negative values are of no relevance for our concerns.

Figure 2.2 shows the Schwarzschild-de Sitter case for a mass of $M = 1.3 \cdot 10^{12} M_\odot$, corresponding to our Local Group of galaxies, in comparison to the Schwarzschild case ($\Lambda = 0$). In order to display the values on the vertical axis of the second graphic

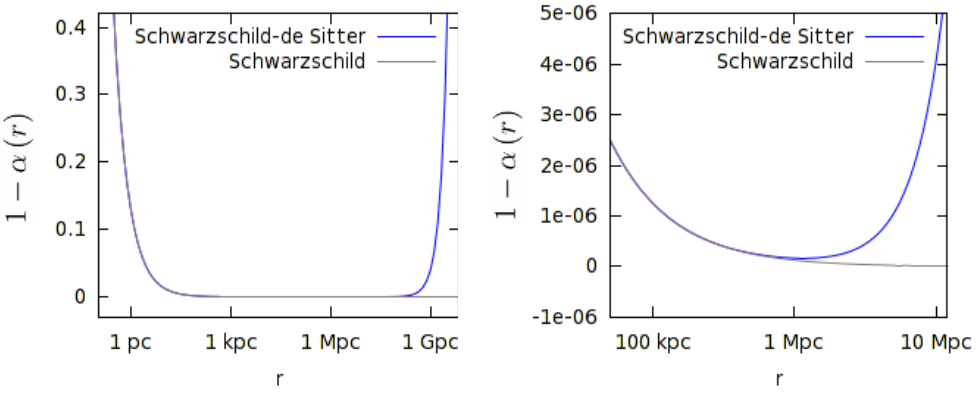

FIGURE 2.2. The function $f = 1 - \alpha(r)$ in Schwarzschild-de Sitter (Kottler) and Schwarzschild case. It is $g_{00} = c^2\alpha(r)$. The graphic shows $f_K = \frac{r_g}{r} + \left(\frac{r}{r_\Lambda}\right)^2$ and $f_S = \frac{r_g}{r}$. Here, r_g is the gravitational radius $r_{LG} \approx 0.125\,\mathrm{pc}$ of the Local Group. Obviously, the influence of Λ appreciably increases at $r \sim 1\,\mathrm{Mpc}$.

with adequate accuracy, we plot $1 - \alpha(r)$ in stead of $\alpha(r)$. For the mass of our Local Group, the extremum of $\alpha(r) = 1 - \frac{r_g}{r} - \left(\frac{r}{r_\Lambda}\right)^2$ is located at $r_* \approx 1.15\,\mathrm{Mpc}$. The influence of the cosmological constant noticeably ascends in the range of $r \sim 1\,\mathrm{Mpc}$. Schwarzschild's solution (i.e. the $\Lambda = 0$ case) is asymptotically flat. The above graphic indicates that the Schwarzschild-de Sitter spacetime is not asymptotically flat. Since the Schwarzschild-de Sitter metric is a solution of Einstein's vacuum equations, there is no pressure in this model.

3. The McVittie problem - Earlier research

After Schwarzschild and Friedmann found their solutions of Einstein's equations, the problem of fitting local and global geometry occurred. Gravitationally bound systems do not take part in the expansion of our universe. A static gravitational field, generated by a central mass, has to be embedded into an expanding cosmological background. But where is the limit of the non-expanding area? And what is a suitable model to describe both, local and global geometry, in the framework of Einstein's general relativity? We review some earlier research that has been concerned with this problem. At first we outline the basic terminology and notation, which is used in this section.

A spacetime manifold is described by its metric tensor, which can be expressed in different coordinate systems. It seems natural to choice a comoving frame for an expanding cosmological model, since it is easier to work with. A comoving coordinate system expands together with the universe. Roughly speaking, the cosmic material itself (i.e. matter which moves along with the Hubble flow) constitutes the comoving coordinate system. A comoving observer has constant spatial coordinate values. On the other hand, we have static spacetimes like the Schwarzschild or Schwarzschild-de Sitter model. Obviously, a natural coordinate choice would be a static frame. In a static coordinate frame, "*the distance between two points at relative rest is independent of time*" [79]. Following McVittie, we will call these coordinates "*observer coordinates*". Both coordinate frames are related as follows: A radial observer coordinate r is related to the corresponding comoving coordinate $\overline{r}$ by $r = a\,(t)\,\overline{r}$, where $a\,(t)$ is the scale factor of the universe.

The adjective 'isotropic' can be defined[44] as "*having a physical property which has the same value when measured in different directions*". Due to this definition, Schwarzschild's spacetime would not be isotropic, except for an observer located at the coordinate singularity. Nevertheless, Schwarzschild's metric (2.29) can be transformed into 'isotropic coordinates', see section 5.2. In general relativity, a metric tensor is called isotropic if the 3-space of constant time is conformal[45] Euclidean.

[44] Oxford Dictionaries. April 2010. Oxford University Press. 13 January 2013 http://oxforddictionaries.com/definition/english/isotropic?

[45] "When two Riemann spaces are so related that the line element of one is merely a multiple of the line element of the other they are said to be conformal." see [13].

In other words, a metric is called isotropic if its spatial component is a multiple of the Euclidean line element, which in spherical coordinates $\{q, \theta, \phi\}$ is given by

$$d\sigma^2 = dq^2 + q^2 d\theta^2 + q^2 \sin^2\theta \, d\phi^2 \tag{3.1}$$

where q is the radial coordinate. Thus, an isotropic line element has the form $ds^2 = g_{00}dt^2 - g_{11}d\sigma^2$.

Notation:
In order to compare the articles, we change the originally used notations and use the following consistent notation:

1. If more than one coordinate system is used (observer and comoving coordinates), time and radial coordinates in comoving systems are overlined.

2. r_g is the gravitational radius (Schwarzschild radius).

3. The spherical coordinates are $\{t, r, \theta, \phi\}$ and it is $d\Omega_2 := d\theta^2 + r^2 d\phi^2$.

4. We use q as radial coordinate in an isotropic frame and the shortcut (3.1). The notation $d\sigma^2$ is also used in comoving systems (and not $d\bar{\sigma}^2$).

5. The general isotropic line element is

$$ds^2 = c^2 e^{\xi} dt^2 - e^{\mu} d\sigma^2$$

where ξ and μ depend on the time and the radial coordinate.

Examples:
In our notation, Schwarzschild's metric (2.29) takes the form:

$$ds^2 = \left[1 - \frac{r_g}{r}\right] c^2 dt^2 - \frac{1}{1 - \frac{r_g}{r}} dr^2 - r^2 d\Omega_2 \tag{3.2}$$

The spatially flat FLRW line element is

$$ds^2 = c^2 d\bar{t}^2 - a^2\left(\bar{t}\right) d\sigma^2 \tag{3.3}$$

where $a\left(\bar{t}\right)$ is the scale factor. With respect to Cartesian coordinates $\left\{\bar{t}, \overline{x}_1, \overline{x}_2, \overline{x}_3\right\}$ the spatially flat FLRW interval reads:

$$ds^2 = c^2 d\bar{t}^2 - a^2\left(\bar{t}\right)\left(d\overline{x}_1^2 + d\overline{x}_2^2 + d\overline{x}_3^2\right) \tag{3.4}$$

3.1. **The first discussion of the problem: G. C. McVittie 1933.**

George McVittie was the first who proposed the problem how to connect local and global geometry of our universe using a simple model. In 1933, he found a solution which is of Schwarzschild-type in the neighborhood of the central mass-point, and which turns into the spatially flat FLRW[46] metric for increasing distance.

The local geometry, e.g. gravitational bound systems like the Sun and the bodies moving in orbit around it, can be described by:

$$ds^2 = \left(\frac{1-\frac{r_g}{4q}}{1+\frac{r_g}{4q}}\right)^2 c^2dt^2 - \left(1+\frac{r_g}{4q}\right)^4 d\sigma^2 \tag{3.5}$$

This is the isotropic form of Schwarzschild's solution. The transformation of Schwarzschild's interval (2.29) into the isotropic form (3.5) is given in subsection 5.2. The isotropic coordinates are $\{t, q, \theta, \phi\}$, where q is the radial coordinate. q "*is what we shall call an observer's co-ordinate, i.e. it is one based on the assumption that the distance between two points at relative rest is independent of time.*" [79]. On the other hand, we use non-static metrics to model the global geometry of our expanding universe. McVittie used the following classification: Metrics of the form

$$ds^2 = c^2d\bar{t}^2 - a^2\left(\bar{t}\right)\frac{d\sigma^2}{\left(1+\bar{q}^2/4R^2\right)^2} \tag{3.6}$$

are called Lemaître class metrics. Metrics of the form

$$ds^2 = c^2d\bar{t}^2 - a^2\left(\bar{t}\right)d\sigma^2 \tag{3.7}$$

are called De Sitter class metrics. Global curvature of space (as a whole) is given by the constant $1/R^2$, which may be positive or negative[47] in (3.6). The spatial curvature in (3.7) is zero. The function $a\left(\bar{t}\right)$ represents the scale factor. De Sitter's metric is a particular case of (3.7) where $a\left(\bar{t}\right) = \exp\left[\sqrt{\Omega_\Lambda}\cdot H_0\bar{t}\right]$. The $\bar{q}$ coordinate in (3.6) and (3.7) is the radial coordinate in the comoving system. This coordinate "*is one which is called cosmical. It is used when the system of nebulae is taken as the basis of reference.*" [79].

McVittie's calculations were based on the "*most general form of metric which is orthogonal, isotropic in the space co-ordinates and which expresses the condition for spherical symmetry around the origin.*" [79]. In our notation, this metric takes the form:

$$ds^2 = c^2e^{\xi}d\bar{t}^2 - e^{\mu}d\sigma^2 \tag{3.8}$$

[46]Friedmann–Lemaître–Robertson–Walker

[47]Perhaps, it would be more favorable to use K instead of $1/R^2$ in order to avoid misconception about the case $1/R^2 < 0$.

The functions ξ and μ depend on the time and the radial coordinate. The cosmic matter outside the mass-particle "*is evenly spread out through space if it were a gas*" [79]. McVittie assumed that there "*is no flow of the matter as a whole either towards or away from the origin* [...]". Consequently, he claimed that the pressure is isotropic at any point in the universe. The stress-energy tensor is that of a cosmic fluid, cf. (2.3). Its nonzero components are:

$$T_t^t = c^2\rho; \quad T_r^r = T_\theta^\theta = T_\phi^\phi = -p$$

Based on (3.8) and (2.3), McVittie derived a couple of equations from Einstein's equation (1.1), which lead *"to our two fundamental equations for determining the coefficients of the metric* [...]":

$$\dot{\mu}' - \frac{1}{2}\dot{\mu}\xi' = 0 \tag{3.9}$$

$$\xi'' + \mu'' - \frac{1}{\overline{q}}\left(\xi' + \mu'\right) - \mu'\xi' - \frac{1}{2}\left(\mu'\right)^2 + \frac{1}{2}\left(\xi'\right)^2 = 0 \tag{3.10}$$

Overdots and primes stand for partial differentiation with respect to the time and the radial coordinate, respectively. McVittie established a line element from (3.9) and (3.10). Using our notation, this interval can be written in the form:

$$ds^2 = \left[\frac{1 - \frac{k_0}{2a\left(\bar{t}\right)\overline{q}}\left(1 + \frac{\overline{q}^2}{4R^2}\right)^{\frac{1}{2}}}{1 + \frac{k_0}{2a\left(\bar{t}\right)\overline{q}}\left(1 + \frac{\overline{q}^2}{4R^2}\right)^{\frac{1}{2}}}\right]^2 c^2 d\bar{t}^2 - a^2\left(\bar{t}\right)\frac{\left[1 + \frac{k_0}{2a\left(\bar{t}\right)\overline{q}}\left(1 + \frac{\overline{q}^2}{4R^2}\right)^{\frac{1}{2}}\right]^4}{\left(1 + \frac{\overline{q}^2}{4R^2}\right)^2} d\sigma^2$$

k_0 is a constant of integration, which is set to $k_0 = r_g/2$ in the following. If the spatial curvature of the space is supposed to be zero, i.e. for $R = \infty$, McVittie's interval reads:

$$ds^2 = \left[\frac{1 - \frac{r_g}{4a\left(\bar{t}\right)\overline{q}}}{1 + \frac{r_g}{4a\left(\bar{t}\right)\overline{q}}}\right]^2 c^2 d\bar{t}^2 - a^2\left(\bar{t}\right)\left[1 + \frac{r_g}{4a\left(\bar{t}\right)\overline{q}}\right]^4 d\sigma^2 \tag{3.11}$$

The latter interval reduces to the Schwarzschild solution (3.5) for $a\left(\bar{t}\right) = 1$. For large $\overline{q}$, interval (3.11) approximates the de Sitter class (3.7).

In part IV of his article [79], McVittie analyzed planetary orbits. His investigations were based on the assumption that planets move on geodesic lines of the spacetime given by (3.11). Due to the spherical symmetry of the system, it is sufficient to deal with movements in the $\theta = \frac{\pi}{2}$ plane. McVittie established an equation of motion, which in our notation reads:

$$\frac{1}{\overline{q}^2}\frac{d\overline{q}}{d\bar{t}} = -\frac{\dot{a}\left(\bar{t}\right)r_g}{2h^2}\left(1 + \epsilon\cos\phi\right)$$

This equation describes the movement of a planet that "*has a period short compared with the rate of change of* β $[\beta = 2 \ln a]$ *and moves with a velocity small compared with that of light* [...]" [79]. ϵ is the eccentricity of the orbit and $h \in \mathbb{R}$ is a constant of integration. A gravitationally bound system, like a planet orbiting a star, does not take part in the general expansion of the universe. Accordingly, in the comoving coordinate system the orbit should shrink in size: "*from the point of view of cosmical coordinates* [comoving system]*, the configuration of the nebulae is unchanging, but the mass particle*[48] *and its planetary system perpetually shrink in size.*" [79]. From the observer's point of view the orbit is given by

$$\frac{1}{q} = \frac{r_g}{2h^2} \left(1 + \epsilon \cos \phi\right)$$

where r_g is the gravitational radius of the central mass particle which is embedded in the cosmological background. In the static coordinate system, the orbit of the planet does not vary in size, but e.g. the distance of remote galaxies increases with time. "[...] *for the observer* [static coordinate system]*, the orbit of the planet and the mass of the central particle remain fixed, whilst the system of nebulae increases in size.*" [79].

Part V of the article [79], McVittie pointed out that the requirement of non-negative density and pressure gives a lower limit for the cosmological constant: "[...] *our observer would necessarily take* $[\Lambda]$ *to be a positive constant.*" [79].

As previously mentioned, McVittie assumed that there is no flow of cosmic matter towards or away from the coordinate origin. But what we observe (in our real universe) is the following: Surrounding matter falls towards the central body under the influence of gravity. Far away from its gravitational influence, cosmic material moves along with the Hubble flow. 2010 Kaloper, Kleban and Martin noticed in [65] that the lack of accretion is "*an odd property for a physical black hole in a universe full of matter or radiation.*" Another point is the following: If the density ρ depends on the time, the pressure p will not longer be homogeneous, cf. for example [61]. We establish the general relation of pressure and density in a McVittie model with nonzero cosmological constant in section 4, see equation (4.7). Faraoni and Jacques remarked in [40]: "*However, in general, the* [McVittie] *metric can not be interpreted as describing a black hole embedded in a FLRW universe* [...]". The central mass in McVittie's model is surrounded by a spacelike singularity, which is difficult to interpret: Except for a model with de Sitter background, the pressure diverges at $\overline{q} = r_g / (4a)$.

[48] The central star of a planetary system, for example our Sun.

3.2. **A. Einstein and E. G. Straus 1945.**
Einstein and Straus proposed a model where the central body is surrounded by a static, spherical, void region, embedded in an expanding cosmological background. The central body consists of the material that was initially spread evenly in the present void region. The goal is to fit together the stationary gravitational field, which is generated by a single mass like a star or a black hole, with an expanding (and thus time dependent) cosmological model. Einstein and Straus proved in [37] that such a solution exists, but they did not give an explicit solution for the problem they posed.

Schwarzschild's (stationary) field goes over asymptotically into the flat Minkowskian space. Since we know that real space is expanding, these boundary conditions are not valid for a real star. In the model proposed by Einstein and Straus, there is still a delimited static neighborhood of the central mass where the expansion of space has no effect. The continuum is divided into two parts. One of these parts is the region where the central mass at $x_1 = x_2 = x_3 = 0$ generates a static field. Outside the singularity the field shall satisfy the empty space equations $R_{ik} = 0$. The other part is the region where the field is based on the cosmological solutions of Einstein's equations for a pressure free, spatially constant density of matter. At a given radius (*"Region G"* [37]) the static field shall pass continuously into the field of the expanding spacetime. "*At this passage the g_{ik} and their first derivates shall remain continuous.*" [37]. Einstein and Straus started with a general centrally-symmetric field. In our notation the corresponding line element can be written as

$$ds^2 = c^2 e^{\xi} dt^2 - e^{\mu} \delta_{ik} dx_i dx_k \qquad i,k = 1,2,3 \tag{3.12}$$

where μ and ξ are functions of the time t and the radial coordinate q. Based on the metric (3.12) they established "*Field Equations for the Interior of the Region G*" [37]. For the outer region "*the remaining space with homogeneous distribution of matter is a field of constant spatial curvature"* [37]:

$$ds^2 = c^2 d\bar{t}^2 - \frac{T^2\left(\bar{t}\right)}{\left[1 + \frac{z}{4}\left(\overline{x}_1^2 + \overline{x}_2^2 + \overline{x}_3^2\right)\right]^2} \delta_{ik} d\overline{x}_i d\overline{x}_k \tag{3.13}$$

T is a function of $\bar{t}$ alone and z determines the spatial curvature: "*The spherical case corresponds to $z = 1$, the pseudo-spherical to $z = -1$, the spatially plane case to $z = 0$.*" [37]. In case of $z = 0$, the interval (3.13) reduces to

$$ds^2 = c^2 d\bar{t}^2 - T^2\left(\bar{t}\right) \delta_{ik} d\overline{x}_i d\overline{x}_k.$$

Obviously, T represents the scale factor, cf. equation (3.4). The gravitational field given by (3.12) shall go over continuously up to the first derivative[49] into the field (3.13). "*These boundary conditions are always sufficient, but not always necessary,* [...]" [37]. Einstein and Straus established equations from these boundary conditions and studied their first order approximation. They proved that the interior solution is entirely static and that in the first approximation it is identical to Schwarzschild's solution. "*The time dependence implied by the expansion does not make the* [interior] *solution time-dependent. What becomes time-dependent is the boundary of G where the Schwarzschild field goes over into the field generated by homogeneously distributed matter.*" [37].

Schücking resumed the work of Einstein and Straus. He presented in [105] a modification of Schwarzschild's field (2.29) to describe the interior region of the Einstein-Straus model, so that the time coordinate of the interior field is matched to the cosmological time. Schücking's solution[50] is equal to Schwarzschild's metric (2.29) except for the g_{00} component, which is multiplied by a correction term: The interior gravitational field is given by

$$ds^2 = \frac{1 - R_0^2 K}{\left(1 - \frac{r_g}{a(t) R_0}\right)^2} \left(1 - \frac{r_g}{r}\right) c^2 dt^2 - \frac{1}{1 - \frac{r_g}{r}} dr^2 - r^2 d\theta^2 - r^2 \sin^2\theta \, d\phi^2 \tag{3.14}$$

where R_0 is the radius of the vacuole and $K \in \{-1; 0; 1\}$ represents the spatial curvature of the exterior cosmological model (outside the vacuole). Schücking pointed out, that transforming his solution into a static form leads to mismatching of the time scales.

Schücking as well as Einstein and Straus did not take into account a nonzero cosmological constant. In 1988, Balbinot, Bergamini and Comastri extended the matching proposed by Schücking in case of a nonzero cosmological constant, see [5]. Several other articles are based on the model first proposed by Einstein and Straus, and the name 'Swiss Cheese model' was coined, cf. for example [23].

Naturally, the vacuole radius is related to the enclosed mass. Carrera and Giulini remarked in [20] that the vacuole radius corresponding to a single solar mass is "*almost two orders of magnitude larger than the average distance of stars in our Galaxy*". Hence, this model "*cannot provide a realistic model for the environment of small structures in our Universe*" [20].

---

[49] The question remains whether the chosen boundary conditions are too strong. Conceivably, the postulation of continuous first derivatives at the boundary can be dropped.

[50] See equation (34) in [105].

3.3. **P. D. Noerdlinger and V. Petrosian 1971.**

In their article "*The effect of cosmological expansion on self-gravitating ensembles of particles*" [83], Noerdlinger and Petrosian considered "*the possible expansion of clusters or superclusters of galaxies* [...]*, immersed in a universe containing a gas of particles having zero rest mass and having energy density* ρc^2." This paper does not take into account the cosmological constant. It was shown that the clusters or superclusters expand with the universe, if their rest-mass density ρ_c is smaller than ρ, and that the expansion is reduced in the ratio ρ/ρ_c if $\rho_c \gg \rho$. The authors predicted a small expansion of gravitationally bound systems like galaxy clusters or superclusters, if the energy density $\rho_c c^2$ exceeds the energy density ρc^2 of the particles with zero rest mass. This small expansion can be described by an equivalent 'Hubble' constant $J_0 = 4\epsilon H_0$, where $\epsilon = \rho/\rho_c$. Noerdlinger and Petrosian remarked that these effects are completely negligible for other bound systems like a galaxy or a planetary system. Section II of [83] contains Newtonian considerations, concerning the problem of point condensation and the cosmic substratum. The Newtonian potential $\psi_N = -\gamma M r^{-1} + \frac{2}{3}\pi\gamma\rho r^2$ for a point condensation at the center leads to

$$\frac{d^2 r}{dt^2} + \gamma M r^{-2} - L^2 r^{-3} = -\frac{8\pi\gamma}{3} r\rho\left(t\right) \tag{3.15}$$

where L is the angular momentum per unit mass and γ the gravitational constant. By averaging the latter equation of motion, Noerdlinger and Petrosian established the above mentioned relation for the 'Hubble-like expansion' of bound systems. In order to support their Newtonian considerations, the authors studied a general-relativistic model, cf. section III in [83]. In our notation, the corresponding line element reads

$$ds^2 = \left(1 - \frac{r_g}{\overline{q}a\left(\bar{t}\right)}\right) c^2 d\bar{t}^2 - \left(1 + \frac{r_g}{\overline{q}a\left(\bar{t}\right)}\right) a^2\left(\bar{t}\right) d\sigma^2 \tag{3.16}$$

where $r_g = 2\gamma M/c^2$ is the gravitational radius of the mass M. For $M = 0$, interval (3.16) reduces to the spatially flat FLRW metric. If $M \neq 0$ and $a\left(t\right)$ is a constant, say $a\left(t\right) \equiv 1$, the line element (3.16) reduces to:

$$ds^2 = \left(1 - \frac{r_g}{q}\right) c^2 d\bar{t}^2 - \left(1 + \frac{r_g}{q}\right) d\sigma^2 \tag{3.17}$$

Consider Schwarzschild's isotropic solution (3.5). It is[51]

$$\left(\frac{1 - \frac{r_g}{4q}}{1 + \frac{r_g}{4q}}\right)^2 = 1 - \frac{r_g}{q} + \mathcal{O}\left(\left[\frac{r_g}{4q}\right]^2\right) \text{ and } \left(1 + \frac{r_g}{4q}\right)^4 = 1 + \frac{r_g}{q} + \mathcal{O}\left(\left[\frac{r_g}{4q}\right]^2\right).$$

[51] With $(1+x)^m = 1 + mx + \mathcal{O}\left(x^2\right)$ we get $\left(\frac{1-x}{1+x}\right)^2 = \left(1-x\right)^2\left(1+x\right)^{-2} = 1 - 4x + \mathcal{O}\left(x^2\right)$

Accordingly, (3.17) is the first order approximation of Schwarzschild's isotropic solution (3.5), i.e. it represents the static gravitational field of a point mass.

Noerdlinger and Petrosian remarked that metric (3.16) will not be valid for a dust-filled universe, since the conditions (spatially isotropic coordinates comoving with the cosmic fluid, so T^{ik} diagonal, $a(t)$ independent of space coordinates) are too restrictive. But if the universe is filled with particles of zero rest mass ($p = \frac{1}{3}\rho c^2$), the metric is valid approximately, and one can determine the sizes of Keplerian orbits to first order in $\alpha = \frac{r_g}{2\overline{q}a(t)}$. Moreover, Noerdlinger and Petrosian introduced a modified ansatz, including higher-order terms, which could be used to study effects like the advance of perihelion. A consideration of geodesic equations for the general-relativistic model again results in (3.15), if terms of order $(v/c)^2$, the pressure and the cosmological constant are neglected. If the pressure is non-negligible, the equation of motion (3.15) includes a $3p/c^2$ correction term. It was shown in [83] that "*in low-pressure cosmologies clusters of galaxies, etc., do not expand, while in high-pressure, high-density models there would have been an epoch when the cosmologic density was nearly that in the clusters, in which case clusters would have been forced to expand and hardly seem able to have formed at all.*" Noerdlinger and Petrosian concluded that it "*seems unlikely that clusters of galaxies could have formed prior to the epoch corresponding to the redshift* $z \approx 2$" [83]. On the other hand, L. Pentericci et al. found galaxies at redshift ~ 7 in 2011, see [92].

3.4. **M. Israelit and N. Rosen 1992.**
In [61], Israelit and Rosen considered a $\Lambda = 0$ universe and presented a solution of Einstein's field equations "*for the case of a massive particle at rest in a universe which without the particle would be homogeneous, isotropic and spatially flat.*" In our notation, their ansatz for a spatially flat and spherically symmetric universe is given by

$$ds^2 = e^{\xi} c^2 d\bar{t}^2 - e^{\mu} d\sigma^2 \tag{3.18}$$

where ξ and μ depend on the time $\bar{t}$ and the radial coordinate $\bar{q}$. At first, Israelit and Rosen set up Einstein's equations[52] for (3.18) in case that "*the universe is filled with matter characterized by a density $\rho(t,r)$ and a pressure $p(t,r)$*" [61]. Accordingly, in our notation, the stress-energy-momentum tensor is given by

$$T_t^t = c^2\rho; \quad T_r^r = T_\theta^\theta = T_\phi^\phi = -p; \quad \text{and} \quad T_k^i = 0 \text{ for } i \neq k$$

and the equations read:

$$\frac{3\dot{\mu}^2 e^{-\xi}}{4c^2} - e^{-\mu}\left(\mu'' + \frac{1}{4}\mu'^2 + \frac{2}{\bar{q}}\mu'\right) = \frac{8\pi\gamma}{c^2}\rho \tag{3.19}$$

$$e^{-\mu}\left(\dot{\mu}' - \frac{1}{2}\dot{\mu}\xi'\right) = 0 \tag{3.20}$$

$$\frac{e^{-\xi}}{c^2}\left(\ddot{\mu} + \frac{3}{4}\dot{\mu}^2 - \frac{1}{2}\dot{\mu}\dot{\xi}\right) - e^{-\mu}\left(\frac{\mu'\xi'}{2} + \frac{\mu'^2}{4} + \frac{\mu'+\xi'}{\bar{q}}\right) = -\frac{8\pi\gamma}{c^4}p \tag{3.21}$$

$$\frac{e^{-\xi}}{c^2}\left(\ddot{\mu} + \frac{3}{4}\dot{\mu}^2 - \frac{1}{2}\dot{\mu}\dot{\xi}\right) - e^{-\mu}\left(\frac{\mu''+\xi''}{2} + \frac{\xi'^2}{4} + \frac{\mu'+\xi'}{2\bar{q}}\right) = -\frac{8\pi\gamma}{c^4}p \tag{3.22}$$

Overdots and primes stand for partial differentiation with respect to t and $\bar{q}$, respectively. Next, Israelit and Rosen considered two special cases: A homogeneous, isotropic (and spatially flat) universe without mass particle, which they called the 'unperturbed case'. The second one was called 'perturbed case', since it additionally contains a point mass at the origin.

In the unperturbed case, density and pressure only depend on the time coordinate. Israelit and Rosen used $\xi = 0$ and $e^{\mu} = a^2\left(\bar{t}\right)$ in (3.18) and the density $\rho = \rho_0(t)$ and pressure $p = p_0(t)$ to model the (unperturbed) homogeneous, isotropic universe without mass particle. Consequently, the above equations reduce to Friedmann's

[52] Israelit and Rosen used units with $c = \gamma = 1$, where c is the speed of light and γ the gravitational constant. Further, they used another convention where $G_k^i = -8\pi T_k^i$.

equations:

$$\left(\frac{\dot{a}}{a}\right)^2 = \frac{8\pi}{3}\rho_0 \quad \text{and} \quad 2\frac{\ddot{a}}{a} + \left(\frac{\dot{a}}{a}\right)^2 = -8\pi p_0$$

In the perturbed case, Israelit and Rosen assumed that the density remains the same as in the unperturbed case. They established a set of equations wherein time and space are decoupled. In our notation, this set is given by:

$$\begin{aligned} \dot{\mu}' - \frac{1}{2}\dot{\mu}\xi' &= 0 \\ \mu'' + \frac{1}{4}\mu'^2 + \frac{2\mu'}{\overline{q}} &= 0 \\ \mu'' + \xi'' - \frac{1}{2}\mu'^2 + \frac{1}{2}\xi'^2 - \mu'\xi' - \frac{\mu' + \xi'}{\overline{q}} &= 0 \end{aligned}$$

Israelit and Rosen obtained the solution

$$e^{\mu} = \left[\frac{1 - \frac{m_0}{2a(\bar{t})\overline{q}}}{1 + \frac{m_0}{2a(\bar{t})\overline{q}}}\right]^2 \quad \text{and} \quad e^{\xi} = a^2\left(\bar{t}\right)\left(1 + \frac{m_0}{2a\left(\bar{t}\right)\overline{q}}\right)^4. \tag{3.23}$$

which is similar to the solution (3.11) found by McVittie in 1933. A gravitating mass is located at the coordinate origin. The parameter m_0 can be interpreted as the fixed mass of the gravitating body. Since Israelit and Rosen used units with $c = \gamma = 1$, the gravitational radius is $r_g = 2m_0$ and the interval (3.23) equals McVittie's line element (3.11).

Moreover, Israelit and Rosen studied the influence of the mass point on the pressure of the cosmic background. As mentioned above, the density in the perturbed model is set to be the same as in the unperturbed case, $\rho = \rho_0(t)$. Israelit and Rosen noticed that the presence of the central mass changes the pressure of the cosmic matter. "[...] *for the pressure must provide a force to balance the gravitational field of the* [mass] *particle.*"[61]. In the perturbed case, the pressure is no longer homogeneous. Instead of $p = p_0(t)$, they found:

$$p = p_0 + \frac{2m}{2\overline{q} - m}\left(p_0 + \rho_0\right) \tag{3.24}$$

McVittie's article [79] did not handle this problem.

McVittie investigated the motion of a test particle based on his metric (3.11). Israelit and Rosen, who found the identical interval (3.23), likewise studied the motion of a test particle. But they derived the geodesic equations for the line

element[53]

$$ds^2 = \left(1 - \frac{2m}{\overline{q}}\right) dt^2 - a^2\left(\overline{t}\right) \left(1 + \frac{2m}{\overline{q}}\right) \left(d\overline{x}^2 + d\overline{y}^2 + d\overline{z}^2\right) \tag{3.25}$$

which represents the approximation of (3.23) to the first order in m/r for $m/r \ll 1$. It is[54]:

$$\left(\frac{1 - \frac{m}{2\overline{q}}}{1 + \frac{m}{2\overline{q}}}\right)^2 = 1 - \frac{2m}{\overline{q}} + \mathcal{O}\left(\left[\frac{2m}{\overline{q}}\right]^2\right) \text{ and } \left(1 + \frac{2m}{\overline{q}}\right)^4 = 1 + \frac{2m}{\overline{q}} + \mathcal{O}\left(\left[\frac{2m}{\overline{q}}\right]^2\right)$$

Notice, that Noerdlinger and Petrosian used a similar approximation in [83]. Based on their results, Israelit and Rosen proposed "*that one has motion under an attractive force that is the sum of the Newtonian force plus a force arising from the deceleration of the universe expansion.*" [61].

In 1996 Israelit and Rosen published another article concerning "*the internal structure and the metric of a spherically symmetric mass in an FRW universe*" [62], in which they presented the same result (3.23) for the gravitational field outside the mass. In both articles [61] and [62], Israelit and Rosen considered cosmological backgrounds without cosmological constant. According to recent WMAP data [63], our universe is made up of over 70% dark energy, which can be modeled with a nonzero cosmological constant.

---

[53] Obviously, it is $\overline{q} = \sqrt{\overline{x}^2 + \overline{y}^2 + \overline{z}^2}$ in (3.25).

[54] With $(1+x)^m = 1 + mx + \mathcal{O}\left(x^2\right)$ we get $\left(\frac{1-x}{1+x}\right)^2 = (1-x)^2 (1+x)^{-2} = 1 - 4x + \mathcal{O}\left(x^2\right)$

3.5. **P. J. E. Peebles 1993.**
Among other things, Peebles studied in his book [91] a $\Lambda = 0$ Swiss Cheese model, i.e. the embedding of a Schwarzschild mass into a $\Lambda = 0$ cosmological model. Expanding cosmological models, which contain at least one static region are commonly called Swiss-Cheese model, cf. for example [23]. "*Birkhoff's theorem tells us that in a homogeneous zero-pressure cosmological model we can evacuate a spherical region and replace the material with a compact mass $\mathcal{M}$ at the center, without affecting spacetime outside the region.*" Peebles presented a method to *"find the relation between the mass $\mathcal{M}$ and the rest mass evacuated from the cavity in this compensated rearrangement of the mass distribution.*" [91].

The Idea for the Swiss Cheese model was first proposed by Einstein and Straus [37], who proved the existence of such a solution. An explicit solution was first given by Schücking [105]: He modified the g_{00} component of Schwarzschild's metric (2.29) in order to match the time coordinate of the interior field to the cosmological time, cf. equation (3.14) in section 3.2. Schücking noted in [105], that his interior solution (3.14) can be transformed into Schwarzschild's metric (2.29). As Carrera and Guilini pointed out, "*the matched solution is really such that for radii smaller than a certain matching radius* [...] *it is exactly given by the Schwarzschild solution (exterior for a black hole, exterior plus interior for a star) and for radii above this radius it is exactly given by a FLRW universe for dust matter without cosmological constant.*" [20].

Peebles determined the mass $\mathcal{M}'$ of the evacuated matter and the mass $\mathcal{M}$ of the compact mass condensation (which replaced the evacuated material of a cosmological model with generic spatial curvature) by directly matching time and radial coordinate of Schwarzschild's metric (2.29) and the FLRW metric (2.1):

Provided that there is no cosmological constant, space-time inside the cavity is described by Schwarzschild's line element

$$ds^2 = \left(1 - \frac{r_g}{r}\right) c^2 dt^2 - \frac{dr^2}{1 - r_g/r} - r^2 d\Omega_2 \tag{3.26}$$

and outside the cavity by the FLRW line element, which in our notation (2.1) reads:

$$ds^2 = c^2 d\bar{t}^2 - a^2\left(\bar{t}\right)\left(\frac{d\bar{r}^2}{1 - K\bar{r}^2} + \bar{r}^2 d\Omega_2\right). \tag{3.27}$$

K determines the spatial curvature of the FLRW background. The sphere with fixed comoving radius $\overline{R}$ represents the edge of the cavity with respect to the coordinates

(3.27). $R(t)$ represents the radius of that sphere[55] with respect to (3.26). Since the circumference of the cavity has to be the same measured either way, it applies $2\pi R(t) = 2\pi a(\bar{t})\,\overline{R}$ and therefore $R(t) = a(\bar{t})\,\overline{R}$. The latter equation leads to[56]:

$$\frac{1}{a}\frac{da}{d\bar{t}} = \frac{1}{R}\frac{dR}{dt}\cdot\frac{dt}{d\bar{t}} \tag{3.28}$$

For an observer at rest at the edge of the cavity holds $ds^2 = c^2 d\bar{t}^2$, so that

$$c^2 d\bar{t}^2 = ds^2 = \left[c^2\left(1-\frac{r_g}{R}\right) - \left(1-\frac{r_g}{R}\right)^{-1}\left(\frac{dR}{dt}\right)^2\right]dt^2. \tag{3.29}$$

With the $i = 0$ component of the geodesic equation for the observer, which is[57]

$$\left(1-\frac{r_g}{r}\right)\frac{dt}{ds} = 1/\sqrt{E} \tag{3.30}$$

the result of eliminating $\frac{dt}{ds}$ in (3.29) is:

$$\frac{dR}{dt} = \left(1-\frac{r_g}{R}\right)\left[c^2 - E\left(1-\frac{r_g}{R}\right)\right]^{\frac{1}{2}} \tag{3.31}$$

With $ds^2 = c^2 d\bar{t}^2$ equation (3.30) gives $\left(\frac{dt}{d\bar{t}}\right)^2 = \frac{c^2}{E}\left(1-\frac{r_g}{r}\right)^{-2}$. Together with (3.31) and $R(t) = a(\bar{t})\,\overline{R}$, equation (3.28) leads to

$$\left(\frac{1}{a}\frac{da}{d\bar{t}}\right)^2 = \frac{c^2 r_g}{\left(a\overline{R}\right)^3} + \frac{c^2\left(\frac{c^2}{E}-1\right)}{\left(a\overline{R}\right)^2}. \tag{3.32}$$

On the other hand, Friedmann's equation (2.4) in a homogeneous cosmological model gives

$$\left(\frac{1}{a}\frac{da}{d\bar{t}}\right)^2 = \frac{8\pi\gamma}{3}\rho - \frac{Kc^2}{a^2}. \tag{3.33}$$

Comparing equations (3.32) and (3.33), one obtains

$$\mathcal{M} = \frac{4}{3}\pi\rho\left(a\overline{R}\right)^3 \text{ and } K = \frac{1}{\overline{R}^2}\left(1-\frac{c^2}{E}\right)$$

which "*fixes the value of the compact mass $\mathcal{M}$ that has replaced what has been evacuated from the homogeneous solution to make the void.*" [91]. The mass of the evacuated matter amounts to

$$\mathcal{M}' = 4\pi\rho a^3\int_0^{\overline{R}}\frac{\bar{r}^2 d\bar{r}}{\sqrt{1-K\bar{r}^2}}. \tag{3.34}$$

---

[55]Peebles used the notation $\bar{r}_e$ and $r_e(t)$ for the radius of that sphere in [91]. He further used $1/R^2$ to describe the spatial curvature of the FLRW background, which is in our notation represented by K.

[56]From $a(\bar{t}) = \frac{R(t)}{\overline{R}}$ we get $\frac{da}{d\bar{t}} = \frac{dR}{\overline{R}dt}\frac{dt}{d\bar{t}}$ and therefore (3.28).

[57]This condition corresponds to the conservation of energy, $1/\sqrt{E}$ is a constant. For more details see lemma 14.

For $R = \infty$ the integral equation (3.34) reduces to $\mathcal{M}' = \frac{4}{3}\pi\rho a^3 \overline{R}^3$, which agrees with the value for the compact mass $\mathcal{M}$. Hence, in a cosmologically flat model it is $\mathcal{M}' = \mathcal{M}$, in a closed model $\mathcal{M}' > \mathcal{M}$. Peebles concluded in [91]: "*In an informal way of describing this, the net gravitational mass* $\mathcal{M}$ *seen by an observer at* $\bar{r}_e$ [in our notation $\overline{R}$] *in the homogeneous case is the sum of the rest mass* $\mathcal{M}'$ *within* $\bar{r}_e$ [in our notation $\overline{R}$]*, the positive kinetic energy of expansion, and the negative gravitational potential energy of the smoothly distributed matter.*"

The preceding considerations are based on $\Lambda = 0$. Contemporary measurements indicate that a nonzero cosmological constant has to be taken into consideration. In section 7, we extend the above method to establish a differential equation for the matching radius R in a ΛCDM Swiss Cheese model.

3.6. **N. Kaloper, M. Kleban and D. Martin 2010.**
In their article "*McVittie's Legacy: Black Holes in an Expanding Universe*" [65], the authors proved that the McVittie class of solutions includes regular black holes embedded in Friedmann–Lemaître–Robertson–Walker (FLRW) cosmologies. The article is concerned with the spatially flat McVittie metric, which is characterized by the mass of the central point mass and the scale factor $a(t)$ of the FLRW background. In our notation, the metric reads

$$ds^2 = -\left(\frac{1-u}{1+u}\right)^2 dt^2 + (1+u)^4 a^2(t)\, d\vec{x}^2, \qquad u = \frac{r_g}{4a(t)\,|\vec{x}|} \tag{3.35}$$

where $\vec{x} = 0$ is the center of the spherical symmetry. The interval (3.35) is an exact solution of Einstein's equations if

$$H^2 = \frac{8\pi\gamma}{3}\rho(t)\,, \text{ where } H := \frac{\dot{a}(t)}{a(t)}. \tag{3.36}$$

ρ is the energy density, and the overdot denotes differentiation with respect to the time coordinate. Obviously, the cosmological background is either entirely filled with a homogeneous fluid (whose energy density is ρ) or it is empty ($\rho = 0$). For generic expanding FLRW background, McVittie's model (3.35) has a curvature singularity at $u = 1$, corresponding to $\overline{q} = r_g/(4a)$ in (3.11). This "*can be seen by evaluating e.g. the Ricci scalar*" [65], which is:

$$R = 12H^2 + 6\frac{1+u}{1-u}\dot{H} \tag{3.37}$$

On fixed $t-$slices, the pressure p is given by

$$p = \frac{1}{8\pi\gamma}\left(-3H^2 - 2\frac{1+u}{1-u}\dot{H}\right). \tag{3.38}$$

Except in the case of $\dot{H} = 0$ (pure cosmological constant), the pressure (3.38) is inhomogeneous and diverges together with the Ricci scalar at the hypersurface $u = 1$. Kaloper, Kleban and Martin proposed, that "*the McVittie solution should be thought of as a special case of a larger class of geometries describing masses in FRW: McVittie is the special class where the mass parameter is a constant and the energy density is homogeneous, and its inhomogeneous pressure is the necessary and sufficient price one pays for these features.*" [65].

The authors showed, that the black hole interpretation of McVittie's metric (3.35) is valid if "*the McVittie scale factor asymptotes to de Sitter space*" [65]. Apparently, the expression $(1+u)^2 a(t)$ is what Kaloper, Kleban and Martin called the McVittie scale factor, see metric (3.35). In other words, the black hole interpretation is valid if the cosmological background is a de Sitter model, see section 2.4. In this case

one has $\dot{H} = \frac{d}{dt}\left[\dot{a}/a\right] = 0$, cf. equation (2.20). As a consequence of $\dot{H} = 0$, density and pressure are constant, see (3.36) and (3.38).

In order to confirm the black hole interpretation, Kaloper, Kleban and Martin studied several features[58] of the McVittie model. We will not discuss all details of their work, but the section "Coordinate Covers" of [65] is most interesting for our purpose. It is concerned with a transformation of McVittie's interval (3.35). The result of this transformation is a line element, which in case of H =constant, represents the Schwarzschild-de Sitter metric "*in coordinates which are analogous to outgoing Eddington-Finkelstein coordinates for a flat space Schwarzschild black hole.*" [65].

It is well known, that McVittie's metric reduces to the FLRW space-time if the mass, and with that the gravitational radius r_g, is taken to be zero. Provided $r_g \neq 0$, it reduces to the Schwarzschild solution if $a\left(t\right)$ =constant, i.e. in case of $H = 0$. Kaloper, Kleban and Martin remarked that (3.35) reduces to the Schwarzschild-de Sitter case if H is a nonzero constant[59]. They introduce the new radial coordinate

$$\vec{r} = \left(1+u\right)^2 a\left(t\right)\vec{x} \tag{3.39}$$

further $r = |\vec{r}| = \left(1+u\right)^2 a\left(t\right)|\vec{x}|$, which is the spherical area coordinate. Equation (3.39) implies the relation

$$a\left(t\right)|\vec{x}| = \frac{r_g}{4}\left(\frac{2r}{r_g} - 1 \pm \sqrt{\left(\frac{2r}{r_g}-1\right)^2 - 1}\right)^{-1}. \tag{3.40}$$

The authors claimed that McVittie's metric (3.35) transforms to a metric, which in our notation reads:

$$ds^2 = -\left(1 - \frac{r_g}{r} - H^2 r^2\right)dt^2 - \frac{2Hr}{\sqrt{1-r_g/r}}drdt + \frac{dr^2}{1-r_g/r} + r^2 d\Omega_2 \tag{3.41}$$

Their article [65] does not contain the corresponding calculations. In the following we show how to obtain (3.41) by coordinate transformation, which is not quite trivial.

---

[58] There is "*a null or spacelike FRW future infinity at large radial distance r and late time t, [...] a surface $r = r_-, t = \infty$ which is null and at finite affine distance along ingoing null geodesics from any point in the bulk; this null surface is a soft, null naked singularity in an FRW spacetime if the FRW Hubble constant $H\left(t\right) = \dot{a}\left(t\right)/a\left(t\right)$ goes to zero at late times; the addition of any positive cosmological constant (so that $\lim_{t\to\infty} H\left(t\right) \equiv H_0 > 0$) eliminates this singularity; all curvature invariants on the null surface in this case are exactly equal to their values on the horizon of a Schwarzschild-de Sitter black hole of mass m and Hubble constant $H_0 > 0$; therefore, at least in the case $H_0 > 0$ the McVittie metric describes a regular (on the horizon) black hole embedded in an FRW spacetime.*" [65].

[59] As it is in case of a de Sitter background, cf. (2.20). It is $H \neq 0$ and $\dot{H} = 0$.

3.6.1. ***Transformation of McVittie's metric.***
Our goal is to transform (3.35) into (3.41). At first we have to establish (3.40) from (3.39). From $u = \frac{r_g}{4a(t)|\vec{x}|}$ together with $r = (1+u)^2 a(t) |\vec{x}|$ we get $u = \frac{r_g}{4r}(1+u)^2$ and thus the quadratic equation:

$$u^2 + 2\left(1 - \frac{2r}{r_g}\right)u + 1 = 0 \tag{3.42}$$

The solution of (3.42) is given by

$$u = \frac{2r}{r_g} - 1 \pm \sqrt{\left(1 - \frac{2r}{r_g}\right)^2 - 1} \tag{3.43}$$

and $a(t)|\vec{x}| = \frac{r_g}{4u}$ leads to the term (3.40). Notice, that (3.40) can be rewritten by

$$\begin{aligned} a(t)|\vec{x}| &= \frac{\frac{r_g}{4}}{\frac{2r}{r_g} - 1 \pm \sqrt{\left(\frac{2r}{r_g} - 1\right)^2 - 1}} \cdot \frac{\frac{2r}{r_g} - 1 \mp \sqrt{\left(\frac{2r}{r_g} - 1\right)^2 - 1}}{\frac{2r}{r_g} - 1 \mp \sqrt{\left(\frac{2r}{r_g} - 1\right)^2 - 1}} \\ &= \frac{r_g}{4}\left(\frac{2r}{r_g} - 1 \mp \sqrt{\left(\frac{2r}{r_g} - 1\right)^2 - 1}\right) = \frac{r_g}{4}\left(\frac{2r}{r_g} - 1 \mp \sqrt{\frac{4r^2}{r_g^2} - \frac{4r}{r_g}}\right). \end{aligned}$$

Now we transform the $(1-u)/(1+u)$ term with the help of (3.43):

$$\begin{aligned} \frac{1-u}{1+u} &= \frac{2 - \left(\frac{2r}{r_g} \pm \sqrt{\frac{4r^2}{r_g^2} - \frac{4r}{r_g}}\right)}{\frac{2r}{r_g} \pm \sqrt{\frac{4r^2}{r_g^2} - \frac{4r}{r_g}}} \cdot \frac{\frac{2r}{r_g} \mp \sqrt{\frac{4r^2}{r_g^2} - \frac{4r}{r_g}}}{\frac{2r}{r_g} \mp \sqrt{\frac{4r^2}{r_g^2} - \frac{4r}{r_g}}} \\ &= \frac{2\left(\frac{2r}{r_g} \mp \sqrt{\frac{4r^2}{r_g^2} - \frac{4r}{r_g}}\right) - \frac{4r}{r_g}}{\frac{4r}{r_g}} = \mp\frac{r_g}{2r}\sqrt{\frac{4r^2}{r_g^2} - \frac{4r}{r_g}} = \mp\sqrt{1 - \frac{r_g}{r}} \end{aligned}$$

From this we get

$$\left(\frac{1-u}{1+u}\right)^2 = 1 - \frac{r_g}{r}. \tag{3.44}$$

Now we transform the $(1+u)^4 a^2(t)\, d\vec{x}^2$ term. Let us use the notations

$$x := |\vec{x}| \text{ and } a = a(t).$$

It is important to notice that $dx^2 = d|\vec{x}|^2 \neq d\vec{x}^2$. The following lemma shows how to deal with $d\vec{x}$ and $d|\vec{x}|$.

Lemma 5.
Let $n \in \mathbb{N}$ and $\vec{x} \in \mathbb{R}^n$. One has

$$x dx = |\vec{x}|\, d\,|\vec{x}| = \vec{x} \circ d\vec{x} \tag{3.45}$$

where '$\circ$' denotes the scalar product and $x = |\vec{x}| := \sqrt{\vec{x} \circ \vec{x}}$.

Proof. On the one hand we have $d\left[|\vec{x}|^2\right] = 2\,|\vec{x}|\, d\,|\vec{x}|$, and on the other hand $d\,[\vec{x} \circ \vec{x}] = 2\vec{x} \circ d\vec{x}$. From $|\vec{x}|^2 = \vec{x} \circ \vec{x}$ we get (3.45). □

Equation (3.39) gives $\vec{x} = (1+u)^{-2}\, a^{-1}\vec{r}$ and thus

$$d\vec{x} = -\frac{2\,du}{a\,(1+u)^3}\vec{r} - \frac{\dot{a}\,dt}{a^2\,(1+u)^2}\vec{r} + \frac{1}{a\,(1+u)^2}d\vec{r}.$$

Multiplication by $a\,(1+u)^2$ yields

$$a\,(1+u)^2\, d\vec{x} = d\vec{r} - H\,dt\,\vec{r} - \frac{2\,du}{1+u}\vec{r} \tag{3.46}$$

Now it is necessary to calculate du:

Lemma 6. *One has:*

$$du = -\frac{1+u}{1-u} \cdot \frac{u}{r} dr \tag{3.47}$$

Proof. We calculate du from $u = \frac{r_g}{4a(t)x}$:

$$du = \frac{r_g}{4}\left(-\frac{\dot{a}\,dt}{a^2 x} - \frac{dx}{ax^2}\right) = -\frac{r_g}{4ax}\left(H\,dt + \frac{dx}{x}\right) = -u\left(H\,dt + \frac{dx}{x}\right) \tag{3.48}$$

This expression contains dx/x, which can be rewritten as follows. Equation (3.39) gives $r = (1+u)^2\, ax$ and thus:

$$\begin{aligned} dx = d\left[\frac{r}{a\,(1+u)^2}\right] &= -\frac{2r\,du}{a\,(1+u)^3} - \frac{\dot{a}r\,dt}{a^2\,(1+u)^2} + \frac{dr}{a\,(1+u)^2} \\ &= -\frac{2x}{1+u}du - Hx\,dt + \frac{x}{r}dr \end{aligned}$$

Now we use (3.48) and it remains:

$$\begin{aligned} dx &= \frac{2xu}{1+u}\left(H\,dt + \frac{dx}{x}\right) - Hx\,dt + \frac{x}{r}dr \\ &= \frac{2xuH\,dt}{1+u} + \frac{2u\,dx}{1+u} - Hx\,dt + \frac{x}{r}dr \end{aligned}$$

From this we get

$$\left(1-\frac{2u}{1+u}\right)dx=\left(\frac{2u}{1+u}-1\right)Hx\,dt+\frac{x}{r}dr$$

and therewith

$$\frac{1-u}{1+u}dx=-\frac{1-u}{1+u}Hx\,dt+\frac{x}{r}dr.$$

The latter equation can be solved to:

$$\frac{dx}{x}=-H\,dt+\frac{1+u}{1-u}\cdot\frac{dr}{r} \tag{3.49}$$

Now we use (3.49) in equation (3.48) and get (3.47). □

With lemma 6 we replace du in equation (3.46)

$$a\,(1+u)^2\,d\vec{x}=d\vec{r}-H\,dt\,\vec{r}-\frac{2\,du}{1+u}\vec{r}=d\vec{r}-H\,dt\,\vec{r}+\frac{2dr}{1-u}\cdot\frac{u}{r}\vec{r}$$

so that

$$\begin{aligned}a^2\,(1+u)^4\,d\vec{x}^2 &= \left(d\vec{r}-H\,dt\,\vec{r}+\frac{2dr}{1-u}\cdot\frac{u}{r}\vec{r}\right)^2\\ &= d\vec{r}^2+H^2r^2dt^2+\frac{4u^2}{(1-u)^2}dr^2\\ &\quad +2\left(-H\,dt+\frac{2\,dr}{1-u}\cdot\frac{u}{r}\right)\vec{r}\circ d\vec{r}-\frac{4Hru}{1-u}dt\,dr.\end{aligned}$$

From lemma 5 we know that $\vec{r}\circ d\vec{r}=r dr$, see (3.45). We can collect and simplify some terms:

$$\begin{aligned}a^2\,(1+u)^4\,d\vec{x}^2 &= d\vec{r}^2+H^2r^2dt^2\\ &\quad +\frac{4u}{1-u}\left(\frac{u}{1-u}+1\right)dr^2-2Hr\left(1+\frac{2u}{1-u}\right)dt\,dr\\ &= d\vec{r}^2+H^2r^2dt^2+\frac{4u}{(1-u)^2}dr^2-2Hr\frac{1+u}{1-u}dt\,dr\end{aligned}$$

Now we have to split the $d\vec{r}^2$ term into $d\vec{r}^2=dr^2+r^2d\Omega_2$. With that we have

$$\begin{aligned}a^2\,(1+u)^4\,d\vec{x}^2 &= dr^2+r^2d\Omega_2+H^2r^2dt^2-2Hr\frac{1+u}{1-u}dt\,dr+\frac{4u}{(1-u)^2}dr^2\\ &= H^2r^2dt^2+\left(1+\frac{4u}{(1-u)^2}\right)dr^2-2Hr\frac{1+u}{1-u}dt\,dr+r^2d\Omega_2\\ &= H^2r^2dt^2+\left(\frac{1+u}{1-u}\right)^2dr^2-2Hr\frac{1+u}{1-u}dt\,dr+r^2d\Omega_2.\end{aligned}$$

Together with equation (3.44) the latter expression reads:

$$a^2\,(1+u)^4\,d\vec{x}^2 = H^2r^2dt^2 + \frac{dr^2}{1-\frac{r_g}{r}} - \frac{2Hr\,dt\,dr}{\sqrt{1-\frac{r_g}{r}}} + r^2d\Omega_2 \tag{3.50}$$

Finally, (3.44) and (3.50) yield:

$$\begin{aligned} ds^2 &= -\left(\frac{1-u}{1+u}\right)^2 dt^2 + (1+u)^4\,a^2\,(t)\,d\vec{x}^2 \\ &= -\left(1-\frac{r_g}{r}\right)dt^2 + H^2r^2dt^2 + \frac{dr^2}{1-\frac{r_g}{r}} - \frac{2Hr\,dt\,dr}{\sqrt{1-\frac{r_g}{r}}} + r^2d\Omega_2 \\ &= -\left(1-\frac{r_g}{r}-H^2r^2\right)dt^2 + \frac{dr^2}{1-\frac{r_g}{r}} - \frac{2Hr\,dt\,dr}{\sqrt{1-\frac{r_g}{r}}} + r^2d\Omega_2 \end{aligned}$$

For some inexplicable reason, Kaloper, Kleban and Martin presented non of the calculations given in subsection 3.6.1 in their article [65].

As mentioned in section 3.2, in a Swiss-Cheese model (first proposed by Einstein and Straus), the central mass is surrounded by an empty, static cavity, which in turn is embedded in an expanding cosmological background. Naturally, the vacuole radius is several orders of magnitude larger than the gravitational radius of the central mass. The situation in McVittie's generic model is basically different: The curvature singularity at $u = 1$, which is surrounding the singularity at the origin, is directly exposed to the cosmological background. Nevertheless, there is no accretion of mass, which can be regarded as "*an odd property for a physical black hole in a universe full of matter or radiation*" [65]. Naturally, the (lack of) accretion problem disappears if there is no matter or radiation in the cosmological background: McVittie's model includes regular black holes embedded in de Sitter cosmologies. But an empty universe contradicts to the observations. In 2011, Lake and Abdelqader proposed "*a specific* [McVittie] *solution that asymptotes to the CDM cosmology*" [72]. They chose $H = H_0 \coth(3H_0t/2)$ in order to model an asymptotic ΛCDM universe. But, based on investigations concerning the structure of spacetime, Lake and Abdelqader noticed "*that the McVittie solution cannot represent a physically realistic inhomogeneity* [...]" [72]. However, they concluded "*that the McVittie solution is an instructive idealization*" [72]. In 2012, da Silva, Fontanini and Guariento "*developed a working method to determine the causal structure of McVittie metrics* [...]" and "*proved that the form of the expansion function* [which is $H(t)$] *is the sole responsible factor for the structure of the boundaries in McVittie spacetime*", cf. [30].

4. McVittie Solution with cosmological constant

Most recently, in 2012, Landry, Abdelqader and Lake pointed out[60]: "*The McVittie solution has been known for many years, but it continues to attract interest*" [74]. As seen above in section 3.6, several current articles are concerned with this topic, cf. for example [19, 30, 65, 72, 74, 82]. In this section, we also deal with McVittie's model.

We establish a McVittie-type metric by a coordinate replacement and proof that this metric is an exact solution of Einstein's equations with cosmological constant. In section 3, we overlined comoving (time and radial) coordinates, in order to distinguish between different coordinate frames. We now drop this overline notation, which is slightly cumbersome.

Coordinate replacement and field equations

Consider Schwarzschild's solution (2.29). By transformation of $r = q\left(1+\frac{r_g}{4q}\right)^2$ we get the isotropic line element

$$ds^2 = \left(\frac{1-\frac{r_g}{4q}}{1+\frac{r_g}{4q}}\right)^2 c^2dt^2 - \left(1+\frac{r_g}{4q}\right)^4 d\sigma^2 \tag{4.1}$$

where $r_g = 2M\gamma/c^2$ and $d\sigma^2 = dq^2 + q^2d\theta^2 + q^2\sin^2\theta\, d\phi^2$. Subsection 5.2 is concerned with a detailed derivation of the isotropic line element. Now we replace the q coordinate by $a\,(t)\,q$ and the dq differential by $a\,(t)\,dq$ in (5.26). This replacement is different from a coordinate transformation $q = a\bar{q}$, since we ignore the $\dot{a}\bar{q}dt$ term in $dq = \dot{a}\bar{q}dt + ad\bar{q}$. Our coordinate replacement results in:

$$ds^2 = \left[\frac{1-\frac{r_g}{4a(t)q}}{1+\frac{r_g}{4a(t)q}}\right]^2 c^2dt^2 - a^2\,(t)\left[1+\frac{r_g}{4a\,(t)\,q}\right]^4 d\sigma^2 \tag{4.2}$$

This is McVittie's metric, see (3.11), (3.23) and (3.35), cf. [30, 19, 65, 72, 79]. Let us assume that the stress–energy–momentum tensor has the form:

$$T_t^t = c^2\rho\,(q,t)\,; \quad T_q^q = T_\theta^\theta = T_\phi^\phi = -p\,(q,t)\,; \quad \text{and} \quad T_k^i = 0 \text{ for } i \neq k \tag{4.3}$$

Now we set up Einstein's equations for metric (4.2) together with the stress–energy tensor (4.3). The calculations concerning Einstein's tensor for the metric (4.2) are

[60] Landry, Abdelqader and Lake *"examined the McVittie solution with a negative cosmological constant $\Lambda < 0$. A detailed construction of the global structure has been given for the case of a background of dust."* [74].

presented in appendix C.6. Einstein's field equations (1.1) yield

$$\frac{3}{c^2}\left(\frac{\dot{a}}{a}\right)^2 - \Lambda = \frac{8\pi\gamma}{c^2}\rho \tag{4.4}$$

$$\frac{2\,(1+u)}{c^2\,(1-u)}\frac{\ddot{a}}{a} + \frac{(1-5u)}{c^2\,(1-u)}\left(\frac{\dot{a}}{a}\right)^2 - \Lambda = -\frac{8\pi\gamma}{c^4}p \tag{4.5}$$

where $u = \frac{r_g}{4aq}$. Obviously, the McVittie ansatz (4.2) prescribes that the left side of equation (4.4) depends solely on the time t. Hence, the right side of (4.4) should depend solely on the time t too. As a consequence, it is $\rho = \rho\,(t)$. In the following we show that Einstein's equations (4.4) and (4.5) predetermine a relation between the functions ρ and p. Similar expressions are given in [65, 72].

Theorem 7. *(McVittie metric and stress–energy–momentum tensor) Consider a model universe which is determined by the McVittie interval (4.2) and the stress–energy–momentum tensor (4.3). One has:*

$$p = \frac{c^2}{8\pi\gamma}\left\{c^2\Lambda - 3H^2 - 2\left(\frac{1+u}{1-u}\right)\dot{H}\right\},\ \textit{where } H := \dot{a}/a \tag{4.6}$$

The components $T_t^t = c^2\rho$ and $T_q^q = T_\theta^\theta = T_\phi^\phi = -p$ are related by

$$p = -c^2\rho - \frac{c^2\dot{\rho}}{\sqrt{24\pi\gamma\rho + 3c^2\Lambda}}\left(\frac{1+u}{1-u}\right). \tag{4.7}$$

A dot denotes differentiation with respect to the t coordinate, and it is $u = \frac{r_g}{4aq}$.

Proof. Since $\dot{H} = \frac{d}{dt}\left[\frac{\dot{a}}{a}\right] = \frac{\ddot{a}}{a} - \left(\frac{\dot{a}}{a}\right)^2 = \frac{\ddot{a}}{a} - H^2$ we have

$$\frac{\ddot{a}}{a} = \dot{H} + H^2. \tag{4.8}$$

Now consider Einstein's equation (4.5), which can be written in the form

$$p = \frac{c^2}{8\pi\gamma}\left\{c^2\Lambda - 2\left(\frac{1+u}{1-u}\right)\frac{\ddot{a}}{a} - \frac{(1-5u)}{(1-u)}\left(\frac{\dot{a}}{a}\right)^2\right\}. \tag{4.9}$$

Using $H = \dot{a}/a$ and (4.8) in equation (4.9) we get (4.6). In [65], Kaloper, Kleban and Martin present a similar relation, see (3.38), but equation (4.6) includes a Λ term. Now let us establish equation (4.7). From (4.4) we get

$$H^2 = \frac{c^2\Lambda}{3} + \frac{8\pi\gamma}{3}\rho. \tag{4.10}$$

Differentiation with respect to the t coordinate yields $2H\dot{H} = \frac{8\pi\gamma}{3}\dot{\rho}$ and thus

$$\dot{H} = \frac{4\pi\gamma}{3H}\dot{\rho} = \frac{4\pi\gamma\dot{\rho}}{\sqrt{24\pi\gamma\rho + 3c^2\Lambda}}. \tag{4.11}$$

Using (4.10) and (4.11) in equation (4.6) we get (4.7). □

As noticed above, McVittie's model prescribes $\rho = \rho(t)$. Thus, the cosmological background in McVittie's model has a homogeneous density It is obvious from equation (4.7) that the pressure is inhomogeneous (remember that u depends on the $q-$coordinate), except in case of $\dot{\rho} = 0$, cf. [19, 61, 65].

4.0.2. ***Cosmological background with constant, nonzero density.***
At first, let us study the special case $\dot{\rho} = 0$, which implies a constant density $\rho = \rho_1$. From (4.7) one gets for the pressure $p = -c^2\rho_1$. In the latter case, Einstein's equations (4.4) and (4.5) reduce to

$$\frac{3}{c^2}\left(\frac{\dot{a}}{a}\right)^2 - \Lambda = \frac{8\pi\gamma}{c^2}\rho_1 \tag{4.12}$$

$$\frac{2(1+u)}{c^2(1-u)}\frac{\ddot{a}}{a} + \frac{(1-5u)}{c^2(1-u)}\left(\frac{\dot{a}}{a}\right)^2 - \Lambda = \frac{8\pi\gamma}{c^2}\rho_1 \tag{4.13}$$

Using the definition $\Omega_\Lambda = \frac{c^2\Lambda}{3H_0^2}$, equation (4.12) yields:

$$\frac{\dot{a}}{a} = \sqrt{\frac{c^2\Lambda}{3} + \frac{8\pi\gamma}{3}\rho_1} = H_0\sqrt{\Omega_\Lambda + \frac{8\pi\gamma}{3H_0^2}\rho_1}$$

The solution is given by

$$a = a_0 \exp\left(\sqrt{\Omega_\Lambda + \frac{8\pi\gamma}{3H_0^2}\rho_1}\cdot H_0 t\right). \tag{4.14}$$

Obviously, a cosmological background with density $\rho_1 > 0$ acts like a cosmological constant. We could define a new parameter $\Omega_D := \Omega_\Lambda + \frac{8\pi\gamma}{3H_0^2}\rho_1$, so that (4.14) reads

$$a = a_0 \exp\left(\sqrt{\Omega_D}\cdot H_0 t\right).$$

Mathematically speaking, this case represents the "pure cosmological constant solutions", but with a different dark energy parameter Ω_D instead of Ω_Λ. This is not in accordance with the observations of our universe.

Ω_D is positive as long as $\rho_1 > -3H_0^2\Omega_\Lambda/(8\pi\gamma)$. But, in case of $\rho_1 < -3H_0^2\Omega_\Lambda/(8\pi\gamma)$, one gets $\Omega_D < 0$. Accordingly, we may write $\Omega_D = -|\Omega_D|$ and the scale factor becomes

$$a = a_0 \exp\left(i\sqrt{|\Omega_D|}\cdot H_0 t\right).$$

Indeed, this is an even more unphysical condition. Nevertheless, one has a mathematical solution of Einstein's equations (4.4) and (4.5). Let us now draw attention to the $\rho = 0$ McVittie model, which asymptotes to the de Sitter cosmology[61].

[61] sole dominated by the cosmological constant Λ.

4.1. **Cosmological background with $\Omega_M = 0$ and $\Omega_\Lambda \neq 0$.**
Consider an empty background universe with nonzero cosmological constant, i.e. it is $\Omega_M = 0$ and $\Omega_\Lambda \neq 0$. The following theorem proves, that there is an exact solution of Einstein's field equations (4.4) and (4.5) for $\rho = p = 0$.

Theorem 8. *(McVittie solution including a nonzero cosmological constant) A solution for the gravitational field outside of a single point mass, which is embedded in an spatially flat, expanding (empty) FLRW background, is given by*
(4.15)

$$ds^2 = \left[\frac{1 - \frac{r_g}{4a_0 \exp\left(\frac{ct}{r_\Lambda}\right) q}}{1 + \frac{r_g}{4a_0 \exp\left(\frac{ct}{r_\Lambda}\right) q}}\right]^2 c^2 dt^2 - a_0^2 \exp\left(\frac{2ct}{r_\Lambda}\right) \left[1 + \frac{r_g}{4a_0 \exp\left(\frac{ct}{r_\Lambda}\right) q}\right]^4 d\sigma^2$$

where $r_\Lambda = \sqrt{3/\Lambda}$, see (2.39).

Proof. Metric (4.2) represents (4.15) if $a(t)$ is given by

$$a_E := a_0 \exp\left(\frac{ct}{r_\Lambda}\right) \tag{4.16}$$

which is similar to the scale factor in de Sitter's spacetime, see (2.20) in subsection 2.4. According to (4.4) and (4.5), $R_{ik} - \frac{1}{2} R\, g_{ik} - \Lambda g_{ik} = 0$ Einstein's empty space equations for the line element (4.15) reduce to

$$\frac{3}{c^2}\left(\frac{\dot{a}_E}{a_E}\right)^2 - \Lambda = 0 \tag{4.17}$$

$$\frac{2(1+u_E)}{c^2(1-u_E)}\frac{\ddot{a}_E}{a_E} + \frac{(1-5u_E)}{c^2(1-u_E)}\left(\frac{\dot{a}_E}{a_E}\right)^2 - \Lambda = 0 \tag{4.18}$$

where

$$u_E := \frac{r_g}{4a_E q}$$

Equation (4.17) already occurred in subsection 2.4. It represents the corresponding equation for the de Sitter model. From (4.16) we get

$$\dot{a}_E^2 = \left(\frac{c}{r_\Lambda}\right)^2 a_E^2 \equiv \frac{c^2\Lambda}{3} a_E^2$$

Obviously, equation (4.17) is identically fulfilled. Now we have to show that (4.18) is fulfilled too. One has:

$$\begin{aligned}\frac{2(1+u_E)}{c^2(1-u_E)}\frac{\ddot{a}_E}{a_E} + \frac{(1-5u_E)}{c^2(1-u_E)}\left(\frac{\dot{a}_E}{a_E}\right)^2 &= \frac{1}{c^2(1-u_E)}(2+2u_E+1-5u_E)\frac{c^2\Lambda}{3} \\ &= \frac{\Lambda}{3(1-u_E)}(3-3u_E) \quad \equiv \quad \Lambda\end{aligned}$$

Because of $G_1^1 = G_2^2 = G_3^3 = 0$ and $G_k^i \equiv 0$ for $i \neq k$ the theorem is proved. □

4.2. **McVittie model with ΛCDM background.**
The Lambda Cold Dark Matter (ΛCDM) model is frequently referred to as the standard model of big bang cosmology. Let us assume that the density is given by $\rho(t) = \frac{\rho_0}{a^3(t)}$ (see section 2.3), where ρ_0 is the average density of the current universe. Einstein's equation (4.4) reads

$$\left(\frac{\dot{a}}{a}\right)^2 = H_0^2\left(\frac{\Omega_M}{a^3} + \Omega_\Lambda\right)$$

We already solved this equation in subsection 2.6, the solution is:

$$a(t) = \sqrt[3]{\frac{\Omega_M}{\Omega_\Lambda}}\sinh^{\frac{2}{3}}\left[\frac{3}{2}\sqrt{\Omega_\Lambda}\cdot H_0\,(t-t_0)\right]$$

Using the shortcut

$$\eta := \frac{3}{2}\sqrt{\Omega_\Lambda}\cdot H_0\,(t-t_0)$$

and $\Omega_\Lambda H_0^2 = c^2\Lambda/3$, equation (4.6) in Theorem 7 yields:

$$p = \frac{c^4\Lambda}{8\pi\gamma}\left[1 - \frac{16}{81}\left(\cosh^2\eta - \frac{1 + \frac{r_g}{4q\sqrt[3]{\frac{\Omega_M}{\Omega_\Lambda}}\sinh^{\frac{2}{3}}\eta}}{1 - \frac{r_g}{4q\sqrt[3]{\frac{\Omega_M}{\Omega_\Lambda}}\sinh^{\frac{2}{3}}\eta}}\right)\sinh^{-2}\eta\right] \tag{4.19}$$

In subsection 2.6 we showed that there is no pressure in the ΛCDM model. The above equation (4.19) gives

$$\lim_{q\to\infty} p = \frac{65c^4\Lambda}{648\pi\gamma} \approx 5\cdot 10^{-10}\frac{\mathrm{N}}{\mathrm{m}^2} \neq 0.$$

A physical ΛCDM-McVittie model should asymptote to the ΛCDM cosmology. But even in the $q \to \infty$ limit there is nonzero pressure in the McVittie model with ΛCDM background.

4.2.1. ***Drawbacks of the McVittie model.***
McVittie's ansatz (4.2) leads to an exact solution if the mass density parameter of the cosmological background is given by $\Omega_M = 0$, so that $\Omega_{tot} \equiv \Omega_\Lambda + \Omega_M \neq 1$. This contradicts to the assumption that our universe is flat. Even the metric of Theorem 8 is valid only for flat space. Perhaps it would be more consequent to use the value $\Omega_\Lambda = 1$, but this contradicts to the observations, see [63]. Fortunately, the decision if $\Omega_\Lambda = 1$ or $\Omega_\Lambda = 0.7$ does not take influence on the order of magnitude estimations. Indeed, as mentioned in section 3.6, Kaloper, Kleban and Martin showed in 2010 that the McVittie model describes regular black holes, if the metric asymptotes to the de Sitter cosmology, cf. [65]. But what we observe is a universe which contains matter and radiation. The ΛCDM cosmological model is in good

accordance with current observations, cf. [63]. Indeed, Lake and Abdelqader found in 2011 a McVittie metric, which asymptotes to the ΛCDM cosmology. Unfortunately, their analysis of the spacetime's structure led them to the conviction that McVittie's solution cannot represent a physically realistic model, cf. [72].

A major problem arises from the fact that there is no flow of matter towards or away from the central body, cf. [79]. Faraoni and Jacques noticed in [40] that McVittie's solution "*is accretion-free, describes a general FLRW background universe, and does not expand.*" This contradicts to the observations: Distant cosmic matter moves along with the Hubble flow. The surrounding matter falls towards the central body, due to the influence of gravity. Gravity may resorb the dust in the neighborhood of the mass. Hence we should assume that the space near the mass is empty, so we have an exact solution in this area (case $\rho = 0$).

An exact solution of the entire problem might be found if we are able to modify the term $H_0^2 \left(\frac{\Omega_M}{a^3} + \Omega_\Lambda\right)$ in the following manner. We search for a function $f(t, q)$ with:

$$\lim_{q\to 0} f = 0 \qquad \text{and} \qquad \lim_{q\to\infty} f = H_0^2 \left(\frac{\Omega_M}{a^3} + \Omega_\Lambda\right) \tag{4.20}$$

Consequently, the left side of Einstein's equations should depend on the spatial coordinate q too. The ansatz (4.2), where a depends solely on the time, does not fit the boundary conditions (4.20). With regard to the drawbacks of McVittie's model, we search for alternative approaches to describe the gravitational field, generated by a spherically symmetric massive body, which is embedded in an expanding cosmological background. Due to the cosmological principle, we should search for an isotropic metric, i.e. an interval of the form $ds^2 = g_{00}dt^2 - g_{11}d\sigma^2$.

A spherically symmetric solution of Einstein's equations is not necessarily isotropic. The next section is concerned with the question weather a spherically symmetric interval of the form (2.35) can be transformed into an isotropic line element by introducing a new radial coordinate.

5. Isotropic coordinates for spherical spacetimes

Matching of local and global geometry in our universe may require local solutions in isotropic form. Consider the spherically symmetric, but non-isotropic line element[62]

$$ds^2 = \alpha(r)\, c^2 dt^2 - \alpha^{-1}(r)\, dr^2 - r^2 d\theta^2 - r^2 \sin^2\theta\, d\phi^2 \tag{5.1}$$

which corresponds to the Schwarzschild case if $\alpha(r) = 1 - \frac{r_g}{r}$, the de Sitter case if $\alpha(r) = 1 - \left(\frac{r}{r_\Lambda}\right)^2$, and which represents Kottler's Schwarzschild-de Sitter metric in case of $\alpha(r) = 1 - \frac{r_g}{r} - \left(\frac{r}{r_\Lambda}\right)^2$. Our goal is to find a transformation $r = r(q)$ for the radial coordinate, so that interval (5.1) transforms into an isotropic and static line element:

$$ds^2 = A(q)\, c^2 dt^2 - B(q)\, \left\{dq^2 + q^2 d\theta^2 + q^2 \sin^2\theta\, d\phi^2\right\} \tag{5.2}$$

Comparing the components of (5.1) and (5.2) leads to:

$$\alpha^{-1}(r)\, dr^2 = B(q)\, dq^2 \tag{5.3}$$

$$r^2 = B(q)\, q^2 \tag{5.4}$$

$$A(q) = \alpha(r) \tag{5.5}$$

From (5.3) and (5.4) we get $\alpha^{-1}(r)\, dr^2 = \frac{r^2}{q^2} dq^2$ or

$$\frac{dr}{r\sqrt{\alpha(r)}} = \frac{dq}{q}. \tag{5.6}$$

The corresponding integral equation is

$$\int_{r_0}^{r} \frac{dx}{x\sqrt{\alpha(x)}} = \int_{q_0}^{q} \frac{dy}{y}$$

where r_0 and q_0 are the constants of integration. It follows $\ln q = \ln q_0 + \int_{r_0}^{r} \frac{dx}{x\sqrt{\alpha(x)}}$, and for the q coordinate one gets:

$$q = q_0 \exp\left(\int_{r_0}^{r} \frac{dx}{x\sqrt{\alpha(x)}}\right) \tag{5.7}$$

If we solve (5.7) to r, we get the static and isotropic form (5.2) from (5.4) and (5.5). Alternatively, one can directly use the radial transformation $r(q)$ in (5.1) to obtain the isotropic interval. First, we will use this method to get isotropic coordinates for the de Sitter metric (2.22) and the Schwarzschild metric (2.29) in section 5.1 and 5.2. After that, we study weather the Schwarzschild-de Sitter interval (2.40)

[62] This line element was previously established in section 2.7, see (2.35).

can be transformed into an isotropic line element by transformation of the radial coordinate solely.

Indeed, a transformation of the Schwarzschild-de Sitter metric was given by Robertson in [99]. His approach additionally requires a time transformation. In our notation, Robertson's transformation reads as follows: The Schwarzschild-de Sitter metric (2.40)

$$(5.8)\quad ds^2 = \left[1 - \frac{r_g}{r} - \left(\frac{r}{r_\Lambda}\right)^2\right] c^2 dt^2 - \frac{1}{1 - \frac{r_g}{r} - \left(\frac{r}{r_\Lambda}\right)^2} dr^2 - r^2 d\theta^2 - r^2 \sin^2\theta \, d\phi^2$$

can be transformed by

$$(5.9)\quad r = \overline{q} \exp\left(\frac{c\bar{t}}{r_\Lambda}\right)\left(1 + \frac{r_g}{4\overline{q}\exp\left(\frac{c\bar{t}}{r_\Lambda}\right)}\right)^2 ; \quad t = \bar{t} + \frac{4r_g^2}{c r_\Lambda} F\left(\frac{1 - \frac{r_g}{4\overline{q}\exp\left(\frac{c\bar{t}}{r_\Lambda}\right)}}{1 + \frac{r_g}{4\overline{q}\exp\left(\frac{c\bar{t}}{r_\Lambda}\right)}}\right)$$

where

$$F(\xi) = \int \frac{d\xi}{(1-\xi^2)\left[\xi^2(1-\xi^2) - \left(\frac{r_g}{r_\Lambda}\right)^2\right]}$$

into the isotropic line element

$$(5.10)\qquad ds^2 = \left[\frac{1 - \frac{r_g}{4\overline{q}\exp\left(\frac{c\bar{t}}{r_\Lambda}\right)}}{1 + \frac{r_g}{4\overline{q}\exp\left(\frac{c\bar{t}}{r_\Lambda}\right)}}\right]^2 c^2 d\bar{t}^2 - \exp\left(\frac{2c\bar{t}}{r_\Lambda}\right)\left[1 + \frac{r_g}{4\overline{q}\exp\left(\frac{c\bar{t}}{r_\Lambda}\right)}\right]^4 d\sigma^2.$$

The latter interval represents McVittie's solution (3.11) in case of $a\left(\bar{t}\right) = \exp\left(\frac{c\bar{t}}{r_\Lambda}\right)$. McVittie's metric with de Sitter background has already been the subject of detailed study, cf. for example [65]. As mentioned before, an empty de Sitter cosmology is not in accordance with the observation that our universe is filled with matter and radiation. Lake and Abdelqader introduced a McVittie model which asymptotes to the ΛCDM cosmology in 2011, cf. [72]. But they concluded (based on their analysis of the spacetime's structure) that McVittie's metric cannot represent a physically realistic model.

In section 5.3, we investigate an alternative to Robertson's transformation (5.9). Our approach is based on transformation of the radial coordinate by equation (5.7), which contains an elliptic integral in the Schwarzschild-de Sitter case. We solve this equation numerically. In section 5.6, we introduce a new isotropic metric, whose g_{ik} are composed of (products of) de Sitter and Schwarzschild components. This 'Product metric' is not directly obtained by transformation of the Schwarzschild-de Sitter metric, but a comparison with the numerical results indicates that it

represents a good approximation for an isotropic and static Schwarzschild-de Sitter line element.

Robertson's approach (5.9) also contains an elliptic integral for the time transformation. Due to the structure of the Schwarzschild-de Sitter metric (5.8), it is not necessary to solve the integral: It is sufficient to determine dt^2 since the g_{ik} do not depend on the time t. The transformation of the radial coordinate is given by a simple function, cf. (5.9). Thus, Robertson's result of the isotropic transformation, the McVittie metric (5.10), can be written down explicitly.

In our case, the elliptic integral emerges for the radial transformation. There is no simple form to write down the exact isotropic line element explicitly, since the g_{ik} of the Schwarzschild-de Sitter metric (5.8) depend on the radial coordinate.

5.1. **De Sitter solution in isotropic coordinates.**
We use again $r_\Lambda = \sqrt{3/\Lambda}$. In subsection 2.4.1 we showed that de Sitter's metric (2.21) can be transformed into the static form

$$ds^2 = \left[1 - \left(\frac{r}{r_\Lambda}\right)^2\right] c^2 dt^2 - \frac{1}{1 - \left(\frac{r}{r_\Lambda}\right)^2} dr^2 - r^2 d\theta^2 - r^2 \sin^2\theta \, d\phi^2 \tag{5.11}$$

cf. equation (2.22). We use the previously established conditions for the transformation of interval (5.1), which represents the de Sitter metric (5.11) in case of $\alpha(r) = 1 - (r/r_\Lambda)^2$. From (5.7) we obtain:

$$q = q_0 \exp\left(\int_{r_0}^{r} \frac{dx}{x\sqrt{\alpha(x)}}\right) = q_0 \exp\left(r_\Lambda \int_{r_0}^{r} \frac{dx}{x\sqrt{r_\Lambda^2 - x^2}}\right) \tag{5.12}$$

For the integral on we need the following lemma:

Lemma 9. *For $m \in \mathbb{R}$ with $m \neq 0$ one has*

$$\int \frac{dx}{x\sqrt{m^2 \pm x^2}} = \begin{cases} -\frac{1}{m}\mathrm{Arsinh}\left(\frac{m}{x}\right) + c_0, & \text{if the sign is } + \\ -\frac{1}{m}\mathrm{Arcosh}\left(\frac{m}{x}\right) + c_0, & \text{if the sign is } - \end{cases} \tag{5.13}$$

where $c_0 \in \mathbb{R}$ is the constant of integration.

Proof. With $x = \frac{1}{y}$ it is $\frac{dx}{dy} = -\frac{1}{y^2} = -\frac{x}{y}$ so that $\frac{dx}{x} = -\frac{dy}{y}$. We get

$$\int \frac{dx}{x\sqrt{m^2 \pm x^2}} = -\int \frac{dy}{y\sqrt{m^2 \pm \left(\frac{1}{y}\right)^2}} = -\int \frac{dy}{\sqrt{m^2 y^2 \pm 1}}. \tag{5.14}$$

Now we replace $z = my$ so that $dy = \frac{1}{m}dz$ and

$$-\int \frac{dy}{\sqrt{m^2 y^2 \pm 1}} = -\frac{1}{m}\int \frac{dz}{\sqrt{z^2 \pm 1}}.$$

First consider the case that the sign is "+". The transformation $z = \sinh\varphi$ leads to

$$-\frac{1}{m}\int \frac{dz}{\sqrt{z^2+1}} = -\frac{1}{m}\int \frac{\cosh\varphi \, d\varphi}{\sqrt{\sinh^2\varphi + 1}} = -\frac{1}{m}\int d\varphi = -\frac{1}{m}\varphi = -\frac{1}{m}\mathrm{Arsinh}(z)$$

since $dz = \cosh\varphi \, d\varphi$ and $\cosh^2 y - \sinh^2 y = 1$. For the case "−" we use $z = \cosh\varphi$ and obtain

$$-\frac{1}{m}\int \frac{dz}{\sqrt{z^2-1}} = -\frac{1}{m}\int \frac{\sinh\varphi \, d\varphi}{\sqrt{\cosh^2\varphi - 1}} = -\frac{1}{m}\int d\varphi = -\frac{1}{m}\varphi = -\frac{1}{m}\mathrm{Arcosh}(z).$$

Finally, we replace again $z = my = \frac{m}{x}$ in both cases, so we are left with (5.13). □

5.1.1. ***Transformation***.
We use lemma 9 with $m = r_\Lambda$ and obtain

$$\int \frac{dx}{x\sqrt{r_\Lambda^2 - x^2}} = -\frac{1}{r_\Lambda}\text{Arcosh}\left(\frac{r_\Lambda}{x}\right) + c_0$$

for the integral. Hence, equation (5.12) reads

$$kq = \exp\left\{-\text{Arcosh}\left(\frac{r_\Lambda}{r}\right)\right\} \tag{5.15}$$

where k contains the constants of integration. With $\ln(kq) = -\text{Arcosh}(r_\Lambda/r)$ it applies $\cosh\{\ln(1/kq)\} = r_\Lambda/r$ and because of $\cosh(x) = \frac{1}{2}\{\exp(x) + \exp(-x)\}$ it remains

$$\frac{r}{r_\Lambda} = \frac{1}{\frac{1}{2}\left(\frac{1}{kq} + kq\right)} = \frac{2kq}{1 + k^2q^2} \tag{5.16}$$

Now we get $A(q)$ from (5.5) and $B(q)$ from (5.4):

$$\begin{aligned} A(q) &= 1 - \left(\frac{r}{r_\Lambda}\right)^2 = 1 - \left(\frac{2kq}{1+k^2q^2}\right)^2 = \frac{\left(1+k^2q^2\right)^2 - 4k^2q^2}{\left(1+k^2q^2\right)^2} = \left(\frac{1-k^2q^2}{1+k^2q^2}\right)^2 \\ B(q) &= \frac{r^2}{q^2} = \frac{r_\Lambda^2}{q^2}\left(\frac{2kq}{1+k^2q^2}\right)^2 = 4r_\Lambda^2k^2\left(\frac{1}{1+k^2q^2}\right)^2 \end{aligned}$$

With (5.2) de Sitter's metric with respect to the coordinates $[t, q, \theta, \phi]$ reads

$$ds^2 = \left(\frac{1-k^2q^2}{1+k^2q^2}\right)^2 c^2dt^2 - 4r_\Lambda^2k^2\left(\frac{1}{1+k^2q^2}\right)^2 d\sigma^2 \tag{5.17}$$

where k is an arbitrary constant and $d\sigma^2$ is given by (3.1). If we choose $k = 1/2r_\Lambda$ we are left with

$$ds^2 = \left[\frac{1-\left(\frac{q}{2r_\Lambda}\right)^2}{1+\left(\frac{q}{2r_\Lambda}\right)^2}\right]^2 c^2dt^2 - \left[\frac{1}{1+\left(\frac{q}{2r_\Lambda}\right)^2}\right]^2 d\sigma^2 \tag{5.18}$$

where $r_\Lambda = \sqrt{3/\Lambda}$.

Remark 10. The transformation of the interval (5.11) into (5.18) is given by:

$$r = \frac{q}{1+\left(\frac{q}{2r_\Lambda}\right)^2} \tag{5.19}$$

Equation (5.19) directly results from (5.16) for $k = 1/2r_\Lambda$.

5.2. **Schwarzschild solution in isotropic coordinates.**
Schwarzschild's metric is given by the interval

$$ds^2 = \left(1 - \frac{r_g}{r}\right) c^2 dt^2 - \frac{1}{1 - \frac{r_g}{r}} dr^2 - r^2 d\theta^2 - r^2 \sin^2\theta \, d\phi^2 \tag{5.20}$$

which is metric (5.1) with $\alpha(r) = 1 - \frac{r_g}{r}$. We refer again to the above mentioned conditions for the transformation of an non-isotropic interval. For the q coordinate (5.7) we get:

$$q = q_0 \exp\left(\int_{r_0}^{r} \frac{dx}{x\sqrt{\alpha(x)}}\right) = q_0 \exp\left(\int_{r_0}^{r} \frac{dx}{\sqrt{x^2 - r_g x}}\right) \tag{5.21}$$

The following lemma will help to solve the integral in (5.21):

Lemma 11. *For $m \in \mathbb{R}$ with $m \neq 0$ one has*

$$\int \frac{dx}{\sqrt{x^2 - mx}} \quad = \quad 2\mathrm{Arcosh}\left(\sqrt{\frac{x}{m}}\right) + c_0 \tag{5.22}$$

where $c_0 \in \mathbb{R}$ is the constant of integration.

Proof. At first we rewrite the integral

$$\int \frac{dx}{\sqrt{x^2 - mx}} = \int \frac{dx}{\sqrt{x}\sqrt{x - m}} = \frac{1}{m} \int \frac{dx}{\sqrt{\frac{x}{m}}\sqrt{\frac{x}{m} - 1}}$$

and use the $y = x/m$ coordinate. With $dx = mdy$ it is

$$\int \frac{dx}{\sqrt{x^2 - mx}} = \int \frac{dy}{\sqrt{y}\sqrt{y - 1}} \tag{5.23}$$

Now we use the transformation $y = \cosh^2(\alpha)$, $dy = 2\cosh(\alpha)\sinh(\alpha)\, d\alpha$ and the $\cosh^2(\alpha) - 1 = \sinh^2(\alpha)$ identity. It remains:

$$\int \frac{dy}{\sqrt{y}\sqrt{y - 1}} = \int \frac{2\cosh(\alpha)\sinh(\alpha)\, d\alpha}{\cosh(\alpha)\sqrt{\cosh^2(\alpha) - 1}} = 2\int d\alpha = 2\alpha + c_0$$

$c_0 \in \mathbb{R}$ is an arbitrary constant. Finally we retransform

$$\alpha = \mathrm{Arcosh}(\sqrt{y}) = \mathrm{Arcosh}\left(\sqrt{\frac{x}{m}}\right)$$

Together with (5.23) we obtain equation (5.22). □

5.2.1. ***Transformation***.

From lemma 11 we get $\int \frac{dx}{\sqrt{x^2 - r_g x}} = 2\text{Arcosh}\left(\sqrt{\frac{x}{r_g}}\right) + c_0$ and equation (5.21) becomes

$$kq = \exp\left\{2\text{Arcosh}\left(\sqrt{\frac{r}{r_g}}\right)\right\} \tag{5.24}$$

where k contains the constants of integration. Now we solve equation (5.24) to r. With $\frac{1}{2}\ln(kq) = \text{Arcosh}\left(\sqrt{\frac{r}{r_g}}\right)$ we get

$$\cosh\left(\ln\sqrt{kq}\right) = \sqrt{\frac{r}{r_g}}$$

and because of $\cosh(x) = \frac{1}{2}\{\exp(x) + \exp(-x)\}$ we are left with

$$\sqrt{\frac{r}{r_g}} = \frac{1}{2}\left(\sqrt{kq} + \frac{1}{\sqrt{kq}}\right) = \frac{1}{2\sqrt{kq}}(kq+1).$$

Accordingly, the r coordinate is given by:

$$\frac{r}{r_g} = \frac{1}{4kq}(kq+1)^2 \tag{5.25}$$

Now we obtain $A(q)$ from (5.5) and $B(q)$ from (5.4):

$$\begin{aligned} A(q) &= 1 - \frac{r_g}{r} = 1 - \frac{1}{\frac{1}{4kq}(kq+1)^2} = \frac{(kq+1)^2 - 4kq}{(kq+1)^2} = \left(\frac{1-\frac{1}{kq}}{1+\frac{1}{kq}}\right)^2 \\ B(q) &= \frac{r^2}{q^2} = \left\{\frac{r_g}{4kq^2}(kq+1)^2\right\}^2 = \frac{r_g^2 k^2}{16}\left(1+\frac{1}{kq}\right)^4 \end{aligned}$$

and the isotropic metric (5.2) reads

$$ds^2 = \left(\frac{1-\frac{1}{kq}}{1+\frac{1}{kq}}\right)^2 c^2 dt^2 - \frac{r_g^2 k^2}{16}\left(1+\frac{1}{kq}\right)^4 d\sigma^2$$

where k is an arbitrary constant. We choose $k = \frac{4}{r_g}$ with $r_g = \frac{2\gamma M}{c^2}$ in the following. Schwarzschild's metric with respect to the $\{t, q, \theta, \phi\}$ coordinates reads

$$ds^2 = \left(\frac{1-\frac{r_g}{4q}}{1+\frac{r_g}{4q}}\right)^2 c^2 dt^2 - \left(1+\frac{r_g}{4q}\right)^4 d\sigma^2 \tag{5.26}$$

where $d\sigma^2$ is given by (3.1) again. This solution is given in [73].

Remark 12. The transformation of the interval (5.20) into (5.26) is given by:

$$r = q\left(1+\frac{r_g}{4q}\right)^2 \tag{5.27}$$

Equation (5.27) directly results from (5.25) with $k = 4/r_g$.

5.3. **Isotropic coordinates for the Schwarzschild-de Sitter solution.**
The Schwarzschild-de Sitter solution represents the gravitational field of a spherical mass (located at the coordinate origin) in case of a nonzero cosmological constant. We consider the exterior field, i.e. it is at least $r > r_g$. In the neighborhood of r_g, the cosmological constant can be neglected. Far away from the central mass, say $r \sim r_\Lambda$, the gravitational field passes over into de Sitter's solution. But there is a wide range where $r_g \ll r \ll r_\Lambda$, within we have to deal with $\alpha(r) = 1 - \frac{r_g}{r} - \left(\frac{r}{r_\Lambda}\right)^2$. According to (5.7), the equation for the q coordinate is:

$$q = q_0 \exp\left(\int_{r_0}^{r} \frac{dx}{x\sqrt{\alpha(x)}}\right) = q_0 \exp\left(\int_{r_0}^{r} \frac{dx}{x\sqrt{1 - \frac{r_g}{x} - \left(\frac{x}{r_\Lambda}\right)^2}}\right) \tag{5.28}$$

Unfortunately, there exists no simple analytic solution for this integral. We propose two methods for approximating the q coordinate in the following. In the first approach, we replace the square root term on the right side of (5.28) with its Taylor series. Second order terms are neglected. We obtain an integral which can be solved analytically. The second approach is to solve equation (5.28) numerically.

5.3.1. ***Taylor approximation for*** $r \ll r_\Lambda$.
Let us now assume that $r \ll r_\Lambda \approx 5\,\mathrm{Gpc}$. We establish the first order approximation of (5.28) in the following. The square root term in (5.39) can be rewritten as

$$\frac{1}{x\sqrt{1 - \frac{r_g}{x} - \left(\frac{x}{r_\Lambda}\right)^2}} = \frac{1}{x\sqrt{1 - \frac{r_g}{x}}} \cdot \frac{1}{\sqrt{1 - \frac{x^2}{r_\Lambda^2\left(1 - \frac{r_g}{x}\right)}}} = \frac{1}{x\sqrt{1 - \frac{r_g}{x}}} \cdot (1 - z)^{-\frac{1}{2}}$$

where $z = (x/r_\Lambda)^2 / \left(1 - \frac{r_g}{x}\right)$. Now we use the Taylor series:

$$(1 + z)^{-\frac{1}{2}} = 1 - \frac{1}{2}z + \mathcal{O}\left(z^2\right) \tag{5.29}$$

see [52]. Terms of higher order than the second may be neglected, we get

$$\left(1 - \frac{x^2}{r_\Lambda^2\left(1 - \frac{r_g}{x}\right)}\right)^{-\frac{1}{2}} \approx 1 + \frac{x^2}{2r_\Lambda^2\left(1 - \frac{r_g}{x}\right)}$$

and thus:

$$\frac{1}{x\sqrt{1 - \frac{r_g}{x} - \left(\frac{x}{r_\Lambda}\right)^2}} \approx \frac{1}{x\sqrt{1 - \frac{r_g}{x}}} + \frac{x}{2r_\Lambda^2\left(1 - \frac{r_g}{x}\right)^{\frac{3}{2}}} = \frac{1}{\sqrt{x^2 - r_g x}} + \frac{x^{\frac{5}{2}}}{2r_\Lambda^2\left(x - r_g\right)^{\frac{3}{2}}}$$

Accordingly, equation (5.28) yields:

$$q \approx q_0 \exp\left(\int_{r_0}^{r} \frac{dx}{\sqrt{x^2 - r_g x}} + \frac{1}{2r_\Lambda^2}\int_{r_0}^{r} \frac{x^{\frac{5}{2}}\,dx}{\left(x - r_g\right)^{\frac{3}{2}}}\right)$$

The left integral corresponds to the Schwarzschild case. It already occurred in subsection 5.2. As a consequence we obtained equation (5.24). Let us assume that q_1 contains q_0 and the other constants of integration. Together with (5.24) our approximation for the q coordinate reads:

$$q \approx q_1 \exp\left(2\mathrm{Arcosh}\left(\sqrt{\frac{r}{r_g}}\right) + \frac{1}{2r_\Lambda^2}\int_{r_0}^{r} \frac{x^{\frac{5}{2}}dx}{(x-r_g)^{\frac{3}{2}}}\right) \tag{5.30}$$

The remaining integral is solved in the following lemma:

Lemma 13.
For $m \in \mathbb{R}$ with $m \neq 0$ one has

$$\int \frac{x^{\frac{5}{2}}dx}{(x-m)^{\frac{3}{2}}} = m^2\left\{\left(\frac{x}{4m} + \frac{1}{1-\frac{x}{m}} + \frac{7}{8}\right)\sqrt{\frac{x}{m}\left(\frac{x}{m}-1\right)} + \frac{15}{8}\mathrm{Arcosh}\left(\sqrt{\frac{x}{m}}\right)\right\} + c_0$$

where $c_0 \in \mathbb{R}$ is a constant of integration.

Proof. We introduce the new coordinate $y = x/m$ so that $dx = mdy$ and

$$\int \frac{x^{\frac{5}{2}}dx}{(x-m)^{\frac{3}{2}}} = m^2\int \frac{y^{\frac{5}{2}}dy}{(y-1)^{\frac{3}{2}}}. \tag{5.31}$$

The latter integral is transformed by $y = \cosh^2\alpha$ and $dy = 2\cosh\alpha\sinh\alpha\, d\alpha$. We use the $\cosh^2\alpha - \sinh^2\alpha = 1$ identity and get:

$$\begin{aligned}
\int \frac{y^{\frac{5}{2}}dy}{(y-1)^{\frac{3}{2}}} &= \int \frac{\cosh^6\alpha}{\sinh^2\alpha}d\alpha = \int \frac{\left(1+\sinh^2\alpha\right)^3}{\sinh^2\alpha}d\alpha \\
&= \int\left(\frac{1}{\sinh^2\alpha} + 3 + 3\sinh^2\alpha + \sinh^4\alpha\right)d\alpha \\
&= \int \frac{d\alpha}{\sinh^2\alpha} + 3\int\cosh^2\alpha\, d\alpha + \int\sinh^4\alpha\, d\alpha
\end{aligned}$$

The three remaining integrals are easy to solve:

$$\int \frac{d\alpha}{\sinh^2\alpha} = -\int\frac{\sinh^2\alpha - \cosh^2\alpha}{\sinh^2\alpha}d\alpha = -\int\frac{d}{d\alpha}\left[\frac{\cosh\alpha}{\sinh\alpha}\right]d\alpha = -\frac{\cosh\alpha}{\sinh\alpha} + c_1$$

$$\int\cosh^2\alpha\, d\alpha = \frac{1}{4}\int\left(e^{2\alpha} + 2 + e^{-2\alpha}\right)d\alpha = \frac{1}{2}\alpha + \frac{1}{4}\sinh(2\alpha) + c_2$$

$$\begin{aligned}
\int\sinh^4\alpha\, d\alpha &= \frac{1}{16}\int\left(e^{4\alpha} - 4e^{2\alpha} + 6 - 4e^{-2\alpha} + e^{-4\alpha}\right)d\alpha \\
&= \frac{3}{8}\alpha - \frac{1}{8}\left(e^{2\alpha} - e^{-2\alpha}\right) + \frac{1}{64}\left(e^{4\alpha} - e^{-4\alpha}\right) + c_3 \\
&= \frac{3}{8}\alpha - \frac{1}{4}\sinh(2\alpha) + \frac{1}{32}\sinh(4\alpha) + c_3
\end{aligned}$$

c_1, c_2 and c_3 are constants of integration. As a result we get

$$\int \frac{y^{\frac{5}{2}}dy}{(y-1)^{\frac{3}{2}}} = \frac{15}{8}\alpha + \frac{1}{2}\sinh(2\alpha) + \frac{1}{32}\sinh(4\alpha) - \frac{\cosh\alpha}{\sinh\alpha} + c_4 \tag{5.32}$$

where $c_4 = c_1 + c_2 + c_3$. Before transforming back to the y coordinate, we rewrite the terms which contain a hyperbolic sine. At first we need:

$$\cosh(2\alpha) = \frac{1}{2}\left(e^{2\alpha} + e^{-2\alpha}\right) = \frac{1}{2}\left(e^{2\alpha} + 2 + e^{-2\alpha}\right) - 1 = 2\cosh^2\alpha - 1$$

Therewith we have

$$\begin{aligned}
\sinh(2\alpha) &= \sqrt{\cosh^2(2\alpha) - 1} = \sqrt{\left(2\cosh^2\alpha - 1\right)^2 - 1} = 2\cosh\alpha\sqrt{\cosh^2\alpha - 1} \\
\sinh(4\alpha) &= 2\cosh(2\alpha)\sqrt{\cosh^2(2\alpha) - 1} \\
&= 2\left(2\cosh^2\alpha - 1\right)\sqrt{\left(2\cosh^2\alpha - 1\right)^2 - 1} \\
&= 4\cosh\alpha\left(2\cosh^2\alpha - 1\right)\sqrt{\cosh^2\alpha - 1}
\end{aligned}$$

and with $\alpha = \operatorname{Arcosh}\left(\sqrt{y}\right)$ integral (5.32) transforms to

$$\begin{aligned}
\int \frac{y^{\frac{5}{2}}dy}{(y-1)^{\frac{3}{2}}} &= \frac{15}{8}\operatorname{Arcosh}\left(\sqrt{y}\right) + \sqrt{y(y-1)} + \frac{1}{8}(2y-1)\sqrt{y(y-1)} - \sqrt{\frac{y}{y-1}} + c_4 \\
&= \sqrt{y(y-1)}\left[1 + \frac{1}{8}(2y-1) - \frac{1}{y-1}\right] + \frac{15}{8}\operatorname{Arcosh}\left(\sqrt{y}\right) + c_4 \\
&= \left(\frac{1}{4}y + \frac{1}{1-y} + \frac{7}{8}\right)\sqrt{y(y-1)} + \frac{15}{8}\operatorname{Arcosh}\left(\sqrt{y}\right) + c_4.
\end{aligned}$$

Now we have to retransform $y = x/m$. Together with (5.31) and $c_0 = m^2 c_4$ lemma 13 is proved. □

Now we are able to solve the second integral. With lemma 13 it remains

$$\begin{aligned}
\frac{1}{2r_\Lambda^2}\int_{r_0}^{r} \frac{x^{\frac{5}{2}}dx}{(x-r_g)^{\frac{3}{2}}} &= \frac{1}{2}\left(\frac{r_g}{r_\Lambda}\right)^2\left(\frac{r}{4r_g} + \frac{1}{1-\frac{r}{r_g}} + \frac{7}{8}\right)\sqrt{\frac{r}{r_g}\left(\frac{r}{r_g} - 1\right)} \\
&\quad + \frac{15}{16}\left(\frac{r_g}{r_\Lambda}\right)^2 \operatorname{Arcosh}\left(\sqrt{\frac{r}{r_g}}\right) + c_5.
\end{aligned}$$

Let us use the abbreviation $\varepsilon := (r_g/r_\Lambda)^2$ in the following. The first order approximation (5.30) for the Schwarzschild-de Sitter q coordinate reads

$$q \approx q_2 \exp\left\{\frac{\varepsilon}{2}\left(\frac{r}{4r_g} + \frac{1}{1-\frac{r}{r_g}} + \frac{7}{8}\right)\sqrt{\frac{r}{r_g}\left(\frac{r}{r_g} - 1\right)} + \left(2 + \frac{15}{16}\varepsilon\right)\operatorname{Arcosh}\left(\sqrt{\frac{r}{r_g}}\right)\right\}$$

where q_2 contains all the constants of integration. In order to establish an isotropic

Schwarzschild-de Sitter metric in the form (5.2), we additionally need the inverse function $r(q)$. It does not seem that the above equation can be solved to r analytically. Nevertheless, we will compare our result with the Schwarzschild case and the de Sitter case.

Schwarzschild case:
The isotropic Schwarzschild $q-$coordinate is related to r by equation (5.24). We chose $k = \frac{4}{r_g}$, so we are left with $q = \frac{r_g}{4}\exp\left\{2\text{Arcosh}\left(\sqrt{\frac{r}{r_g}}\right)\right\}$. The inverse hyperbolic cosine fulfills the identity[63]:

$$\text{Arcosh}(z) = \ln\left(z \pm \sqrt{z^2-1}\right) = \pm\ln\left(z+\sqrt{z^2-1}\right), \quad z \geq 1 \tag{5.33}$$

According to this identity, the 'Schwarzschild q coordinate' is given by

$$q = \frac{r_g}{4}\exp\left\{2\ln\left(\sqrt{\frac{r}{r_g}}+\sqrt{\frac{r}{r_g}-1}\right)\right\} = \frac{r_g}{4}\left(\sqrt{\frac{r}{r_g}}+\sqrt{\frac{r}{r_g}-1}\right)^2. \tag{5.34}$$

The "$-$" branch of (5.33) leads to a negative coordinate q. Therefore, we only consider the "$+$" branch.

De Sitter case:
In the de Sitter case, the q coordinate is given by equation (5.15). We chose $k = 1/2r_\Lambda$, so that the equation reads

$$q = 2r_\Lambda \exp\left\{-\text{Arcosh}\left(\frac{r_\Lambda}{r}\right)\right\}$$

where $r_\Lambda = \sqrt{3/\Lambda}$. We use again identity (5.33) for the inverse hyperbolic cosine and get:

$$q = 2r_\Lambda \exp\left\{-\ln\left(\frac{r_\Lambda}{r}+\sqrt{\left(\frac{r_\Lambda}{r}\right)^2-1}\right)\right\} = \frac{2r_\Lambda}{\frac{r_\Lambda}{r}+\sqrt{\left(\frac{r_\Lambda}{r}\right)^2-1}} \tag{5.35}$$

For the purpose of comparison we choose $M = 1.3\cdot 10^{12} M_\odot$, which corresponds to the mass of our Local Group of galaxies. Accordingly, the gravitational radius is $r_g \approx 0.125\,\text{pc}$. Figure 5.1 shows the first order approximation of the Schwarzschild-de Sitter q coordinate for $q_2 = r_g/4$

(5.36)

$$q = \frac{r_g}{4}\exp\left\{\frac{\varepsilon}{2}\left(\frac{r}{4r_g}+\frac{1}{1-\frac{r}{r_g}}+\frac{7}{8}\right)\sqrt{\frac{r}{r_g}\left(\frac{r}{r_g}-1\right)}+\left(2+\frac{15}{16}\varepsilon\right)\text{Arcosh}\left(\sqrt{\frac{r}{r_g}}\right)\right\}$$

[63] Let $y = \text{Arcosh}(z)$. From $z = \cosh(y) = \frac{1}{2}\left(e^y + e^{-y}\right)$ we get $e^{2y} - 2ze^y + 1 = 0$. The solutions are $e^y = z \pm \sqrt{z^2-1}$, hence it applies $\text{Arcosh}(z) = y = \ln\left(z \pm \sqrt{z^2-1}\right)$. It is easy to check that $\ln\left(z-\sqrt{z^2-1}\right) = -\ln\left(z+\sqrt{z^2-1}\right)$.

in comparison with the Schwarzschild case (5.34) and de Sitter case (5.35). Figure 5.2 shows (5.36) in the region $r \sim r_g$.

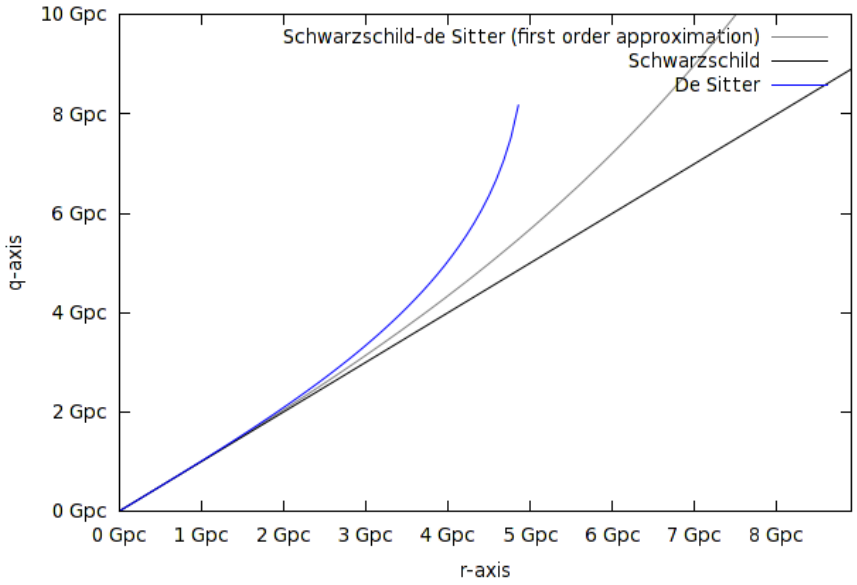

FIGURE 5.1. Relation of q and r for de Sitter, Schwarzschild and Schwarzschild-de Sitter case.

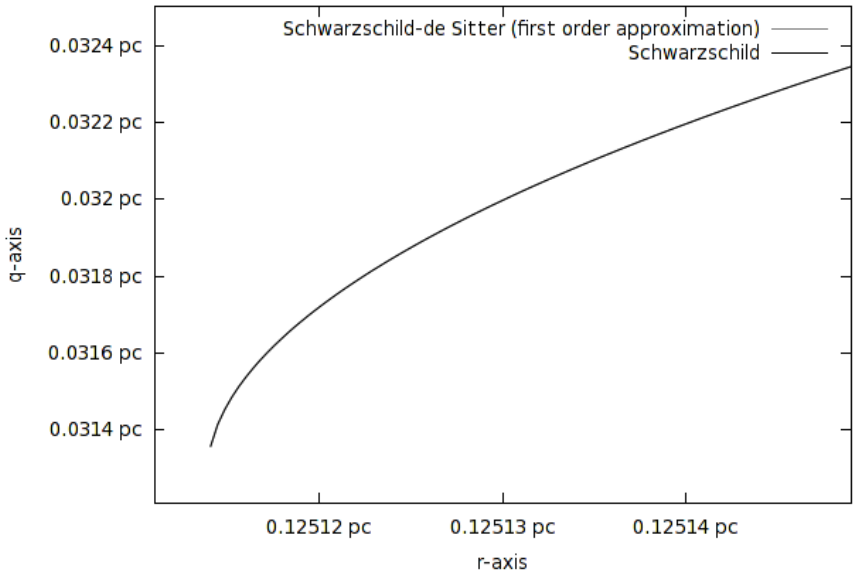

FIGURE 5.2. The Schwarzschild-de Sitter q coordinate coincides with the Schwarzschild q coordinate if $r \sim r_g$.

5.4. **Numerical approximation.**
As mentioned at the beginning of subsection 5.3, our second approach is to solve equation (5.28) numerically. We study the corresponding differential equation. Equation (5.28) can be retransformed into

$$\ln q - \ln q_0 = \int_{r_0}^{r} \frac{dx}{x\sqrt{1 - \frac{r_g}{x} - \left(\frac{x}{r_\Lambda}\right)^2}}.$$

Differentiation with respect to the r coordinate yields[64]

$$\frac{d}{dr}\left[\ln q\right] = \frac{1}{r\sqrt{1 - \frac{r_g}{r} - \left(\frac{r}{r_\Lambda}\right)^2}} \tag{5.37}$$

which can be numerically solved within a suitable interval. For the purpose of numerical approximation we rescale the coordinate system by introducing new coordinates x and u:

$$r = r_g e^x \quad \text{and} \quad q = r_g e^u \tag{5.38}$$

Hence, it follows $dr = r_g e^x dx = r dx$ and from $u = \ln\left(q/r_g\right) = \ln q - \ln r_g$ we get $\ln q = u - \ln r_g$, so that

$$\frac{d}{dr}\left[\ln q\right] = \frac{d}{rdx}\left[u - \ln r_g\right] = \frac{du}{rdx}$$

and equation (5.37) transforms to

$$\frac{du}{dx} = \frac{1}{\sqrt{1 - e^{-x} - \left(\frac{r_g}{r_\Lambda}\right)^2 e^{2x}}} = \frac{1}{\sqrt{1 - e^{-x} - \varepsilon e^{2x}}}. \tag{5.39}$$

where we have used again $\varepsilon = \left(r_g/r_\Lambda\right)^2$. Our goal is to establish a numerical solution for the isotropic Schwarzschild-de Sitter metric. For our purpose it is not necessary to plot the $q\left(r\right)$ transformation, since we can directly approximate the metric components $g_{00} = A\left(q\right)$ and $g_{11} = -B\left(q\right)$. In section 5 we established equations for the transformation of $ds^2 = \alpha\left(r\right)c^2dt^2 - \alpha^{-1}\left(r\right)dr^2 - r^2d\theta^2 - r^2\sin^2\theta\, d\phi^2$ into the corresponding isotropic interval (5.2):

$$ds^2 = A\left(q\right)\, c^2dt^2 - B\left(q\right)\, \left\{dq^2 + q^2d\theta^2 + q^2\sin^2\theta\, d\phi^2\right\}$$

Based upon the conditions (5.3), (5.4) and (5.5) we search functions for the tensor components $g_{00} = A$ and $g_{11} = -B$ of the isotropic Schwarzschild-de Sitter metric. There is a simple relation between A and α given by $A\left(q\right) = \alpha\left(r\left(q\right)\right)$, where r and q are determined by (5.6): $\frac{dr}{r\sqrt{\alpha(r)}} = \frac{dq}{q}$. As earlier mentioned, there is no exact solution for the latter differential equation in the Schwarzschild-de Sitter

[64]Of course we get the same result directly from (5.6): $\frac{dr}{r\sqrt{\alpha(r)}} = \frac{dq}{q}$.

case, and we have to deal with a numerical approximation for $r\,(q)$. The differential equation was transformed by $r = r_g e^x$ and $q = r_g e^u$. We can approximate $u\,(x)$ or alternatively $x\,(u)$ from (5.39), and with that we obtain an $A\,(u)$ by[65]

$$A = \alpha\left(r_g e^{x(u)}\right) = 1 - e^{-x(u)} - \left(\frac{r_g}{r_\Lambda}\right)^2 e^{2x(u)}.$$

Analogously, we establish the function which represents the $g_{11} = -B$ tensor component of the isotropic metric (5.2). Later we use the result (5.40) to plot the function g_{11} for the isotropic Schwarzschild-de Sitter case. B is given by $B = r^2/q^2$, see equation (5.4). According to transformation (5.38), it applies $u = \ln q - \ln r_g$ and $x = \ln r - \ln r_g$ so that

$$\exp^2(x-u) = \exp^2(\ln r - \ln q) = \exp^2\left[\ln\left(\frac{r}{q}\right)\right] = \left(\frac{r}{q}\right)^2$$

and we finally have:

$$B = \exp^2(x-u) \tag{5.40}$$

Thus, our function graph for $g_{11} = -B\,(u)$ in the Schwarzschild-de Sitter case consists of the points $P_n\left(u_n \mid -\exp^2(x_n - u_n)\right)$, which we approximated numerically with algorithm 3, see appendix. Alternatively, we may plot the points $P_n\left(x_n \mid -\exp^2(x_n - u_n)\right)$ to get a function which depends on the x coordinate. Our numerical calculations are confined to the investigation of $g_{11} = -B$. Based on the numerical results for B, we introduce a new metric in subsection 5.6, which is a very good approximation for the isotropic Schwarzschild-de Sitter case. Hence, an additional numerical investigation of $A = g_{00}$ does not seem to be necessary. Nevertheless, algorithm 3 in appendix D could be easily modified for this purpose.

5.4.1. ***Initial conditions.***

At first let us determine a suitable interval for the numerical approximation. Consider again equation (5.37). The term on the right side has poles at $r = 0$ and $1 - \frac{r_g}{r} - \left(\frac{r}{r_\Lambda}\right)^2 = 0$. Solutions of the latter equation are given by (2.43). The roots are roughly located at $r_1 \approx r_\Lambda - \frac{1}{2}r_g$, $r_2 \approx -r_\Lambda - \frac{1}{2}r_g$ and $r_3 \approx r_g$, see section 2.8. Accordingly, we approximate our differential equation (5.39) within an interval $[x_a, x_b]$ where $x_a > \ln(r_3/r_g) \approx 0$ and $x_b < \ln(r_1/r_g) \approx \ln(r_\Lambda/r_g)$. We suppose that the solution of (5.39) largely coincides with the Schwarzschild case, as long as the distance r is small enough, say $r \lesssim 10 r_g$. In this case, the $q-$coordinate is given by $q = \frac{r_g}{4}\left(\sqrt{\frac{r}{r_g}} + \sqrt{\frac{r}{r_g} - 1}\right)^2$, see (5.34). Correspondingly, the relation between

[65] Perhaps it would be better to write $\bar{A}\,(u) = A\,(r_g e^u) = A\,(q)$ instead of $A\,(u)$.

the $u = \ln(q/r_g)$ and $x = \ln(r/r_g)$ coordinates is:

$$e^u = \frac{1}{4}\left(\sqrt{e^x} + \sqrt{e^x - 1}\right)^2 = \frac{1}{2}e^x - \frac{1}{4} + \frac{1}{2}\sqrt{e^{2x} - e^x} \tag{5.41}$$

In terms of the gravitational radius r_g, i.e. for $r = \kappa r_g$, the start values for the numerical algorithm with respect to the coordinates x and u are

$$x_0 = \ln\kappa\,; \quad u_0 = \ln\left[\frac{1}{2}\kappa - \frac{1}{4} + \frac{1}{2}\sqrt{\kappa^2 - \kappa}\right]. \tag{5.42}$$

For example, our Fortran77 algorithm 3 was started at[66] $r = 4r_g$ to get figure 5.3. Let us compare the first order approximation (5.36) of the Schwarzschild-de Sitter coordinate (say q_K) with the (5.34) Schwarzschild coordinate (say q_S) at $r = 4r_g$:

$$q_K(4r_g) = \frac{r_g}{4}\exp\left\{\frac{37\sqrt{3}}{24}\varepsilon + \left(2 + \frac{15}{16}\varepsilon\right)\operatorname{Arcosh}\sqrt{4}\right\}, \quad q_S(4r_g) = r_g\left(\frac{7}{4} + \sqrt{3}\right)$$

We may assume that q_K coincides with the Schwarzschild case at $r = 4r_g$ since

$$\frac{q_K(4r_g)}{q_S(4r_g)} - 1 \approx 1.7 \cdot 10^{-21}.$$

5.4.2. ***Results***.

In order to display the values on the vertical axis with adequate accuracy, we evaluate the function

$$f := 1 + g_{11} = 1 - B$$

instead of the metric component g_{11}. Since we intend to compare our numerical solution with the exact solutions in the Schwarzschild case and the de Sitter case, we have to transform the corresponding functions by $q = r_g e^u$. From the isotropic Schwarzschild metric (5.26) we get

$$f_s = 1 - B_s = 1 - \left(1 + \frac{r_g}{4q}\right)^4 = 1 - \left[1 + \frac{1}{4}\exp(-u)\right]^4$$

and from the isotropic de Sitter metric (5.18):

$$f_d = 1 - B_d = 1 - \left(\frac{1}{1 + \frac{1}{4r_\Lambda^2}q^2}\right)^2 = 1 - \left[1 + \frac{1}{4}\left(\frac{r_g}{r_\Lambda}\right)^2\exp(2u)\right]^{-2}$$

Figure 5.3 suggests that the Schwarzschild-de Sitter graph is entirely covered by the two other solutions. Indeed, our numerical result largely coincides with either the Schwarzschild case or the de Sitter case, but in fact the Schwarzschild-de Sitter solution represents the transition between them. The results were double checked with the help of Maple. The numerical error is smaller than the line width.

[66] $r = 4r_g$ corresponds to $\kappa = 4$ in (5.42)

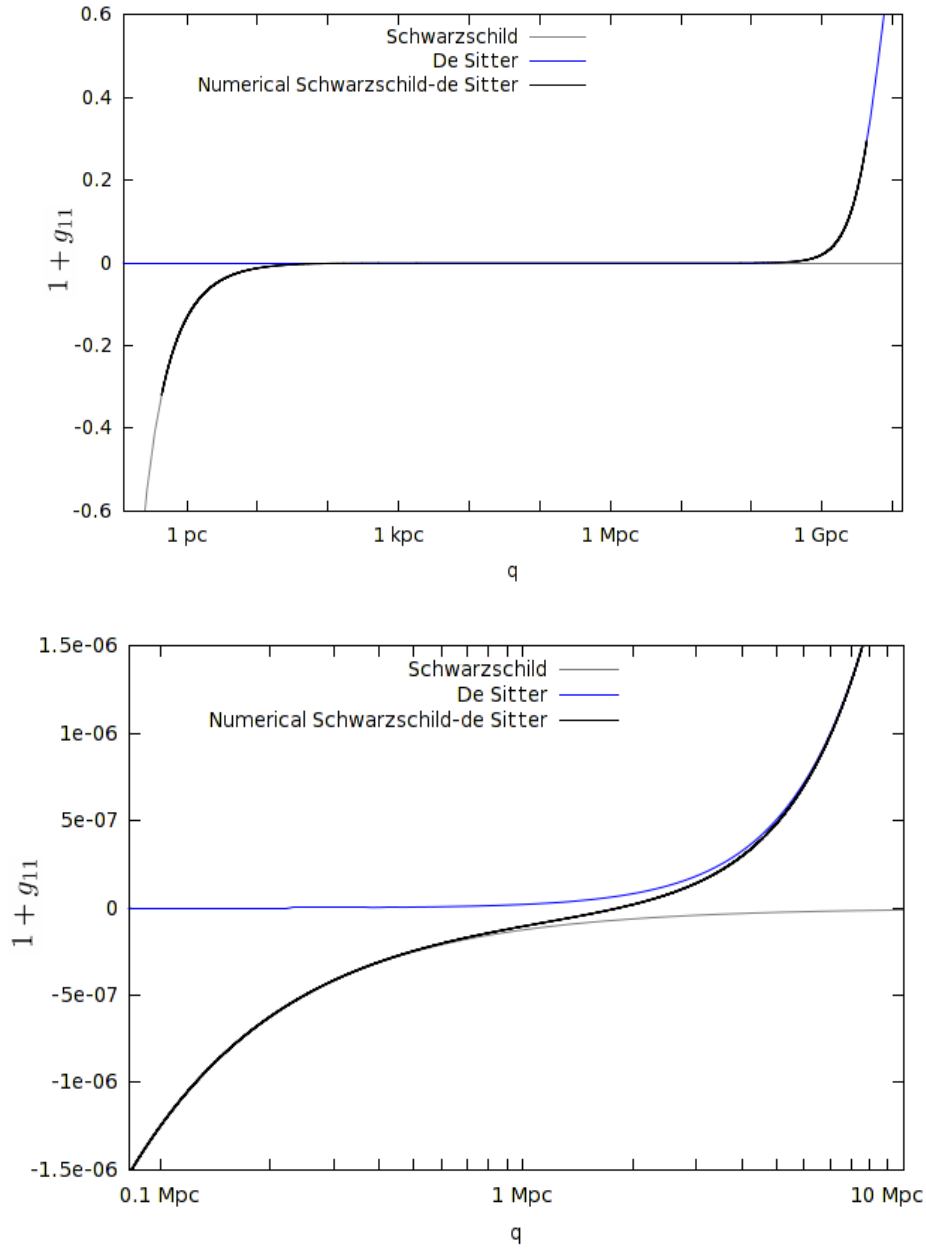

FIGURE 5.3. Numerical result for $f = 1 + g_{11}$, according to a system where the central mass $M = 1.3 \cdot 10^{12} M_{\odot}$ corresponds to the mass of our Local Group of galaxies. The gravitational radius is $r_g \approx 0.125\,\mathrm{pc}$. The second graphic shows the 'Schwarzschild-de Sitter transition' between de Sitter and Schwarzschild solution.

5.5. **A function for the isotropic Schwarzschild-de Sitter g_{11}.**
In the following we propose an approximate solution for g_{11}, which can be expressed as a functional term. Indeed, we introduce two acceptable terms for $B = -g_{11}$ in the Schwarzschild-de Sitter case. First, we set B as a sum of B_s (Schwarzschild case), B_d (de Sitter case) and -1. In order to avoid ambiguity, this solution is denoted by S in the following:

$$S(u) := B_s(u) + B_d(u) - 1$$

Therefore we have

$$S(u) = \left[1 + \frac{1}{4}\exp(-u)\right]^4 + \left[1 + \frac{1}{4}\left(\frac{r_g}{r_\Lambda}\right)^2 \exp(2u)\right]^{-2} - 1. \tag{5.43}$$

Alternatively, we obtain an acceptable solution for the Schwarzschild-de Sitter case if we set B as the product of B_s and B_d. This solution is denoted by P

$$P(u) := B_s(u) \cdot B_d(u)$$

so that finally

$$P(u) = \left[1 + \frac{1}{4}\exp(-u)\right]^4 \left[1 + \frac{1}{4}\left(\frac{r_g}{r_\Lambda}\right)^2 \exp(2u)\right]^{-2}. \tag{5.44}$$

Both functions (5.43) and (5.44) cover the numerical graph for B in the Schwarzschild-de Sitter case, see figure 5.4:

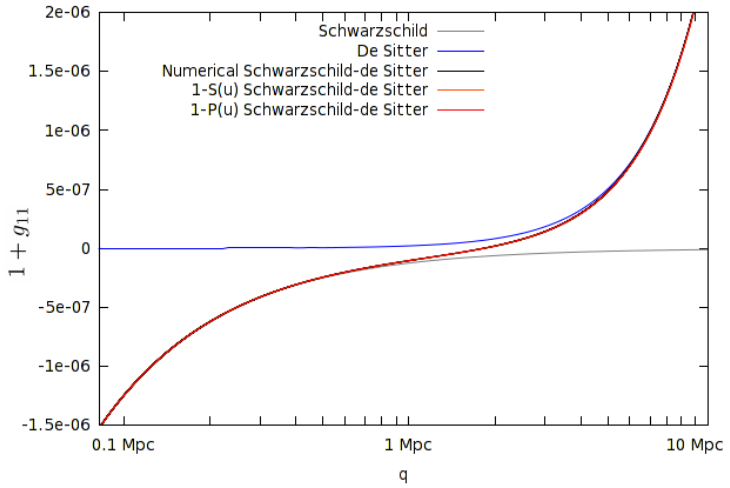

FIGURE 5.4. The isotropic $f = 1 + g_{11}$ functions $f_S = 1 - S(u)$ and $f_P = 1 - P(u)$ for the Schwarzschild-de Sitter case compared with the corresponding numerical result and the Schwarzschild case $f_s = 1 - B_s(u)$ and de Sitter case $f_d = 1 - B_d(u)$; $r_g \approx 0.125\,\mathrm{pc}$.

Figure 5.4 shows the $f = 1+g_{11}$ functions $f_S = 1-S(u)$ and $f_P = 1-P(u)$ for the Schwarzschild-de Sitter case compared with the corresponding numerical result, the $f_s = 1-B_s(u)$ Schwarzschild case and the $f_d = 1-B_d(u)$ de Sitter case. Again, the central mass was set to $M = 1.3 \cdot 10^{12} M_\odot$, the mass of our Local Group of galaxies. Accordingly, the gravitational radius is $r_{LG} \approx 0.125\,\mathrm{pc}$. By slightly modifying the scripts, which are given in the appendix, it is easy to examine that (5.43) and (5.44) also cover the corresponding numerical graph for other mass condensations M.

S and P approximate the numerical result for the Schwarzschild-de Sitter case with high accuracy. It seems natural to construct an isotropic metric, which is at least a high-precision approximation of the isotropic Schwarzschild-de Sitter space-time, by using one of the two above mentioned methods. If we use the sum of the related components of the metric tensors, we will call the resulting interval 'Sum-metric':

$$ds^2 = \left[\left(\frac{1-\frac{r_g}{4q}}{1+\frac{r_g}{4q}}\right)^2 + \left(\frac{1-\frac{q^2}{4r_\Lambda^2}}{1+\frac{q^2}{4r_\Lambda^2}}\right)^2 - 1\right] c^2 dt^2 - \left[\left(1+\frac{r_g}{4q}\right)^4 + \left(1+\frac{q^2}{4r_\Lambda^2}\right)^{-2} - 1\right] d\sigma^2$$

Alternatively, we can construct an isotropic Schwarzschild-de Sitter approximation by multiplying the related components of the Schwarzschild and the de-Sitter metric. We will call the resulting interval 'Product-metric':

$$ds^2 = \left(\frac{1-\frac{r_g}{4q}}{1+\frac{r_g}{4q}}\right)^2 \cdot \left(\frac{1-\frac{q^2}{4r_\Lambda^2}}{1+\frac{q^2}{4r_\Lambda^2}}\right)^2 c^2 dt^2 - \left(1+\frac{r_g}{4q}\right)^4 \cdot \left(1+\frac{q^2}{4r_\Lambda^2}\right)^{-2} d\sigma^2$$

Product-metric and Sum-metric are studied in the following subsection.

5.6. **Product-metric.**

Our new metric resembles some kind of product of Schwarzschild and de-Sitter case. As mentioned above, this 'Product-metric' is given by the interval

$$ds^2 = \left(\frac{1-\frac{r_g}{4q}}{1+\frac{r_g}{4q}}\right)^2 \left(\frac{1-\frac{q^2}{4r_\Lambda^2}}{1+\frac{q^2}{4r_\Lambda^2}}\right)^2 c^2dt^2 - \left(1+\frac{r_g}{4q}\right)^4 \left(\frac{1}{1+\frac{q^2}{4r_\Lambda^2}}\right)^2 d\sigma^2 \tag{5.45}$$

where $d\sigma^2 = dq^2 + q^2d\theta^2 + q^2\sin^2\theta\, d\phi^2$. In the following section we determine the required stress–energy–momentum tensor T_k^i, so that our Product-metric becomes an exact solution of $G_k^i = \frac{8\pi\gamma}{c^4}T_k^i$ Einstein's field equations, including a cosmological constant. It turned out that this stress–energy–momentum tensor remains negligibly small outside the gravitational sphere[67]. This confirms that the Product-metric is a good approximation for Einstein's empty space equations. Later we show that the first order approximation of the Product-metric is given by the above mentioned Sum-metric. Let us use the abbreviations[68]

(5.46)

$$A_d = \left(\frac{1-\frac{q^2}{4r_\Lambda^2}}{1+\frac{q^2}{4r_\Lambda^2}}\right)^2,\ B_d = \left(\frac{1}{1+\frac{q^2}{4r_\Lambda^2}}\right)^2,\ A_s = \left(\frac{1-\frac{r_g}{4q}}{1+\frac{r_g}{4q}}\right)^2,\ B_s = \left(1+\frac{r_g}{4q}\right)^4$$

for the components of de Sitter and Schwarzschild metric. With the latter shortcuts, de Sitter's case is given by $ds^2 = A_dc^2dt^2 - B_d d\sigma^2$ and the Schwarzschild interval reads $ds^2 = A_sc^2dt^2 - B_s d\sigma^2$. The Product metric (5.45) takes the simple form

$$ds^2 = A_dA_sc^2dt^2 - B_dB_s d\sigma^2. \tag{5.47}$$

With the help of Maple, see algorithm 8 in the appendix, it is easy to calculate Einstein's tensor G_i^k with respect to the coordinates $\{t, q, \theta, \phi\}$ for (5.47):

$$G_t^t = \frac{3+\frac{r_g}{4q}-\frac{r_g}{8r_\Lambda^2}q}{r_\Lambda^2\left(1+\frac{r_g}{4q}\right)^5} - \Lambda \tag{5.48}$$

$$G_q^q = \frac{3+\frac{7r_g^2}{64r_\Lambda^2}+\frac{3r_g^2}{16q^2}-\frac{r_g}{q}-\frac{r_g}{4r_\Lambda^2}q-\frac{1}{r_\Lambda^2}\left(\frac{3}{4}+\frac{r_g^2}{128r_\Lambda^2}\right)q^2}{r_\Lambda^2\left(1+\frac{r_g}{4q}\right)^5\left(1-\frac{r_g}{4q}\right)\left(1-\frac{q^2}{4r_\Lambda^2}\right)} - \Lambda \tag{5.49}$$

$$G_\theta^\theta = \frac{3+\frac{3r_g^2}{64r_\Lambda^2}-\frac{3r_g^2}{16q^2}+\frac{r_g}{q}+\frac{r_g}{4r_\Lambda^2}q-\frac{3}{4r_\Lambda^2}q^2}{r_\Lambda^2\left(1+\frac{r_g}{4q}\right)^5\left(1-\frac{r_g}{4q}\right)\left(1-\frac{q^2}{4r_\Lambda^2}\right)} - \Lambda \tag{5.50}$$

$$G_\phi^\phi = G_\theta^\theta \quad \text{and} \quad G_k^i = 0 \quad \text{for} \ \ i \neq k \tag{5.51}$$

[67]The sphere with radius $r = r_g$, with respect to the $q-$coordinate this is $q = r_g/4$.
[68]Remember that $r_\Lambda = \sqrt{3/\Lambda}$ and $r_g = 2M\gamma/c^2$

Einstein's field equations yield $T_k^i = \frac{c^4}{8\pi\gamma} G_k^i$. By using $r_\Lambda = \sqrt{3/\Lambda}$ we can place Λ outside the brackets. It remains:

$$T_t^t = \frac{c^4\Lambda}{8\pi\gamma}\left[\frac{1+\frac{r_g}{12q}-\frac{r_g}{24r_\Lambda^2}q}{\left(1+\frac{r_g}{4q}\right)^5}-1\right] \tag{5.52}$$

$$T_q^q = \frac{c^4\Lambda}{8\pi\gamma}\left[\frac{1+\frac{7r_g^2}{192r_\Lambda^2}+\frac{r_g^2}{16q^2}-\frac{r_g}{3q}-\frac{r_g}{12r_\Lambda^2}q-\frac{1}{r_\Lambda^2}\left(\frac{1}{4}+\frac{r_g^2}{384r_\Lambda^2}\right)q^2}{\left(1+\frac{r_g}{4q}\right)^5\left(1-\frac{r_g}{4q}\right)\left(1-\frac{q^2}{4r_\Lambda^2}\right)}-1\right] \tag{5.53}$$

$$T_\theta^\theta = \frac{c^4\Lambda}{8\pi\gamma}\left[\frac{1+\frac{r_g^2}{64r_\Lambda^2}-\frac{r_g^2}{16q^2}+\frac{r_g}{3q}+\frac{r_g}{12r_\Lambda^2}q-\frac{1}{4r_\Lambda^2}q^2}{\left(1+\frac{r_g}{4q}\right)^5\left(1-\frac{r_g}{4q}\right)\left(1-\frac{q^2}{4r_\Lambda^2}\right)}-1\right] \tag{5.54}$$

The unit[69] of the above stress–energy–momentum tensor T_k^i is $\frac{\mathrm{g}}{\mathrm{ms}^2} = 10^{-3}\frac{\mathrm{N}}{\mathrm{m}^2}$, which is the physical unit of a pressure. Figure 5.5 shows the functions (5.52), (5.53) and (5.54):

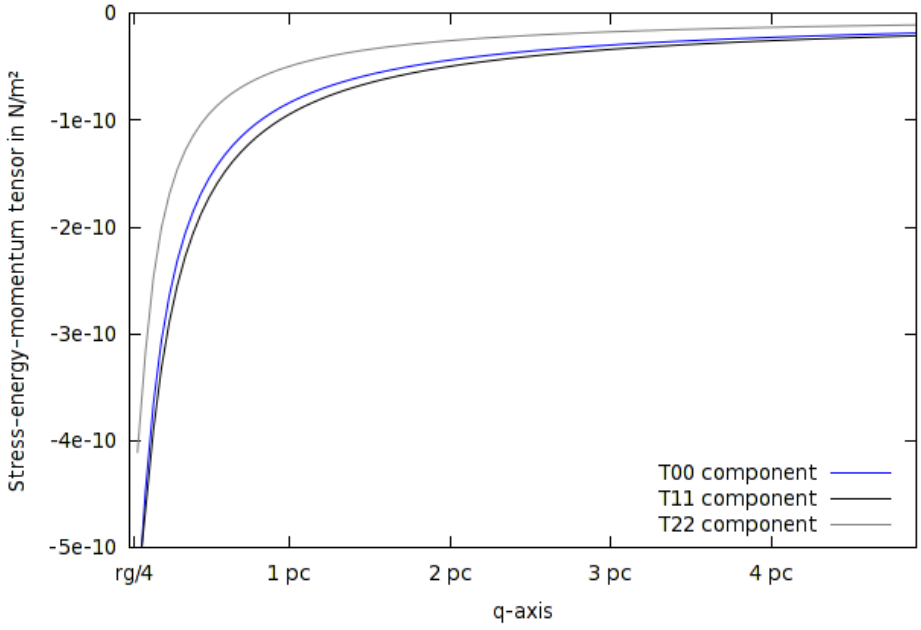

FIGURE 5.5. Stress–energy–momentum tensor for the Product-metric (5.45) with $r_g \approx 0.125\,\mathrm{pc}$, corresponding to our Local Group of galaxies. The T_k^i are negligibly small, except very close to the gravitational radius, which is located at $q = r_g/4$. They go to zero for increasing distance to the coordinate origin.

[69] $\gamma \approx 6.67 \cdot 10^{-14}\frac{\mathrm{m}^3}{\mathrm{s}^2\mathrm{g}}$, $\Lambda \approx 1.29 \cdot 10^{-52}\frac{1}{\mathrm{m}^2}$ and $c \approx 3 \cdot 10^8\frac{\mathrm{m}}{\mathrm{s}}$

5.6.1. ***Interpretation of the data.***
If we would assume that the cosmological background is filled with a perfect fluid, the functions T^q_q, T^θ_θ and T^ϕ_ϕ must coincide, i.e. $T^q_q = T^\theta_\theta = T^\phi_\phi$. These components of the stress–energy–momentum tensor represent the pressure p of the fluid. The function T^t_t/c^2 is related to the density ρ of the fluid. Appropriate to the signature of the Product-metric interval (5.45), the stress–energy–momentum tensor of a perfect cosmic fluid is given by:

$$(T^i_k) = \begin{pmatrix} c^2\rho & 0 & 0 & 0 \\ 0 & -p & 0 & 0 \\ 0 & 0 & -p & 0 \\ 0 & 0 & 0 & -p \end{pmatrix}$$

In cosmology, pressure p and energy density ρ (of a perfect fluid) are related by $p = w\rho$, where w is a dimensionless number. In our case it is $T^q_q \neq T^\theta_\theta$, and the function T^t_t/c^2, which might represent the energy-density ρ of the model universe, is not either related to T^q_q or T^θ_θ in a suitable manner. Obviously, the stress–energy–momentum tensor, which is given by (5.52), (5.53) and (5.54), corresponds to an anisotropic distribution of cosmic material, although the Product-metric provides isotropic spacetime geometry. It is uncertain what the nature of this cosmological background material is. But in fact, the graph of T^t_t in figure 5.5 indicates that a large part of this material clusters around the central mass M at the coordinate origin.

The asymptotic behavior of the T^i_k for $q \to \infty$ coincides with the de Sitter case ($r_g = 0$) where $T^i_k = 0$. Anyway, the functions T^i_k are negligibly small in the region $r_g \ll q \ll r_\Lambda$, thus the Product metric can be at least regarded as a good approximation of Einstein's empty space equations.

For the evaluation of (5.52), (5.53) and (5.54) we considered at first a system whose central mass $M = 1.3 \cdot 10^{12} M_\odot$ corresponds to that of our Local Group of galaxies. Accordingly, the gravitational radius is $r_{LG} \approx 0.125\,\mathrm{pc}$. All T^i_k remain negligibly small, except very close to $q = r_{LG}/4$. Even at $q = 1.01 r_{LG}/4$ it is

$$(5.55) \qquad \left|T^t_t\right| \approx 6 \cdot 10^{-10} \frac{\mathrm{N}}{\mathrm{m}^2}, \quad \left|T^q_q\right| \approx 7 \cdot 10^{-10} \frac{\mathrm{N}}{\mathrm{m}^2}, \quad \left|T^\theta_\theta\right| \approx 2 \cdot 10^{-9} \frac{\mathrm{N}}{\mathrm{m}^2}$$

and the magnitude of the energy density is $\left|T^t_t/c^2\right| \approx 6.6 \cdot 10^{-24} \mathrm{g/m}^3$. These values are highly stable against variations of the mass M within realistic range. For example, let $M = M_\odot$ (the mass of our sun) so that $r_g \approx 3\,\mathrm{km}$. The $\left|T^i_k\right|$ values for the corresponding distance at $q = 1.01 r_g/4 \approx 758\,\mathrm{m}$ coincide with (5.55) for at least six decimal places.

5.6.2. ***Sum-metric as first order approximation.***
As previously mentioned, an alternative method to construct an interval for the isotropic Schwarzschild-de Sitter space-time is to summate the related metric components of de Sitter and Schwarzschild metric. With respect to the shortcuts (5.46), the Sum-metric is:

$$ds^2 = (A_d + A_s - 1)\, c^2 dt^2 - (B_d + B_s - 1)\, d\sigma^2 \tag{5.56}$$

We show that (5.56) is the first order approximation of the Product-metric (5.45) $ds^2 = A_d A_s c^2 dt^2 - B_d B_s d\sigma^2$ within the region $r_g \ll q \ll r_\Lambda$:

Let $I \subseteq \mathbb{R}$ be an interval, and f_1, f_2 functions with $f_1(x) \approx 1$ and $f_2(x) \approx 1$ for all $x \in I$. Let us assume that the product $(f_1(x) - 1)(f_2(x) - 1)$ can be neglected on the interval I. As a consequence of $(f_1 - 1)(f_2 - 1) = f_1 f_2 - f_1 - f_2 + 1$ it applies

$$f_1(x)\, f_2(x) \approx f_1(x) + f_2(x) - 1 \quad \text{for all } x \in I. \tag{5.57}$$

Consequently, we have to study the terms $(A_d - 1)(A_s - 1)$ and $(B_d - 1)(B_s - 1)$. For this purpose we use the Taylor series

$$(1-x)^{-2} = 1 - 2x + \mathcal{O}\left(x^2\right) \quad \text{and} \quad (1+x)^n = 1 + nx + \mathcal{O}\left(x^2\right) \text{ for } n \in \mathbb{N}$$

see [52]. Second order terms are neglected in the following. Together with (5.46) it remains:

$$\begin{aligned} A_d - 1 &= \left(1 - \frac{q^2}{4r_\Lambda^2}\right)^2 \left(1 + \frac{q^2}{4r_\Lambda^2}\right)^{-2} - 1 \approx -\frac{q^2}{r_\Lambda^2} \\ A_s - 1 &= \left(1 - \frac{r_g}{4q}\right)^2 \left(1 + \frac{r_g}{4q}\right)^{-2} - 1 \approx -\frac{r_g}{q} \end{aligned}$$

Since $r_\Lambda \approx 5\,\mathrm{Gpc}$, the product $(A_d - 1)(A_s - 1) \approx r_g q / r_\Lambda^2$ is negligibly small. Analogously, it is:

$$\begin{aligned} B_d - 1 &= \left(1 + \frac{q^2}{4r_\Lambda^2}\right)^{-2} - 1 \approx -\frac{q^2}{2r_\Lambda^2} \\ B_s - 1 &= \left(1 + \frac{r_g}{4q}\right)^4 - 1 \approx \frac{r_g}{q} \end{aligned}$$

The product $(B_d - 1)(B_s - 1) \approx -r_g q / \left(2r_\Lambda^2\right)$ is negligibly small again. Hence, equation (5.57) holds for $g_{00} = A_d A_s c^2$ and $g_{11} = -B_d B_s$. Accordingly, we get

$$A_d A_s \approx A_d + A_s - 1 \quad \text{and} \quad B_d B_s \approx B_d + B_s - 1$$

within the region $r_g \ll q \ll r_\Lambda$ and thus finally:

$$ds^2 = A_d A_s c^2 dt^2 - B_d B_s d\sigma^2 \;\approx\; (A_d + A_s - 1)\, c^2 dt^2 - (B_d + B_s - 1)\, d\sigma^2$$

5.7. **General isotropic and spherically symmetric spacetime.**
Many astronomical observations, for example those of the cosmic microwave background radiation, indicate that the global geometry of our universe is very close to be homogeneous and isotropic. Based on coordinate transformation, we previously worked out an approximation for the isotropic Schwarzschild-de Sitter metric and proposed a suitable model, given by the Product-metric interval (5.45). An alternative approach to establish (and confirm) our preceding result is given in the following. We directly solve Einstein's equations for

$$ds^2 = c^2 e^{\xi(q,t)} dt^2 - e^{\mu(q,t)} \left(dq^2 + q^2 d\theta^2 + q^2 \sin^2\theta \, d\phi^2 \right) \tag{5.58}$$

which represents the most general form of an orthogonal, isotropic and spherically symmetric ansatz. Assuming that the content of our universe could be regarded as a cosmic fluid[70] with density ρ and pressure p, the stress-energy-momentum tensor is given by equation (2.3), i.e.

$$T_t^t = c^2\rho; \quad T_r^r = T_\theta^\theta = T_\phi^\phi = -p; \quad \text{and} \quad T_k^i = 0 \text{ for } i \neq k$$

where $\rho = \rho(t,q)$ and $p = p(t,q)$. Accordingly, Einstein's equations become

$$\frac{8\pi\gamma}{c^2}\rho = \frac{3\dot{\mu}^2 e^{-\xi}}{4c^2} - e^{-\mu}\left(\mu'' + \frac{1}{4}\mu'^2 + \frac{2}{q}\mu'\right) - \Lambda \tag{5.59}$$

$$0 = e^{-\mu}\left(\dot{\mu}' - \frac{1}{2}\dot{\mu}\xi'\right) \tag{5.60}$$

$$-\frac{8\pi\gamma}{c^4}p = \frac{e^{-\xi}}{c^2}\left(\ddot{\mu} + \frac{3}{4}\dot{\mu}^2 - \frac{1}{2}\dot{\mu}\dot{\xi}\right) - e^{-\mu}\left(\frac{\mu'\xi'}{2} + \frac{\mu'^2}{4} + \frac{\mu'+\xi'}{q}\right) - \Lambda \tag{5.61}$$

$$-\frac{8\pi\gamma}{c^4}p = \frac{e^{-\xi}}{c^2}\left(\ddot{\mu} + \frac{3}{4}\dot{\mu}^2 - \frac{1}{2}\dot{\mu}\dot{\xi}\right) - e^{-\mu}\left(\frac{\mu''+\xi''}{2} + \frac{\xi'^2}{4} + \frac{\mu'+\xi'}{2q}\right) - \Lambda \tag{5.62}$$

where overdots and primes stand for partial differentiation with respect to t and r, respectively. The corresponding calculations concerning the Einstein tensor for (5.58) are presented in the appendix, section C.

In section 3.4, we summarized the article [61], written by Israelit and Rosen in 1992. They published Einstein's equations in case of $\Lambda = 0$ for the metric (5.58). In their original paper [61], Israelit and Rosen used $c = \gamma = 1$ and the different notation $G_k^i = -\frac{8\pi\gamma}{c^4}T_{ik}$. Correspondingly, the Ricci tensor has to be $R_{nk} := R^a_{\ ank}$ and the result for the Einstein tensor is opposite in sign.

[70] This should be a good approximation on a scale large

5.7.1. ***The system of differential equations.***
A line element, which represents a homogeneous, isotropic and spherically symmetric spacetime, needs to fulfill Einstein's equations (5.59) to (5.62). As mentioned above, the main goal is to confirm our preceding result for the isotropic Schwarzschild-de Sitter metric. For this purpose, it is adequate to consider a system consisting of equations (5.59) and (5.60) which can be written as:

$$\left(\mu'' + \frac{1}{4}\mu'^2 + \frac{2}{q}\mu'\right) e^{-\mu} = \frac{3\dot{\mu}^2 e^{-\xi}}{4c^2} - \Lambda - \frac{8\pi\gamma}{c^2}\rho \tag{5.63}$$

$$\left(\dot{\mu}' - \frac{1}{2}\dot{\mu}\xi'\right) e^{-\mu} = 0 \tag{5.64}$$

Let α be a function which depends on the time t solely. Equation (5.64) is fulfilled if the time derivative of μ is related to ξ by

$$\dot{\mu} = \alpha(t) \exp\left(\frac{1}{2}\xi\right). \tag{5.65}$$

This is easy to confirm, since the derivative of equation (5.65) with respect to the spatial coordinate q reads

$$\dot{\mu}' = \frac{1}{2}\xi'\alpha(t) \exp\left(\frac{1}{2}\xi\right) = \frac{1}{2}\xi'\dot{\mu}.$$

We use (5.65) in equation (5.63) and get

$$\mu'' + \frac{1}{4}\mu'^2 + \frac{2}{q}\mu' = \left(\frac{3\alpha^2(t)}{4c^2} - \Lambda - \frac{8\pi\gamma}{c^2}\rho\right) e^{\mu}. \tag{5.66}$$

Coordinate transformations
In order to simplify the differential equation, we transform to the coordinate

$$y = e^{\frac{\mu}{4}}. \tag{5.67}$$

It is $\mu = 4\ln y$, the first and second derivative of μ is given by

$$\mu' = 4\frac{y'}{y}, \quad \text{and} \quad \mu'' = 4\frac{y''}{y} - 4\left(\frac{y'}{y}\right)^2.$$

Equation (5.66) transforms into

$$y'' = -\frac{2}{q}y' + \frac{1}{4}\left(\frac{3\alpha^2(t)}{4c^2} - \Lambda - \frac{8\pi\gamma}{c^2}\rho\right) y^5. \tag{5.68}$$

Additionally, we use again the u coordinate given by $q = r_g e^u$, which was previously introduced for the numerical approximation of isotropic Schwarzschild-de Sitter

coordinates, see (5.38). It applies $dq = r_g e^u du$ and therewith:

$$\begin{aligned} y' &= \frac{dy}{dq} = \frac{dy}{r_g e^u du} \\ y'' &= \frac{d}{dq}\left[\frac{dy}{dq}\right] = \frac{d}{r_g e^u du}\left[\frac{dy}{r_g e^u du}\right] = \frac{1}{r_g^2 e^{2u}}\left(\frac{d^2y}{du^2} - \frac{dy}{du}\right) \end{aligned}$$

Accordingly, equation (5.68) transforms into:

$$\frac{d^2y}{du^2} = -\frac{dy}{du} + \frac{r_g^2}{4}\left(\frac{3\alpha^2(t)}{4c^2} - \Lambda - \frac{8\pi\gamma}{c^2}\rho\right) y^5 e^{2u} \tag{5.69}$$

Let us now introduce the abbreviation

$$K = K(t,u) := \frac{r_g^2}{4}\left(\frac{3\alpha^2(t)}{4c^2} - \Lambda - \frac{8\pi\gamma}{c^2}\rho\right). \tag{5.70}$$

Finally, our second order differential equation reads

$$\frac{d^2y}{du^2} = -\frac{dy}{du} + K(t,u)\, y^5 e^{2u}. \tag{5.71}$$

This equation can be reformulated to the equivalent first-order system

$$\frac{dy}{du} = z, \qquad \frac{dz}{du} = -z + K(t,u)\, y^5 e^{2u}. \tag{5.72}$$

5.7.2. ***Initial conditions.***

Consider again a gravitationally bound system, which is embedded in an expanding cosmological background. Let us assume that the gravitationally bound system can be regarded as a point mass at the coordinate origin. Presuming that the spacetime is of Schwarzschild type in the neighborhood of the central mass point, we determine the initial values for our numerical solution from Schwarzschild's isotropic interval (5.26) where

$$y^4 = e^{\mu} = \left(1 + \frac{r_g}{4q}\right)^4.$$

With respect to the $u = \ln(q/r_g)$ coordinate we get:

$$y_0 := 1 + \frac{r_g}{4q_0} = 1 + \frac{1}{4}e^{-u_0} \quad \text{and} \quad z_0 := \left.\frac{dy}{du}\right|_{u_0} = -\frac{1}{4}e^{-u_0}$$

Now we can approximate further points $\left(u \mid y^4\right)$ and plot the graph of the g_{11} tensor component for a constant time. Since we used the transformation (5.67) and $q = r_g e^u$ it applies $y^4 = \exp\left[\mu\left(q(u), t_0\right)\right] = g_{11}(u, t_0)$ where t_0 is a time constant.

5.8. **Results of the numerical approximation.**
We approximated the system of differential equations (5.72) with the fourth order Runge Kutta method in case of K =constant. Algorithm 10, which is given in appendix D.3, can be used to calculate the points $\left(u \mid y^4\right)$. For the numerical calculations the mass parameter is set to $M = 2.6 \cdot 10^{45}$g (mass of the Local Group).

Consider at first the case $\alpha = 0$ and $\rho = 0$. The K parameter reduces to

$$K = -\frac{r_g^2}{4}\Lambda = -\frac{3}{4}\left(\frac{r_g}{r_\Lambda}\right)^2 \tag{5.73}$$

see (5.70), and we get $\dot{\mu} = 0$ directly from equation (5.65). In this case we get back the isotropic Schwarzschild-de Sitter solution. Figure 5.6 shows, that the numerical

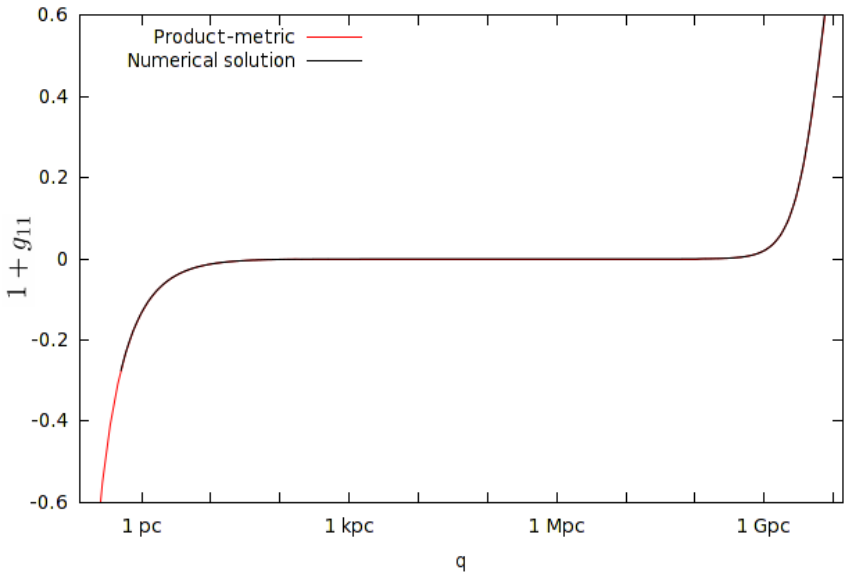

FIGURE 5.6. $f = 1+g_{11}$ for the Product metric in comparison with the corresponding numerical result $f = 1-e^u$. The mass parameter is set to $M = 2.6 \cdot 10^{45}$g, which is the mass of our Local Group. Correspondingly, the gravitational radius is $r_{LG} \approx 0.125\,\mathrm{pc}$. We obtain the Schwarzschild-de Sitter case from equation (5.72) with $K = -0.75\left(r_{LG}/r_\Lambda\right)^2 \approx -4.8 \cdot 10^{-22}$.

result for $e^\mu = -g_{11}$ coincides quite good with our isotropic Schwarzschild-de Sitter approximation P, which is given by

$$e^\mu = P(u) := \left[1 + \frac{1}{4}\exp(-u)\right]^4 \left[1 + \frac{1}{4}\left(\frac{r_g}{r_\Lambda}\right)^2 \exp(2u)\right]^{-2} \tag{5.74}$$

see (5.44). In subsection 5.6, the Product-metric (5.45)

$$ds^2 = \left(\frac{1 - \frac{r_g}{4q}}{1 + \frac{r_g}{4q}} \cdot \frac{1 - \frac{q^2}{4r_\Lambda^2}}{1 + \frac{q^2}{4r_\Lambda^2}} \right)^2 c^2 dt^2 - \left(1 + \frac{r_g}{4q} \right)^4 \left(1 + \frac{q^2}{4r_\Lambda^2} \right)^{-2} d\sigma^2$$

was introduced as a good approximation for the isotropic Schwarzschild-de Sitter model. As before, we plot again $f = 1 + g_{11}$ instead of g_{11}. Based on the Product metric we directly obtain an approximation for ξ. With respect to the coordinate transformation $q = r_g e^u$ it remains

$$e^\xi = \left[\frac{1 - \frac{1}{4}\exp(-u)}{1 + \frac{1}{4}\exp(-u)} \cdot \frac{1 - \frac{1}{4}\left(\frac{r_g}{r_\Lambda}\right)^2 \exp(2u)}{1 + \frac{1}{4}\left(\frac{r_g}{r_\Lambda}\right)^2 \exp(2u)} \right]^2 \tag{5.75}$$

The equations (5.74) and (5.75) represent a good approximate solution for Einstein's empty space equations with $\dot{\mu} = 0$. The latter considerations did not lead to another new solution, but they confirmed our preceding results. It is interesting that one obtains an isotropic Schwarzschild-de Sitter model on the one hand by coordinate transformation (section 5.3) and on the other hand directly from Einstein's equations.

Even at (theoretical) distances, much larger than the radius of the observable universe ($r \sim 4\,\mathrm{Gpc}$), our numerical result fits perfect to the g_{11} component of the Product-metric. The solution passes over into de Sitter's exact solution for large q:

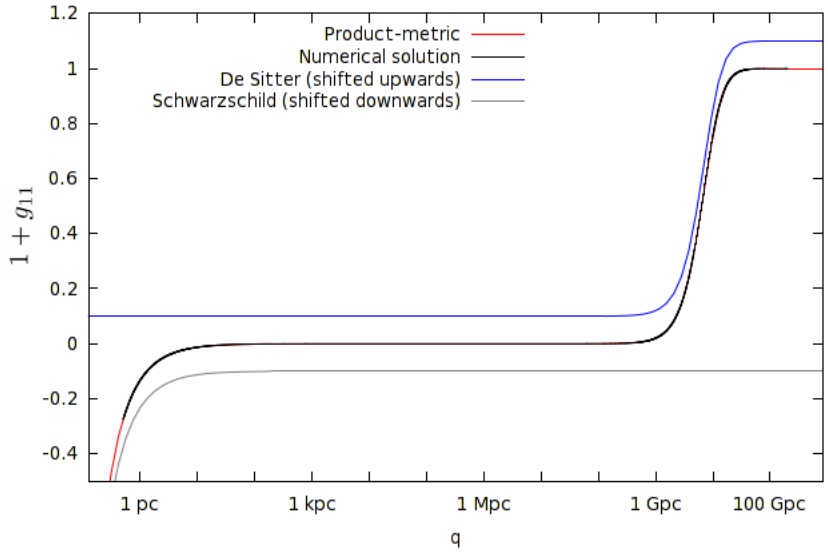

FIGURE 5.7. Behavior of $f = 1 + g_{11}$ for large q. The gravitational radius is $r_{LG} \approx 0.125\,\mathrm{pc}$.

5.9. **Influence of the K parameter.**

In the following we allow a nonzero density, but our considerations are still restricted to the assumption that K does not depend on the u coordinate. Our numerical solutions are based on the differential equation[71]

$$\frac{d^2y}{du^2} = -\frac{dy}{du} + Ky^5e^{2u}, \quad \text{where} \quad K = \frac{r_g^2}{4}\left(\frac{3\alpha^2}{4c^2} - \Lambda - \frac{8\pi\gamma}{c^2}\rho\right) \tag{5.76}$$

respectively on the corresponding first order system (5.72). Equation (5.76) can be solved for different K parameters in order to study the parameter's influence of the model spacetime. We already presented the $\alpha = 0$, $\rho = 0$ case, where $K = -0.75\,(r_{LG}/r_\Lambda)^2$, see figure 5.6 and 5.7. Figure 5.7 indicates that the image of our solution can be roughly divided into four major zones: Initially, the values are distinctly increasing (first region). In the second region the values are impalpably increasing, apparently the solutions resemble a horizontal line. After that, the values are notably increasing again (third region). Finally, at distances exceeding the radius of the observable universe, the slope tends to zero (fourth region). The fourth region is only of theoretical interest. In the following we study the influence of K with regard to the first three areas. Figure 5.8 shows some results. Our solutions coincide within the first region. The extent of the second region is

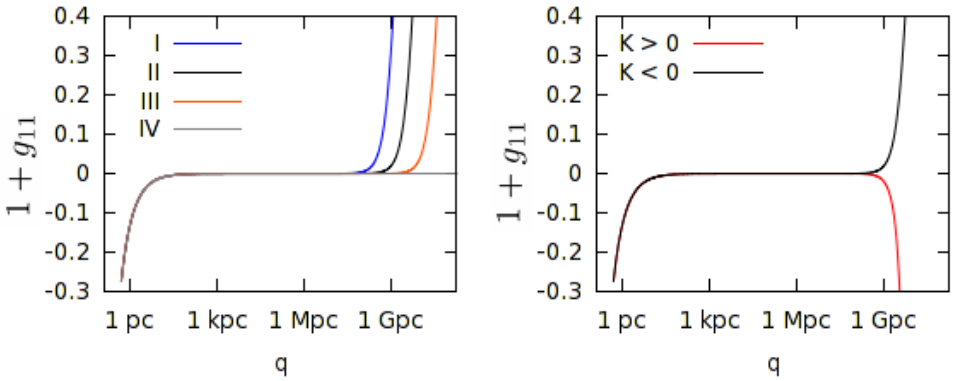

FIGURE 5.8. Solutions of (5.76) for sundry K in comparison to $K = -0.75\,(r_{LG}/r_\Lambda)^2 \approx -4.8 \cdot 10^{-22}$ (Schwarzschild-de Sitter). $K = 0$ represents Schwarzschild's solution. On the left side:
I) $K = -10^{-20}$ II) $K \approx -4.8 \cdot 10^{-22}$ III) $K = -10^{-23}$ IV) $K = 0$
The second graphic shows the solutions for $K = \pm 0.75\,(r_{LG}/r_\Lambda)^2$.
The gravitational radius is again $r_{LG} \approx 0.125\,\text{pc}$ (Local Group).

determined by K. The smaller $|K|$, the larger is the second area. In the $K = 0$ Schwarzschild case, the second region is extended to infinity. If K falls appreciably

[71] It is $y = \sqrt[4]{g_{11}}$ and $u = \ln(q/r_g)$

short of $-0.75\,(r_{LG}/r_\Lambda)^2$, we obtain a different graph which is dominated by the third region. At several orders of magnitude lower[72] algorithm 10 generates oscillating solutions, whose amplitude tends to zero rapidly for increasing distance u. But these oscillations appear to be artifacts of the numerical calculations, since they are not reproducible with a fourth order Runge Kutta program in Maple. If K takes small positive values, for example $K = 0.75\,(r_{LG}/r_\Lambda)^2$, the solution resembles the corresponding $K < 0$ case within the first two regions, but decreases at the third area.

5.9.1. ***Discussion of the results***.
We compare our results with the $K = -0.75\,(r_{LG}/r_\Lambda)^2$ Schwarzschild-de Sitter case in the following. The K parameter in (5.76) is determined by the cosmological constant Λ, the density ρ and the value of the function α, which was introduced in equation (5.65). Higher values of Λ cause smaller values of K. Accordingly, the influence of Λ becomes more important at medium and small distances, the second region shrinks in size. But this is a trivial interpretation. Besides that, the value of the cosmological constant is very well known, cf. [63].

Surprisingly, a nonzero density affects the K parameter in the same way. As consequence of $\rho > 0$ it follows $K < -0.75\,(r_{LG}/r_\Lambda)^2$. Our numerical result indicates that in a model with a higher density, the influence of the cosmological constant increases 'earlier', i.e. closer to the coordinate origin. In fact, one would expect that ρ acts in an opposite manner. This would happen if ρ is replaced by $-\rho$ in (5.59) or if Λ is replaced by $-\Lambda$, but the above convention in Einstein's equations (5.59) to (5.62) is in accordance with all other results, see for example Friedmann's equations[73] in subsection 2.1, which lead to the ansatz for the ΛCDM model, subsection 2.6. On the other hand, our numerical result resembles the g_{11} component of the Schwarzschild-de Sitter interval, which is an empty-space solution of Einstein's equations. Hence, it seems probable that $\rho = 0$ has to be assumed anyway.

Obviously, α can antagonize the repulsive effect. If $-0.75\,(r_{LG}/r_\Lambda)^2 < K < 0$ the effect increases 'later', i.e. at a greater distance to the origin (as compared to the $K = -0.75\,(r_{LG}/r_\Lambda)^2$ Schwarzschild-de Sitter case). The $K = 0$ case represents Schwarzschild's solution.

---

[72] For example $K = -3$

[73] With $e^\xi = 1$ and $e^\mu = a^2\,(t)$ Einstein's equations (5.59) to (5.62) reduce to $\frac{3}{c^2}\left(\frac{\dot a}{a}\right)^2 - \Lambda = \frac{8\pi\gamma}{c^2}\rho$ and $\frac{1}{c^2}\left[2\frac{\ddot a}{a} + \left(\frac{\dot a}{a}\right)^2\right] - \Lambda = -\frac{8\pi\gamma}{c^4}p$. We obtain the same equations for the spatially flat FLRW model from (2.4) and (2.5).

6. Expansion versus Gravitation

Dark energy is the most popular explanation for the accelerating expansion of our universe. It turned out that the antigravity effect of dark energy can be modeled by assuming a positive cosmological constant. Since gravitationally bound systems, like our Local Group for example, do not individually expand, there must be a surface where gravitational attraction and the repulsive force reach equilibrium. This region is called 'zero-gravity surface'. A. D. Chernin introduced a method to estimate the radius of the zero-gravity surface: "*In a simple model, a* [galaxy-] *group may be represented by a spherical mass M of dark matter and baryons, embedded in the uniform dark energy background. Out of the mass at a distance R from the mass center, the gravity force is given by Newton's inverse square law in the reference frame related to the group barycenter. The antigravity force produced by the DE density v is given by Einstein's linear law*" [26]. According to Chernin et. al., gravitational force $F_N = -\gamma M/r^2$ (force per unit mass) and antigravity $F_E = \frac{8\pi}{3}\gamma\rho_\Lambda r = H_0^2\Omega_\Lambda r$ are exactly balanced at the zero-gravity surface of $R = R_v$. The same idea is used in [57]: "[...] *the local gravity field around the LG* [Local Group] *can be decomposed into the contribution of the LG, modeled as a point particle, and the contribution of the DE* [Dark Energy]". The radius R_v of the zero-gravity surface is given by $gpp\,(R_v) = 0$ where $gpp\,(r) = -\frac{\gamma M}{r^2} + H_0^2\Omega_\Lambda r$, cf. [57]. The radius R_v is the solution of

$$0 = -\frac{\gamma M}{R_v^2} + H_0^2\Omega_\Lambda R_v \tag{6.1}$$

and thus given by

$$R_v = \sqrt[3]{\frac{\gamma M}{H_0^2\Omega_\Lambda}}. \tag{6.2}$$

Consequently, our Local Group with $M = 1.3 \cdot 10^{12} M_\odot$ has a zero-gravity surface at a radius of $R_v \approx 1.15\,\mathrm{Mpc}$.

Interestingly, the value R_v represents a local maximum of $\alpha\,(r) = 1 - \frac{r_g}{r} - \left(\frac{r}{r_\Lambda}\right)^2$ in the Schwarzschild-de Sitter case, see metric (2.40). In the following it is shown that $g_{00} = c^2\alpha$ and $g_{11} = -\alpha^{-1}$ have a local maximum, which is located at the radius of zero-gravity, proposed by the above mentioned model. Furthermore, we study our 'Product-metric' model concerning the interaction of gravitation and expansion. It turned out, that the inflection point of g_{11} largely coincides with the zero-gravity radius, corresponding to M_{LG}.

6.1. **'Zero-gravity surface' in Schwarzschild-de Sitter spacetime.**
Evidently, the zero-gravity surface in a Schwarzschild-de Sitter model has to be spherically symmetric, since the spacetime is spherically symmetric. Thus we may presume θ, ϕ =constant, so that the line element (2.40) reduces to

$$ds^2 = \alpha(r)\, c^2 dt^2 - \alpha^{-1}(r)\, dr^2. \tag{6.3}$$

where $\alpha(r) = 1 - \frac{r_g}{r} - \left(\frac{r}{r_\Lambda}\right)^2$. As shown before in subsection 2.8.2, the function $\alpha(r)$ has a local maximum at

$$r_* = \left(\frac{1}{2} r_g r_\Lambda^2\right)^{\frac{1}{3}}.$$

Therefore $g_{00} = c^2\alpha$ and as a consequence $g_{11} = -\alpha^{-1}(r)$ have a local maximum at r_* too[74]. Since both components g_{00} and g_{11} have a local maximum at r_*, this point represents a local maximum for the interval (6.3).

The preceding considerations correspond to the interval (2.40), which has the signature $(1 \mid 3)$. Alternatively, a Schwarzschild-de Sitter model with signature $(3 \mid 1)$ is given by

$$ds^2 = -\alpha(r)\, c^2 dt^2 + \alpha^{-1}(r)\, dr^2 + r^2 d\theta^2 + r^2 \sin^2\theta\, d\phi^2.$$

Evidently, g_{00} and g_{11} have a local minimum instead of a maximum in this case.

If we use the definitions

$$r_g = \frac{2\gamma M}{c^2}, \quad r_\Lambda = \sqrt{\frac{3}{\Lambda}}, \quad \Omega_\Lambda = \frac{c^2\Lambda}{3H_0^2}$$

it is easy to show that r_* is equal to the radius R_v of the zero-gravity surface:

$$r_*(M) = R_v = \left(\frac{\gamma M}{H_0^2 \Omega_\Lambda}\right)^{\frac{1}{3}} \tag{6.5}$$

Obviously, the zero-gravity radius R_v is proportional to the cube root of the mass M.

---

[74]The necessary condition is given by $\alpha'(r) = 0$ since $g'_{11} = \frac{\alpha'(r)}{\alpha(r)^2}$. We already know that $\alpha'(r) = 0$ is fulfilled at $r_* = \left(\frac{1}{2} r_g r_\Lambda^2\right)^{\frac{1}{3}}$. For the second derivation we get

$$g''_{11} = \frac{\alpha''(r)\,\alpha(r) - 2\alpha'^2(r)}{\alpha^3(r)}. \tag{6.4}$$

If we use the necessary condition $\alpha'(r) = 0$ in (6.4) it remains

$$g''_{11}(\alpha' = 0) = \frac{\alpha''(r)}{\alpha^2(r)}.$$

It applies $\alpha^2(r_*) > 0$ and $\alpha''(r_*) = -6/r_\Lambda^2 < 0$. Thus we have $g''_{11}(r_*) < 0$.

6.2. **Considerations based on the Product-metric model.**
In this section we study the predictions of our 'Product-metric' (5.45), regarding the expansion of a spacetime. At first we consider again a gravitationally bound system with a central mass similar to that of our Local Group, $M_{LG} = 2.6 \cdot 10^{45}$g. It turned out, that the inflection point of g_{11} largely coincides with the zero-gravity radius, corresponding to M_{LG}. Finally, we apply our method to the data for the Virgo cluster.

The Product-metric (5.45) in subsection 5.5 depends on the q coordinate. Naturally, we are more accustomed to deal with the r coordinate, which directly represents the distance[75] to the coordinate origin. Hence, we consider the g_{11} function graph which consists of the points $P_n\left(x_n \mid -\exp^2\left(x_n - u_n\right)\right)$ in the following, i.e. we deal with $B = B\left(u\left(x\right)\right)$. The $P = -g_{11}$ component of our Product-metric (5.45) is the product of the B_d and B_s functions, which represent the de Sitter and the Schwarzschild case, i.e. $P := B_s \cdot B_d$. Thus, we transform the B_d and B_s functions for de Sitter and Schwarzschild case to u and x coordinates at first.

Transformation in the Schwarzschild case
According to (5.41), one has:

$$e^u = \frac{1}{2}e^x - \frac{1}{4} + \frac{1}{2}\sqrt{e^{2x} - e^x}$$

From equation (5.40) we get:

$$B_s = \left(\frac{e^x}{e^u}\right)^2 = \left(\frac{e^x}{\frac{1}{2}e^x - \frac{1}{4} + \frac{1}{2}\sqrt{e^{2x} - e^x}}\right)^2 = \frac{4}{\left(1 - \frac{1}{2}e^{-x} + \sqrt{1 - e^{-x}}\right)^2} \tag{6.6}$$

Transformation in the de Sitter case
The relation between q and r is given by (5.35) in the de Sitter case. We rewrite this equation:

$$q = \frac{2r_\Lambda}{\frac{r_\Lambda}{r} + \sqrt{\left(\frac{r_\Lambda}{r}\right)^2 - 1}} = \frac{2}{\frac{1}{r} + \sqrt{\frac{1}{r^2} - \frac{1}{r_\Lambda^2}}} = \frac{2r_g}{\frac{r_g}{r} + \sqrt{\left(\frac{r_g}{r}\right)^2 - \left(\frac{r_g}{r_\Lambda}\right)^2}}.$$

With the transformations $q = r_g e^u$ and $r = r_g e^x$ this equation reads

$$e^u = \frac{2}{e^{-x} + \sqrt{e^{-2x} - \left(\frac{r_g}{r_\Lambda}\right)^2}}. \tag{6.7}$$

[75] In order to avoid problems with the singularity, we may define this distance with respect to the sphere around the origin whose surface area is $4\pi r^2$.

Now we use again (5.40) and obtain:

$$B_d = \left(\frac{e^x}{e^u}\right)^2 = \frac{1}{4}\left\{1 + \sqrt{1 - \left(\frac{r_g}{r_\Lambda} e^x\right)^2}\right\}^2 \tag{6.8}$$

Transformation of the Product-metric

Together with (6.6) and (6.8) we obtain the function $P = -g_{11}$, which represents a good approximation for the isotropic Schwarzschild-de Sitter case, by

$$P(x) := B_s(x) \cdot B_d(x) = \left(\frac{1 + \sqrt{1 - \left(\frac{r_g}{r_\Lambda} e^x\right)^2}}{1 - \frac{1}{2}e^{-x} + \sqrt{1 - e^{-x}}}\right)^2 . \tag{6.9}$$

In order that Gnuplot displays the values on the vertical axis with adequate accuracy, we plot again $f = 1 + g_{11}$ instead of g_{11}. A Gnuplot script to generate the following graphic is given in the appendix, algorithm 7.

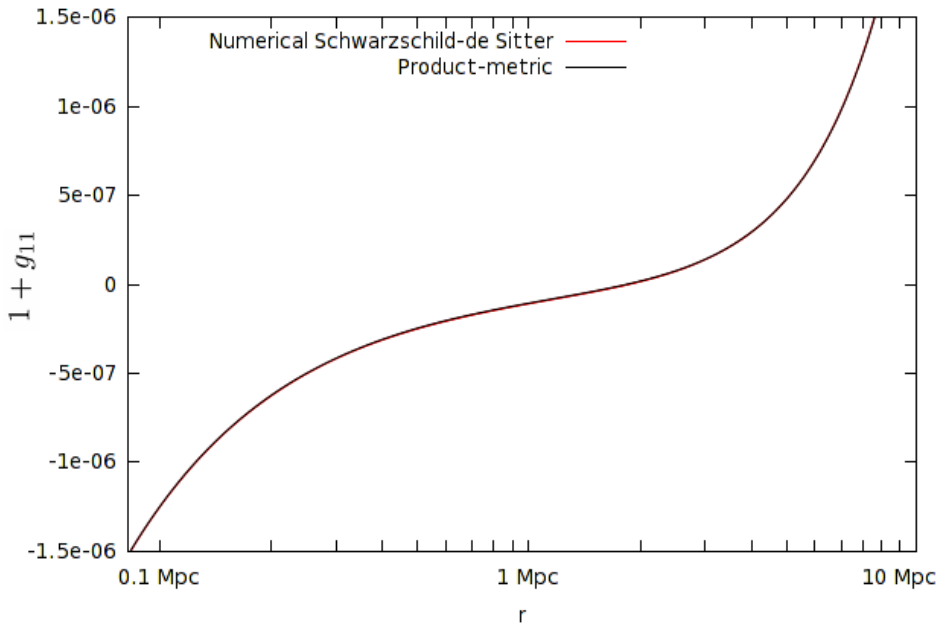

FIGURE 6.1. $f = 1 + g_{11}$ with respect to the r coordinate, evaluated in the neighborhood of the inflection point at $\sim 1\,\text{Mpc}$. r represents the distance to the coordinate origin. The graphic shows the numerical result in comparison to the Product-metric for a central mass of $M = 1.3 \cdot 10^{12} M_\odot$ (Local Group). Correspondingly, the gravitational radius is $r_{LG} \approx 0.125\,\text{pc}$.

Figure 6.1 reconfirms that the Product-metric approximates the Schwarzschild-de Sitter case with high accuracy. Further it shows that there is an inflection point of P located at $r \sim 1\,\mathrm{Mpc}$.

6.2.1. *Inflection point.*

We presume that the Schwarzschild-de Sitter case is given by (6.9), which is at least a high-precision approximation. Based on this assumption, it is possible to determine the location of the inflection point more exactly. Let the central mass be similar to that of our Local Group $M_{LG} = 1.3 \cdot 10^{12} M_\odot$ again. With the help of Maple[76] we solved $P''(x) = 0$, the necessary condition for an inflection point. Our Maple-result $x \approx 16.04$ has to be retransformed by $r = r_g e^x$ where $r_g \approx 0.125\,\mathrm{pc}$ is the gravitational radius of M_{LG}. We get:

$$r \approx 1.15\,\mathrm{Mpc} \tag{6.10}$$

The location of the inflection point in figure 6.1 largely[77] coincides with the radius

$$R_v = \left(\frac{\gamma M}{H_0^2 \Omega_\Lambda} \right)^{\frac{1}{3}}$$

of the zero-gravity sphere, see (6.5). The disparity is roughly $\sim 0.1\,\mathrm{pc}$ and therewith at the order of $10^{-5}\,\%$. Conceivably, this method is appropriate to determine the radius of the zero-gravity surface. But it should be remarked that the results do not vary significantly from the results of Chernin's method.

6.2.2. *Virgo Cluster test.*

We analyze a system whose central mass is similar to that of the Virgo Cluster. 2010 Chernin et. al. published in [27] an estimation for the zero-gravity radius (here R_{ZG}): "*According to various estimates (Sect.2), the total mass of the Virgo cluster is* 1–2 *times the virial mass:* $M = (0.6\text{–}1.2) \times 10^{15} M_\odot$. *Then the known global* ρ_Λ *gives* $R_{ZG} = (9\text{–}11)\mathrm{Mpc}$." For the lower bound $M = 0.6 \cdot 10^{15} M_\odot$ the inflection point of $P(x)$ is located at 8.90 Mpc, for the upper bound $M = 1.2 \cdot 10^{15} M_\odot$ we obtain 11.21 Mpc. This is in good accordance with the results given in [27].

---

[76] The "*fsolve*" Maple command is appropriate to search for a numerical solution in a specified region. We used the maple source (define the values for rg=r_g and rL=r_Λ before):
BS := 4/(1-.5*exp(-x)+sqrt(1-exp(-x)))^2;
BD := .25*(1+sqrt(1-(rg*exp(x)/rL)^2))^2;
B := BS*BD;
fsolve(diff(B, x, x) = 0, x = 16);

[77] more precise $r \approx 1.151752464\,\mathrm{Mpc}$ and $R_v \approx 1.151752340\,\mathrm{Mpc}$

7. The ΛCDM Swiss-Cheese model

Consider an expanding (quasi-) FLRW universe with slight density inhomogeneities. Dense regions contract, as a consequence of gravity, and under-dense regions expand. Material starts clumping together, and gravitation "evacuates" the surrounding area, empty intermediate spaces emerge. This section concerns a FLRW cosmological model, which contains a static Schwarzschild-de Sitter region. A spherical region of cosmic fluid is replaced by a compact mass condensation at the coordinate origin, which is surrounded by an empty cavity. A similar model for $\Lambda = 0$ was previously suggested by Einstein and Straus in [37]. As mentioned in section 3.2, they proved that such a solution exists, but they did not give an explicit solution for the problem they posed. Schücking resumed the work of Einstein and Straus in [105]. He established the metric (3.14) by modifying the g_{00} component of Schwarzschild's field (2.29). His solution (3.14) describes the interior region of the Einstein-Straus model, so that the time coordinate of the interior field is matched to the cosmological time. Balbinot, Bergamini and Comastri extended Schücking's model to the case of a nonzero cosmological constant in [5]. As Carrera and Giulini pointed out in 2009, "*the matched solution* [Swiss Cheese model] *is really such that for radii smaller than a certain matching radius* [...] *it is exactly given by the Schwarzschild solution (exterior for a black hole, exterior plus interior for a star) and for radii above this radius it is exactly given by a FLRW universe*" [20].

In [91], Peebles also studied the embedding of a static gravitational field in an expanding cosmology, see section 3.5. He stuck together Schwarzschild's field (2.29) and the FLRW field (2.1) by matching of the time and the vacuole radius with respect to both coordinate systems, in order to get a relation between the mass of the evacuated cosmic material and the mass condensation. Peebles assumed $\Lambda = 0$, which contradicts to recent observations, see [63].

We extend Peebles' approach and establish a differential equation for the matching radius R in a ΛCDM Swiss Cheese model. Further, we solve the differential equation and study the expansion of the static field's boundary. In section 7.6, the results will be used to investigate the influence of Λ on galaxies, clusters and voids. As Carrera and Giulini noticed "[...] *the Swiss-Cheese model cannot apply at the scale of stars in galaxies*", since the vacuole radius corresponding to a single solar mass is "*almost two orders of magnitude larger than the average distance of stars in our Galaxy.* [...] *This changes as one goes to larger scales.*" [20].

7.1. **Matching condition for the ΛCDM Swiss-Cheese model.**
An expanding cosmological model which contains a static region (bounded by a sphere) is commonly called "Swiss-Cheese" model, cf. [23]. A spherical region of a cosmological model, as for instance the ΛCDM model, is evacuated and replaced by a compact mass condensation at the center, which is surrounded by an empty cavity. Conceivably, the ΛCDM Swiss-Cheese model is suitable to describe the cosmic voids in the large scale structure of our universe, see for example [16, 111]. Capozziello, Funaro and Stornaiolo proposed in 2004: "[...] *in the center of each void there is a black hole whose mass M compensates the mass which the void would have if it were completely filled with matter having a cosmological density.*" [16]. Observations of the Sloan Digital Sky Survey confirm that cosmic voids were emptied by gravity. In 2008 Tinker et al. found "*that the sizes and emptiness of observed voids are in excellent agreement with straightforward theoretical predictions.*" [116]. Figure 7.1 illustrates the construction of a Swiss-Cheese model. The following considerations are concerned with the matching of local Schwarzschild-de Sitter geometry and global FLRW geometry in the ΛCDM Swiss-Cheese model. Each Schwarzschild-de Sitter coordinate r can be associated with a comoving FLRW coordinate $\overline{r}$. We match the radius of the evacuated sphere with respect to both coordinate systems. Then we match the times, measured in Schwarzschild-de Sitter and FLRW coordinates. The time is universal within the FLRW system. In Schwarzschild-de Sitter coordinates, the running of the clock depends on the r coordinate. Consequently, the matching of time is possible only for a given radius R. This determines the radius of the Schwarzschild-de Sitter sphere, which depends on the mass M of the inclosed material, i.e. $R = R(M)$. Inside the cavity, spacetime is given by the static Schwarzschild-de Sitter interval

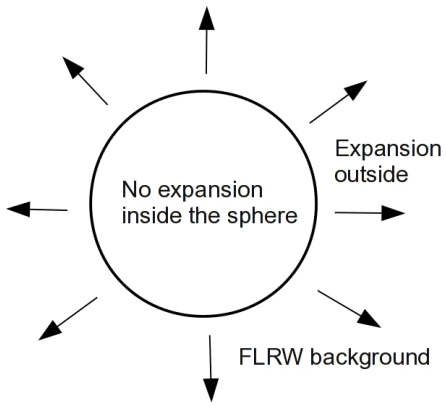

FIGURE 7.1.
Swiss-Cheese model.

$$ds^2 = \alpha(r)\, c^2 dt^2 - \alpha^{-1}(r)\, dr^2 - r^2 d\theta^2 - r^2 \sin^2\theta\, d\phi^2 \tag{7.1}$$

where $\alpha(r) = 1 - \frac{r_g}{r} - \frac{1}{3}\Lambda r^2$. Due to the WMAP data [63] we assume that the space-time outside the cavity is spatially flat. Correspondingly, the outer field is:

$$ds^2 = c^2 d\overline{t}^2 - a^2\left(\overline{t}\right)\left(d\overline{r}^2 + \overline{r}^2 d\theta^2 + \overline{r}^2 \sin^2\theta\, d\phi^2\right) \tag{7.2}$$

Let us assume that $R(t)$ represents the radius of that sphere with respect to the Schwarzschild-de Sitter coordinates (7.1) and that $\overline{R}$ denotes the fixed comoving radius of that sphere with respect to the FLRW coordinates (7.2). $R(t)$ and the comoving coordinate $\overline{R}$ are related by $R(t) = a\left(\bar{t}\right)\overline{R}$, where $a\left(\bar{t}\right)$ is the scale factor of the cosmological background. Consequently, it is

$$a\left(\bar{t}\right) = \frac{R(t)}{\overline{R}}. \tag{7.3}$$

Matching of the clocks is done by comparing the velocity of a point on the edge of the cavity. Derivation of (7.3) with respect to the time coordinate $\bar{t}$ and division by $a\left(\bar{t}\right)$ leads to:

$$\frac{1}{a}\frac{da}{d\bar{t}} = \frac{1}{a}\frac{d}{d\bar{t}}\left[\frac{R(t)}{\overline{R}}\right] = \frac{1}{a\overline{R}}\frac{dR}{dt}\frac{dt}{d\bar{t}} = \frac{1}{R}\frac{dR}{dt}\frac{dt}{d\bar{t}}$$

Now square both sides to get back the left side of Friedmann's equation (2.4):

$$\left(\frac{1}{a}\frac{da}{d\bar{t}}\right)^2 = \frac{1}{R^2}\left(\frac{dR}{dt}\right)^2\left(\frac{dt}{d\bar{t}}\right)^2 \tag{7.4}$$

In 7.1.1, we will use (7.4) to establish a matching condition for the interior field (7.1) and the exterior field (7.2). As Balbinot, Bergamini and Comastri pointed out, "*the matching takes place along the world line of a typical comoving observer* [...]" [5]. This trajectory is free falling in both coordinate systems and thus a geodesic line[78]. For a geodesic line, there exists the proper time τ, which is analogous to the arc length of the curve[79].

Lemma 14.
Consider a geodesic line in a model universe, which is given by (2.31):

$$ds^2 = \alpha(r)\,c^2dt^2 - \beta(r)\,dr^2 - r^2d\theta^2 - r^2\sin^2\theta\,d\phi^2$$

Then there exists a constant $1/\sqrt{E}$ *of geodesic motion, so that*

$$\alpha(r)\frac{dt}{ds} = \frac{1}{\sqrt{E}} \tag{7.5}$$

where s *is related to the proper time* τ *by* $s = c\tau$*, and* t *is the coordinate time.*

Proof. Let $x^m \in \{t, r, \theta, \phi\}$, the geodesic equations are

$$\frac{d^2x^m}{ds^2} + \Gamma^m_{ik}\frac{dx^i}{ds}\frac{dx^k}{ds} = 0 \tag{7.6}$$

[78] World lines of free-falling objects are geodesic lines.
[79] With $ds^2 = c^2d\tau^2$ one has $\tau = \frac{1}{c}\int ds = \frac{1}{c}\int\sqrt{g_{ik}dx^idx^k}$.

cf. [91]. Since $\Gamma^0_{01} = \Gamma^0_{10} = \frac{1}{2\alpha}\frac{d\alpha}{dr}$ and otherwise $\Gamma^0_{ik} = 0$, equation (7.6) with $m = 0$ yields

$$0 = \frac{d^2t}{ds^2} + \frac{1}{\alpha}\frac{d\alpha}{dr}\frac{dt}{ds}\frac{dr}{ds} = \frac{1}{\alpha}\left(\alpha\frac{d^2t}{ds^2} + \frac{d\alpha}{ds}\frac{dt}{ds}\right) = \frac{1}{\alpha}\cdot\frac{d}{ds}\left[\frac{dt}{ds}\alpha\right]$$

and we are left with

$$\frac{d}{ds}\left[\alpha\left(r\right)\frac{dt}{ds}\right] = 0. \tag{7.7}$$

Integration of (7.7) with respect to the parameter s gives equation (7.5) where $1/\sqrt{E}$ is the constant of integration. □

7.1.1. ***Observer at the edge of the cavity.***
Consider an observer at rest, located at the boundary of the spherical region, so that the observer's coordinates θ and ϕ are constant and $r = R\left(t\right)$. Hence, it follows $d\theta = d\phi = 0$ and $dr = \frac{dR}{dt}dt$. Accordingly, equation (7.1) reads:

$$ds^2 = \left[\alpha\left(R\right)c^2 - \alpha^{-1}\left(R\right)\left(\frac{dR}{dt}\right)^2\right]dt^2 \tag{7.8}$$

We can solve the latter equation to $\left(\frac{dR}{dt}\right)^2$ so that

$$\left(\frac{dR}{dt}\right)^2 = \alpha^2\left(R\right)c^2 - \alpha\left(R\right)\left(\frac{ds}{dt}\right)^2 = \alpha^2\left(R\right)c^2\left[1 - \frac{1}{\alpha\left(R\right)c^2}\left(\frac{ds}{dt}\right)^2\right].$$

As mentioned above, the world line of the observer is a geodesic line. Lemma 14 tells us that $\left(\frac{ds}{dt}\right)^2 = E\alpha^2\left(R\right)$ at $r = R$, see (7.5), and the above equation results in

$$\left(\frac{dR}{dt}\right)^2 = \alpha^2\left(R\right)c^2\left[1 - \frac{E}{c^2}\alpha\left(R\right)\right]. \tag{7.9}$$

After taking the square root and dividing by c it remains

$$\frac{dR}{cdt} = \pm\alpha\left(R\right)\sqrt{1 - \frac{E}{c^2}\alpha\left(R\right)}$$

In the Schwarzschild-de Sitter case, we are left with

$$\frac{dR}{cdt} = \pm\left[1 - \frac{r_g}{R} - \left(\frac{R}{r_\Lambda}\right)^2\right]\sqrt{1 - \frac{E}{c^2}\left[1 - \frac{r_g}{R} - \left(\frac{R}{r_\Lambda}\right)^2\right]}. \tag{7.10}$$

In the following, we study how spatial curvature determines the constant of geodesic motion (which is $1/\sqrt{E}$, see lemma 14). We prove, that the matching condition yields $E = c^2$ if the outer FLRW region is spatially flat.

Theorem 15. *(ΛCDM Swiss-Cheese model)*
Consider a ΛCDM Swiss-Cheese model with spatially flat cosmological background. The expansion of a spherical region is given by

$$\frac{dR}{cdt} = \pm\left[1 - \frac{r_g}{R} - \left(\frac{R}{r_\Lambda}\right)^2\right]\sqrt{\frac{r_g}{R} + \left(\frac{R}{r_\Lambda}\right)^2} \tag{7.11}$$

where r_g is the gravitational radius of the central mass and $r_\Lambda = \sqrt{3/\Lambda}$.

Proof. The condition $r = R(t)$ for the observer at the edge of the cavity corresponds to a fixed comoving coordinate $\overline{r} = \overline{R}$. Consequently, equation (7.2) reduces to $ds^2 = c^2 d\overline{t}^2$. Equation (7.5) in lemma 14 yields $ds^2 = E\alpha^2(R)\,dt^2$ and thus

$$\left(\frac{dt}{d\overline{t}}\right)^2 = \frac{c^2}{E\alpha^2(R)}. \tag{7.12}$$

Now we use (7.9) and (7.12) in equation (7.4). For $\alpha(R) = 1 - (r_g/R) - (R/r_\Lambda)^2$, the Schwarzschild-de Sitter case, it remains

$$\left(\frac{1}{a}\frac{da}{d\overline{t}}\right)^2 = \frac{c^4}{R^2E}\left[1 - \frac{E}{c^2}\alpha(R)\right] = c^2\left[\frac{c^2}{R^2E} - \frac{\alpha(R)}{R^2}\right] = c^2\left(\frac{1}{r_\Lambda^2} + \frac{\frac{c^2}{E} - 1}{R^2} + \frac{r_g}{R^3}\right).$$

Equation (7.3) implies $R = a\overline{R}$. Furthermore we use $r_\Lambda = \sqrt{3/\Lambda}$, $r_g = 2M\gamma/c^2$ and $\Omega_\Lambda = \frac{c^2\Lambda}{3H_0^2}$, see (2.9). As a result we get:

$$\begin{aligned}\left(\frac{1}{a}\frac{da}{d\overline{t}}\right)^2 &= H_0^2\left(\frac{c^2\Lambda}{3H_0^2} + \frac{c^2}{H_0^2}\cdot\frac{\frac{c^2}{E} - 1}{\overline{R}^2a^2} + \frac{c^2r_g}{H_0^2\overline{R}^3a^3}\right)\\ &= H_0^2\left[\Omega_\Lambda - \frac{c^2}{H_0^2\overline{R}^2E}\left(E - c^2\right)\cdot\frac{1}{a^2} + \frac{2M\gamma}{H_0^2\overline{R}^3}\cdot\frac{1}{a^3}\right]\end{aligned}$$

Following the method suggested by Peebles in [91], we compare the latter equation with the expansion rate in a FLRW model, where

$$\left(\frac{da}{a\,d\overline{t}}\right)^2 = H_0^2\left(\Omega_\Lambda - \frac{\Omega_K}{a^2} + \frac{\Omega_M}{a^3}\right) = H_0^2\left(\Omega_\Lambda - \Omega_K\cdot\frac{1}{a^2} + \frac{8\pi\gamma\rho_0}{3H_0^2}\cdot\frac{1}{a^3}\right)$$

see (2.14). Comparing these two equations yields

$$\Omega_K = \frac{c^2}{H_0^2\overline{R}^2E}\left(E - c^2\right) \quad \text{and} \quad M = \frac{4}{3}\pi\overline{R}^3\rho_0. \tag{7.13}$$

Obviously, the mass condensation M is equal to the mass M' of the evacuated material if the cosmological background is spatially flat[80]. Since $\Omega_K = 0$, equation (7.13) claims $E = c^2$. Therewith, equation (7.10) directly yields (7.11). It turned out that E represents the energy per unit mass. □

[80]Peebles proved in [91] that the mass of the evacuated material is equal to the value of the point mass in the spatially flat case with $\Lambda = 0$ (see section 3.5).

7.2. **Expansion of the edge of the cavity in case of $\Lambda = 0$.**
From now on we assume that the expanding cosmic background is spatially flat. Following Theorem 15, the expansion of the boundary of that cavity is given by (7.11). In case of $\Lambda = 0$ and $r_g > 0$, equation (7.11) reduces to

$$\frac{dR}{cdt} = \pm\left(1 - \frac{r_g}{R}\right)\sqrt{\frac{r_g}{R}} \tag{7.14}$$

which can be transformed to

$$\int_{R_1}^{R} \frac{\sqrt{r}}{1-\frac{r_g}{r}} dr = \pm c\sqrt{r_g}\,(t - t_1)\,. \tag{7.15}$$

The integral on the left side of (7.15) is solved with the following lemma:

Lemma 16. *Integral for $\Lambda = 0$*
Let us assume that $r > r_g$, then one has

$$\int \frac{\sqrt{r}}{1-\frac{r_g}{r}} dr = 2r_g^{\frac{3}{2}}\left[\frac{1}{3}\sqrt{\frac{r}{r_g}}^3 + \sqrt{\frac{r}{r_g}} - \operatorname{Arcoth}\left(\sqrt{\frac{r}{r_g}}\right) + k\right] \tag{7.16}$$

where k is a constant of integration. Alternatively, the solution is given by:

$$\int \frac{\sqrt{r}}{1-\frac{r_g}{r}} dr = 2r_g^{\frac{3}{2}}\left[\frac{1}{3}\sqrt{\frac{r}{r_g}}^3 + \sqrt{\frac{r}{r_g}} + \frac{1}{2}\ln\left(\frac{\sqrt{\frac{r}{r_g}}-1}{\sqrt{\frac{r}{r_g}}+1}\right) + k\right]$$

Proof. Let us introduce the new coordinate x by $x^2 = r/r_g$, so that $dr = 2r_g x dx$ and

$$\int \frac{\sqrt{r}}{1-\frac{r_g}{r}} dr = 2r_g^{\frac{3}{2}} \int \frac{x^2}{1-\frac{1}{x^2}} dx = 2r_g^{\frac{3}{2}} \int \frac{x^4}{x^2-1} dx. \tag{7.17}$$

From polynomial long division we get:

$$\int \frac{x^4}{x^2-1} dx = \int \left(x^2 + 1 + \frac{1}{x^2-1}\right) dx = \frac{1}{3}x^3 + x + \int \frac{dx}{x^2-1} \tag{7.18}$$

The integral $\int \frac{dx}{x^2-1}$ can be solved easily with the transformation[81] $x = \tanh(\varphi)$ in case of $x < 1$ and with the transformation[82] $x = \coth(\varphi)$ if $x > 1$. It remains:

$$\int \frac{dx}{x^2-1} = \begin{cases} -\operatorname{Artanh}(x) + k, & x < 1 \\ -\operatorname{Arcoth}(x) + k, & x > 1 \end{cases} \tag{7.19}$$

[81] **Case $x < 1$:** With $x = \tanh(\varphi)$ it applies $dx = \frac{\cosh^2(\varphi)-\sinh^2(\varphi)}{\cosh^2(\varphi)} d\varphi = \left[1 - \tanh^2(\varphi)\right] d\varphi$ and therewith $\int \frac{dx}{x^2-1} = -\int d\varphi = -\varphi = -\operatorname{Artanh}(x)$.

[82] **Case $x > 1$:** With $x = \coth(\varphi)$ it applies $dx = \frac{\sinh^2(\varphi)-\cosh^2(\varphi)}{\sinh^2(\varphi)} d\varphi = \left[1 - \coth^2(\varphi)\right] d\varphi$ and therewith $\int \frac{dx}{x^2-1} = -\int d\varphi = -\varphi = -\operatorname{Arcoth}(x)$.

We only deal with the $r > r_g$ case, so the Integral is given by the $x > 1$ branch of (7.19). Anyway, it is $x \neq 1$ and the integral can be alternatively solved by

$$\int \frac{dx}{x^2-1} = \frac{1}{2}\int \left(\frac{1}{x-1} - \frac{1}{x+1}\right) dx = \frac{1}{2}\ln\left|\frac{x-1}{x+1}\right| + k \tag{7.20}$$

where k is a constant of integration. Since we are interested in the $x > 1$ case, we may drop the absolute value bars. In either case we use the $x > 1$ branch of (7.19) or alternatively (7.20) in equation (7.18) and get

$$\int \frac{x^4}{x^2-1}dx = \frac{1}{3}x^3 + x - \operatorname{Arcoth}(x) + k = \frac{1}{3}x^3 + x + \frac{1}{2}\ln\left(\frac{x-1}{x+1}\right) + k.$$

Finally, we retransform $x = \sqrt{r/r_g}$. Together with (7.17) we obtain (7.16) . □

Let us now return to our integral equation (7.15), which prescribes the relation between time t and radius R. For $R > r_g$ we get

$$t(R) = \mp\frac{2r_g}{c}\left[\frac{1}{3}\sqrt{\frac{R}{r_g}}^3 + \sqrt{\frac{R}{r_g}} - \operatorname{Arcoth}\left(\sqrt{\frac{R}{r_g}}\right) + k\right] \tag{7.21}$$

from lemma 16. k is a constant of integration again. With regard to the domain of the inverse hyperbolic cotangent Arcoth, the function is not defined at $R = r_g$. Indeed, we expect that a sphere with initial radius r_g does not take part in the cosmic expansion.

We can not solve (7.21) to R analytically. Certainly, it is easy to produce numerical data for the inverse function $R(t)$. Algorithm 13 in the appendix can be used to calculate this numerical data. Generally, we deal with the $\Lambda > 0$ case. Since there is no exact solution of the corresponding differential equation, we approximate the $R(t)$ data with the Euler algorithm. Later we will compare the $\Lambda = 0$ and $\Lambda > 0$ case. It turned out, that it is more comfortable to use the numerical algorithm for the $\Lambda = 0$ data as well. Hence, we don't need the inverse function of (7.21).

7.3. **The zero-mass case.**

Now let us study the differential equation (7.11) for $r_g = 0$ but with nonzero cosmological constant. This solution may be used to approximately describe the general case within the $R \sim r_\Lambda$ region, where the influence of the gravitating mass is negligible. For $r_g = 0$ and $\Lambda \neq 0$ equation (7.11) reduces to

$$\frac{dR}{cdt} = \pm \left[1 - \left(\frac{R}{r_\Lambda}\right)^2\right] \frac{R}{r_\Lambda}$$

and the corresponding integral equation reads

$$\int_{R_1}^{R} \frac{dr}{\left[1 - \left(\frac{r}{r_\Lambda}\right)^2\right] \frac{r}{r_\Lambda}} = \pm c\,(t - t_1)\,. \tag{7.22}$$

The integral on the left side can be solved with the following lemma:

Lemma 17. *Integral for $r_g = 0$*
Let us assume that $r \neq r_\Lambda$, one has

$$\int \frac{dr}{\left[1 - \left(\frac{r}{r_\Lambda}\right)^2\right] \frac{r}{r_\Lambda}} = r_\Lambda \cdot \begin{cases} \ln\left(\sinh\left[\operatorname{Artanh}\left(\frac{r}{r_\Lambda}\right)\right]\right) + k, \text{ if } r < r_\Lambda \\ \\ \ln\left(\cosh\left[\operatorname{Arcoth}\left(\frac{r}{r_\Lambda}\right)\right]\right) + k, \text{ if } r > r_\Lambda \end{cases} \tag{7.23}$$

where k is a constant of integration. Alternatively, the solution is given by[83]*:*

$$\int \frac{dr}{\left[1 - \left(\frac{r}{r_\Lambda}\right)^2\right] \frac{r}{r_\Lambda}} = \frac{1}{2} r_\Lambda \ln \left| \frac{\left(\frac{r}{r_\Lambda}\right)^2}{1 - \left(\frac{r}{r_\Lambda}\right)^2} \right| \tag{7.24}$$

Proof. First, we introduce the new coordinate $x = r/r_\Lambda$ so that $dr = r_\Lambda dx$ and

$$\int \frac{dr}{\left[1 - \left(\frac{r}{r_\Lambda}\right)^2\right] \frac{r}{r_\Lambda}} = r_\Lambda \int \frac{dx}{(1 - x^2)\, x}. \tag{7.25}$$

In case of $x^2 < 1$ we transform to $x = \tanh(\varphi)$, it is:

$$dx = \frac{\cosh^2(\varphi) - \sinh^2(\varphi)}{\cosh^2(\varphi)} d\varphi = \left[1 - \tanh^2(\varphi)\right] d\varphi$$

[83]Certainly, it is easy to confirm the equivalence of the antiderivatives (7.23) and (7.24). We get $\ln(\sinh[\operatorname{Artanh}(x)]) = \frac{1}{2}\ln\left(\frac{x^2}{1-x^2}\right)$ and $\ln(\cosh[\operatorname{Arcoth}(x)]) = \frac{1}{2}\ln\left(\frac{x^2}{x^2-1}\right)$ after a short calculation.

Furthermore we use $z = \sinh(\varphi)$ and $d\varphi = dz/\cosh(\varphi)$ and get

$$\begin{aligned}\int \frac{dx}{(1-x^2)\,x} &= \int \frac{d\varphi}{\tanh(\varphi)} = \int \frac{\cosh(\varphi)}{\sinh(\varphi)} d\varphi = \int \frac{1}{z} dz \\ &= \ln(z) + k = \ln[\sinh(\varphi)] + k = \ln(\sinh[\operatorname{Artanh}(x)]) + k\end{aligned}$$

where k is a constant of integration. Analogously, in case of $x^2 > 1$ we transform to $x = \coth(\varphi)$. It is

$$dx = \frac{\sinh^2(\varphi) - \cosh^2(\varphi)}{\sinh^2(\varphi)} d\varphi = \left[1 - \coth^2(\varphi)\right] d\varphi$$

and together with a second transformation $z = \cosh(\varphi)$ it remains

$$\begin{aligned}\int \frac{dx}{(1-x^2)\,x} &= \int \frac{d\varphi}{\coth(\varphi)} = \int \frac{\sinh(\varphi)}{\cosh(\varphi)} d\varphi = \int \frac{1}{z} dz \\ &= \ln(z) + k = \ln[\cosh(\varphi)] + k = \ln(\cosh[\operatorname{Arcoth}(x)]) + k\end{aligned}$$

where k is a constant of integration again. Now we have to retransform $x = r/r_\Lambda$ in either case and get (7.23) from (7.25).

Alternatively, we can solve (7.25) with $\int \frac{dx}{(1-x^2)x} = \frac{1}{2}\ln\left|\frac{x^2}{1-x^2}\right|$ in order to get (7.24). This indefinite integral is given in [14], it can be easily solved by using partial fraction decomposition. □

With lemma 17, our integral equation (7.22) directly yields:

$$t(R) = \mp\frac{r_\Lambda}{c}\begin{cases} \ln(\sinh[\operatorname{Artanh}(R/r_\Lambda)]) + k, & R < r_\Lambda \\ \ln(\cosh[\operatorname{Arcoth}(R/r_\Lambda)]) + k, & R > r_\Lambda \end{cases}$$

Now it is easy to work out the inverse function $R(t)$. Together with the identities[84] $\tanh(\operatorname{Arsinh} z) = \frac{z}{1+z^2}$ and $\coth(\operatorname{Arcosh} z) = \frac{z}{z^2-1}$ we get

$$R(t) = r_\Lambda \tanh\left[\operatorname{Arsinh}\left(\exp\left[\pm\frac{ct}{r_\Lambda} - k\right]\right)\right] = \frac{r_\Lambda \exp\left[\pm\frac{ct}{r_\Lambda} - k\right]}{\exp\left[2\left(\pm\frac{ct}{r_\Lambda} - k\right)\right] + 1}$$

in case of $R < r_\Lambda$ and

$$R(t) = r_\Lambda \coth\left[\operatorname{Arcosh}\left(\exp\left[\pm\frac{ct}{r_\Lambda} - k\right]\right)\right] = \frac{r_\Lambda \exp\left[\pm\frac{ct}{r_\Lambda} - k\right]}{\exp\left[2\left(\pm\frac{ct}{r_\Lambda} - k\right)\right] - 1}$$

in case of $R > r_\Lambda$. Let us now study the general case where $\Lambda \neq 0$ and $r_g \neq 0$.

---

[84] Since $\cosh^2 x - \sinh^2 x = 1$ it is $\tanh x = \frac{\sinh x}{\cosh x} = \frac{\sinh x}{1+\sinh^2 x}$ and $\coth x = \frac{\cosh x}{\sinh x} = \frac{\cosh x}{\cosh^2 x - 1}$. Hence, we directly obtain that $\tanh(\operatorname{Arsinh} z) = \frac{z}{1+z^2}$ and $\coth(\operatorname{Arcosh} z) = \frac{z}{z^2-1}$.

7.4. **Expansion including nonzero mass and cosmological constant.** Consider a static Schwarzschild-de Sitter sphere embedded in a spatially flat FLRW background. From Theorem 15 we know that the expansion of the cavity boundary is determined by the differential equation

$$\frac{dR}{cdt} = \left[1 - \frac{r_g}{R} - \left(\frac{R}{r_\Lambda}\right)^2\right] \sqrt{\frac{r_g}{R} + \left(\frac{R}{r_\Lambda}\right)^2} \tag{7.26}$$

see (7.11). The initial radius R_0 it is determined by equation (7.13), it depends on the mass M and the density ρ_0 of the FLRW model. Naturally, in the real universe it is $R_0 \gg r_g$. For the purpose of illustration, we choose $R_0 \sim r_g$ in the following. Transformation of (7.26) to the dimensionless coordinates $y = R/r_g$ and $x = ct/r_g$ yields

$$\frac{dy}{dx} = \left(1 - \frac{1}{y} - \varepsilon y^2\right) \sqrt{\frac{1}{y} + \varepsilon y^2} \tag{7.27}$$

where $\varepsilon := (r_g/r_\Lambda)^2 \ll 1$ again. The differential equation[85] (7.27) was solved with the Euler method. A Fortran77 source code is given in the appendix, see algorithm 14. The numerical results are presented in figure 7.2. If the numerical calculation

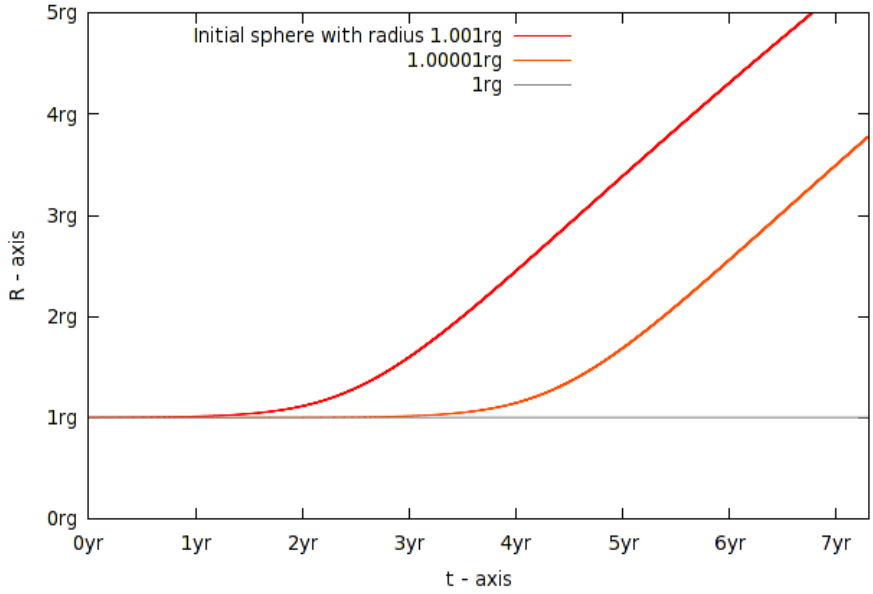

FIGURE 7.2. Expansion of the cavity. Here, r_g is the gravitational radius $r_{LG} \approx 0.125\,\mathrm{pc}$ of the Local Group. Anything outside the gravitational radius expands. The gravitational sphere itself does not noticeably take part in cosmic expansion.

[85]Since we intend to deal with the time given in years, we have to multiply the x values by $r_g/\left(c \cdot 365 \cdot 24 \cdot 3600\mathrm{s}\right) \approx 0.41$.

starts at $y_0 = 1$, which corresponds to $R_0 = r_g$, the data of algorithm 14 indicates that there is no expansion of the initial-sphere with radius r_g. To be exact, the Euler algorithm for (7.26) is given by:

$$R_{n+1} = R_n + hc\left[1 - \frac{r_g}{R_n} - \left(\frac{R_n}{r_\Lambda}\right)^2\right]\sqrt{\frac{r_g}{R_n} + \left(\frac{R_n}{r_\Lambda}\right)^2} \tag{7.28}$$

What does really happen if we start at $R_0 = r_g$? According to (7.28), the next data point of the Euler algorithm is given by

$$R_1 = r_g - hc\left(\frac{r_g}{r_\Lambda}\right)^2\sqrt{1 + \left(\frac{r_g}{r_\Lambda}\right)^2} \neq r_g.$$

Thus, we do not obtain the function $R(t) = r_g$, actually. Certainly, the term including $(r_g/r_\Lambda)^2$ is negligibly small[86]. But there is another initial R_0, very close to r_g, for which the Euler algorithm returns $R(t)$ =constant. In subsection 2.8 we analyzed the function $\alpha(r) = 1 - \frac{r_g}{r} - \left(\frac{r}{r_\Lambda}\right)^2$, which occurs in the components $g_{00} = c^2\alpha$ and $g_{11} = -\alpha^{-1}$ of the Schwarzschild-de Sitter field. The zeros of α are given by equation (2.43). Indeed, the Schwarzschild radius r_g is not an exact solution of $\alpha = 0$, but one has

$$\widetilde{r}_g = -\frac{2}{\sqrt{3}}r_\Lambda \cos\left\{\frac{1}{3}\arccos\left(-\frac{3\sqrt{3}}{2}\cdot\frac{r_g}{r_\Lambda}\right) + \frac{\pi}{3}\right\} \approx r_g$$

see equation (2.43) in subsection 2.8. Let us now theoretically start the Euler algorithm (7.28) at $R_0 = \widetilde{r}_g$. Since $\widetilde{r}_g$ is an exact solution of $\alpha = 0$ we get

$$R_1 = \widetilde{r}_g + hc\underbrace{\left[1 - \frac{r_g}{\widetilde{r}_g} - \left(\frac{\widetilde{r}_g}{r_\Lambda}\right)^2\right]}_{=0}\sqrt{\frac{r_g}{\widetilde{r}_g} + \left(\frac{\widetilde{r}_g}{r_\Lambda}\right)^2} = \widetilde{r}_g$$

and further on $R_n = \widetilde{r}_g$ for all $n \in \mathbb{N}$. Hence, our model predicts that cosmic expansion has no effect on a sphere with radius $\widetilde{r}_g$, which could be considered as the 'Schwarzschild-de Sitter gravitational sphere'. As a matter of fact, the difference between Schwarzschild radius r_g and $\widetilde{r}_g$ is negligibly small. For the mass of our Local Group, $r_g = r_{LG} \approx 0.125\,\mathrm{pc}$ and $\widetilde{r}_{LG}$ coincide up to the $20th$ decimal place[87]. In other words, the difference between r_{LG} and $\widetilde{r}_{LG}$ amounts to some μm. Altogether, we suppose that a sphere with gravitational radius r_g does not expand itself. An initial-sphere with $R_0 > r_g$ ($y_0 > 1$), whose radius perceptibly exceeds the gravitational radius, undergoes expansion, see figure 7.2.

---

[86]For example if we choose the gravitational radius $r_{LG} \approx 0.125\,\mathrm{pc}$ of the our Local Group, it remains $c\left(\frac{r_g}{r_\Lambda}\right)^2\sqrt{1 + \left(\frac{r_g}{r_\Lambda}\right)^2} \approx 1.14 \cdot 10^{-13}\mathrm{m}$

[87]Maple command: evalf[25](solve(1-rg/r-(1/3)*Lambda*r^2 = 0, r))

7.4.1. ***Expansion in the region*** $R(t) \gg r_g$.

Now let us study the behavior of the function $R(t)$ for $R \gg r_g$. Figure 7.3 shows, that the cosmological constant Λ dominates at $R(t) \gg r_g$, but it has no measurable influence in the neighborhood of the gravitational radius r_g. Since the data covers

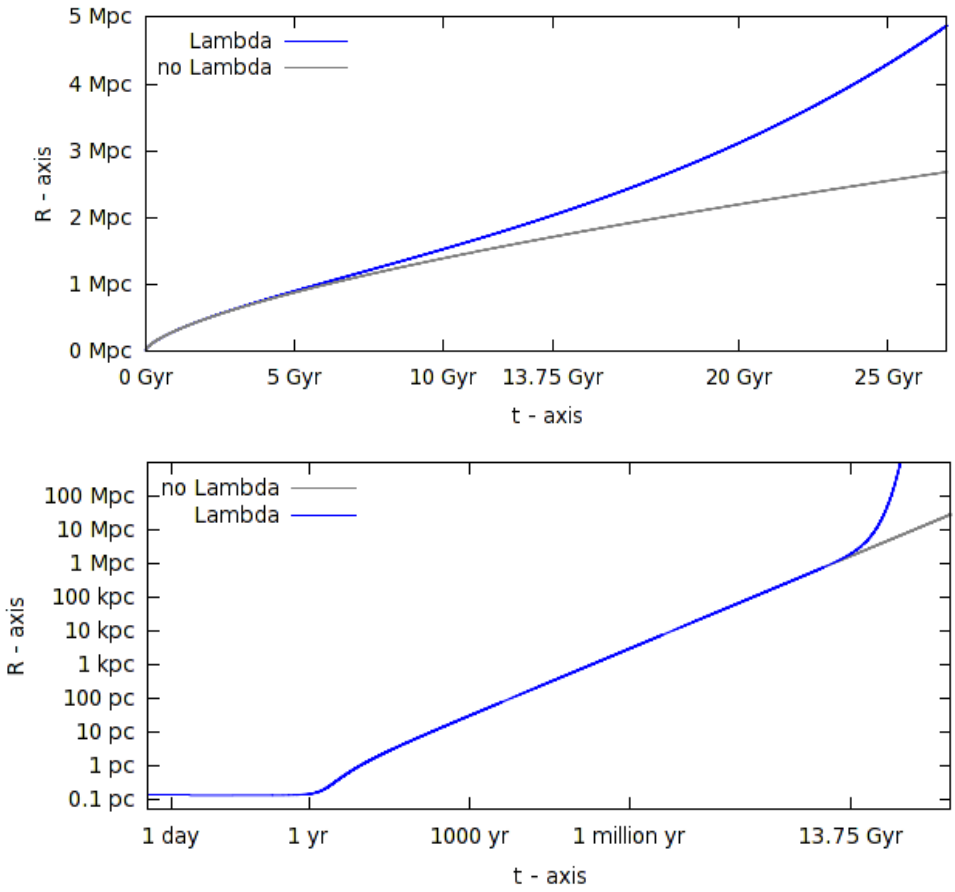

FIGURE 7.3. Influence of Λ on the Expansion of $R(t)$ in comparison with a $\Lambda = 0$ model. The lower graph shows the Expansion of $R(t)$ on a logarithmic scale: From the neighborhood of the gravitational radius up to over 100 Mpc. The radius of the initial sphere is $R_0 = 1.01 r_{LG}$, where $r_{LG} \approx 0.125$ pc is the gravitational radius of the Local Group. The current age of our universe is marked at 13.75 Gyr.

a large range of values, a logarithmic scale is appropriate. As it was expected, there is only tiny expansion in the neighborhood of r_g. At a medium distance, the spacetime expands but the rate of expansion is slightly slowing down. The rate of expansion increases again at a great distance, where the cosmological constant dominates.

7.4.2. ***Influence of the cosmological constant.***
Since Λ has no influence on the neighborhood of the gravitational radius r_g, the corresponding cosmological-constant-term in (7.26) is negligible in the region near to r_g. Certainly, cosmic expansion is dominated by the $\Lambda-$term at large scales. But from which distance, the cosmological constant should be taken appropriately into account? We estimated the threshold, where this effect makes at least 1% of the expansion. Due to equation (7.27), the radial expansion is given by

$$\frac{dy}{dx} = \begin{cases} \left(1 - \frac{1}{y} - \varepsilon y^2\right)\sqrt{\frac{1}{y} + \varepsilon y^2}, & \text{if } \Lambda > 0 \\ \left(1 - \frac{1}{y}\right)\sqrt{\frac{1}{y}}, & \text{if } \Lambda = 0 \end{cases} \tag{7.29}$$

where $y = R/r_g$, $x = ct/r_g$ and $\varepsilon := (r_g/r_\Lambda)^2$. Let us denote the $\Lambda > 0$ solution by y_L and the corresponding $\Lambda = 0$ solution by y_N. For a given mass M, there exists a unique value x_1 where the condition

$$\frac{y_L(x_1)}{y_N(x_1)} = 1.01 \tag{7.30}$$

is fulfilled. Accordingly, we define the '1% - threshold' R_1 by

$$R_1 := r_g y_L(x_1) \tag{7.31}$$

Figure 7.4 shows how the 1% - threshold is related to the central mass M. The data

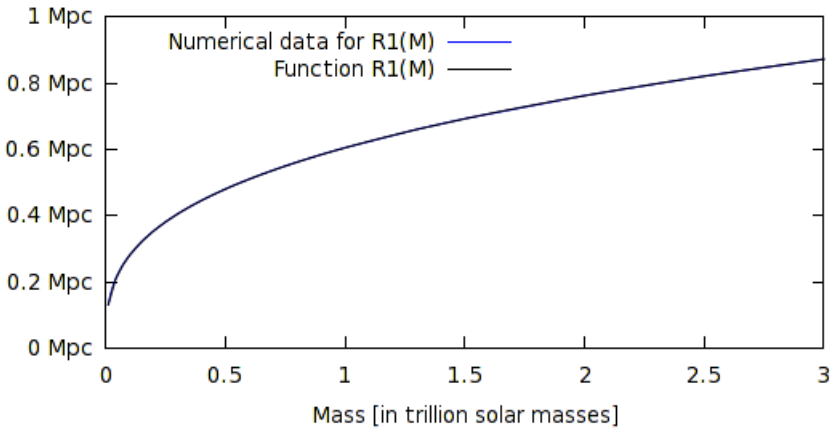

FIGURE 7.4. Mass to '1% - threshold' relation. At this distance (1% - threshold), the cosmological-constant effect makes 1% of the expansion. The graphic shows data in the range of $10^{10} M_\odot$ to $3 \cdot 10^{12} M_\odot$ in comparison to the function $R_1(M) = C_1 M^{1/3}$, where $C_1 \approx 1.48 \cdot 10^7 \mathrm{g\,m}^{-\frac{1}{3}}$.

can be approximated with Algorithm 17, see appendix. For example, if we analyze a model whose central mass is $M = 1.3 \cdot 10^{12} M_{\odot}$ (mass of our Local Group), the 1% - threshold is located at $R_1 \approx 0.66\,\mathrm{Mpc}$. One can easily estimate the 1% - threshold for several masses and finally plot the function $R_1(M)$. The numerical results indicate, that the 1% - threshold R_1 is proportional to $M^{1/3}$. The function is given by:

$$R_1(M) = C_1 M^{\frac{1}{3}}, \text{ where } C_1 \approx 1.48 \cdot 10^7 \mathrm{g\,m}^{-\frac{1}{3}}$$

The value of C_1, with respect to the physical units of the data in figure 7.4, is given by

$$C_1 \approx 0.61 \frac{\mathrm{Mpc}}{(10^{12} M_{\odot})^{\frac{1}{3}}}.$$

A table with the numerical data is given in the appendix, see table 1.

7.5. **Cosmic voids in the ΛCDM Swiss-Cheese model.**
As mentioned before, some authors proposed the idea that each cosmic void was emptied by gravity of a giant black hole in its center, cf. [16]. The ΛCDM Swiss-Cheese model should be taken into consideration when establishing a model to describe this scenario. The current density ρ_0 of the FLRW model universe is given

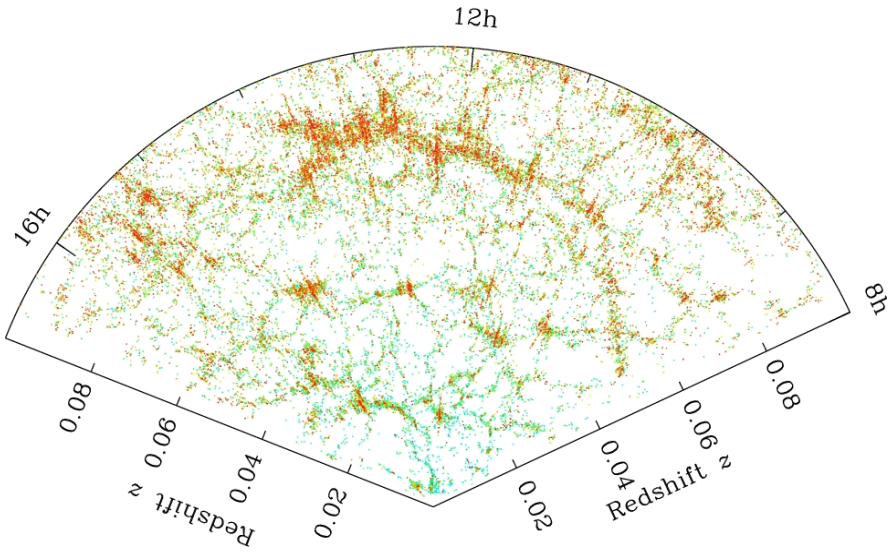

FIGURE 7.5. Filaments and cosmic voids: Distribution of galaxies from the Sloan Digital Sky Survey, SDSS Press Release Images: http://www.astronomy.ohio-state.edu/~dhw/SDSS08/voidfigs.html

by $\rho_0 = \frac{3H_0^2\Omega_M}{8\pi\gamma}$, see (2.9). Since our model universe is spatially flat, we assume that the mass M of the black hole is equal to the mass of a sphere with radius R_a and density ρ_0:

$$M = \frac{4}{3}\pi R_a^3 \rho_0 = \frac{H_0^2\Omega_M}{2\gamma} R_a^3 \tag{7.32}$$

In a spatially curved universe, the compact mass would not be equal to the mass of the evacuated cosmic material. Following [91], the mass $\mathcal{M}'$ of the evacuated material within a sphere with radius R_a is given by

$$\mathcal{M}' = 4\pi\rho a^3 \int_0^{R_a} \frac{r^2 dr}{\sqrt{1-\frac{r^2}{R_K^2}}} \tag{7.33}$$

where R_K is the curvature radius of the universe, ρ its density and a the scale factor. Since R_k is very large, there is only a slight difference to the spatially flat model. A spatially flat model has an infinite curvature radius R_K, and consequently we get back (7.32). According to (7.32), the mass of a $R_a = 10\,\text{Mpc}$ void black hole is about $1.55 \cdot 10^{14} M_\odot$.

7.5.1. ***Size of cosmic voids in the early universe.***
Consider a (model) universe, where a cosmic void contains a black hole whose mass corresponds to the mass of the material which has been evacuated from a cosmological model to make the void. Equation (7.32) determines the mass of the central body from the radius R_a of the void. The "$-$" branch of equation (7.11)

$$\frac{dR}{cdt} = -\left[1 - \frac{r_g}{R} - \left(\frac{R}{r_\Lambda}\right)^2\right]\sqrt{\frac{r_g}{R} + \left(\frac{R}{r_\Lambda}\right)^2} \tag{7.34}$$

can be used to estimate the former size of the void in our model. For the calculations we used the dark energy parameter $\Omega_\Lambda \approx 0.728$ and the mass density parameter $\Omega_M \approx 0.273$, which is in accordance with the WMAP data [63]. Algorithm 18 in appendix D.4.4 can be used to estimate the former size of cosmic voids, for example some hundred thousand or some billion years after the big bang.

This begs the question, which expansion time seems to be appropriate for our numerical calculations? Francis et al discovered in 2004 a large filament structure at $z = 2.38$, see [41]. This corresponds to a time of roughly three billion years after the big bang. On the other hand, the gravitational collapse of a supermassive void black hole should have emitted large amounts of energy in the form of electromagnetic radiation, e.g. light. But there is no observational evidence for the incurrence of void black holes. A possible explanation for the absence of observational evidence may be that these void black holes already formed at the epoch of recombination, before our universe became permeable to light. Today, the universe has an age of $13.75 \cdot 10^9$ years, recombination occurred roughly $3.8 \cdot 10^5$ years after the big bang. Hence, let us choose an expansion time of 13.75 Gyr for the numerical calculations.

At first we study a void, which has a radius of $R_a = 10\,\mathrm{Mpc}$ today. Following equation (7.32), there is a $1.55 \cdot 10^{14} M_\odot$ mass condensation at the center of this void. The gravitational radius of the mass is roughly 15 pc. Equation (7.34) was solved with algorithm 18 in the appendix. According to our model, this 10 Mpc void had a 24 kpc radius 13.75 billion years ago.

Now consider a void with a current radius of $R_a = 1.5\,\mathrm{Mpc}$. The mass condensation is about $5.28 \cdot 10^{11} M_\odot$ with a gravitational radius of 0.05 pc. The 1.5 Mpc void had a 3 kpc radius 13.75 billion years ago.

7.6. **Influence of Λ on galaxies, clusters and voids.**
As mentioned at the beginning of section 7, Carrera and Giulini remarked in [20] that the Swiss Cheese model can only apply on large scales. The vacuole radius corresponding to a single solar mass is much larger than the average distance of stars in a Galaxy. *"This changes as one goes to larger scales."* [20].

We compare the ΛCDM Swiss-Cheese model with a $\Lambda = 0$ Swiss-Cheese model and study the repulsive effect of the cosmological constant on galaxies, clusters and voids. Again, our considerations are based on (7.26):

$$\frac{dR}{cdt} = \left[1 - \frac{r_g}{R} - \left(\frac{R}{r_\Lambda}\right)^2\right] \sqrt{\frac{r_g}{R} + \left(\frac{R}{r_\Lambda}\right)^2}$$

At first let us consider a typical galaxy like our Milky Way. Baryonic matter roughly spans a region of about $\sim 15\,\text{kpc}$ radius around a supermassive black hole at its center, "*Dark matter halos appear to extend to at least* $\sim 50\,kpc$" [103]. The zero-gravity surface is located at about 1 Mpc distance from the galactic center, where the space up to about 1 Mpc is empty. According to (7.32) the material inside a sphere with 1 Mpc radius has a mass of $1.56 \cdot 10^{11} M_\odot$. This value roughly corresponds to the amount of baryonic matter in our galaxy. Indeed, the total mass of the Milky Way is $\sim 10^{12} M_\odot$. We used algorithm 19 to approximate the later size of a sphere with initial radius 50 kpc, which encloses a mass of $10^{12} M_\odot$. After an expansion time of 1 Gyr, the 50 kpc radius has grown to $\approx 287.34\,\text{kpc}$. In a $\Lambda = 0$ model we have only $\approx 287.02\,\text{kpc}$. Thus, the influence of the cosmological constant is roughly 0.1% for this galaxy.

Analogously we proceed with a galaxy cluster. Consider a sphere with initial radius 1.5 Mpc, that encloses a mass of $10^{14} M_\odot$ to $10^{15} M_\odot$. After 1 Gyr of expansion, the influence of the cosmological constant is about $0.2 - 0.4\%$.

Finally, let us consider again the void with a radius of $R_a = 10\,\text{Mpc}$ and a $1.55 \cdot 10^{14} M_\odot$ mass condensation in its center. The influence of the cosmological constant is roughly 3.5% for an expansion time of 1 Gyr.

Obviously, the repulsive effect of Λ is negligibly small for a galaxy or a galaxy cluster. But for a void, the cosmological constant has a substantial effect on the expansion.

8. Lemaitre Tolman Bondi model

For the purpose of matching local and global geometry in our universe we studied in section 7 the ΛCDM Swiss-Cheese model, which is a generalization of the $\Lambda = 0$ Einstein-Straus vacuole (a spherical Schwarzschild region immersed in a FLRW universe, cf. section 3.2). It refers to a spherical Schwarzschild-de Sitter region immersed in a ΛCDM cosmology. Another method to generalize the Einstein-Straus model was used by Bonnor, cf. [12]. His model is similar in construction, except that there is a Lemaitre-Tolman-Bondi (LTB) background instead of the FLRW cosmology: "*The Einstein–Straus vacuole, which refers to a spherical Schwarzschild region immersed in a Friedmann universe, is generalized to the case in which the exterior is an inhomogeneous Lemaitre–Tolman–Bondi model.*" [12]. This LTB Swiss-Cheese model[88] represents a spherical Schwarzschild region immersed in a LTB cosmology. As distinguished from the situation in a ΛCDM Swiss-Cheese model, the vacuole radius in the LTB Swiss-Cheese model is independent of cosmological background density and mass condensation, cf. [12]. Based on the LTB Swiss-Cheese model, Bonnor pointed out: "*Evidence is presented that we may be living in a vacuole approximating to the local group of galaxies. This implies that the cosmic expansion has no effect on dynamics even on the scale of the Milky Way.*" [12].

In section 8.3, we also study the LTB Swiss-Cheese model and establish a relationship between observer time and world time from the the matching condition. But first, let us draw attention to the LTB cosmology in the following.

In 1934 Richard Tolman studied "[...] *simple models composed of dust particles (nebulae) which exert negligible pressure and which are distributed non-uniformly but nevertheless with spherical symmetry around some particular origin*" [117]. The LTB model, which was created by Georges Lemaître, Richard Tolman and Hermann Bondi during the period of time from 1933 to 1947, describes an expanding or collapsing spherical cloud of dust. The LTB interval is

$$ds^2 = c^2 dt^2 - e^{\lambda(t,r)} dr^2 - R^2(t,r)\left(d\theta^2 + \sin^2\theta\, d\phi^2\right). \tag{8.1}$$

[88] Another model, which also could be called 'LTB Swiss-Cheese model', was given by Biswas and Notari [9] in 2008: They studied a Swiss-Cheese model, where inhomogeneous LTB patches are embedded in a flat FLRW background. In this case, the LTB model is used for the interior field. Anyhow, we will use the name LTB Swiss-Cheese model for a Schwarzschild vacuole in an expanding LTB cosmology.

Notice that the general LTB metric (8.1) is not necessary isotropic. Hence, it is uncertain if the following considerations are helpful to find an adequate model for the real universe (which is homogeneous and isotropic). Since the pressure of the dust is negligible, $T_0^0 = c^2\rho$ is the only nonzero component of the stress-energy tensor. Einstein's field equations for the LTB model are for example given in [54, 73, 117]. For the interval (8.1) we get

$$\frac{8\pi\gamma}{c^2}\rho = \frac{1}{R^2} - e^{-\lambda}\frac{R'^2}{R^2} + \frac{\dot{R}^2}{c^2R^2} - 2e^{-\lambda}\frac{R''}{R} + \frac{\dot{R}\dot{\lambda}}{c^2R} + e^{-\lambda}\frac{R'\lambda'}{R} - \Lambda \tag{8.2}$$

$$0 = 2\dot{R}' - \dot{\lambda}R' \tag{8.3}$$

$$0 = \frac{1}{R^2} - e^{-\lambda}\frac{R'^2}{R^2} + \frac{\dot{R}^2}{c^2R^2} + 2\frac{\ddot{R}}{c^2R} - \Lambda \tag{8.4}$$

$$0 = -e^{-\lambda}\frac{R''}{R} + \frac{\ddot{R}}{c^2R} + e^{-\lambda}\frac{R'\lambda'}{2R} + \frac{\dot{R}\dot{\lambda}}{2c^2R} + \frac{\ddot{\lambda}}{2c^2} + \frac{\dot{\lambda}^2}{4c^2} - \Lambda \tag{8.5}$$

where overdots and primes stand for partial differentiation with respect to the time t and the radial coordinate r, respectively. In the following we integrate the equations for the LTB model. It applies $\frac{\partial}{\partial t}\left[\ln R'\right] = \dot{R}'/R'$ and equation (8.3) yields

$$0 = 2\frac{\dot{R}'}{R'} - \dot{\lambda} = 2\frac{\partial}{\partial t}\left[\ln R'\right] - \dot{\lambda} = \frac{\partial}{\partial t}\left[\ln R'^2 - \lambda\right].$$

As the integral of this equation we may evidently write $\ln R'^2 - \lambda = k\left(r\right)$, where $k\left(r\right)$ is an undetermined function of r. Correspondingly, we get:

$$e^{\lambda} = R'^2 e^{-k(r)} \tag{8.6}$$

Multiplying (8.4) by c^2R^2 results in

$$c^2\left(1 - e^{-\lambda}R'^2\right) + \dot{R}^2 + 2\ddot{R}R = c^2R^2\Lambda.$$

Together with (8.6) we may rewrite the latter equation in the form

$$\dot{R}^2 + 2\ddot{R}R = c^2\left(e^{k(r)} - 1\right) + c^2R^2\Lambda.$$

We introduce the dimensionless, undetermined function

$$\mathcal{E}\left(r\right) := e^{k(r)} - 1$$

and multiply by $\dot{R}$, so that

$$\dot{R}^3 + 2\ddot{R}\dot{R}R = c^2\left(\mathcal{E}\left(r\right)\dot{R} + R^2\dot{R}\Lambda\right). \tag{8.7}$$

The left side can be rewritten by

$$\frac{\partial}{\partial t}\left[\dot{R}^2R\right] = 2\dot{R}\ddot{R}R + \dot{R}^3$$

further it is $\frac{\partial}{\partial t}\left[\frac{1}{3}R^3\right] = R^2\dot{R}$. Therewith, equation (8.7) reads

$$\frac{\partial}{\partial t}\left[\dot{R}^2 R\right] = c^2 \frac{\partial}{\partial t}\left[\mathcal{E}(r) R + \frac{1}{3}R^3\Lambda\right]. \tag{8.8}$$

Integration of (8.8) leads to

$$\dot{R}^2 R = c^2\left(\mathcal{E}(r) R + \frac{1}{3}R^3\Lambda + \mathcal{M}(r)\right) \tag{8.9}$$

where $\mathcal{M}(r)$ is a second undetermined function of r, which has the dimension of length. Now we use again $r_\Lambda = \sqrt{3/\Lambda}$, see (2.39). Division by R results in:

$$\dot{R}^2 = c^2\left[\mathcal{E}(r) + \frac{\mathcal{M}(r)}{R} + \left(\frac{R}{r_\Lambda}\right)^2\right] \tag{8.10}$$

Equation (8.10) enables us to gain further insights into the physical meaning of $\mathcal{E}$ and $\mathcal{M}$. Consider a dust particle (mass m), which is radial moving in the gravitational field of the mass M. Conservation of energy in classical mechanics implies that the total energy is given by $E = \frac{1}{2}m\dot{R}^2 - \gamma Mm/R$. Hence, we get

$$\dot{R}^2 = \frac{2E}{m} + \frac{2M\gamma}{R} = c^2\left[\frac{2E}{mc^2} + \frac{r_g}{R}\right] \tag{8.11}$$

where $r_g = 2M\gamma/c^2$ is the gravitational radius of M. By comparing (8.11) and (8.10) in case of $\Lambda = 0$ (since there is no Λ in Newtonian mechanics) we obtain $\mathcal{E}(r) = \frac{2E}{mc^2}$, where E is the energy of a dust particle, and $\mathcal{M}(r) = r_g$ is the gravitational radius of the material inside the sphere with radius r.

8.0.1. ***Density in the LTB model with nonzero cosmological constant.*** Landau and Lifschitz established an expression for the density in a LTB universe without cosmological constant, see [73]. We generalize the proof in case of an nonzero cosmological constant.

Lemma 18. *Density in the LTB model*
The density ρ in the Lemaitre-Tolman-Bondi model with line element (8.1) $ds^2 = c^2dt^2 - e^{\lambda(t,r)}dr^2 - R^2(t,r)\left(d\theta^2 + \sin^2\theta\, d\phi^2\right)$ is given by

$$\frac{8\pi\gamma}{c^2}\rho = \frac{\mathcal{M}'}{R^2 R'} \tag{8.12}$$

where primes stand for partial differentiation with respect to the r coordinate. $\mathcal{M}$ is the same undetermined function of r that already occurred in equation (8.9).

Proof. We will use (8.6) and (8.9) in Einstein's equation (8.2) to proof the lemma. Equation (8.6) yields $e^{-\lambda} = (1+\mathcal{E})/R'^2$ so that (8.2) reads

$$\frac{8\pi\gamma}{c^2}\rho = -\frac{\mathcal{E}}{R^2} + \frac{\dot{R}^2}{c^2R^2} - 2\frac{R''(1+\mathcal{E})}{RR'^2} + \frac{\dot{R}\dot{\lambda}}{c^2R} + \frac{\lambda'(1+\mathcal{E})}{RR'} - \Lambda.$$

Since $\lambda = \ln R'^2 - \ln(1+\mathcal{E})$ it is

$$\lambda' = 2\frac{R''}{R'} - \frac{\mathcal{E}'}{1+\mathcal{E}} \quad \text{and} \quad \dot{\lambda} = 2\frac{\dot{R}'}{R'}.$$

Hence, it remains

$$\frac{8\pi\gamma}{c^2}\rho = -\frac{\mathcal{E}}{R^2} + \frac{\dot{R}^2}{c^2R^2} + 2\frac{\dot{R}\dot{R}'}{c^2RR'} - \frac{\mathcal{E}'}{RR'} - \Lambda. \tag{8.13}$$

Equation (8.9) leads to

$$\mathcal{E} = \frac{\dot{R}^2}{c^2} - \frac{1}{3}R^2\Lambda - \frac{\mathcal{M}}{R} \tag{8.14}$$

and accordingly

$$\mathcal{E}' = \frac{2\dot{R}\dot{R}'}{c^2} - \frac{2}{3}RR'\Lambda - \frac{\mathcal{M}'}{R} + \frac{\mathcal{M}R'}{R^2}. \tag{8.15}$$

We exert (8.14) and (8.15) to (8.13) and obtain the density equation (8.12):

$$\begin{aligned}\frac{8\pi\gamma}{c^2}\rho \;=\; & -\left(\frac{\dot{R}^2}{c^2R^2} - \frac{1}{3}\Lambda - \frac{\mathcal{M}}{R^3}\right) + \frac{\dot{R}^2}{c^2R^2} + 2\frac{\dot{R}\dot{R}'}{c^2RR'} \\ & -\left(\frac{2\dot{R}\dot{R}'}{c^2RR'} - \frac{2}{3}\Lambda - \frac{\mathcal{M}'}{R^2R'} + \frac{\mathcal{M}}{R^3}\right) - \Lambda \qquad \equiv \; \frac{\mathcal{M}'}{R^2R'}\end{aligned}$$

□

8.1. **Well-solvable special cases of the equation for $R(t,r)$.**
The previously established equation $\dot{R}^2 = c^2\left[\mathcal{E}(r) + \mathcal{M}(r)/R + (R/r_\Lambda)^2\right]$, see (8.10), can be transformed into the corresponding integral equation

$$\int_{R_0}^{R} \frac{dx}{\sqrt{\mathcal{E}(r) + \frac{\mathcal{M}(r)}{x} + \left(\frac{x}{r_\Lambda}\right)^2}} = \pm c\,(t - t_0) \tag{8.16}$$

where R_0 and t_0 are undetermined functions of r. Occasionally, we will abbreviate $\mathcal{E} = \mathcal{E}(r)$ and $\mathcal{M} = \mathcal{M}(r)$ again. We only deal with solutions of (8.16) for the radial function R. In order to establish the complete space-time model, one has to determine the function $\lambda(t,r)$ from Einstein's field equations (8.2), (8.3), (8.4) and (8.5) as well. Further, it might be necessary to specify some of the undetermined functions, which will occur in the solutions for R. Last but not least, equation (8.12) in lemma 18 prescribes a relation between R, $\mathcal{M}$ and a given density ρ. The following considerations are mainly restricted to solutions of integral equation (8.16). Some special cases of (8.16) are studied first.

8.1.1. ***Empty space with cosmological constant and $\mathcal{E} = 0$.***
As above mentioned, $\mathcal{E}(r)$ is related to the energy of the dust particles and $\mathcal{M}(r)$ represents the gravitational radius of the material inside a sphere with radius r. The case $\mathcal{E} = 0$, $\mathcal{M} = 0$ and $\Lambda \neq 0$ describes the expansion or contraction of empty space. Equation (8.16) gives

$$\pm\frac{c}{r_\Lambda}(t - t_0) = \int_{R_0}^{R} \frac{dx}{x} = \ln R - \ln R_0$$

and the solution is

$$R(t,r) = R_B(r)\exp\left(\pm\frac{ct}{r_\Lambda}\right)$$

where R_B is another undetermined function of r, which is related to t_0 and R_0 by $R_B = R_0\exp(\mp ct_0/r_\Lambda)$. Case 8.1.1 includes de Sitter's space-time, where

$$R(t,r) = ra_0\exp\left(\frac{ct}{r_\Lambda}\right) \quad \text{and} \quad e^{\lambda(t,r)} = a_0^2\exp^2\left(\frac{ct}{r_\Lambda}\right).$$

a_0 is an arbitrary constant. Notice that $c/r_\Lambda = H_0\sqrt{\Omega_\Lambda}$. For de Sitter's spacetime see subsection 2.4.

8.1.2. ***Empty space with cosmological constant and $\mathcal{E} > 0$.***
For $\mathcal{E} > 0$ ($\mathcal{M} = 0$ and $\Lambda \neq 0$) equation (8.16) reduces to

$$\int_{R_0}^{R} \frac{dx}{\sqrt{\mathcal{E} + \left(\frac{x}{r_\Lambda}\right)^2}} = \pm c\,(t - t_0)\,. \tag{8.17}$$

We transform to $x = \sqrt{\mathcal{E}} r_\Lambda y$, so that the integral on the left side of (8.17) reads[89]

$$\int_{R_0}^{R} \frac{dx}{\sqrt{\mathcal{E} + \left(\frac{x}{r_\Lambda}\right)^2}} = r_\Lambda \int_{y(R_0)}^{y(R)} \frac{dy}{\sqrt{1+y^2}} = r_\Lambda \text{Arsinh}\left(\frac{R}{r_\Lambda\sqrt{\mathcal{E}}}\right) + k_0. \tag{8.18}$$

k_0 is an undetermined function of r which contains the "R_0"-terms. Equation (8.17) yields:

$$R = r_\Lambda \sqrt{\mathcal{E}(r)} \sinh\left(\pm\frac{c}{r_\Lambda}(t - t_B(r))\right) = \pm r_\Lambda \sqrt{\mathcal{E}(r)} \sinh\left(\frac{c}{r_\Lambda}(t - t_B(r))\right)$$

where $t_B(r)$ contains the t_0 and k_0 terms.

8.1.3. ***Empty space with cosmological constant and*** $\mathcal{E} < 0$.
In this case we can replace $\mathcal{E}$ by $-|\mathcal{E}|$ in equation (8.17) and use the transformation $x = \sqrt{|\mathcal{E}|} r_\Lambda y$. The integral becomes[90]

$$\int_{R_0}^{R} \frac{dx}{\sqrt{\left(\frac{x}{r_\Lambda}\right)^2 - |\mathcal{E}|}} = r_\Lambda \int_{y(R_0)}^{y(R)} \frac{dy}{\sqrt{y^2-1}} = r_\Lambda \text{Arcosh}\left(\frac{R}{r_\Lambda\sqrt{|\mathcal{E}|}}\right) + k_0$$

and equation (8.17) yields:

$$R(t,r) = r_\Lambda \sqrt{|\mathcal{E}|} \cosh\left(\pm\frac{c}{r_\Lambda}(t - t_B(r))\right) = r_\Lambda \sqrt{|\mathcal{E}|} \cosh\left(\frac{c}{r_\Lambda}(t - t_B(r))\right)$$

$t_B(r)$ contains the t_0 and k_0 terms again.

8.1.4. ***Solution without cosmological constant and*** $\mathcal{M} \neq 0$***,*** $\mathcal{E} = 0$.
Now let's shift attention to a model universe without cosmological constant. The simplest case is $\mathcal{E} = 0$. Equation (8.16) reduces to

$$\pm c(t - t_0) = \frac{1}{\sqrt{\mathcal{M}}} \int_{R_0}^{R} \sqrt{x} dx = \frac{2}{3\sqrt{\mathcal{M}}} R^{3/2} - k_0$$

---

[89] It is easy to solve the middle integral. With $y = \sinh\varphi$ one has

$$\int \frac{dy}{\sqrt{1+y^2}} = \int \frac{\cosh\varphi d\varphi}{\sqrt{1+\sinh^2\varphi}} = \int d\varphi = \varphi + c = \text{Arsinh}(y) + c$$

where c is a constant of integration.

[90] The second integral can be solved with the transformation $y = \cosh\varphi$. We get

$$\int \frac{dy}{\sqrt{y^2-1}} = \int \frac{\sinh\varphi d\varphi}{\sqrt{\cosh^2\varphi - 1}} = \int d\varphi = \varphi + c = \text{Arcosh}(y) + c$$

where c is a constant of integration.

so that R is given by:

$$R = \sqrt[3]{\frac{9\mathcal{M}c^2}{4}\left(t - t_B\left(r\right)\right)^2} \tag{8.19}$$

8.1.5. ***Solution without cosmological constant and*** $\mathcal{M} \neq 0$***,*** $\mathcal{E} > 0$.
For $\Lambda = 0$ but $\mathcal{E} \neq 0$ and $\mathcal{M} \neq 0$ the integral equation (8.16) reduces to

$$\int_{R_0}^{R} \frac{dx}{\sqrt{\mathcal{E}\left(r\right) + \frac{\mathcal{M}(r)}{x}}} = \pm c\left(t - t_0\right). \tag{8.20}$$

We introduce the new coordinate η by

$$x = \frac{\mathcal{M}}{2\mathcal{E}}\left(\cosh\eta - 1\right) \tag{8.21}$$

According to the definition of η, it is $dx = \frac{\mathcal{M}}{2\mathcal{E}}\sinh\eta\, d\eta$ and the integral reads

$$\int_{R_0}^{R} \frac{dx}{\sqrt{\mathcal{E} + \frac{\mathcal{M}}{x}}} = \frac{\mathcal{M}}{2\mathcal{E}} \int_{\eta(R_0)}^{\eta(R)} \frac{\sinh\eta\, d\eta}{\sqrt{\mathcal{E} + \frac{2\mathcal{E}}{\cosh\eta - 1}}} = \frac{\mathcal{M}}{2\mathcal{E}^{3/2}} \int_{\eta(R_0)}^{\eta(R)} \sqrt{\frac{\cosh\eta - 1}{\cosh\eta + 1}}\sinh\eta\, d\eta.$$

Since $\sinh^2\eta = \cosh^2\eta - 1 = \left(\cosh\eta + 1\right)\left(\cosh\eta - 1\right)$ we have:

$$\sinh\eta = \sqrt{\left(\cosh\eta + 1\right)\left(\cosh\eta - 1\right)} \tag{8.22}$$

We exert (8.22) to the integral and get

$$\frac{\mathcal{M}}{2\mathcal{E}^{3/2}} \int_{\eta(R_0)}^{\eta(R)} \left(\cosh\eta - 1\right) d\eta = \frac{\mathcal{M}}{2\mathcal{E}^{3/2}}\left(\sinh\eta - \eta\right) - k_0. \tag{8.23}$$

The $x = \frac{\mathcal{M}}{2\mathcal{E}}\left(\cosh\eta - 1\right)$ relation gives $\frac{x\mathcal{E}}{\mathcal{M}} = \frac{1}{2}\left(\cosh\eta - 1\right) = \sinh^2\left(\frac{\eta}{2}\right)$ and thus:

$$\eta = 2\mathrm{Arsinh}\left(\sqrt{\frac{x\mathcal{E}}{\mathcal{M}}}\right) \tag{8.24}$$

Finally, we get the solution of the integral in equation (8.20) by retransforming the η coordinate (8.24) in (8.23):

$$\int_{R_0}^{R} \frac{dx}{\sqrt{\mathcal{E} + \frac{\mathcal{M}}{x}}} = \frac{\mathcal{M}}{2\mathcal{E}^{3/2}}\left(\sinh\left[2\mathrm{Arsinh}\left(\sqrt{\frac{R\mathcal{E}}{\mathcal{M}}}\right)\right] - 2\mathrm{Arsinh}\left(\sqrt{\frac{R\mathcal{E}}{\mathcal{M}}}\right)\right) - k_0 \tag{8.25}$$

where k_0 contains all the R_0-terms. Nevertheless, we can not solve equation (8.20) to the $R\left(t\right)$ function without using a parametric form. One gets the most common (and simplest) notation of the $\mathcal{E} > 0$ solution in parametric form by using (8.23) together with (8.21):

$$R = \frac{\mathcal{M}}{2\mathcal{E}}\left(\cosh\eta - 1\right), \quad \frac{\mathcal{M}}{2\mathcal{E}^{3/2}}\left(\sinh\eta - \eta\right) = \pm c\left(t - t_B\left(r\right)\right) \tag{8.26}$$

8.1.6. ***Solution without cosmological constant and*** $\mathcal{M} \neq 0$, $\mathcal{E} < 0$.
In this case we may replace $\mathcal{E}$ by $-|\mathcal{E}|$ in equation (8.20) and introduce the coordinate η by $x = \frac{\mathcal{M}}{2|\mathcal{E}|}(1 - \cos\eta)$. Consequently, it applies $dx = \frac{\mathcal{M}}{2|\mathcal{E}|}\sin\eta\, d\eta$ and the integral in equation (8.20) transforms to

$$\int_{R_0}^{R} \frac{dx}{\sqrt{-|\mathcal{E}| + \frac{\mathcal{M}}{x}}} = \frac{\mathcal{M}}{2\,|\mathcal{E}|^{3/2}} \int_{\eta(R_0)}^{\eta(R)} \sqrt{\frac{1-\cos\eta}{1+\cos\eta}}\sin\eta\, d\eta.$$

Together with $\sin\eta = \sqrt{1-\cos^2\eta} = \sqrt{(1-\cos\eta)(1+\cos\eta)}$ equation (8.20) reads

$$\pm c\,(t - t_0) = \frac{\mathcal{M}}{2\,|\mathcal{E}|^{3/2}} \int_{\eta(R_0)}^{\eta(R)} (1-\cos\eta)\, d\eta = \frac{\mathcal{M}}{2\,|\mathcal{E}|^{3/2}} (\eta - \sin\eta) + k_0.$$

Hence, the $\mathcal{E} < 0$ solution is given by:

$$R = \frac{\mathcal{M}}{2\,|\mathcal{E}|}(1-\cos\eta)\,, \quad \frac{\mathcal{M}}{2\,|\mathcal{E}|^{3/2}}(\eta - \sin\eta) = \pm c\,(t - t_B\,(r)) \tag{8.27}$$

Figure 8.1 presents an outline of the LTB solutions for $\Lambda = 0$.

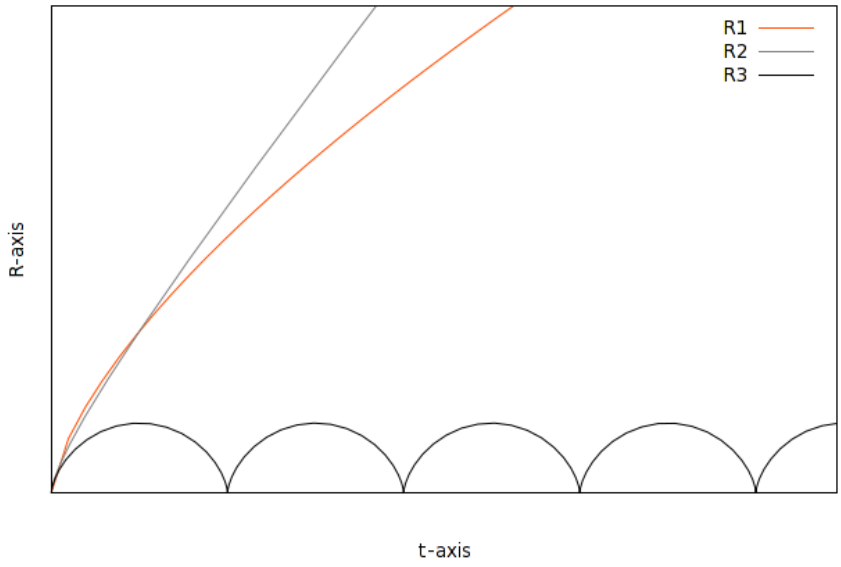

FIGURE 8.1. Outline of the LTB solutions without cosmological constant. The graphic shows the functions $R_1 : \left(\eta \mid \frac{9}{4}\eta^{2/3}\right)$, $R_2 : \frac{1}{2}(\sinh\eta - \eta \mid \cosh\eta - 1)$ and $R_3 : \frac{1}{2}(\eta - \sin\eta \mid 1 - \cos\eta)$ which represent the "+" branch of the solutions (8.19), (8.26) and (8.27) for $c = 1$, $\mathcal{M}(r) \equiv 1$, $t_B(r) \equiv 0$ and further $\mathcal{E}(r) \equiv 1$ in (8.26) and (8.27). The initial big bang occurs at the coordinate origin.

8.2. **General solution including a nonzero cosmological constant.**
This section is concerned with the general case of our differential equation (8.10), respectively with the corresponding integral equation (8.16), in case of nonzero Λ, $\mathcal{E}(r)$ and $\mathcal{M}(r)$. The following considerations are restricted to the "+" branch of (8.10) and (8.16). Thus, our equations are:

$$\dot{R} = c\sqrt{\mathcal{E}(r) + \frac{\mathcal{M}(r)}{R} + \left(\frac{R}{r_\Lambda}\right)^2} \tag{8.28}$$

$$\int_{R_0}^{R} \frac{dx}{\sqrt{\mathcal{E}(r) + \frac{\mathcal{M}(r)}{x} + \left(\frac{x}{r_\Lambda}\right)^2}} = c(t - t_0) \tag{8.29}$$

Generally, the integral on the left side of equation (8.29) is of elliptic type. Our first approach is to solve equation (8.29) approximately by using the Taylor series expansion for the function in the integral. After that we work out a numerical solution of the corresponding differential equation (8.28).

8.2.1. ***The Taylor approximation.***
In order to simplify the calculations, we define $f(x) := \mathcal{E}(r) + \frac{\mathcal{M}(r)}{x} + \left(\frac{x}{r_\Lambda}\right)^2$ and further $h(x) = 1/\sqrt{f(x)}$. One has:

$$h' = -\frac{1}{2} f^{-\frac{3}{2}} f' = -\frac{1}{2f^{\frac{3}{2}}}\left(-\frac{\mathcal{M}}{x^2} + \frac{2x}{r_\Lambda^2}\right) \tag{8.30}$$

We evaluate the function h, which is the function in the integral of equation (8.29), at the point

$$R_* := \sqrt[3]{\frac{1}{2}\mathcal{M} r_\Lambda^2}. \tag{8.31}$$

We obtain $f'(R_*) = 0$ as well as $h'(R_*) = 0$, see equation (8.30). The second and third derivative of h have the structure

$$h'' = -\frac{1}{2} f^{-\frac{3}{2}} f'' + \frac{3}{4} f^{-\frac{5}{2}} f'^2 \quad \text{and} \quad h''' = -\frac{1}{2} f^{-\frac{3}{2}} f''' + (\dots) \cdot f'$$

so that

$$h''(R_*) = \left.\frac{dh}{dx}\right|_{f'=0} = -\frac{1}{2f^{\frac{3}{2}}(R_*)} f''(R_*) = -\frac{1}{2\sqrt{f(R_*)}^3} \cdot \frac{6}{r_\Lambda^2} = -\frac{3}{r_\Lambda^2} h^3(R_*)$$

$$h'''(R_*) = \left.\frac{d^2h}{dx^2}\right|_{f'=0} = -\frac{1}{2f^{\frac{3}{2}}(R_*)} f'''(R_*) = \frac{6}{R_* r_\Lambda^2} h^3(R_*)$$

The Taylor series expansion for h at R_* is given by $h(x) = \sum_{k=0}^{\infty} \frac{1}{k!} \cdot h^{(k)}(R_*)(x - R_*)^k$ where $h^{(k)}$ stands for the $k-$th derivative of h with respect to the x coordinate.

Neglecting the terms of fourth and higher order we obtain $h(x) \approx \widetilde{h}(x)$ where

$$\begin{aligned}\widetilde{h}(x): &= h(R_*) + h'(R_*)(x-R_*) + \frac{1}{2}h''(R_*)(x-R_*)^2 + \frac{1}{6}h'''(R_*)(x-R_*)^3 \\ &= h(R_*) - \frac{3}{2r_\Lambda^2}h^3(R_*)(x-R_*)^2 + \frac{1}{r_\Lambda^2 R_*}h^3(R_*)(x-R_*)^3.\end{aligned}$$

8.2.2. ***Splitting up the integral.***
Now we split up the elliptic integral in equation (8.29) into three parts. As mentioned above, $\mathcal{M}(r)$ represents the gravitational radius r_g of the material (e.g. dust) inside the sphere with radius r. The gravitational radius r_g and $r_\Lambda = \sqrt{3/\Lambda}$ are located far apart from each other. In the neighborhood of r_g we may neglect the r_Λ-term and vice versa. Hence, there are constants $R_1 < R_* < R_2$, so that the following ansatz is a good approximation:
If $R \leq R_1$ one has

$$\int_{R_0}^{R} h(x)\,dx \approx \int_{R_0}^{R} \frac{dx}{\sqrt{\mathcal{E} + \frac{\mathcal{M}}{x}}}, \tag{8.32}$$

for $R_1 < R \leq R_2$ we have

$$\int_{R_0}^{R} h(x)\,dx \approx \int_{R_0}^{R_1} \frac{dx}{\sqrt{\mathcal{E} + \frac{\mathcal{M}}{x}}} + \int_{R_1}^{R} \widetilde{h}(x)\;dx \tag{8.33}$$

and in case of $R > R_2$ it is

$$\int_{R_0}^{R} h(x)\,dx \approx \int_{R_0}^{R_1} \frac{dx}{\sqrt{\mathcal{E} + \frac{\mathcal{M}}{x}}} + \int_{R_1}^{R_2} \widetilde{h}(x)\;dx + \int_{R_2}^{R} \frac{dx}{\sqrt{\mathcal{E} + \left(\frac{x}{r_\Lambda}\right)^2}}. \tag{8.34}$$

We already solved (8.32). Together with the $\operatorname{Arsinh}(x) = \ln\left(x + \sqrt{x^2+1}\right)$ identity our solution reads

$$\begin{aligned}\int \frac{dx}{\sqrt{\mathcal{E} + \frac{\mathcal{M}}{x}}} &= \frac{\mathcal{M}}{2\mathcal{E}^{3/2}}\left(\sinh\left[2\operatorname{Arsinh}\left(\sqrt{\frac{x\mathcal{E}}{\mathcal{M}}}\right)\right] - 2\operatorname{Arsinh}\left(\sqrt{\frac{x\mathcal{E}}{\mathcal{M}}}\right)\right) + k_0 \\ &= \frac{\mathcal{M}}{4\mathcal{E}^{3/2}}\left[\left(\sqrt{\frac{x\mathcal{E}}{\mathcal{M}}} + \sqrt{\frac{x\mathcal{E}}{\mathcal{M}}+1}\right)^2 - \frac{1}{\left(\sqrt{\frac{x\mathcal{E}}{\mathcal{M}}} + \sqrt{\frac{x\mathcal{E}}{\mathcal{M}}+1}\right)^2}\right] \\ &\quad -\frac{\mathcal{M}}{\mathcal{E}^{3/2}}\ln\left(\sqrt{\frac{x\mathcal{E}}{\mathcal{M}}} + \sqrt{\frac{x\mathcal{E}}{\mathcal{M}}+1}\right) + k_0\end{aligned}$$

The (8.33) integral is easy to solve:

$$\int \widetilde{h}(x)\;dx = h(R_*) - \frac{1}{2r_\Lambda^2}h^3(R_*)(x-R_*)^3 + \frac{1}{4r_\Lambda^2 R_*}h^3(R_*)(x-R_*)^4 + k_0$$

Furthermore, from equation (8.18) we obtain the solution of the (8.34) integral:

$$\int \frac{dx}{\sqrt{\mathcal{E}+\left(\frac{x}{r_\Lambda}\right)^2}} = r_\Lambda \mathrm{Arsinh}\left(\frac{x}{r_\Lambda\sqrt{\mathcal{E}}}\right)+k_0 = r_\Lambda \ln\left(\frac{x}{r_\Lambda\sqrt{\mathcal{E}}}+\sqrt{\frac{x^2}{r_\Lambda^2\mathcal{E}}+1}\right)+k_0$$

Now it is easy to calculate some data points from equation (8.29). If we use $t_0 = 0$, equation (8.29) gives

$$t(R) = \frac{1}{c}\int_{R_0}^{R} h(x)\,dx$$

where the integral is given by (8.32), (8.33) or (8.34). In the most bulky case $R > R_2$, the latter equation gives:

(8.35)

$$\begin{aligned} t(R) \;=\; & \frac{r_\Lambda}{c}\ln\left(\frac{R}{r_\Lambda\sqrt{\mathcal{E}}}+\sqrt{\frac{R^2}{r_\Lambda^2\mathcal{E}}+1}\right)-\frac{r_\Lambda}{c}\ln\left(\frac{R_2}{r_\Lambda\sqrt{\mathcal{E}}}+\sqrt{\frac{R_2^2}{r_\Lambda^2\mathcal{E}}+1}\right) \\ & +\frac{1}{2cr_\Lambda^2}h^3(R_*)\left[(R_1-R_*)^3-(R_2-R_*)^3\right] \\ & +\frac{1}{4cr_\Lambda^2R_*}h^3(R_*)\left[(R_2-R_*)^4-(R_1-R_*)^4\right] \\ & +\frac{\mathcal{M}}{4c\mathcal{E}^{3/2}}\left[\left(\sqrt{\frac{R_1\mathcal{E}}{\mathcal{M}}}+\sqrt{\frac{R_1\mathcal{E}}{\mathcal{M}}+1}\right)^2-\left(\sqrt{\frac{R_0\mathcal{E}}{\mathcal{M}}}+\sqrt{\frac{R_0\mathcal{E}}{\mathcal{M}}+1}\right)^2\right. \\ & \left.+\left(\sqrt{\frac{R_0\mathcal{E}}{\mathcal{M}}}+\sqrt{\frac{R_0\mathcal{E}}{\mathcal{M}}+1}\right)^{-2}-\left(\sqrt{\frac{R_1\mathcal{E}}{\mathcal{M}}}+\sqrt{\frac{R_1\mathcal{E}}{\mathcal{M}}+1}\right)^{-2}\right] \\ & +\frac{\mathcal{M}}{c\mathcal{E}^{3/2}}\left[\ln\left(\sqrt{\frac{R_0\mathcal{E}}{\mathcal{M}}}+\sqrt{\frac{R_0\mathcal{E}}{\mathcal{M}}+1}\right)-\ln\left(\sqrt{\frac{R_1\mathcal{E}}{\mathcal{M}}}+\sqrt{\frac{R_1\mathcal{E}}{\mathcal{M}}+1}\right)\right] \end{aligned}$$

The calculations can be done with a computer algebra system. A table with some data is given in the appendix. Later we compare these results with our numerical solution for (8.28), which we work out in the following.

8.2.3. ***Numerical approximation.***

In order to get an impression of the influence of Λ, it is enough to solve (8.28) for constant $\mathcal{E}(r)$ and $\mathcal{M}(r)$, say $\mathcal{E} \equiv 1$ and $\mathcal{M} \equiv 0.125\,pc$ (the gravitational radius of the Local Group). We introduce the new coordinate $\xi = ct$. The resulting equation

$$\frac{dR}{d\xi} \approx \sqrt{1+\frac{r_{LG}}{R}+\left(\frac{R}{r_\Lambda}\right)^2} \tag{8.36}$$

can be solved by numerical integration. Unfortunately, the algorithm cannot start at $R = 0$, since there is a discontinuity on the right side of (8.36). Due to the

tiny order of magnitude of the cosmological constant we proceed on the assumption that the general solution coincides with the $\Lambda = 0$ solution (8.26) for small R. Corresponding to $\mathcal{E} = 1$ and $\mathcal{M} = r_{LG}$, we obtain initial values from

$$\xi_0 \approx \frac{r_{LG}}{2}\left(\sinh\eta - \eta\right), \quad R_0 \approx \frac{r_{LG}}{2}\left(\cosh\eta - 1\right) \tag{8.37}$$

where η has to be small, say $\eta = 0.1$. The numerical data was produced with algorithm 20, see appendix.

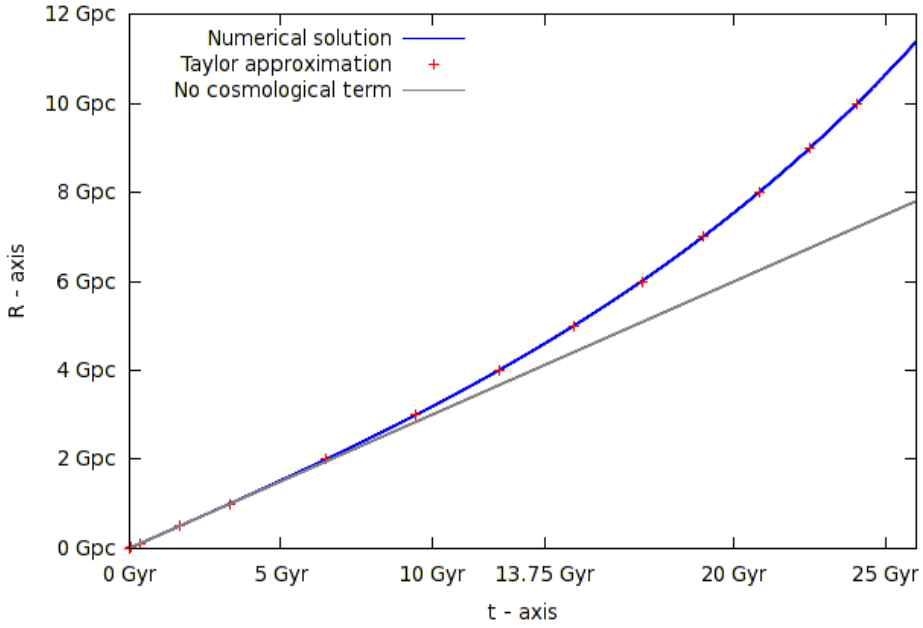

FIGURE 8.2. Radial function R of the LTB interval (8.1), it is $R^2 = -g_{22}$. The graphic shows the numerical solution of (8.36):

$$\frac{dR}{d\xi} \approx \sqrt{1 + \frac{r_{LG}}{R} + \left(\frac{R}{r_\Lambda}\right)^2}$$

We used $r_{LG} \approx 0.125\,\text{pc}$, $r_\Lambda \approx 5\,\text{Gpc}$ and $\xi = ct$ where the speed of light is $c \approx 3 \cdot 10^8\text{m/s} \approx 0.3\,\text{Gpc/Gyr}$. Additionally, the graphic shows an approximation based on Taylor series and the well-solvable $\Lambda = 0$ case. The current age of our universe is marked at 13.75 Gyr.

8.3. **The LTB Swiss-Cheese model.**

This section is concerned with a matching condition for a static Schwarzschild vacuole embedded in an expanding Lemaitre-Tolman-Bondi (LTB) universe. Subsection 7.1 dealt with a similar problem, the matching condition in a ΛCDM Swiss-Cheese model. As already mentioned, the ΛCDM Swiss-Cheese model, which refers to a spherical Schwarzschild-de Sitter region immersed in a ΛCDM cosmology, is a generalization of the $\Lambda = 0$ Einstein-Straus vacuole. In 2000, Bonnor pointed out, that "*the ES* [Einstein-Straus] *vacuole imposes a boundary condition which relates the central Schwarzschild mass to the size of the vacuole and the cosmic density. The condition implies, roughly, that the Schwarzschild mass, averaged over the vacuole, must equal the cosmic density. This seriously restricts the astronomical systems to which the ES theory can be applied. For example, it could not be applied to the solar system because the average density is much too high.*" [12]. Naturally, same holds for the ΛCDM Swiss-Cheese model. Bonnor used another method to generalize the Einstein-Straus model: "*I take a Schwarzschild vacuole and match it to a general spherically symmetric dust universe, i.e. a Lemaitre–Tolman–Bondi (LTB) model*" [12]. Evidently, this method is similar to the construction of the ΛCDM Swiss-Cheese model, except that there is LTB background instead of the FLRW cosmology: A spherical region in an expanding LTB cosmology is evacuated, and the material is replaced by a compact mass condensation, which is surrounded by an empty cavity. What we now have is a LTB Swiss-Cheese model, a static gravitational field, embedded in a nonstatic, expanding cosmological LTB background. Bonnor found, "*that the matching can be achieved for a vacuole of any radius, and with any central mass* [...]" [12].

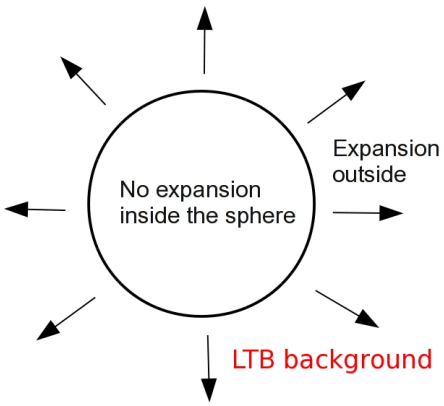

FIGURE 8.3.
LTB Swiss-Cheese.

Now we construct a "LTB Swiss-Cheese" model, where the LTB background is filled with dust or material of negligible pressure. Since we have no exact solution for the general LTB model including a cosmological constant, we consider the case $\Lambda = 0$ in the following. The LTB background is given by (8.1) together with (8.6) and $e^k = 1 + \mathcal{E}$, see section 8. In the following, time and radial coordinates of the LTB

spacetime are overlined:

$$ds^2 = c^2 d\bar{t}^2 - \frac{R'^2\left(\bar{t},\bar{r}\right)}{1+\mathcal{E}\left(\bar{r}\right)} d\bar{r}^2 - R^2\left(\bar{t},\bar{r}\right)\left(d\theta^2 + \sin^2\theta\, d\phi^2\right) \tag{8.38}$$

For the expanding $\Lambda = 0$ model we obtained (8.26)

$$R = \frac{\mathcal{M}\left(\bar{r}\right)}{2\mathcal{E}\left(\bar{r}\right)}\left(\cosh\eta - 1\right), \quad \frac{\mathcal{M}\left(\bar{r}\right)}{2\mathcal{E}^{3/2}\left(\bar{r}\right)}\left(\sinh\eta - \eta\right) = \pm c\left(\bar{t} - \bar{t}_B\left(\bar{r}\right)\right). \tag{8.39}$$

To simplify the following considerations, we choose suitable functions $\mathcal{E}$, $\mathcal{M}$:

$$\mathcal{E}\left(\bar{r}\right) = \sinh^2\left(\bar{r}\right), \quad \mathcal{M}\left(\bar{r}\right) = 2a_0 \sinh^3\left(\bar{r}\right) \tag{8.40}$$

Now we fit the (8.38) interval to the Schwarzschild interval, which is given by

$$ds^2 = \left(1 - \frac{r_g}{r}\right) dt^2 - \frac{1}{1-\frac{r_g}{r}} dr^2 - r^2\left(d\theta^2 + \sin^2\theta\, d\phi^2\right). \tag{8.41}$$

8.3.1. ***Matching condition for Schwarzschild and LTB.***
With the functions $\mathcal{E}$ and $\mathcal{M}$ given by (8.40), equation (8.39) reads

$$R = a_0 \sinh\left(\bar{r}\right)\left(\cosh\eta - 1\right), \quad a_0\left(\sinh\eta - \eta\right) = \pm c\left(\bar{t} - \bar{t}_B\left(\bar{r}\right)\right) \tag{8.42}$$

and it remains

$$\frac{R'^2}{1+\mathcal{E}} = \frac{a_0^2 \cosh^2\left(\bar{r}\right)\left(\cosh\eta - 1\right)^2}{1+\sinh^2\left(\bar{r}\right)} = a_0^2\left(\cosh\eta - 1\right)^2.$$

In common with section 7.1, consider again an observer at rest in the comoving coordinate system, located at the boundary of the spherical cavity. The observer's coordinates θ and ϕ are constant and thus $d\theta = d\phi = 0$. Let $r_0\left(t\right)$ represent the radius of the boundary sphere with respect to the Schwarzschild coordinates (8.41) and $\bar{r}_0$ denotes the fixed comoving radius of that sphere with respect to the LTB coordinates (8.38). In the comoving system it is $d\bar{r} = 0$, so that (8.38) yields $ds^2 = c^2 d\bar{t}^2$. Hence, the connection between t and $\bar{t}$ is given by:

$$c^2 d\bar{t}^2 = \left(1 - \frac{r_g}{r_0}\right) dt^2 - \frac{1}{1-\frac{r_g}{r_0}} dr_0^2 \tag{8.43}$$

Matching of the intervals (8.38) and (8.41) at $\bar{r}_0$ requires $R\left(\bar{t},\bar{r}_0\right) = r_0\left(t\right)$. The motion of the shell in LTB coordinates is given by

$$r_0\left(t\right) = R\left(\bar{t},\bar{r}_0\right) = a_0 \sinh\bar{r}_0\left(\cosh\eta - 1\right), \quad a_0\left(\sinh\eta - \eta\right) = \pm c\left(\bar{t} - \bar{t}_B\left(\bar{r}_0\right)\right) \tag{8.44}$$

so that $dr_0 = a_0 \sinh\bar{r}_0 \sinh\eta d\eta$ and $a_0\left(\cosh\eta - 1\right) d\eta = \pm c d\bar{t}$. Using r_0, dr_0 and $cd\bar{t}$ in (8.43), the condition reads

$$a_0^2\left(\cosh\eta - 1\right)^2 d\eta^2 = \left(1 - \frac{r_g}{a_0 \sinh\bar{r}_0\left(\cosh\eta - 1\right)}\right) dt^2 - \frac{a_0^2 \sinh^2\bar{r}_0 \sinh^2\eta d\eta^2}{1 - \frac{r_g}{a_0 \sinh\bar{r}_0\left(\cosh\eta - 1\right)}}.$$

We choose an appropriate a_0 by $a_0 = r_g/\left(2\sinh^3\overline{r}_0\right)$ so that

$$1 - \frac{r_g}{a_0\sinh\overline{r}_0\left(\cosh\eta - 1\right)} = \frac{\cosh\eta - 1 - 2\sinh^2\overline{r}_0}{\cosh\eta - 1}$$

and therewith

$$dt^2 = \left(a_0^2\left(\cosh\eta - 1\right) + \frac{a_0^2\sinh^2\overline{r}_0\sinh^2\eta}{\cosh\eta - 1 - 2\sinh^2\overline{r}_0}\right)\frac{\left(\cosh\eta - 1\right)^2}{\cosh\eta - 1 - 2\sinh^2\overline{r}_0}d\eta^2.$$

Adding the fractions in the brackets on the right side results in

$$\begin{aligned} dt^2 &= a_0^2\left[\left(\cosh\eta - 1\right)^2 - 2\sinh^2\overline{r}_0\left(\cosh\eta - 1\right) + \sinh^2\overline{r}_0\sinh^2\eta\right]\times \\ &\qquad \times\left(\frac{\cosh\eta - 1}{\cosh\eta - 1 - 2\sinh^2\overline{r}_0}\right)^2 d\eta^2 \end{aligned}$$

which can be rearranged to

$$\begin{aligned} dt^2 &= a_0^2\left[\left(\cosh\eta - 1\right)^2 + \sinh^2\overline{r}_0\left(\sinh^2\eta - 2\cosh\eta + 2\right)\right]\times \\ &\qquad \times\left(\frac{\cosh\eta - 1}{\cosh\eta - 1 - 2\sinh^2\overline{r}_0}\right)^2 d\eta^2. \end{aligned}$$

Together with the $\sinh^2\eta = \cosh^2\eta - 1$ identity, the term in the second inner parentheses reads

$$\sinh^2\eta - 2\cosh\eta + 2 = \cosh^2\eta - 2\cosh\eta + 1 = \left(\cosh\eta - 1\right)^2$$

so that the equation reduces to

$$dt^2 = \frac{a_0^2\cosh^2\overline{r}_0\left(\cosh\eta - 1\right)^4}{\left(\cosh\eta - 1 - 2\sinh^2\overline{r}_0\right)^2}d\eta^2 \tag{8.45}$$

which can be integrated analytically. Using the abbreviations

$$\mathcal{C}\left(\eta\right) := \cosh\eta - 1, \quad \beta := 2\sinh^2\overline{r}_0$$

one gets from (8.45)

$$dt = \pm\frac{a_0\cosh\overline{r}_0\left(\cosh\eta - 1\right)^2}{\cosh\eta - 1 - 2\sinh^2\overline{r}_0}d\eta = \pm a_0\cosh\overline{r}_0\frac{\mathcal{C}^2\left(\eta\right)}{\mathcal{C}\left(\eta\right) - \beta}d\eta. \tag{8.46}$$

By polynomial long division we get

$$\frac{\mathcal{C}^2\left(\eta\right)}{\mathcal{C}\left(\eta\right) - \beta} = \mathcal{C}\left(\eta\right) + \beta + \frac{\beta^2}{\mathcal{C}\left(\eta\right) - \beta}$$

and integration of (8.46) leads to

$$\begin{aligned} t - t_1 &= \pm a_0\cosh\overline{r}_0\int_{\eta_1}^{\eta}\left[\mathcal{C}\left(x\right) + \beta + \frac{\beta^2}{\mathcal{C}\left(x\right) - \beta}\right]dx \\ &= \pm a_0\cosh\overline{r}_0\left(\sinh\eta - \eta + \beta\eta - k_1 + \beta^2\int_{\eta_1}^{\eta}\frac{dx}{\mathcal{C}\left(x\right) - \beta}\right) \end{aligned} \tag{8.47}$$

where $k_1 = \sinh\eta_1 - \eta_1 + \beta\eta_1$. Now we use the $\cosh x = \frac{1}{2}\left(e^x + e^{-x}\right)$ identity and $y = e^x$ to solve the last integral:

$$\int_{\eta_1}^{\eta} \frac{dx}{\mathcal{C}(x) - \beta} = 2\int_{\eta_1}^{\eta} \frac{dx}{e^x + e^{-x} - 2(\beta+1)} = 2\int_{y(\eta_1)}^{y(\eta)} \frac{dy}{y^2 + 1 - 2(\beta+1)\,y} \tag{8.48}$$

This integral is given in [14]: For $a \neq 0$, $D := 4ac - b^2 < 0$ and $|2ax + b| > \sqrt{-D}$ one has

$$\int \frac{dx}{ax^2 + bx + c} = \frac{1}{\sqrt{-D}} \ln\left(\frac{2ax + b - \sqrt{-D}}{2ax + b + \sqrt{-D}}\right) + k \tag{8.49}$$

where k is a constant of integration. For the (8.48) integral we have $a = c = 1$, $b = -2(\beta+1)$ and $D = 4 - 4(\beta+1)^2$. Since we may assume that $\overline{r}_0 > 0$, it is $\beta = 2\sinh^2\overline{r}_0 > 0$ and therewith $D < 0$. Accordingly, we get from[91] (8.49):

$$\int \frac{dy}{y^2 + 1 - 2(\beta+1)\,y} = \frac{1}{2\sqrt{\beta^2 + 2\beta}} \ln\left[\frac{y - (\beta+1) - \sqrt{\beta^2 + 2\beta}}{y - (\beta+1) + \sqrt{\beta^2 + 2\beta}}\right] + k$$

With the latter formula we can now solve the integral (8.48). After retransformation to the η coordinate it remains

$$\int_{\eta_1}^{\eta} \frac{dx}{\mathcal{C}(x) - \beta} = \frac{1}{\sqrt{\beta^2 + 2\beta}} \ln\left(\frac{e^\eta - (\beta+1) - \sqrt{\beta^2 + 2\beta}}{e^\eta - (\beta+1) + \sqrt{\beta^2 + 2\beta}}\right) - k_2$$

where k_2 contains the "η_1"- terms. The argument of the logarithm can be appreciably simplified by replacing $\beta = 2\sinh^2\overline{r}_0$ again. After a short calculation one gets

$$e^\eta - (\beta+1) \pm \sqrt{\beta^2 + 2\beta} = e^\eta - e^{\mp 2\overline{r}_0}$$

and our integral reads

$$\int_{\eta_1}^{\eta} \frac{dx}{\mathcal{C}(x) - \beta} = \frac{1}{2\sinh\overline{r}_0\cosh\overline{r}_0} \ln\left(\frac{e^\eta - e^{2\overline{r}_0}}{e^\eta - e^{-2\overline{r}_0}}\right) - k_2.$$

Now we use the latter integral in (8.47). Remember that we chose $a_0 = r_g/\left(2\sinh^3\overline{r}_0\right)$. The relationship between the observer time and the world time is

$$t = t_0 \pm \frac{r_g\cosh\overline{r}_0}{2\sinh^3\overline{r}_0}\left[\sinh\eta - \eta + 2\eta\sinh^2\overline{r}_0 + \frac{2\sinh^3\overline{r}_0}{\cosh\overline{r}_0}\ln\left(\frac{e^\eta - e^{2\overline{r}_0}}{e^\eta - e^{-2\overline{r}_0}}\right)\right]$$

and[92]

$$\overline{t} = \overline{t}_B(\overline{r}_0) \mp \frac{r_g}{2c\sinh^3\overline{r}_0}(\sinh\eta - \eta).$$

---

[91] Alternatively, the integral in (8.48) can be solved by completing the square in the denominator. Let $B_\pm := -(\beta+1) \pm \sqrt{\beta^2 + 2\beta}$ so that $y^2 + 1 - 2(\beta+1)\,y = (y + B_-)(y + B_+)$. Our integral can be rewritten as

$$\int \frac{dy}{y^2 + 1 - 2(b+1)\,y} = \frac{1}{B_+ - B_-}\int\left(\frac{1}{y + B_-} - \frac{1}{y + B_+}\right)dy = \frac{1}{B_+ - B_-}\ln\left(\frac{y + B_-}{y + B_+}\right)$$

[92] see equation (8.44)

9. A new empty-space-solution of Einstein's equations

During our investigations concerning the coordinate replacement which transforms the Schwarzschild metric into McVittie's solution, it turned out that there is a new solution of $R_{ik} - \frac{1}{2}R\,g_{ik} - \Lambda g_{ik} = 0$ Einstein's equations, partly based on the de Sitter structure. If we replace the $q-$coordinate of the isotropic Schwarzschild metric (5.26) by $a\,(t)\,q$ and dq by $a\,(t)\,dq$, we obtain McVittie's metric, see section 4. Now we establish a new empty-space-solution of Einstein's equations by using the same coordinate replacement. Consider the metric[93]

$$ds^2 = \left(\frac{1 - Lq^2}{1 + Lq^2}\right)^2 c^2 dt^2 - \left(\frac{1}{1 + Lq^2}\right)^2 d\sigma^2$$

which represents the de Sitter solution (5.18) for $L = \frac{\Lambda}{12}$. The above mentioned coordinate replacement yields

$$ds^2 = \left[\frac{1 - La^2\,(t)\,q^2}{1 + La^2\,(t)\,q^2}\right]^2 c^2 dt^2 - a^2\,(t)\left[\frac{1}{1 + La^2\,(t)\,q^2}\right]^2 d\sigma^2 \tag{9.1}$$

Theorem 19. *Existence theorem*
Let L be an arbitrary constant. Its physical unit has to coincide with the unit of the cosmological constant Λ. In the following $a_0 \in \mathbb{R}$ is a constant of integration.
1) We assume that $L \leq \Lambda/12$. The line element

$$\begin{aligned} ds^2 \;=\; & \left[\frac{1 - La_0^2 \exp\left(2\left(\frac{\Lambda}{3} - 4L\right)^{1/2} ct\right) q^2}{1 + La_0^2 \exp\left(2\left(\frac{\Lambda}{3} - 4L\right)^{1/2} ct\right) q^2}\right]^2 c^2 dt^2 - a_0^2 \exp\left(2\left(\frac{\Lambda}{3} - 4L\right)^{1/2} ct\right) \times \\ & \times \left[\frac{1}{1 + La_0^2 \exp\left(2\left(\frac{\Lambda}{3} - 4L\right)^{1/2} ct\right) q^2}\right]^2 \left(dq^2 + q^2 d\theta^2 + q^2 \sin^2\theta\, d\phi^2\right) \end{aligned}$$

is an exact solution of Einstein's equations.
2) In case of $L = \Lambda/12$ and $a_0 = 1$ the above line element reduces to de Sitter's isotropic solution (5.18)

$$ds^2 = \left(\frac{1 - \frac{1}{4r_\Lambda^2} q^2}{1 + \frac{1}{4r_\Lambda^2} q^2}\right)^2 c^2 dt^2 - \left(\frac{1}{1 + \frac{1}{4r_\Lambda^2} q^2}\right)^2 d\sigma^2$$

where $r_\Lambda = \sqrt{3/\Lambda}$.

[93] $d\sigma^2 = dq^2 + q^2 d\theta^2 + q^2 \sin^2\theta\, d\phi^2$

Proof. Our new solution is represented by metric (9.1) if the scale factor is given by

$$a(t) = a_0 \exp\left[\left(\frac{\Lambda}{3} - 4L\right)^{1/2} ct\right] \tag{9.2}$$

Let $w = La^2(t)\, q^2$. Einstein's equations $G_k^i = 0$ for the metric (9.1) reduce to

$$\frac{3}{c^2}\left(\frac{\dot{a}}{a}\right)^2 = \Lambda - 12L \tag{9.3}$$

$$\frac{2\frac{\ddot{a}}{a}(1+w) + (1-5w)H^2}{c^2(1-w)} = \Lambda - 12L \tag{9.4}$$

The corresponding calculations of Einstein's tensor for (9.1) are given in the appendix, see subsection (C.5).

1) From (9.2) we get $\dot{a} = \left(\sqrt{\frac{\Lambda}{3} - 4L}\right) ca$. Consequently, the left side of (9.3) reads

$$\frac{3}{c^2}\left(\frac{\dot{a}}{a}\right)^2 = \frac{3}{c^2}\left(\sqrt{\frac{\Lambda}{3} - 4L}\right)^2 c^2 = \Lambda - 12L$$

Further, we get $\ddot{a} = \left(\frac{\Lambda}{3} - 4L\right) c^2 a$ and the left side of (9.4) yields

$$\begin{aligned} \frac{2\frac{\ddot{a}}{a}(1+w) + (1-5w)H^2}{c^2(1-w)} &= \frac{2c^2\left(\frac{\Lambda}{3} - 4L\right)(1+w) + c^2\left(\frac{\Lambda}{3} - 4L\right)(1-5w)}{c^2(1-w)} \\ &= c^2\left(\frac{\Lambda}{3} - 4L\right)\frac{3-3w}{c^2(1-w)} = \Lambda - 12L \end{aligned}$$

This completes the proof of the first statement of Theorem 19. Now we consider the second statement:

2) For $L = \Lambda/12$ and $a_0 = 1$ equation (9.2) yields $a(t) \equiv 1$. Since $r_\Lambda = \sqrt{3/\Lambda}$ it remains de Sitter's isotropic solution (5.18). Indeed, it is not necessary to claim $a_0 = 1$. In the $L = \Lambda/12$ limit, equation (9.2) reduces to $a(t) \equiv a_0$ and we obtain de Sitter's isotropic solution in the form (5.17) with $k = \frac{a_0}{2r_\Lambda}$. □

9.1. **Geodesic equations for the new spacetime.**
In this subsection we determine the second order Christoffel symbols and therewith the equations of motion for the new spacetime. If there are no external forces, the motion of a particle is determined by the geometry of spacetime. A particle moves on a curve which is a solution of the geodesic equations

$$\frac{d^2x^m}{ds^2} + \sum_i \sum_k \Gamma^m_{ik} \frac{dx^i}{ds} \frac{dx^k}{ds} = 0 \tag{9.5}$$

where $x^m \in \{t, q, \theta, \phi\}$ are the coordinates of the spacetime manifold, see [73, 91] for example. The parameter s is related to the proper time τ by $s = c\tau$.

9.1.1. ***Second order Christoffel symbols and equations of motion.***
We established the second order Christoffel symbols for the interval (5.58):

$$ds^2 = c^2 e^{\xi(q,t)} dt^2 - e^{\mu(q,t)} \left(dq^2 + q^2 d\theta^2 + q^2 \sin^2(\theta)\, d\phi^2 \right)$$

A list is given in the appendix, see subsection C.1. In the following we use the abbreviations $w = La^2(t)\, q^2$ and $H = \dot{a}/a$. The above metric (5.58) represents (9.1) in case of

$$e^{\xi(t,q)} = \left(\frac{1-w}{1+w} \right)^2 \quad \text{and} \quad e^{\mu(t,q)} = \left(\frac{a}{1+w} \right)^2$$

The calculation for the partial derivatives of the functions ξ and μ with respect to the coordinates t and q are given in the appendix, subsection C.4. It is

$$\dot{\xi} = \frac{8wH}{w^2-1}, \quad \xi' = \frac{8w}{(w^2-1)\, q}, \quad \dot{\mu} = 2H \frac{1-w}{1+w}, \quad \mu' = -\frac{4w}{(1+w)\, q}$$

see equations (C.14) and (C.15). Therewith, it is easy to calculate the nonzero second order Christoffel symbols for the interval (9.1). The following list of Γ^m_{ik} is sorted by the upper index m:

Nonzero Γ^0_{ik} :

$$\Gamma^0_{00} = \frac{1}{2}\dot{\xi} = \frac{4wH}{w^2-1}, \qquad \Gamma^0_{01} = \Gamma^0_{10} = \frac{1}{2}\xi' = \frac{4w}{(w^2-1)\, q},$$

$$\Gamma^0_{11} = \frac{1}{2c^2}\dot{\mu} e^{\mu-\xi} = -\frac{\dot{a}a}{c^2(w^2-1)}, \qquad \Gamma^0_{22} = \frac{1}{2c^2}\dot{\mu} e^{\mu-\xi} q^2 = -\frac{\dot{a}aq^2}{c^2(w^2-1)},$$

$$\Gamma^0_{33} = \Gamma^0_{22} \sin^2\theta = -\frac{\dot{a}aq^2}{c^2(w^2-1)} \sin^2\theta$$

Nonzero Γ^1_{ik} :

$$\Gamma^1_{00} = \frac{1}{2} c^2 \xi' e^{\xi-\mu} = \frac{4c^2 w}{a^2 q} \cdot \frac{w-1}{w+1}, \qquad \Gamma^1_{01} = \Gamma^1_{10} = \frac{1}{2}\dot{\mu} = -H\frac{w-1}{w+1},$$

$$\Gamma^1_{11} = \frac{1}{2}\mu' = -\frac{2w}{(w+1)\,q}, \qquad \Gamma^1_{22} = -\frac{1}{2}\left(\mu' q^2 + 2q\right) = \frac{w-1}{w+1}q,$$

$$\Gamma^1_{33} = \Gamma^1_{22}\sin^2\theta = \frac{w-1}{w+1}q\sin^2\theta$$

Nonzero Γ^2_{ik} :

$$\Gamma^2_{02} = \Gamma^2_{20} = \frac{1}{2}\dot{\mu} = -H\frac{w-1}{w+1}, \qquad \Gamma^2_{12} = \Gamma^2_{21} = \frac{1}{2}\mu' + \frac{1}{q} = -\frac{w-1}{(1+w)\,q},$$

$$\Gamma^2_{33} = -\sin\theta\cos\theta$$

Nonzero Γ^3_{ik} :

$$\Gamma^3_{03} = \Gamma^3_{30} = \frac{1}{2}\dot{\mu} = -H\frac{w-1}{w+1}, \qquad \Gamma^3_{13} = \Gamma^3_{31} = \frac{1}{2}\mu' + \frac{1}{q} = -\frac{w-1}{(1+w)\,q},$$

$$\Gamma^3_{23} = \Gamma^3_{32} = \frac{\cos\theta}{\sin\theta}$$

With the above list of nonzero second order Christoffel symbols for the interval (9.1) it is easy to calculate the geodesic equations from (9.5). Further on, we use $w = La^2(t)\,q^2$ and $H = \dot{a}/a$. Primes stand for the differentiation with respect to the curve parameter s, i.e. $x' = \frac{dx}{ds}$.

$$\begin{aligned}
t'' &= -\frac{1}{w^2-1}\left[4wHt'^2 + \frac{8w}{q}t'q' - \frac{a^2H}{c^2}q'^2 + q^2\left(\theta'^2 + \sin^2(\theta)\,\phi'^2\right)\right] \\
q'' &= -\frac{w-1}{w+1}\left[\frac{4c^2w}{a^2q}t'^2 - 2Ht'q' - \frac{2w}{(w-1)\,q}q'^2 + q\left(\theta'^2 + \sin^2(\theta)\,\phi'^2\right)\right] \\
\theta'' &= 2\frac{w-1}{w+1}\left[Ht' + \frac{q'}{q}\right]\theta' + \sin(\theta)\cos(\theta)\,\phi'^2 \\
\phi'' &= 2\frac{w-1}{w+1}\left[Ht' + \frac{q'}{q}\right]\phi' + 2\cot(\theta)\,\theta'\phi'
\end{aligned}$$

Our set of partial differential equations depends on the curve parameter s, which is related to the proper time[94] τ by $s = c\tau$. It is possible to reduce the system to three equations, which depend on the coordinate time t.

[94]The proper time is the time measured by a clock moving with the particle

9.1.2. ***Coordinate time dependence of the geodesic equations.***
We use the following lemma to convert the geodesic equations from proper time dependence to coordinate time dependence.

Lemma 20. *(Transformation to coordinate time)*
Let $x \in \{t, q, \theta, \phi\}$. The parameter s in (9.5) is given by $s = c\tau$ where τ is the proper time. t is the coordinate time of the spacetime manifold. One has

$$x' = \dot{x}t' \quad \textit{and} \quad x'' = \ddot{x}t'^2 + \dot{x}t'' \tag{9.6}$$

where $x' = \frac{dx}{ds}$ and $\dot{x} = \frac{dx}{dt}$.

Proof. Obviously, it is $x' = \frac{dx}{ds} = \frac{dx}{dt}\frac{dt}{ds} = \dot{x}t'$. With the product rule we get:

$$x'' = \frac{d}{ds}\left[\frac{dx}{dt}\frac{dt}{ds}\right] = \frac{d\left[\frac{dx}{dt}\right]}{ds}\cdot\frac{dt}{ds} + \frac{dx}{dt}\cdot\frac{d^2t}{ds^2} = \frac{d\left[\frac{dx}{dt}\right]}{dt}\left(\frac{dt}{ds}\right)^2 + \frac{dx}{dt}\cdot\frac{d^2t}{ds^2} = \ddot{x}t'^2 + \dot{x}t''$$

□

Let us start with transforming the equation for the $q-$coordinate, which reads

$$q'' = -\frac{w-1}{w+1}\left[\frac{4c^2w}{a^2q}t'^2 - 2Ht'q' - \frac{2w}{(w-1)\,q}q'^2 + q\theta'^2 + q\sin^2(\theta)\,\phi'^2\right].$$

Together with lemma 20, this equation transforms into

$$\ddot{q}t'^2 + \dot{q}t'' = -\frac{w-1}{w+1}\left[\frac{4c^2w}{a^2q}t'^2 - 2Ht'q' - \frac{2w}{(w-1)\,q}q'^2 + q\theta'^2 + q\sin^2(\theta)\,\phi'^2\right].$$

We divide by t'^2 and get:

$$\ddot{q} + \dot{q}\frac{t''}{t'^2} = -\frac{w-1}{w+1}\left[\frac{4c^2w}{a^2q} - 2H\frac{q'}{t'} - \frac{2w}{(w-1)\,q}\left(\frac{q'}{t'}\right)^2 + q\left(\frac{\theta'}{t'}\right)^2 + q\sin^2(\theta)\left(\frac{\phi'}{t'}\right)^2\right]$$

From equation (9.6) in lemma 20 we directly get $x'/t' = \dot{x}$ and thus $q'/t' = \dot{q}$ as well as $\theta'/t' = \dot{\theta}$ and $\phi'/t' = \dot{\phi}$. Our equation reduces to

$$\ddot{q} + \dot{q}\frac{t''}{t'^2} = -\frac{w-1}{w+1}\left[\frac{4c^2w}{a^2q} - 2H\dot{q} - \frac{2w}{(w-1)\,q}\dot{q}^2 + q\left(\dot{\theta}^2 + \sin^2(\theta)\,\dot{\phi}^2\right)\right]. \tag{9.7}$$

Analogously, we use lemma 20 to transform the equations

$$\begin{aligned}
\theta'' &= 2\frac{w-1}{w+1}\left[Ht' + \frac{q'}{q}\right]\theta' + \sin(\theta)\cos(\theta)\,\phi'^2 \\
\phi'' &= 2\frac{w-1}{w+1}\left[Ht' + \frac{q'}{q}\right]\phi' + 2\cot(\theta)\,\theta'\phi'.
\end{aligned}$$

The transformation yields:

$$\begin{aligned}\ddot{\theta}t'^2 + \dot{\theta}t'' &= 2\frac{w-1}{w+1}\left[Ht' + \frac{q'}{q}\right]\theta' + \sin(\theta)\cos(\theta)\,\phi'^2 \\ \ddot{\phi}t'^2 + \dot{\phi}t'' &= 2\frac{w-1}{w+1}\left[Ht' + \frac{q'}{q}\right]\phi' + 2\cot(\theta)\,\theta'\phi'.\end{aligned}$$

Now we divide by t'^2 and use again $q'/t' = \dot{q}$, $\theta'/t' = \dot{\theta}$ as well as $\phi'/t' = \dot{\phi}$. Finally, our equations read

$$\ddot{\theta} + \dot{\theta}\frac{t''}{t'^2} = 2\frac{w-1}{w+1}\left[H + \frac{\dot{q}}{q}\right]\dot{\theta} + \sin(\theta)\cos(\theta)\,\dot{\phi}^2 \tag{9.8}$$

$$\ddot{\phi} + \dot{\phi}\frac{t''}{t'^2} = 2\frac{w-1}{w+1}\left[H + \frac{\dot{q}}{q}\right]\dot{\phi} + 2\cot(\theta)\,\dot{\theta}\dot{\phi}. \tag{9.9}$$

Equations (9.7), (9.8) and (9.9) include a t''/t'^2 term. We can rewrite the equation for the coordinate time

$$t'' = -\frac{1}{w^2-1}\left[4wHt'^2 + \frac{8w}{q}t'q' - \frac{a^2H}{c^2}q'^2 + q^2\left(\theta'^2 + \sin^2(\theta)\,\phi'^2\right)\right]$$

to get an expression for this term. One has

$$\frac{t''}{t'^2} = -\frac{1}{w^2-1}\left[4wH + \frac{8w}{q}\cdot\frac{q'}{t'} - \frac{a^2H}{c^2}\left(\frac{q'}{t'}\right)^2 + q^2\left(\frac{\theta'}{t'}\right)^2 + q^2\sin^2(\theta)\left(\frac{\phi'}{t'}\right)^2\right].$$

Together with $q'/t' = \dot{q}$ and $\phi'/t' = \dot{\phi}$ we are left with

$$\frac{t''}{t'^2} = -\frac{1}{w^2-1}\left[4wH + 8w\frac{\dot{q}}{q} - \frac{a^2H}{c^2}\dot{q}^2 + q^2\left(\dot{\theta}^2 + \sin^2(\theta)\,\dot{\phi}^2\right)\right]. \tag{9.10}$$

In order to obtain equations with coordinate time dependence, we use (9.10) in (9.7), (9.8) and (9.9):

$$\begin{aligned}\ddot{q} &= \frac{1}{w^2-1}\left[4wH + 8w\frac{\dot{q}}{q} - \frac{a^2H}{c^2}\dot{q}^2 + q^2\left(\dot{\theta}^2 + \sin^2(\theta)\,\dot{\phi}^2\right)\right]\dot{q} \\ &\quad -\frac{w-1}{w+1}\left[\frac{4c^2w}{a^2q} - 2H\dot{q} - \frac{2w}{(w-1)\,q}\dot{q}^2 + q\left(\dot{\theta}^2 + \sin^2(\theta)\,\dot{\phi}^2\right)\right]\end{aligned} \tag{9.11}$$

$$\begin{aligned}\ddot{\theta} &= \frac{1}{w^2-1}\left[4wH + 8w\frac{\dot{q}}{q} - \frac{a^2H}{c^2}\dot{q}^2 + q^2\left(\dot{\theta}^2 + \sin^2(\theta)\,\dot{\phi}^2\right)\right]\dot{\theta} \\ &\quad +2\frac{w-1}{w+1}\left[H + \frac{\dot{q}}{q}\right]\dot{\theta} + \sin(\theta)\cos(\theta)\,\dot{\phi}^2\end{aligned} \tag{9.12}$$

$$\begin{aligned}\ddot{\phi} &= \frac{1}{w^2-1}\left[4wH + 8w\frac{\dot{q}}{q} - \frac{a^2H}{c^2}\dot{q}^2 + q^2\left(\dot{\theta}^2 + \sin^2(\theta)\,\dot{\phi}^2\right)\right]\dot{\phi} \\ &\quad +2\frac{w-1}{w+1}\left[H + \frac{\dot{q}}{q}\right]\dot{\phi} + 2\cot(\theta)\,\dot{\theta}\dot{\phi}.\end{aligned} \tag{9.13}$$

9.1.3. ***The $\theta = \pi/2$ subspace.***

Let us now assume that the movement of the particle is constrained to the $\theta = \pi/2$ plain. With $\sin(\pi/2) = 1$, $\cos(\pi/2) = 0$ and $\theta' = 0$ our set of the differential equations (9.11), (9.12) and (9.13) reduces to a simpler system of two equations. Remember that $w = La^2(t)\, q^2$ and $H = \dot{a}/a$. After a short calculation we get:

(9.14)

$$\begin{aligned}
\ddot{q} &= \frac{\left[2H\left(w^2+1\right) + q^2\dot{\phi}^2\right]\dot{q} + 2w\left(w+3\right)\frac{\dot{q}^2}{q} - \frac{a^2H}{c^2}\dot{q}^3}{w^2-1} - \frac{w-1}{w+1}\left(\frac{4c^2w}{a^2q} + q\dot{\phi}^2\right) \\
\ddot{\phi} &= \frac{1}{w^2-1}\left[2H\left(w^2+1\right) + 2\left(6w - w^2 - 1\right)\frac{\dot{q}}{q} - \frac{a^2H}{c^2}\dot{q}^2 + q^2\dot{\phi}^2\right]\dot{\phi}
\end{aligned}$$

The second order system (9.14) can be transformed into a first order system of four equations. Let us introduce the radial velocity v and the angular velocity Ω:

$$v = \frac{dq}{dt} \quad \text{and} \quad \Omega = \frac{d\phi}{dt}$$

We use the capital letter Ω instead of the more frequently used ω in order to avoid any possibility of confusion with the shortcut w, which is given by $w = La^2q^2$. The first order system is:

$$\begin{aligned}
\dot{q} &= v \\
\dot{v} &= \frac{2H\left(w^2+1\right) + q^2\dot{\phi}^2}{w^2-1}\dot{q} + \frac{2w\left(w+3\right)}{\left(w^2-1\right)q}\dot{q}^2 - \frac{a^2H}{c^2\left(w^2-1\right)}\dot{q}^3 \\
&\quad -\frac{w-1}{w+1}\left(\frac{4c^2w}{a^2q} + q\dot{\phi}^2\right) \\
\dot{\phi} &= \Omega \\
\dot{\Omega} &= \frac{2H\left(w^2+1\right)}{w^2-1}\dot{\phi} + \frac{2\left(6w - w^2 - 1\right)}{\left(w^2-1\right)q}\dot{q}\dot{\phi} - \frac{a^2H}{c^2\left(w^2-1\right)}\dot{q}^2\dot{\phi} + \frac{q^2}{w^2-1}\dot{\phi}^3
\end{aligned}$$

9.1.4. ***Radial geodesic equation.***

Let us now consider a particle whose movement is constrained to $\theta, \phi =$constant. In this case (9.11), (9.12) and (9.13) reduce to one equation

(9.15)

$$\ddot{q} = \frac{1}{w^2-1}\left[2H\left(w^2+1\right)\dot{q} + 2w\left(w+3\right)\frac{\dot{q}^2}{q} - \frac{a^2H}{c^2}\dot{q}^3\right] - \frac{4c^2w\left(w-1\right)}{a^2q\left(w+1\right)}$$

which is equivalent to the first order system

$$\begin{aligned}
\dot{q} &= v \\
\dot{v} &= \frac{1}{w^2-1}\left[2H\left(w^2+1\right)v + 2w\left(w+3\right)\frac{v^2}{q} - \frac{a^2H}{c^2}v^3\right] - \frac{4c^2w\left(w-1\right)}{a^2q\left(w+1\right)}
\end{aligned}$$

Even this special case is determined by a cumbersome equation. It is unlikely that it can be solved exactly by analytical methods. We used Maple to approximate the second order differential equation (9.15) with the Runge Kutta Fehlberg method. We chose $a_0 = 1$ and $L = \Lambda/13 \approx 10^{-53}\frac{1}{\mathrm{m}^2}$ in (9.2). Accordingly, it is

$$a = \exp(Ht), \quad w = Lq^2 \exp(2Ht), \quad H = c \cdot \sqrt{\frac{\Lambda}{3} - 4L}$$

Figure 9.1 shows the radial geodesic of a particle, which starts moving with initial speed $v_0 = 1\mathrm{m/s}$ from $q_0 = 1\mathrm{m}$.

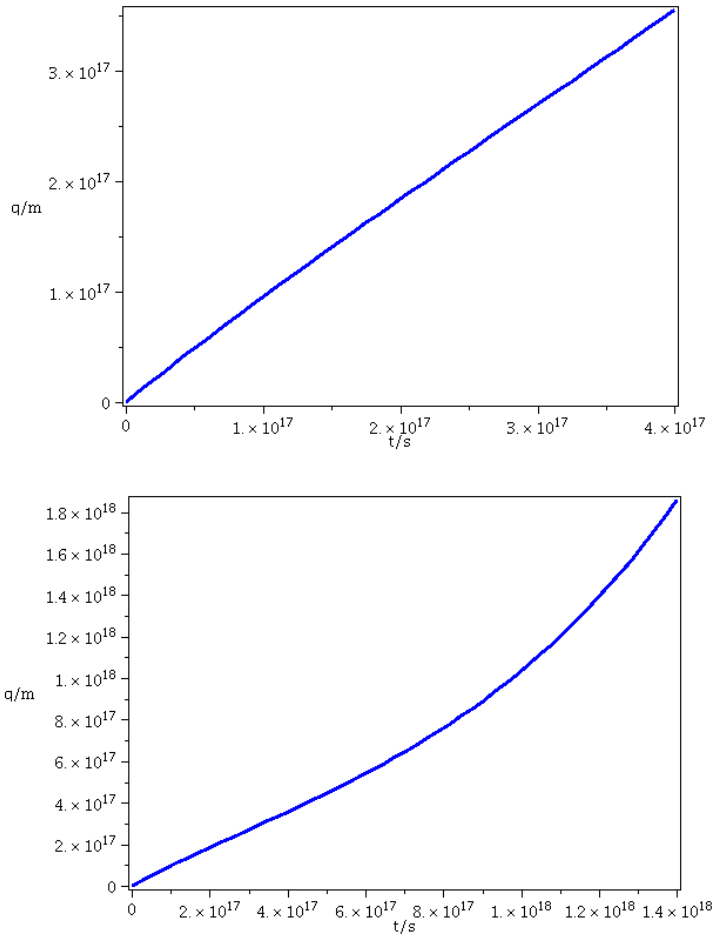

FIGURE 9.1. Radial geodesic in the new spacetime model for $L = \Lambda/13 \approx 10^{-53}\frac{1}{\mathrm{m}^2}$. The first graphic shows that the cosmic expansion has no influence on the particle's movement if $t \lesssim 4 \cdot 10^{17}\mathrm{s}$, which is roughly the current age of our universe ($13.75\,\mathrm{Gyr}$). The second graph shows that finally the particle accelerates, due to the cosmic expansion.

Summary and discussion

Astronomical observations show that in our expanding universe there are non-expanding insulars as galaxies, galaxy clusters and superclusters. This paper is concerned with the matching of these two geometries, the local geometry (gravitational bound systems) and the global geometry (expanding cosmological background) in a universe with non-zero cosmological constant Λ.

In the literature one finds two different models. McVittie was the first who proposed this problem. 1933 he found a new solution of Einstein's equations, an expanding spacetime that contains a point mass at the coordinate origin. Israelit and Rosen presented a similar model "*for the case of a massive particle at rest in a universe which without the particle would be homogeneous, isotropic and spatially flat.*" [61] in 1992. More recently, in 2010, Kaloper, Kleban and Martin showed in their article [65] that McVittie's solution *"includes regular black holes embedded in Friedman-Robertson-Walker cosmologies.*" The black hole interpretation is valid if McVittie's metric asymptotes the de Sitter cosmology. The physical interpretation of McVittie's solution has been debated for almost 80 years, and the discussion is still going on (in case of generic background cosmology), see for example [30, 72].

Assuming a non-zero cosmological constant, we established the McVittie-type solution which asymptotes the de Sitter cosmology by a simple coordinate replacement of Schwarzschild's isotropic metric, see section 4. But there are some crucial drawbacks of the model suggested by McVittie and likewise by Israelit and Rosen. The currently favored cosmological model is the ΛCDM model. McVittie's model does not seem to fit well with a ΛCDM background: In 2011, Lake and Abdelqader pointed out "*that the McVittie solution cannot represent a physically realistic inhomogeneity* [...]" [72].

Another approach of matching local to global geometry is based on an idea which goes back to Einstein and Straus [37]. A spherical region of a cosmological model is removed, and the material is replaced by a compact mass at the center. The non-expanding gravitational field of the mass condensation shall pass continuously into the field of the expanding spacetime. "*At this passage the g_{ik} and their first derivates shall remain continuous.*" [37]. Einstein and Straus proved the existence of such a solution. An explicit solution for the problem was given by Schücking [105], who modified Schwarzschild's field (2.29) to describe the interior region of

the Einstein-Straus model. Schücking's solution can be extended to the case of a nonzero cosmological constant, see [5].

In [91], Peebles proposed the Einstein Straus model without presupposing the condition that the first derivatives of g_{ik} shall remain continuous (which is sufficient but not necessary). He matched the radius of the evacuated sphere with respect to local and global coordinates, in order to get a relation between the evacuated cosmic material and the mass condensation. The matching of time determines the radius[95] $R_a\,(M)$ of the sphere, which depends on the mass M of the inclosed material. Up to now, several other authors worked on this model and coined the name "Swiss-Cheese universe", cf. [23]. In the Swiss-Cheese model, the mass condensation is isolated from the expanding cosmological background by an empty, static sphere. The gravitational field of the mass condensation inside this empty cavity can be modeled with Schwarzschild's solution.

We studied the ΛCDM Swiss-Cheese model, whose local geometry is given by the Schwarzschild-de Sitter solution, the global geometry is a spatially flat ($\Omega_K = 0$) FLRW spacetime with nonzero mass density and dark energy parameters Ω_M and Ω_Λ. Each radial Schwarzschild-de Sitter coordinate can be associated with a radial comoving FLRW coordinate. We match local and global geometry at the edge of the Schwarzschild-de Sitter cavity. For a given mass M, the matching of time is possible only at a certain radius $R_a\,(M,\Lambda)$. This determines the extend of the Schwarzschild-de Sitter sphere. In contrast to Peebles model[96], where $\Omega_\Lambda = 0$ but $\Omega_K \neq 0$ (which contradicts to WMAP data [63]) we have $M = \frac{4}{3}\pi R_a^3 \rho$ since the ΛCDM background is spatially flat. Based on the matching conditions, we established a differential equation, which determines the radial expansion $R\,(t)$ of the boundary sphere in the ΛCDM Swiss-Cheese model. Our solution shows that the material inside the gravitational sphere does not take part in the general expansion. The ΛCDM Swiss-Cheese model can be regarded as a solution of the McVittie problem.

In order to merge local and global spacetime, this paper is also concerned with the question whether the Schwarzschild-de Sitter interval can be transformed into an isotropic line element by transformation of the radial coordinate. We worked

[95]The notation r_e instead of R_a is used in [91].

[96]In [91], the mass $\mathcal{M}'$ of the evacuated material within a sphere with radius R_a is given by

$$\mathcal{M}' = 4\pi\rho a^3 \int_0^{R_a} \frac{r^2 dr}{\sqrt{1-\frac{r^2}{R_K^2}}}$$

where R_K is the curvature radius of the universe, ρ its density and a the scale factor.

out a new isotropic metric, which approximates Einstein's empty space equations (including a cosmological constant) with adequate accuracy. In a way, the structure of our new metric is similar to a product of de Sitter's and Schwarzschild's metric, thus it is called 'Product-metric' in subsection 5.6.

Another Swiss-Cheese model, a static sphere embedded in an expanding Lemaitre-Tolman-Bondi background, is studied in section 8. Based on the matching condition, we established a relation between world time and observer time at the boundary of the static cavity for a given non-expanding mass.

Section 9 presents a new empty space solution of Einstein's equations and the proof of the corresponding existence theorem. This time dependent solution results from a coordinate replacement, applied on a slightly modified de Sitter metric in isotropic form. We used the same coordinate replacement to establish McVittie's solution from the isotropic Schwarzschild interval in section 4. We establish the set of geodesic equations for the new metric and approximate the path of a radial moving particle numerically.

Conclusion.

Observations of distant supernovae indicated that the expansion of the universe is accelerating. S. Perlmutter, B. Schmidt and A. Riess shared the Nobel Prize in Physics 2011 for this discovery, see [115]. Taking into account these results, our investigations are based on Einstein's field equations with non-zero cosmological constant Λ. Conceivably, the ΛCDM Swiss-Cheese model is suited to describe the gravitational field of a galaxy or a cluster in an expanding cosmic background. Baryonic matter in a galaxy like our Milky Way roughly spans a region of about $\sim 15\,\mathrm{kpc}$ radius around a supermassive black hole in its center. It is believed that "*Dark matter halos appear to extend to at least* $\sim 50\,kpc$" [103]. Beyond these halos the space up to about 1 Mpc from the galactic center is empty. Finally, the whole area is embedded in an expanding background, filled with a gas and other galaxies. Interestingly enough, the zero-gravity surface[97] of a galaxy with a total mass of $2 \cdot 10^{45}$g (which is the estimated mass of our Milky Way galaxy including dark matter) is located at about 1 Mpc distance from the galactic center.

Some authors suppose that empty voids in the large scale structure of our universe

[97]Since gravitationally bound systems do not individually expand, there is a surface where gravitational attraction and the repulsive force reach equilibrium. According to a Newtonian approximation proposed by Chernin et. al. [26], gravitational force $F_N = -\gamma M/r^2$ (force per unit mass) and antigravity $F_E = H_0^2 \Omega_\Lambda r$ are exactly balanced at the zero-gravity surface.

(figure 1.9 or 7.5) might contain supermassive 'cosmic black holes' (CBHs), see e.g. [111]: "*we considered the existence of the CBHs, with larger masses and residing at the center of the voids, isolated from any other form of matter.*" The ΛCDM Swiss-Cheese model should be taken into consideration when establishing a model to describe this scenario. Within a galaxy or a galaxy cluster the influence of the cosmological constant can be neglected. The extend of a galaxy or galaxy cluster (baryonic and dark matter) is considerably smaller than the radius of the corresponding zero-gravity surface[98]. The situation is different if we consider a void. Based on the ΛCDM Swiss-Cheese model, the cosmic black hole in a void, which has a radius of, say, $\sim 10\,\mathrm{Mpc}$, has a mass of about $1.55 \cdot 10^{14} M_{\odot}$. The corresponding zero-gravity radius is 5.7 Mpc, much less than the radius of the void. In [91], Peebles studied a $\Lambda = 0$ Swiss Cheese model: He analyzed the matching of local and global geometry in order to compare the mass of the evacuated cosmic material with the mass condensation. We extended the ansatz given by Peebles: A cosmological constant was added, and we determined the expansion of the vacuole's boundary in the ΛCDM Swiss-Cheese model. We studied the expansion of that sphere in a ΛCDM Swiss-Cheese model in comparison to a $\Lambda = 0$ model. These results confirmed that Λ may be neglected for a galaxy or a cluster but not for a void.

Our (approximate) isotropic Schwarzschild-de Sitter interval, the Product-metric, depends on two distance parameters, the gravitational radius r_g and $r_\Lambda = \sqrt{3/\Lambda}$, which are located far apart from each other. There is a large range $r_g \ll r \ll r_\Lambda$ within both are negligible. Hence, the accuracy of the Product-metric is very high. Another approach, a numerical approximation of Einstein's equations for the general form of an isotropic interval[99] confirmed the Product-metric. It turned out that the inflection point of its g_{11} component largely coincides with the zero-gravity radius of the central mass.

Our second Swiss-Cheese model has a Lemaitre-Tolman-Bondi (LTB) background. There is a universal time in LTB models, but on the other hand, the radial expansion does not coincide with the azimuthal expansion[100] generally. A crucial drawback of the LTB model is that we had to restrict the considerations to the $\Lambda = 0$ case in

---

[98] A galaxies zero-gravity radius $\sim 1\,\mathrm{Mpc}$ is much larger than the extend of the dark matter halos $\sim 50\,kpc$. Galaxy clusters typically have total masses of $10^{14} M_{\odot}$ to $10^{15} M_{\odot}$ within a radius of 1 Mpc or 2 Mpc, their zero-gravity radius is in the range of 5 Mpc to 11 Mpc.

[99] $ds^2 = c^2 e^{\xi(q,t)} dt^2 - e^{\mu(q,t)} \left(dq^2 + q^2 d\theta^2 + q^2 \sin^2\theta\, d\phi^2\right)$

[100] The LTB interval is given by $ds^2 = c^2 dt^2 - e^{\lambda(t,r)} dr^2 - R^2(t,r)\left(d\theta^2 + \sin^2\theta\, d\phi^2\right)$. The radial expansion is determined by $e^{\lambda(t,r)}$, the azimuthal expansion by $R^2(t,r)$. In the special case of $e^{\lambda} = R^2$ we get back the FLRW ansatz.

order to obtain an analytic solution. Thus, the ΛCDM Swiss-Cheese model seems to be more useful.

The new metric, which we established in the last section of this paper, is an exact solution of Einstein's equations with nonzero cosmological constant. The examination of a radial geodesic path shows the influence of Λ on large scales. Further studies on the new spacetime are necessary to decide about its astrophysical relevance.

Appendix

Appendix A. Mathematical basics

The following appendix contains, among other things, calculations for the Einstein tensor. Some basic mathematical definitions, for example the signs of Ricci tensor and cosmological constant, are non uniform in literature. In order to have a clear and comprehensible basis, we briefly present some fundamentals of differential geometry in the following. For more detailed treatise see for example [53, 56, 73].

A tensor T of rank (r, s) is given by its components $T^{a_1 \ldots a_r}_{b_1 \ldots b_s}$. For example the components of the $(0, 2)$ metric tensor g are denoted by g_{ik}. Covariant vector fields are $(1, 0)$ tensors, their components are x^k. Contravariant vector fields ω (one forms) are $(0, 1)$ tensors with the components ω_k. Space-time has the structure of a manifold M (dimension 4) with a Lorentz metric and associated affine connection. It is common sense to write the metric in the form:

$$ds^2 = \sum_i \sum_k g_{ik} dx^i dx^k \tag{A.1}$$

Its signature is $(1 \mid 3)$, i.e. the matrix (g_{ik}) has one positive and three negative eigenvalues at a each point $p \in M$. The metric tensor can be used to give an isomorphism between any covariant tensor argument and any contravariant argument, see [56]. We can raise and lower indices with g_{ik} and the components of the inverse metric[101] g^{ik}. For example, if T_{ik} are the components of a tensor T we have to raise indices as follows:

$$T^i{}_k = \sum_a g^{ia} T_{ak} \qquad \text{and} \qquad T_k{}^i = \sum_a g^{ia} T_{ka}$$

If T is a symmetric tensor, so that $T_{ik} = T_{ki}$, we define $T^i_k := T^i{}_k = T_k{}^i$.

The connection ∇ at a point p of the manifold M assigns a differential operator ∇_X to each vector field X at p, so that an arbitrary C^1 vector field Y is mapped into a vector field $\nabla_X Y$ with the conditions[102]:

$$\begin{aligned} \nabla_X (fY) &= X(f) Y + f \nabla_X Y \\ \nabla_X (Y + Z) &= \nabla_X Y + \nabla_X Z \\ \nabla_{fX + hY} Z &= f \nabla_X Z + h \nabla_Y Z \end{aligned}$$

[101] $\sum_l g^{il} g_{lk} = \delta^i_k$, where $\delta^i_k = 1$ for $i = k$ and $\delta^i_k = 0$ for $i \neq k$

[102] f and h are C^1 functions and Z is another C^1vector field.

For $\partial_i = \frac{\partial}{\partial x^i}$ and $\partial_k = \frac{\partial}{\partial x^k}$, the coordinate fields, let us define $\nabla_{ik} := \nabla_{\partial_i}\partial_k$. The components of the covariant derivative ∇_{ik} with respect to the coordinate basis are denoted by Γ^n_{ik}, so that ∇_{ik} reads:

$$\nabla_{ik} = \sum_a \Gamma^a_{ik}\partial_a \tag{A.2}$$

In pseudo-Riemannian manifolds there exists a unique determined, torsion-free[103] connection ∇ with special characteristics[104], determined by Levi-Civita's formula:

$$\begin{aligned} g(\nabla_X Y, Z) &= \frac{1}{2}\{Xg(Y,Z) + Yg(Z,X) - Zg(X,Y) \\ &+ g(Z,[X,Y]) + g(Y,[Z,X]) - g(X,[Y,Z])\} \end{aligned}$$

X, Y and Z are C^1 vector fields, and $[\,,\,]$ is the Lie bracket. For coordinate fields, Levi-Civita's formula reduces to

$$g(\nabla_{ik}, \partial_n) = \frac{1}{2}\{\partial_i g_{kn} + \partial_k g_{ni} - \partial_n g_{ik}\}. \tag{A.3}$$

Equation (A.2) yields:

$$g(\nabla_{ik}, \partial_n) = g\left(\sum_a \Gamma^a_{ik}\partial_a, \partial_n\right) = \sum_a g_{an}\Gamma^a_{ik} = \Gamma_{ikn} \tag{A.4}$$

By combining equations (A.3) and (A.4), we obtain the first order Christoffel symbols

$$\Gamma_{ikn} = \frac{1}{2}\{\partial_i g_{kn} + \partial_k g_{ni} - \partial_n g_{ik}\}$$

and the second order Christoffel symbols

$$\Gamma^h_{ik} = \sum_n g^{hn}\Gamma_{ikn} = \frac{1}{2}\sum_n g^{hn}\{\partial_i g_{kn} + \partial_k g_{ni} - \partial_n g_{ik}\}.$$

A.1. **Riemann curvature tensor.**

The Riemann curvature tensor is a tensor of rank $(1,3)$. Given C^r vector fields X, Y, Z, the curvature tensor is a C^{r-2} vector field defined by

$$R(X,Y)Z = \nabla_X\nabla_Y Z - \nabla_Y\nabla_X Z - \nabla_{[X,Y]}Z \tag{A.5}$$

In classical literature, the Riemann tensor is given by its components $R^a{}_{nik}$. Unfortunately, the sequences of indices is non uniform, compare for example [53, 73]. In order to present comprehensible basics, we evaluate equation (A.5) for coordinate fields.

---

[103] For a torsion-free connection it is $[X,Y] = \nabla_X Y - \nabla_Y X$

[104] The Levi-Civita product rule $Xg(Y,Z) = g(\nabla_X Y, Z) + g(Y, \nabla_X Z)$ holds.

Lemma 21. *Riemann tensor*
If we use coordinate fields in Riemann's curvature tensor (A.5), one has:

$$R\left(\partial_i,\partial_k\right)\partial_n = \sum_a \left(\partial_i\Gamma^a_{kn} - \partial_k\Gamma^a_{in} + \sum_b \left(\Gamma^a_{ib}\Gamma^b_{kn} - \Gamma^a_{kb}\Gamma^b_{in}\right)\right)\partial_a \tag{A.6}$$

Proof. From (A.5) together with (A.2) we get:

$$R\left(\partial_i,\partial_k\right)\partial_n = \nabla_i\nabla_{kn} - \nabla_k\nabla_{in} = \nabla_i\left[\sum_b \Gamma^b_{kn}\partial_b\right] - \nabla_k\left[\sum_b \Gamma^b_{in}\partial_b\right]$$

With the conditions for the differential operator ∇_X the above equation reads:

$$\begin{aligned} R\left(\partial_i,\partial_k\right)\partial_n &= \sum_b \left(\partial_i\Gamma^b_{kn}\cdot\partial_b + \Gamma^b_{kn}\nabla_{ib} - \partial_k\Gamma^b_{in}\cdot\partial_b - \Gamma^b_{in}\nabla_{kb}\right) \\ &= \sum_b \left(\left(\partial_i\Gamma^b_{kn} - \partial_k\Gamma^b_{in}\right)\cdot\partial_b + \Gamma^b_{kn}\sum_c \Gamma^c_{ib}\partial_c - \Gamma^b_{in}\sum_c \Gamma^c_{kb}\partial_c\right) \\ &= \sum_b \left(\left(\partial_i\Gamma^b_{kn} - \partial_k\Gamma^b_{in}\right)\cdot\partial_b + \sum_c \left(\Gamma^b_{kn}\Gamma^c_{ib} - \Gamma^b_{in}\Gamma^c_{kb}\right)\partial_c\right) \end{aligned}$$

Now we collect the ∂_a- terms in the latter expression for an arbitrary fixed value a. This means we have to set $b=a$ in the first part of the sum

$$\sum_{b=a}^{a}\left(\partial_i\Gamma^b_{kn} - \partial_k\Gamma^b_{in}\right)\cdot\partial_b \quad = \quad \left(\partial_i\Gamma^a_{kn} - \partial_k\Gamma^a_{in}\right)\cdot\partial_a$$

and we have to set $c=a$ in the second part of the sum

$$\sum_b\sum_{c=a}^{a}\left(\Gamma^b_{kn}\Gamma^c_{ib} - \Gamma^b_{in}\Gamma^c_{kb}\right)\partial_c \quad = \quad \sum_b \left(\Gamma^b_{kn}\Gamma^a_{ib} - \Gamma^b_{in}\Gamma^a_{kb}\right)\partial_a.$$

Altogether, the remaining ∂_a-component is

$$\mathrm{Term}^a\partial_a = \left(\partial_i\Gamma^a_{kn} - \partial_k\Gamma^a_{in} + \sum_b \left(\Gamma^a_{ib}\Gamma^b_{kn} - \Gamma^a_{kb}\Gamma^b_{in}\right)\right)\partial_a.$$

Finally, summation again gives (A.6). □

Notation of the Riemann tensor components
Following [56, 73], the components of Riemann's curvature tensor are defined by $R\left(\partial_i,\partial_k\right)\partial_n = \sum_a R^a_{nik}\partial_a$, so that

$$R^a_{nik} \quad = \quad \partial_i\Gamma^a_{kn} - \partial_k\Gamma^a_{in} + \sum_b \left(\Gamma^a_{ib}\Gamma^b_{kn} - \Gamma^a_{kb}\Gamma^b_{in}\right). \tag{A.7}$$

Comparatively few authors use a different sequence of indices. See for example [53], Gromoll, Klingenberg and Meyer use R^a_{ikn} instead of R^a_{nik} on the left side of equation (A.7).

Ricci tensor and Ricci curvature scalar

The Ricci tensor is the contraction of Riemann's curvature tensor, its components are defined by:

$$R_{nk} = \sum_a R^a_{\ nak} \tag{A.8}$$

Alternatively, some authors use the definition $R_{nk} = \sum_a R^a_{\ ank} = -\sum_a R^a_{\ nak}$. According to the latter definition, they have to choose $\kappa = -8\pi\gamma/c^4$ in $G_{ik} = \kappa T_{ik}$ Einstein's field equations. Definition (A.8) together with (A.7) yields:

$$R_{nk} = \sum_a \left(\partial_a \Gamma^a_{kn} - \partial_k \Gamma^a_{an} + \sum_b \left(\Gamma^a_{ab}\Gamma^b_{kn} - \Gamma^a_{kb}\Gamma^b_{an} \right) \right) \tag{A.9}$$

The Ricci curvature scalar is the contraction of the Ricci tensor:

$$R = \sum_n \sum_k g^{nk} R_{nk} \tag{A.10}$$

Together with $R^i_k = \sum_n g^{in} R_{nk}$, equation (A.10) gives $R = \sum_k R^k_k$.

A.2. **Einsteintensor and Einstein's field equations.**

The Einstein tensor G_{ik} with cosmological constant Λ is given by

$$G_{ik} = R_{ik} - \frac{1}{2} R\, g_{ik} - \Lambda g_{ik}$$

see e.g. [91]. Spacetime is curved through the influence of its matter content, and vice versa the shape of space-time tells the matter how to move. Einstein's field equations relate the stress-energy-momentum tensor (which describes the content of space-time) to Einstein's tensor. The field equations

$$G_{ik} = \frac{8\pi\gamma}{c^4} T_{ik}$$

see [91], hold on the space-time manifold. With $G^i_k = \sum_l g^{il} G_{lk} = R^i_k - \frac{1}{2} R \delta^i_k - \Lambda \delta^i_k$ and $T^i_k = \sum_l g^{il} T_{lk}$, Einstein's equations take the form:

$$R^i_k - \frac{1}{2} R \delta^i_k - \Lambda \delta^i_k = \frac{8\pi\gamma}{c^4} T^i_k \tag{A.11}$$

It is $\delta^i_k = 1$ for $i = k$ and $\delta^i_k = 0$ for $i \neq k$. Alternatively, one finds Einstein's equations with $+\Lambda$ instead of $-\Lambda$ on the left side, or Λ is included on the other side. Einstein's equations in the form (A.11) correspond to a model where a positive cosmological constant causes expansion. For example, evaluation of (A.11) for the metric $ds^2 = c^2 dt^2 - a^2(t)\, d\sigma^2$ and empty space ($T^i_k = 0$) predicts exponential growth of the $a(t)$ scale factor.

Appendix B. Most important global and local model solutions

Einstein's general relativity theory provides the basis for the local and global models that describe the geometry of our universe. In this section we present some basic calculations concerning the Einstein tensor. In the following let $\partial_k f$ denote the derivation $\partial_k f := \frac{df}{dx^k}$ with respect to the coordinates $x^0 = t,\ x^1 = r,\ x^2 = \theta$ and $x^3 = \phi$, further $f' := \frac{df}{dr}$ and $\dot{f} = \frac{df}{dt}$. During the calculations we use the shortcuts:

$$S := \sin\theta \qquad \text{and} \qquad C := \cos\theta \tag{B.1}$$

B.1. Einstein tensor for the FLRW metric.

An important model for the geometry of the global universe is based on the Friedmann–Lemaître–Robertson–Walker (FLRW) metric. Consider an isotropic an homogeneous universe. These conditions obviously require a spatial subspace of constant curvature. Let $K \in \mathbb{R}$, a suitable model for our purpose is a subspace, embedded in the Euclidean space $\mathbb{R}^4$:

$$dl^2 = dx^2 + dy^2 + dz^2 + dw^2 \quad \text{with} \quad x^2 + y^2 + z^2 + w^2 = \frac{1}{K} \tag{B.2}$$

The spatially flat case corresponds to $K = 0$. Now we transform to spherical coordinates[105] (r, θ, ϕ). Equation (B.2) yields

$$dw = -\frac{xdx + ydy + zdz}{\sqrt{\frac{1}{K} - (x^2 + y^2 + z^2)}} = \frac{rdr}{\sqrt{\frac{1}{K} - r^2}}$$

and with that:

$$dl^2 = \frac{1}{1 - Kr^2} dr^2 + r^2 d\theta^2 + r^2 \sin^2\theta \, d\phi^2$$

The general FLRW metric with constant spatial curvature $ds^2 = c^2 dt^2 - a^2(t)\, dl^2$ reads

$$ds^2 = c^2 dt^2 - a^2(t) \left(\frac{dr^2}{1 - Kr^2} + r^2 d\theta^2 + r^2 \sin^2\theta \, d\phi^2 \right) \tag{B.3}$$

where $K \in \mathbb{R}$. We now compute the Einsteintensor corresponding to the metric (B.3).

---

[105] The spherical coordinates are given by $x = r\sin\theta\cos\phi$, $y = r\sin\theta\sin\phi$ and $z = r\cos\theta$. With

$$\begin{aligned} dx &= \sin\theta\cos\phi\, dr + r\cos\theta\cos\phi\, d\theta - r\sin\theta\sin\phi\, d\phi \\ dy &= \sin\theta\sin\phi\, dr + r\cos\theta\sin\phi\, d\theta + r\sin\theta\cos\phi\, d\phi \\ dz &= \cos\theta\, dr - r\sin\theta\, d\theta \end{aligned}$$

we obtain $xdx + ydy + zdz = rdr$ after some trigonometric calculations.

Partial derivatives of the metric components

The nonzero components of the metric tensor are:

$$g_{00} = c^2, \quad g_{11} = \frac{a^2(t)}{Kr^2 - 1}, \quad g_{22} = -a^2(t)r^2, \quad g_{33} = -a^2(t)r^2S^2$$

The nonzero derivatives of the g_{ik} are:

$$\partial_0 g_{11} = \frac{2a\dot{a}}{Kr^2 - 1}, \quad \partial_1 g_{11} = -\frac{2Kra^2}{\left(Kr^2 - 1\right)^2}, \quad \partial_0 g_{22} = -2a\dot{a}r^2, \quad \partial_1 g_{22} = -2a^2 r,$$
$$\partial_0 g_{33} = -2a\dot{a}r^2S^2, \quad \partial_1 g_{33} = -2a^2 rS^2, \quad \partial_2 g_{33} = -2a^2 r^2 SC$$

First order Christoffel symbols

From $\Gamma_{ikl} = \frac{1}{2}\left(\partial_i g_{kl} + \partial_k g_{li} - \partial_l g_{ik}\right)$ we obtain the nonzero Christoffel symbols:

$$\Gamma_{011} = \frac{a\dot{a}}{Kr^2 - 1}, \quad \Gamma_{022} = -a\dot{a}r^2, \quad \Gamma_{033} = -a\dot{a}r^2S^2, \quad \Gamma_{110} = -\frac{a\dot{a}}{Kr^2 - 1},$$
$$\Gamma_{111} = -\frac{Kra^2}{\left(Kr^2 - 1\right)^2}, \quad \Gamma_{122} = -a^2 r, \quad \Gamma_{133} = -a^2 rS^2, \quad \Gamma_{220} = a\dot{a}r^2,$$
$$\Gamma_{221} = a^2 r, \quad \Gamma_{233} = -a^2 r^2 SC, \quad \Gamma_{330} = a\dot{a}r^2S^2, \quad \Gamma_{331} = a^2 rS^2,$$
$$\Gamma_{332} = a^2 r^2 SC, \text{ further it is } \Gamma_{ikl} = \Gamma_{kil}.$$

Inverse metric

The inverse metric tensor is given by:

$$g^{00} = \frac{1}{c^2}, \quad g^{11} = \frac{Kr^2 - 1}{a^2}, \quad g^{22} = -\frac{1}{a^2 r^2}, \quad g^{33} = -\frac{1}{a^2 r^2 S^2}, \quad g^{ik} = 0 \text{ for } i \neq k$$

Second order Christoffel symbols

The Christoffel symbols are given by $\Gamma^m_{ik} = \sum_{l=0}^{3} g^{ml}\Gamma_{ikl}$. We obtain the nonzero (second order) Christoffel symbols:

$$\Gamma^1_{01} = \Gamma^2_{02} = \Gamma^3_{03} = \frac{\dot{a}}{a}, \quad \Gamma^0_{11} = \frac{a\dot{a}}{\left(1 - Kr^2\right)c^2}, \quad \Gamma^1_{11} = \frac{Kr}{1 - Kr^2}, \quad \Gamma^2_{12} = \Gamma^3_{13} = \frac{1}{r},$$
$$\Gamma^0_{22} = \frac{a\dot{a}r^2}{c^2}, \quad \Gamma^1_{22} = \left(Kr^2 - 1\right)r, \quad \Gamma^3_{23} = \frac{C}{S}, \quad \Gamma^0_{33} = \frac{a\dot{a}r^2S^2}{c^2},$$
$$\Gamma^1_{33} = \left(Kr^2 - 1\right)rS^2, \quad \Gamma^2_{33} = -SC,$$

Further it is $\Gamma^m_{ik} = \Gamma^m_{ki}$.

Components of the Ricci tensor

The Ricci tensor is given by:

$$R_{nk} = \sum_a \left(\partial_a \Gamma^a_{kn} - \partial_k \Gamma^a_{an}\right) + \sum_a \sum_m \left(\Gamma^a_{am}\Gamma^m_{kn} - \Gamma^a_{km}\Gamma^m_{an}\right)$$

We get

$$\begin{aligned} R_{00} &= \sum_a \left(\partial_a \Gamma^a_{00} - \partial_0 \Gamma^a_{a0}\right) + \sum_a \sum_m \left(\Gamma^a_{am}\Gamma^m_{00} - \Gamma^a_{0m}\Gamma^m_{a0}\right) \\ &= -3\partial_0 \left[\frac{\dot{a}}{a}\right] - 3\left(\frac{\dot{a}}{a}\right)^2 = -3\frac{\ddot{a}}{a} \end{aligned}$$

and in an analogous manner after some calculation

$$R_{11} = \frac{2K}{1-Kr^2} + \frac{a\ddot{a} + 2\dot{a}^2}{\left(1-Kr^2\right)c^2}, \quad R_{22} = 2Kr^2 + \frac{a\ddot{a} + 2\dot{a}^2}{c^2} r^2$$

and $R_{33} = R_{22}\sin^2\theta$. The nonzero $R^i_k = \sum_n g^{in} R_{nk}$ are:

$$R^0_0 = -\frac{3\ddot{a}}{c^2 a}, \quad R^1_1 = R^2_2 = R^3_3 = -\frac{2K}{a^2} - \frac{a\ddot{a} + 2\dot{a}^2}{a^2 c^2}$$

Ricci-Scalar

The contraction $R = \sum_k R^k_k$ of the Ricci tensor is:

$$R = -6\left[\frac{K}{a^2} + \frac{\ddot{a}}{c^2 a} + \frac{1}{c^2}\left(\frac{\dot{a}}{a}\right)^2\right]$$

Einstein tensor

Finally we obtain the nonzero components of $G^i_k = R^i_k - \frac{1}{2}R\delta^i_k - \Lambda\delta^i_k$. Corresponding to the coordinates $\{t, r, \theta, \phi\} = \left\{x^0, x^1, x^2, x^3\right\}$ we use the notation:

$$G^t_t := G^0_0\,, \quad G^r_r := G^1_1\,, \quad G^\theta_\theta := G^2_2\,, \quad G^\phi_\phi := G^3_3 \tag{B.4}$$

The Einstein tensor is given by:

$$G^t_t = \frac{3}{c^2}\left(\frac{\dot{a}}{a}\right)^2 + \frac{3K}{a^2} - \Lambda \tag{B.5}$$

$$G^r_r = G^\theta_\theta = G^\phi_\phi = \frac{K}{a^2} + \frac{1}{c^2}\left[2\frac{\ddot{a}}{a} + \left(\frac{\dot{a}}{a}\right)^2\right] - \Lambda \tag{B.6}$$

B.2. **Einstein tensor for a stationary, spherically symmetric line element.** A stationary, spherically symmetric solution of Einstein's field equations has the form:

$$ds^2 = \alpha(r)\, c^2 dt^2 - \beta(r)\, dr^2 - r^2 d\theta^2 - r^2 \sin^2\theta\, d\phi^2 \tag{B.7}$$

We establish the Einstein tensor for the line element (B.7). It is shown in subsection 2.7, that the Schwarzschild-de Sitter metric is a solution of Einstein's vacuum field equations for the ansatz (B.7).

Metric components and their partial derivatives

We use again the shortcuts (B.1). The components of the metric tensor with respect to the coordinates $\{t, q, \theta, \phi\} = \{x^0, x^1, x^2, x^3\}$ are:

$$g_{00} = c^2\alpha, \quad g_{11} = -\beta, \quad g_{22} = -r^2, \quad g_{33} = -r^2 S^2, \quad g_{ik} = 0 \text{ for } i \neq k$$

The nonzero derivatives of the g_{ik} are:
$\partial_1 g_{00} = c^2\alpha', \quad \partial_1 g_{11} = -\beta', \quad \partial_1 g_{22} = -2r, \quad \partial_1 g_{33} = -2rS^2, \quad \partial_2 g_{33} = -2r^2 SC$

First order Christoffel symbols

From $\Gamma_{ikl} = \frac{1}{2}(\partial_i g_{kl} + \partial_k g_{li} - \partial_l g_{ik})$ we obtain $\Gamma_{ikl} = \Gamma_{kil}$ and the following list of nonzero (first order) Christoffel symbols:

$$\begin{array}{llllll} \Gamma_{001} = -\frac{1}{2}c^2\alpha', & \Gamma_{010} = \frac{1}{2}c^2\alpha', & \Gamma_{111} = -\frac{1}{2}\beta', & \Gamma_{122} = -r, & \Gamma_{133} = -rS^2, \\ \Gamma_{221} = r, & \Gamma_{233} = -r^2 SC, & \Gamma_{331} = rS^2, & \Gamma_{332} = r^2 SC & \end{array}$$

Inverse metric

The inverse metric tensor is given by:

$$g^{00} = \frac{1}{c^2\alpha}, \quad g^{11} = -\frac{1}{\beta}, \quad g^{22} = -\frac{1}{r^2}, \quad g^{33} = -\frac{1}{r^2 S^2}, \quad g^{ik} = 0 \text{ for } i \neq k$$

Second order Christoffel symbols

From $\Gamma^m_{ik} = \sum_l g^{ml}\Gamma_{ikl}$ we get $\Gamma^m_{ik} = \Gamma^m_{ki}$ and the following nonzero (second order) Christoffel symbols:

$$\begin{array}{llllll} \Gamma^1_{00} = \frac{c^2\alpha'}{2\beta}, & \Gamma^0_{01} = \frac{\alpha'}{2\alpha}, & \Gamma^1_{11} = \frac{\beta'}{2\beta}, & \Gamma^2_{12} = \frac{1}{r}, & \Gamma^3_{13} = \frac{1}{r}, \\ \Gamma^1_{22} = -\frac{r}{\beta}, & \Gamma^3_{23} = \frac{C}{S}, & \Gamma^1_{33} = -\frac{rS^2}{\beta}, & \Gamma^2_{33} = -SC & \end{array}$$

Ricci tensor and Ricci scalar

The Ricci tensor is given by:

$$R_{nk} = \sum_a (\partial_a \Gamma^a_{kn} - \partial_k \Gamma^a_{an}) + \sum_a \sum_m (\Gamma^a_{am}\Gamma^m_{kn} - \Gamma^a_{km}\Gamma^m_{an})$$

It follows

$$\begin{aligned} R_{00} &= \sum_a (\partial_a \Gamma^a_{00} - \partial_0 \Gamma^a_{a0}) + \sum_a \sum_m (\Gamma^a_{am}\Gamma^m_{00} - \Gamma^a_{0m}\Gamma^m_{a0}) \\ &= \frac{\alpha'' c^2\beta - \alpha' c^2 \beta'}{2\beta^2} + \frac{\alpha' c^2 \beta'}{4\beta^2} + \frac{\alpha' c^2}{\beta r} - \frac{\alpha'^2 c^2}{4\alpha\beta} \\ &= \left(\frac{\alpha''}{2\beta} - \frac{\alpha'\beta'}{4\beta^2} + \frac{\alpha'}{\beta r} - \frac{\alpha'^2}{4\alpha\beta}\right) c^2 \end{aligned}$$

in the same manner we obtain the other nonzero components:

$$\begin{aligned} R_{11} &= -\frac{\alpha''}{2\alpha} + \frac{\alpha'^2}{4\alpha^2} + \frac{\alpha'\beta'}{4\alpha\beta} + \frac{\beta'}{r\beta} \\ R_{22} &= \frac{r\beta'}{2\beta^2} - \frac{r\alpha'}{2\alpha\beta} - \frac{1}{\beta} + 1 \end{aligned}$$

and $R_{33} = R_{22} S^2$. The nonzero $R^i_k = \sum_n g^{in} R_{nk}$ are:

$$\begin{aligned} R^0_0 &= \frac{\alpha''}{2\alpha\beta} - \frac{\alpha'^2}{4\alpha^2\beta} - \frac{\alpha'\beta'}{4\alpha\beta^2} + \frac{\alpha'}{\alpha\beta r} \\ R^1_1 &= \frac{\alpha''}{2\alpha\beta} - \frac{\alpha'^2}{4\alpha^2\beta} - \frac{\alpha'\beta'}{4\alpha\beta^2} - \frac{\beta'}{\beta^2 r} \\ R^2_2 = R^3_3 &= \frac{\alpha'}{2\alpha\beta r} - \frac{\beta'}{2\beta^2 r} + \frac{1}{\beta r^2} - \frac{1}{r^2} \end{aligned}$$

The contraction (Ricci scalar) $R = \sum_k R^k_k$ of the Ricci tensor is:

$$R = \frac{\alpha''}{\alpha\beta} - \frac{\alpha'^2}{2\alpha^2\beta} - \frac{\alpha'\beta'}{2\alpha\beta^2} + \frac{2\alpha'}{\alpha\beta r} - \frac{2\beta'}{\beta^2 r} + \frac{2}{\beta r^2} - \frac{2}{r^2}$$

Einstein tensor

We obtain the components of the Einstein tensor from $G^i_k = R^i_k - \frac{1}{2} R \delta^i_k - \Lambda \delta^i_k$. We use again the notation (B.4):

$$G^t_t = \frac{\beta'}{\beta^2 r} - \frac{1}{\beta r^2} + \frac{1}{r^2} - \Lambda \tag{B.8}$$

$$G^r_r = -\frac{\alpha'}{\alpha\beta r} - \frac{1}{\beta r^2} + \frac{1}{r^2} - \Lambda \tag{B.9}$$

$$G^\theta_\theta = G^\phi_\phi = -\frac{\alpha'}{2\alpha\beta r} + \frac{\beta'}{2\beta^2 r} - \frac{\alpha''}{2\alpha\beta} + \frac{\alpha'^2}{4\alpha^2\beta} + \frac{\alpha'\beta'}{4\alpha\beta^2} - \Lambda \tag{B.10}$$

Appendix C. Einstein's tensor for isotropic spacetimes

This section contains a detailed calculation of Einstein's tensor for

$$ds^2 = c^2 e^{\xi(q,t)} dt^2 - e^{\mu(q,t)} \left(dq^2 + q^2 d\theta^2 + q^2 \sin^2(\theta)\, d\phi^2 \right) \tag{C.1}$$

the most general form of an orthogonal, isotropic and spherically symmetric metric. The nonzero metric components g_{ik} with respect to $\{t, q, \theta, \phi\} = \left\{x^0, x^1, x^2, x^3\right\}$ are: $g_{00} = c^2 e^{\xi}$, $g_{11} = -e^{\mu}$, $g_{22} = -e^{\mu} q^2$, $g_{33} = -e^{\mu} q^2 \sin^2\theta$. The partial derivative of a function f is denoted by $\partial_k f := \frac{df}{dx^k}$ as well as $\dot{f} := \frac{df}{dt}$ and $f' := \frac{df}{dq}$. Each sum $\sum_k$ runs from $k = 0$ to $k = 3$ in the following.

First order Christoffel symbols

We start with the first order Christoffel symbols, which are given by

$$\Gamma_{ikl} \quad = \quad \frac{1}{2} \left(\partial_i g_{kl} + \partial_k g_{li} - \partial_l g_{ik} \right)$$

One has $\Gamma_{ikl} = \Gamma_{kil}$, the following list of nonzero Christoffel symbols is assorted by the first index.

$i = 0$

$$\Gamma_{000} = \frac{1}{2} c^2 \dot{\xi} e^{\xi}, \qquad \Gamma_{001} = -\frac{1}{2} c^2 \xi' e^{\xi}, \qquad \Gamma_{010} = \frac{1}{2} c^2 \xi' e^{\xi}, \qquad \Gamma_{011} = -\frac{1}{2} \dot{\mu} e^{\mu},$$

$$\Gamma_{022} = -\frac{1}{2} \dot{\mu} e^{\mu} q^2, \qquad \Gamma_{03n} = \Gamma_{02n} \sin^2\theta$$

$i = 1$

$$\Gamma_{110} = \frac{1}{2} \dot{\mu} e^{\mu}, \qquad \Gamma_{111} = -\frac{1}{2} \mu' e^{\mu}, \qquad \Gamma_{122} = -\frac{1}{2} \left(\mu' q^2 + 2q \right) e^{\mu},$$

$$\Gamma_{13n} = \Gamma_{12n} \sin^2\theta$$

$i = 2$

$$\Gamma_{220} = \frac{1}{2} \dot{\mu} e^{\mu} q^2, \qquad \Gamma_{221} = \frac{1}{2} \left(\mu' q^2 + 2q \right) e^{\mu}, \qquad \Gamma_{233} = -e^{\mu} q^2 \sin\theta \cos\theta,$$

$i = 3$

$$\Gamma_{330} = \Gamma_{220} \sin^2\theta, \qquad \Gamma_{331} = \Gamma_{221} \sin^2\theta, \qquad \Gamma_{332} = e^{\mu} q^2 \sin\theta \cos\theta$$

C.1. **Second order Christoffel symbols.**
Now we obtain the second order Christoffel symbols from

$$\Gamma^m_{ik} \;=\; \sum_l g^{ml}\Gamma_{ikl} = \frac{1}{2}\sum_l g^{ml}\left(\partial_i g_{kl} + \partial_k g_{li} - \partial_l g_{ik}\right)$$

The components g^{ik} of the inverse metric tensor for (C.1) reduce to $g^{ik} = 1/g_{ik}$ if $i = k$ and $g^{ik} = 0$ for $i \neq 0$. It is $\Gamma^m_{ik} = \Gamma^m_{ki}$, the following list is assorted by the lower left index:

$i = 0$

$$\Gamma^0_{00} = \frac{1}{2}\dot{\xi}, \qquad \Gamma^1_{00} = \frac{1}{2}c^2\xi' e^{\xi-\mu}, \qquad \Gamma^2_{00} = \Gamma^3_{00} = 0,$$

$$\Gamma^0_{01} = \frac{1}{2}\xi', \qquad \Gamma^1_{01} = \Gamma^2_{02} = \Gamma^3_{03} = \frac{1}{2}\dot{\mu}, \qquad \Gamma^2_{01} = \Gamma^3_{01} = 0,$$

$$\Gamma^0_{02} = \Gamma^1_{02} = \Gamma^3_{02} = 0, \qquad \Gamma^0_{03} = \Gamma^1_{03} = \Gamma^2_{03} = 0,$$

$i = 1$

$$\Gamma^0_{11} = \frac{1}{2c^2}\dot{\mu}e^{\mu-\xi}, \qquad \Gamma^1_{11} = \frac{1}{2}\mu', \qquad \Gamma^2_{11} = \Gamma^3_{11} = 0,$$

$$\Gamma^0_{12} = \Gamma^1_{12} = \Gamma^3_{12} = 0, \quad \Gamma^2_{12} = \Gamma^3_{13} = \frac{1}{2}\mu' + \frac{1}{q}, \quad \Gamma^0_{13} = \Gamma^1_{13} = \Gamma^2_{13} = 0$$

$i = 2$

$$\Gamma^0_{22} = \frac{1}{2c^2}\dot{\mu}e^{\mu-\xi}q^2, \qquad \Gamma^1_{22} = -\frac{1}{2}\left(\mu' q^2 + 2q\right), \qquad \Gamma^2_{22} = \Gamma^3_{22} = 0,$$

$$\Gamma^0_{23} = \Gamma^1_{23} = \Gamma^2_{23} = 0, \quad \Gamma^3_{23} = \frac{\cos\theta}{\sin\theta},$$

$i = 3$

$$\Gamma^0_{33} = \Gamma^0_{22}\sin^2\theta, \qquad \Gamma^1_{33} = \Gamma^1_{22}\sin^2\theta, \qquad \Gamma^2_{33} = -\sin\theta\cos\theta, \qquad \Gamma^3_{33} = 0$$

Partial derivatives of the second order Christoffel symbols

For later calculations we need the partial derivatives of some second order Christoffel symbols. It is $\partial_3 \Gamma^m_{ik} = 0$ for all i, k, m. The following derivatives are assorted by the lower left index of the Christoffel symbols.

Derivatives of the $i = 0$ ***Christoffel symbols:***

$$\partial_k \Gamma^0_{00} = \frac{1}{2}\partial_k \dot{\xi}, \quad \partial_k \Gamma^0_{01} = \frac{1}{2}\partial_k \xi', \quad \partial_k \Gamma^1_{01} = \partial_k \Gamma^2_{02} = \partial_k \Gamma^3_{03} = \frac{1}{2}\partial_k \dot{\mu}$$

$$\partial_k \Gamma^1_{00} = \partial_k \left[\frac{1}{2}c^2 \xi' e^{\xi-\mu}\right] = \frac{1}{2}c^2 \left(\partial_k \xi' + \xi' \partial_k \left[\xi - \mu\right]\right) e^{\xi-\mu}$$

We have $\partial_2 \Gamma^m_{0k} = 0$ for all k, m. The remaining nonzero derivatives are:

$$\partial_0 \Gamma^0_{00} = \frac{1}{2}\ddot{\xi}, \quad \partial_1 \Gamma^0_{00} = \frac{1}{2}\dot{\xi}'$$

$$\partial_0 \Gamma^1_{00} = \frac{1}{2}c^2 \left(\dot{\xi}' + \xi'\dot{\xi} - \xi'\dot{\mu}\right) e^{\xi-\mu}, \quad \partial_1 \Gamma^1_{00} = \frac{1}{2}c^2 \left(\xi'' + \xi'^2 - \xi'\mu'\right) e^{\xi-\mu}$$

$$\partial_0 \Gamma^0_{01} = \frac{1}{2}\dot{\xi}', \quad \partial_1 \Gamma^0_{01} = \frac{1}{2}\xi''$$

$$\partial_0 \Gamma^1_{01} = \partial_0 \Gamma^2_{02} = \partial_0 \Gamma^3_{03} = \frac{1}{2}\ddot{\mu}, \quad \partial_1 \Gamma^1_{01} = \partial_1 \Gamma^2_{02} = \partial_1 \Gamma^3_{03} = \frac{1}{2}\dot{\mu}'$$

Derivatives of the $i = 1$ ***Christoffel symbols:***

$$\partial_k \Gamma^0_{11} = \partial_k \left[\frac{1}{2c^2}\dot{\mu} e^{\mu-\xi}\right] = \frac{1}{2c^2}\left(\partial_k \dot{\mu} + \dot{\mu}\partial_k \left[\mu - \xi\right]\right) e^{\mu-\xi}, \quad \partial_k \Gamma^1_{11} = \frac{1}{2}\partial_k \mu'$$

$$\partial_k \Gamma^2_{12} = \partial_k \Gamma^3_{13} = \frac{1}{2}\partial_k \mu' + \partial_k \left[\frac{1}{q}\right]$$

We have $\partial_2 \Gamma^m_{1k} = 0$ for all k, m. The remaining nonzero derivatives are:

$$\partial_0 \Gamma^0_{11} = \frac{1}{2c^2}\left(\ddot{\mu} + \dot{\mu}^2 - \dot{\mu}\dot{\xi}\right) e^{\mu-\xi}, \quad \partial_1 \Gamma^0_{11} = \frac{1}{2c^2}\left(\dot{\mu}' + \dot{\mu}\mu' - \dot{\mu}\xi'\right) e^{\mu-\xi},$$

$$\partial_0 \Gamma^1_{11} = \frac{1}{2}\dot{\mu}', \quad \partial_1 \Gamma^1_{11} = \frac{1}{2}\mu''$$

$$\partial_0 \Gamma^2_{12} = \partial_0 \Gamma^3_{13} = \frac{1}{2}\dot{\mu}', \quad \partial_1 \Gamma^2_{12} = \partial_1 \Gamma^3_{13} = \frac{1}{2}\mu'' - \frac{1}{q^2}$$

Derivatives of the $i = 2$ ***Christoffel symbols:***

$$\partial_k \Gamma^0_{22} = \partial_k \left[q^2 \Gamma^0_{11}\right] = \partial_k \left[q^2\right] \Gamma^0_{11} + q^2 \partial_k \Gamma^0_{11} = \frac{1}{2c^2} \partial_k \left[q^2\right] \dot{\mu} e^{\mu - \xi} q^2 + q^2 \partial_k \Gamma^0_{11}$$

$$\partial_k \Gamma^1_{22} = \partial_k \left[-q^2 \Gamma^2_{12}\right] = -\partial_k \left[q^2\right] \Gamma^2_{12} - q^2 \partial_k \Gamma^2_{12} = -\partial_k \left[q^2\right] \left(\frac{1}{2}\mu' + \frac{1}{q}\right) - q^2 \partial_k \Gamma^2_{12}$$

$$\partial_k \Gamma^3_{23} = \partial_k \frac{\cos\theta}{\sin\theta}$$

It is $\partial_2 \Gamma^m_{22} = 0$ and $\partial_0 \Gamma^3_{23} = \partial_1 \Gamma^3_{23} = 0$. The remaining nonzero derivatives are:

$$\partial_0 \Gamma^0_{22} = q^2 \partial_0 \Gamma^0_{11} = \frac{q^2}{2c^2} \left(\ddot{\mu} + \dot{\mu}^2 - \dot{\mu}\dot{\xi}\right) e^{\mu - \xi}$$

$$\partial_1 \Gamma^0_{22} = \frac{1}{c^2} q^3 \dot{\mu} e^{\mu - \xi} + q^2 \partial_1 \Gamma^0_{11} = \frac{q^2}{2c^2} \left(2q\dot{\mu} + \dot{\mu}' + \dot{\mu}\mu' - \dot{\mu}\xi'\right) e^{\mu - \xi}$$

$$\partial_0 \Gamma^1_{22} = -q^2 \partial_0 \Gamma^2_{12} = -\frac{1}{2} q^2 \dot{\mu}'$$

$$\partial_1 \Gamma^1_{22} = -2q \left(\frac{1}{2}\mu' + \frac{1}{q}\right) - q^2 \partial_1 \Gamma^2_{12} = -q\mu' - 2 - q^2 \left(\frac{1}{2}\mu'' - \frac{1}{q^2}\right) = -\frac{1}{2} q^2 \mu'' - q\mu' - 1$$

$$\partial_2 \Gamma^3_{23} = \partial_2 \left[\frac{\cos\theta}{\sin\theta}\right] = -\frac{1}{\sin^2\theta}$$

Derivatives of the $i = 3$ ***Christoffel symbols:***
The non zero derivatives are:

$$\partial_0 \Gamma^0_{33} = \partial_0 \Gamma^0_{22} \sin^2\theta, \quad \partial_1 \Gamma^0_{33} = \partial_1 \Gamma^0_{22} \sin^2\theta, \quad \partial_2 \Gamma^0_{33} = 2\Gamma^0_{22} \sin\theta\cos\theta,$$

$$\partial_0 \Gamma^1_{33} = \partial_0 \Gamma^1_{22} \sin^2\theta, \quad \partial_1 \Gamma^1_{33} = \partial_1 \Gamma^1_{22} \sin^2\theta, \quad \partial_2 \Gamma^1_{33} = 2\Gamma^1_{22} \sin\theta\cos\theta,$$

$$\partial_2 \Gamma^0_{33} = \partial_2 \left[-\sin\theta\cos\theta\right] = -\cos^2\theta + \sin^2\theta$$

C.2. **Ricci tensor.**
The components of the Ricci tensor are given by the sum:

$$R_{nk} = \sum_a \left(\partial_a \Gamma^a_{kn} - \partial_k \Gamma^a_{an}\right) + \sum_a \sum_m \left(\Gamma^a_{am}\Gamma^m_{kn} - \Gamma^a_{km}\Gamma^m_{an}\right) \tag{C.2}$$

The identity $\Gamma^m_{ik} = \Gamma^m_{ki}$ has to be used repeatedly. Many of the terms are equal to zero. According to the above list of second order Christoffel symbols, we will frequently use the identities

$$\Gamma^1_{01} = \Gamma^2_{02} = \Gamma^3_{03} \quad \text{and} \quad \Gamma^2_{12} = \Gamma^3_{13}. \tag{C.3}$$

The calculations are extensive but not difficult. It applies $R_{ik} = R_{ki}$, the components of the Ricci tensor are assorted by the first index in the following.

Component R_{00}
For $n = 0$, $k = 0$ we get:

$$R_{00} = \sum_a \left(\partial_a \Gamma^a_{00} - \partial_0 \Gamma^a_{a0}\right) + \sum_a \sum_m \left(\Gamma^a_{am}\Gamma^m_{00} - \Gamma^a_{0m}\Gamma^m_{a0}\right)$$

Pursuant to our list of nonzero Christoffel symbols, the sum reduces to:

$$\begin{aligned} R_{00} &= \partial_1\Gamma^1_{00} - \partial_0\Gamma^1_{01} - \partial_0\Gamma^2_{02} - \partial_0\Gamma^3_{03} - \left(\Gamma^1_{01}\right)^2 - \left(\Gamma^2_{02}\right)^2 - \left(\Gamma^3_{03}\right)^2 \\ &\quad + \Gamma^0_{00}\left(\Gamma^1_{01} + \Gamma^2_{02} + \Gamma^3_{03}\right) + \Gamma^1_{00}\left(-\Gamma^0_{01} + \Gamma^1_{11} + \Gamma^2_{12} + \Gamma^3_{13}\right) \end{aligned}$$

By using the identities (C.3) it remains:

$$R_{00} = \partial_1\Gamma^1_{00} - 3\partial_0\Gamma^1_{01} - 3\left(\Gamma^1_{01}\right)^2 + 3\Gamma^0_{00}\Gamma^1_{01} + \Gamma^1_{00}\left(-\Gamma^0_{01} + \Gamma^1_{11} + 2\Gamma^2_{12}\right)$$

Correspondingly, the first component reads:

$$\begin{aligned} R_{00} &= \frac{c^2}{2}\left(\xi'' + \xi'^2 - \xi'\mu'\right)e^{\xi-\mu} - \frac{3}{2}\ddot{\mu} - \frac{3}{4}\dot{\mu}^2 + \frac{3}{4}\dot{\xi}\dot{\mu} + \frac{c^2}{2}\xi' e^{\xi-\mu}\left(\frac{3}{2}\mu' - \frac{1}{2}\xi' + \frac{2}{q}\right) \\ &= \frac{c^2}{2}\left(\xi'' + \frac{1}{2}\xi'^2 + \frac{1}{2}\xi'\mu' + \frac{2}{q}\xi'\right)e^{\xi-\mu} + \frac{3}{4}\left(\dot{\xi}\dot{\mu} - 2\ddot{\mu} - \dot{\mu}^2\right) \end{aligned}$$

Component R_{01}
For $n = 0$, $k = 1$ we get:

$$R_{01} = \sum_a \left(\partial_a \Gamma^a_{10} - \partial_1 \Gamma^a_{a0}\right) + \sum_a \sum_m \left(\Gamma^a_{am}\Gamma^m_{10} - \Gamma^a_{1m}\Gamma^m_{a0}\right)$$

Together with (C.3), the nonzero components reduce to:

$$\begin{aligned} R_{01} &= \partial_0\Gamma^0_{01} - \partial_1\Gamma^0_{00} - \partial_1\Gamma^2_{02} - \partial_1\Gamma^3_{03} \\ &\quad +\Gamma^0_{01}\left(\Gamma^1_{01}+\Gamma^2_{02}+\Gamma^3_{03}\right) - \Gamma^0_{11}\Gamma^1_{00} + \Gamma^1_{01}\left(\Gamma^2_{12}+\Gamma^3_{13}\right) - \Gamma^2_{02}\Gamma^2_{12} - \Gamma^3_{03}\Gamma^3_{13} \\ &= \partial_0\Gamma^0_{01} - \partial_1\Gamma^0_{00} - 2\partial_1\Gamma^1_{01} + 3\Gamma^0_{01}\Gamma^1_{01} - \Gamma^0_{11}\Gamma^1_{00} \end{aligned}$$

and thus it remains:

$$R_{01} = -\dot{\mu}' + \frac{3}{4}\xi'\dot{\mu} - \frac{1}{4}\dot{\mu}\xi' = \frac{1}{2}\dot{\mu}\xi' - \dot{\mu}'$$

The components R_{02} ***and*** R_{03}

For $n = 0,\ k = 2$ we get:

$$R_{02} = \sum_a \left(\partial_a\Gamma^a_{20} - \partial_2\Gamma^a_{a0}\right) + \sum_a\sum_m \left(\Gamma^a_{am}\Gamma^m_{20} - \Gamma^a_{2m}\Gamma^m_{a0}\right)$$

Together with (C.3) it remains

$$R_{02} = \Gamma^3_{23}\Gamma^2_{02} - \Gamma^3_{23}\Gamma^3_{03} = 0.$$

Further $n = 0,\ k = 3$ yields

$$R_{03} = \sum_a \left(\partial_a\Gamma^a_{30} - \partial_3\Gamma^a_{a0}\right) + \sum_a\sum_m \left(\Gamma^a_{am}\Gamma^m_{30} - \Gamma^a_{3m}\Gamma^m_{a0}\right) = 0.$$

Component R_{11}

For $n = 1,\ k = 1$ equation (C.2) reads

$$R_{11} = \sum_a \left(\partial_a\Gamma^a_{11} - \partial_1\Gamma^a_{a1}\right) + \sum_a\sum_m \left(\Gamma^a_{am}\Gamma^m_{11} - \Gamma^a_{1m}\Gamma^m_{a1}\right)$$

and the remaining non zero terms are:

$$\begin{aligned} R_{11} &= \partial_0\Gamma^0_{11} - \partial_1\Gamma^0_{01} - \partial_1\Gamma^2_{12} - \partial_1\Gamma^3_{13} + \Gamma^0_{11}\left(\Gamma^0_{00} - \Gamma^1_{01} + \Gamma^2_{02} + \Gamma^3_{03}\right) \\ &\quad +\Gamma^1_{11}\left(\Gamma^0_{01}+\Gamma^2_{12}+\Gamma^3_{13}\right) - \left(\Gamma^0_{01}\right)^2 - \left(\Gamma^2_{12}\right)^2 - \left(\Gamma^3_{13}\right)^2 \\ &= \partial_0\Gamma^0_{11} - \partial_1\Gamma^0_{01} - 2\partial_1\Gamma^2_{12} + \Gamma^0_{11}\left(\Gamma^0_{00}+\Gamma^1_{01}\right) \\ &\quad +\Gamma^1_{11}\left(\Gamma^0_{01}+2\Gamma^2_{12}\right) - \left(\Gamma^0_{01}\right)^2 - 2\left(\Gamma^2_{12}\right)^2 \end{aligned}$$

Hence we are left with:

$$\begin{aligned} R_{11} &= \frac{1}{2c^2}\left(\ddot{\mu}+\dot{\mu}^2-\dot{\mu}\dot{\xi}\right)e^{\mu-\xi}-\frac{1}{2}\xi''-\mu''+\frac{2}{q^2}+\frac{1}{2c^2}\dot{\mu}e^{\mu-\xi}\left(\frac{1}{2}\dot{\xi}+\frac{1}{2}\dot{\mu}\right) \\ &\quad +\frac{1}{2}\mu'\left(\frac{1}{2}\xi'+\mu'+\frac{2}{q}\right)-\frac{1}{4}\xi'^2-2\left(\frac{1}{2}\mu'+\frac{1}{q}\right)^2 \\ &= \frac{1}{2c^2}\left(\ddot{\mu}+\frac{3}{2}\dot{\mu}^2-\frac{1}{2}\dot{\mu}\dot{\xi}\right)e^{\mu-\xi}-\frac{1}{2}\xi''-\mu''+\frac{1}{4}\mu'\xi'-\frac{1}{4}\xi'^2-\mu'\frac{1}{q} \end{aligned}$$

The components R_{12} ***and*** R_{13}

For $n=1,\ k=2$, equation (C.2) together with (C.3) gives:

$$R_{12}=\sum_a\left(\partial_a\Gamma^a_{21}-\partial_2\Gamma^a_{a1}\right)+\sum_a\sum_m\left(\Gamma^a_{am}\Gamma^m_{21}-\Gamma^a_{2m}\Gamma^m_{a1}\right)=\Gamma^3_{23}\Gamma^2_{12}-\Gamma^3_{23}\Gamma^3_{13}=0$$

Equation (C.2) with $n=1,\ k=3$ yields:

$$R_{13}=\sum_a\left(\partial_a\Gamma^a_{31}-\partial_3\Gamma^a_{a1}\right)+\sum_a\sum_m\left(\Gamma^a_{am}\Gamma^m_{31}-\Gamma^a_{3m}\Gamma^m_{a1}\right)=0$$

Component R_{22}

With $n=2,\ k=2$ equation (C.2) reads:

$$R_{22}=\sum_a\left(\partial_a\Gamma^a_{22}-\partial_2\Gamma^a_{a2}\right)+\sum_a\sum_m\left(\Gamma^a_{am}\Gamma^m_{22}-\Gamma^a_{2m}\Gamma^m_{a2}\right)$$

If we drop all zero terms it remains:

$$\begin{aligned} R_{22} &= \partial_0\Gamma^0_{22}+\partial_1\Gamma^1_{22}-\partial_2\Gamma^3_{23} \\ &\quad +\Gamma^0_{22}\left(\Gamma^0_{00}+\Gamma^1_{01}-\Gamma^2_{02}+\Gamma^3_{03}\right)+\Gamma^1_{22}\left(\Gamma^0_{01}+\Gamma^1_{11}-\Gamma^2_{12}+\Gamma^3_{13}\right)-\left(\Gamma^3_{23}\right)^2 \end{aligned}$$

Because of the identities (C.3) this is equal to

$$R_{22}=\partial_0\Gamma^0_{22}+\partial_1\Gamma^1_{22}-\partial_2\Gamma^3_{23}+\Gamma^0_{22}\left(\Gamma^0_{00}+\Gamma^1_{01}\right)+\Gamma^1_{22}\left(\Gamma^0_{01}+\Gamma^1_{11}\right)-\left(\Gamma^3_{23}\right)^2.$$

Due to $\sin^2\theta+\cos^2\theta=1$ it is $-\partial_2\Gamma^3_{23}-\left(\Gamma^3_{23}\right)^2=\frac{1}{\sin^2\theta}-\frac{\cos^2\theta}{\sin^2\theta}=1$ and thus we are left with

$$R_{22}=\partial_0\Gamma^0_{22}+\partial_1\Gamma^1_{22}+\Gamma^0_{22}\left(\Gamma^0_{00}+\Gamma^1_{01}\right)+\Gamma^1_{22}\left(\Gamma^0_{01}+\Gamma^1_{11}\right)+1. \tag{C.4}$$

During the R_{33} calculation we will refer to the latter equation again. Now, using the Christoffel symbols in (C.4) finally leads to:

$$\begin{aligned} R_{22} &= \frac{q^2}{2c^2}\left(\ddot{\mu}+\dot{\mu}^2-\dot{\mu}\dot{\xi}\right)e^{\mu-\xi}-\frac{1}{2}q^2\mu''-q\mu'-1+\frac{1}{2c^2}\dot{\mu}e^{\mu-\xi}q^2\left(\frac{1}{2}\dot{\xi}+\frac{1}{2}\dot{\mu}\right) \\ &\quad -\frac{1}{2}\left(\mu' q^2+2q\right)\left(\frac{1}{2}\xi'+\frac{1}{2}\mu'\right)+1 \\ &= \frac{q^2}{2c^2}\left(\ddot{\mu}+\frac{3}{2}\dot{\mu}^2-\frac{1}{2}\dot{\mu}\dot{\xi}\right)e^{\mu-\xi}-\frac{1}{2}q^2\mu''-q\mu'-\frac{1}{4}q\left(\mu' q+2\right)\left(\xi'+\mu'\right) \end{aligned}$$

Alternatively, if we expand the second brackets:

$$R_{22}=\frac{q^2}{2c^2}\left(\ddot{\mu}+\frac{3}{2}\dot{\mu}^2-\frac{1}{2}\dot{\mu}\dot{\xi}\right)e^{\mu-\xi}-\frac{1}{2}q^2\mu''-\frac{1}{4}q^2\mu'\xi'-\frac{1}{4}q^2\mu'^2-\frac{1}{2}q\xi'-\frac{3}{2}q\mu'$$

Component R_{23}

Equation (C.2) for $n=2,\ k=3$ yields:

$$R_{23}=\sum_a\left(\partial_a\Gamma^a_{32}-\partial_3\Gamma^a_{a2}\right)+\sum_a\sum_m\left(\Gamma^a_{am}\Gamma^m_{32}-\Gamma^a_{3m}\Gamma^m_{a2}\right)=0$$

Component R_{33}

For $n=3,\ k=3$ we get:

$$R_{33}=\sum_a\left(\partial_a\Gamma^a_{33}-\partial_3\Gamma^a_{a3}\right)+\sum_a\sum_m\left(\Gamma^a_{am}\Gamma^m_{33}-\Gamma^a_{3m}\Gamma^m_{a3}\right)$$

The remaining non zero terms are:

$$\begin{aligned} R_{33} &= \partial_0\Gamma^0_{33}+\partial_1\Gamma^1_{33}+\partial_2\Gamma^2_{33} \\ &\quad +\Gamma^0_{33}\left(\Gamma^0_{00}+\Gamma^1_{01}+\Gamma^2_{02}-\Gamma^3_{03}\right)+\Gamma^1_{33}\left(\Gamma^0_{01}+\Gamma^1_{11}+\Gamma^2_{12}-\Gamma^3_{13}\right)-\Gamma^2_{33}\Gamma^3_{23} \end{aligned}$$

We use the identities (C.3) as well as $\Gamma^0_{33}=\Gamma^0_{22}\sin^2\theta$ and $\Gamma^1_{33}=\Gamma^1_{22}\sin^2\theta$ so that:

$$\begin{aligned} R_{33} &= \left(\partial_0\Gamma^0_{22}+\partial_1\Gamma^1_{22}\right)\sin^2\theta+\partial_2\Gamma^2_{33} \\ &\quad +\Gamma^0_{22}\left(\Gamma^0_{00}+\Gamma^1_{01}\right)\sin^2\theta+\Gamma^1_{22}\left(\Gamma^0_{01}+\Gamma^1_{11}\right)\sin^2\theta-\Gamma^2_{33}\Gamma^3_{23} \end{aligned} \tag{C.5}$$

Since $\partial_2\Gamma^2_{33}-\Gamma^2_{33}\Gamma^3_{23}=\sin^2\theta$ we now obtain R_{33} from equation (C.4):

$$\begin{aligned} R_{33} &= \left(\partial_0\Gamma^0_{22}+\partial_1\Gamma^1_{22}+\Gamma^0_{22}\left(\Gamma^0_{00}+\Gamma^1_{01}\right)+\Gamma^1_{22}\left(\Gamma^0_{01}+\Gamma^1_{11}\right)+1\right)\sin^2\theta \\ &= R_{22}\sin^2\theta \end{aligned}$$

List of nonzero components of the Ricci tensor

We raise the index of the Ricci tensor components by:

$$R^i_k = \sum_n g^{in} R_{nk} \tag{C.6}$$

and obtain the following list of nonzero components:

$$\begin{aligned}
R^0_0 &= \frac{e^{-\mu}}{2}\left(\xi'' + \frac{1}{2}\xi'^2 + \frac{1}{2}\xi'\mu' + \frac{2}{q}\xi'\right) + \frac{3e^{-\xi}}{4c^2}\left(\dot\xi\dot\mu - 2\ddot\mu - \dot\mu^2\right)\\
R^1_0 &= e^{-\mu}\left(\dot\mu' - \frac{1}{2}\dot\mu\xi'\right)\\
R^1_1 &= \frac{e^{-\xi}}{2c^2}\left(\frac{1}{2}\dot\mu\dot\xi - \ddot\mu - \frac{3}{2}\dot\mu^2\right) + e^{-\mu}\left(\frac{1}{2}\xi'' + \mu'' - \frac{1}{4}\mu'\xi' + \frac{1}{4}\xi'^2 + \mu'\frac{1}{q}\right)\\
R^2_2 &= \frac{e^{-\xi}}{2c^2}\left(\frac{1}{2}\dot\mu\dot\xi - \ddot\mu - \frac{3}{2}\dot\mu^2\right) + e^{-\mu}\left(\frac{1}{2}\mu'' + \frac{1}{4}\mu'\xi' + \frac{1}{4}\mu'^2 + \frac{1}{2q}\xi' + \frac{3}{2q}\mu'\right)
\end{aligned}$$

further $R^3_3 = R^2_2$ and $R^0_1 = -\frac{1}{c^2}e^{\mu-\xi}R^1_0$.

The Ricci (curvature) scalar of the metric

The curvature scalar is given by:

$$R = \sum_k R^k_k \tag{C.7}$$

For the general isotropic ansatz (C.1) we found $R^3_3 = R^2_2$, hence the curvature scalar takes the form $R = R^0_0 + R^1_1 + 2R^2_2$.

C.3. **Einstein tensor.**
The Einstein tensor with cosmological constant Λ is defined by:

$$G^i_k = R^i_k - \frac{1}{2}R\delta^i_k - \Lambda\delta^i_k$$

where $\delta^i_k = 1$ for $i = k$ and $\delta^i_k = 0$ for $i \neq k$. Since for (C.1) it is $R = R^0_0 + R^1_1 + 2R^2_2$, we are left with the nonzero components

$$\begin{aligned} G^0_0 &= \frac{1}{2}\left(R^0_0 - R^1_1\right) - R^2_2 - \Lambda \\ G^1_0 &= R^1_0 \\ G^1_1 &= \frac{1}{2}\left(R^1_1 - R^0_0\right) - R^2_2 - \Lambda \\ G^2_2 &= -\frac{1}{2}\left(R^0_0 + R^1_1\right) - \Lambda \end{aligned}$$

further $G^0_1 = R^0_1$ and $G^3_3 = G^2_2$.

Corresponding to the coordinates $\{t, q, \theta, \phi\} = \left\{x^0, x^1, x^2, x^3\right\}$ we use the notation:

$$G^t_t := G^0_0\,, \quad G^q_q := G^1_1\,, \quad G^\theta_\theta := G^2_2\,, \quad G^\phi_\phi := G^3_3 \tag{C.8}$$

According to the list of nonzero R^i_k, the Einstein tensor for (C.1) finally takes the form:

$$\begin{aligned} G^t_t &= \frac{3\dot{\mu}^2 e^{-\xi}}{4c^2} - e^{-\mu}\left(\mu'' + \frac{1}{4}\mu'^2 + \frac{2}{q}\mu'\right) - \Lambda \\ G^q_t &= e^{-\mu}\left(\dot{\mu}' - \frac{1}{2}\dot{\mu}\xi'\right), \qquad G^t_q = -\frac{e^{-\xi}}{c^2}\left(\dot{\mu}' - \frac{1}{2}\dot{\mu}\xi'\right) \\ G^q_q &= \frac{e^{-\xi}}{c^2}\left(\ddot{\mu} + \frac{3}{4}\dot{\mu}^2 - \frac{1}{2}\dot{\mu}\dot{\xi}\right) - e^{-\mu}\left(\frac{\mu'\xi'}{2} + \frac{\mu'^2}{4} + \frac{\mu' + \xi'}{q}\right) - \Lambda \\ G^\theta_\theta &= \frac{e^{-\xi}}{c^2}\left(\ddot{\mu} + \frac{3}{4}\dot{\mu}^2 - \frac{1}{2}\dot{\mu}\dot{\xi}\right) - e^{-\mu}\left(\frac{\mu'' + \xi''}{2} + \frac{\xi'^2}{4} + \frac{\mu' + \xi'}{2q}\right) - \Lambda \\ G^\phi_\phi &= G^\theta_\theta \end{aligned}$$

C.4. **Calculations for the new solution.**

The ansatz for the new solution of Einstein's equation is given by:

$$ds^2 = \left[\frac{1 - La^2(t)\,q^2}{1 + La^2(t)\,q^2}\right]^2 c^2 dt^2 - a^2(t)\left[\frac{1}{1 + La^2(t)\,q^2}\right]^2 d\sigma^2 \tag{C.9}$$

We refer to Einstein's field equations for the general isotropic spacetime, see subsection C.3. For that reason, a couple of derivatives have to be calculated at first. It is convenient to introduce some shortcuts, let us denote $w = La^2(t)\,q^2$ and $H = \dot{a}/a$. Correspondingly, we obtain the relations:

$$\partial_0 w = 2La\dot{a}q^2 = 2wH \tag{C.10}$$

$$\partial_1 w = 2La^2 q = \frac{2}{q}w \tag{C.11}$$

$$\partial_0 H = \frac{\ddot{a}}{a} - H^2 \tag{C.12}$$

With respect to the latter definition of w, the general isotropic ansatz (5.58) represents metric (C.9) if

$$e^{\xi(t,q)} = \left(\frac{1-w}{1+w}\right)^2 \quad \text{and} \quad e^{\mu(t,q)} = \left(\frac{a}{1+w}\right)^2 \tag{C.13}$$

so that

$$\xi = 2\ln\left(\frac{1-w}{1+w}\right) \quad \text{and} \quad \mu = 2\ln\left(\frac{a}{1+w}\right).$$

Derivatives of ξ and μ

The derivation of ξ with respect to the coordinate x^k is given by

$$\partial_k \xi = 2\left(\frac{1-w}{1+w}\right)^{-1} \partial_k\left[\frac{1-w}{1+w}\right] = \frac{4\partial_k w}{w^2-1}$$

so that

$$\dot{\xi} = \frac{8wH}{w^2-1} \quad \text{and} \quad \xi' = \frac{8w}{(w^2-1)\,q}. \tag{C.14}$$

The derivation of μ with respect to the coordinate x^k is given by

$$\partial_k \mu = 2\left(\frac{a}{1+w}\right)^{-1} \partial_k\left[\frac{a}{1+w}\right] = 2\left(\frac{\partial_k a}{a} - \frac{\partial_k w}{1+w}\right)$$

so that

$$\dot{\mu} = 2H - 4H\frac{w}{1+w} = 2H\frac{1-w}{1+w} \quad \text{and} \quad \mu' = -\frac{4w}{(1+w)\,q}. \tag{C.15}$$

Second derivatives

From equation (C.14) we get:

$$\begin{aligned}\ddot{\xi} &= \partial_0\left[\frac{8wH}{w^2-1}\right] = 8\frac{(H\partial_0 w + w\partial_0 H)\left(w^2-1\right) - 2w^2 H\partial_0 w}{\left(w^2-1\right)^2} \\ &= 8\frac{\left(w^2-1\right)w\partial_0 H - \left(w^2+1\right)H\partial_0 w}{\left(w^2-1\right)^2}\end{aligned}$$

Together with (C.10) and (C.12) and after combining like terms, the equation reads:

$$\ddot{\xi} = \frac{8w}{w^2-1}\left(\frac{\ddot{a}}{a} - \frac{3w^2+1}{w^2-1}H^2\right)$$

Analogously, we use (C.10) to obtain:

$$\begin{aligned}\dot{\xi}' &= \partial_0\left[\frac{8w}{\left(w^2-1\right)q}\right] = 8\frac{\left(w^2-1\right)q\partial_0 w - 2w^2 q\partial_0 w}{\left(w^2-1\right)^2 q^2} \\ &= -8\frac{w^2+1}{\left(w^2-1\right)^2 q}\partial_0 w = -\frac{16w\left(w^2+1\right)}{\left(w^2-1\right)^2 q}H\end{aligned}$$

Together with (C.11) we get:

$$\begin{aligned}\xi'' &= \partial_1\left[\frac{8w}{\left(w^2-1\right)q}\right] = 8\frac{\left(w^2-1\right)q\partial_1 w - w\left(2qw\partial_1 w + w^2 - 1\right)}{\left(w^2-1\right)^2 q^2} \\ &= -8\frac{w^3 - w + \left(w^2+1\right)\partial_1 w}{\left(w^2-1\right)^2 q^2} = -8w\frac{3w^2+1}{\left(w^2-1\right)^2 q^2}\end{aligned}$$

Equation (C.15) yields

$$\ddot{\mu} = \partial_0\left[2H\frac{1-w}{1+w}\right] = \frac{2\left(1-w\right)\partial_0 H}{1+w} - \frac{4H\partial_0 w}{\left(1+w\right)^2}$$

and together with (C.10) and (C.12) it remains:

$$\ddot{\mu} = 2\left(\frac{\ddot{a}}{a} - H^2\right)\frac{1-w}{1+w} - \frac{8wH^2}{\left(1+w\right)^2} = 2\frac{\frac{\ddot{a}}{a}\left(1-w^2\right) + H^2\left(w^2-4w-1\right)}{\left(1+w\right)^2}$$

Analogously, we have

$$\dot{\mu}' = \partial_1\left[2H\frac{1-w}{1+w}\right] = -\frac{4H}{\left(1+w\right)^2}\partial_1 w = -\frac{8wH}{\left(1+w\right)^2 q}$$

and

$$\begin{aligned}\mu'' &= \partial_1\left[-\frac{4w}{\left(1+w\right)q}\right] = -4\frac{\left(1+w\right)q\partial_1 w - w\left(q\partial_1 w + w + 1\right)}{\left(1+w\right)^2 q^2} \\ &= -4\frac{q\partial_1 w - w^2 - w}{\left(1+w\right)^2 q^2} = \frac{4w\left(w-1\right)}{\left(1+w\right)^2 q^2}\end{aligned}$$

where we have used (C.11) again.

C.5. **Empty-space equations for the new metric.**
According to Einstein's tensor for the general isotropic ansatz (C.1) in subsection C.3, the empty-space ($T_k^i = 0$) equations are:

$$\text{(C.16)}\quad \Lambda = \frac{3\dot{\mu}^2 e^{-\xi}}{4c^2} - e^{-\mu}\left(\mu'' + \frac{1}{4}\mu'^2 + \frac{2}{q}\mu'\right)$$

$$\text{(C.17)}\quad 0 = \dot{\mu}' - \frac{1}{2}\dot{\mu}\xi'$$

$$\text{(C.18)}\quad \Lambda = \frac{e^{-\xi}}{c^2}\left(\ddot{\mu} + \frac{3}{4}\dot{\mu}^2 - \frac{1}{2}\dot{\mu}\dot{\xi}\right) - e^{-\mu}\left(\frac{\mu'\xi'}{2} + \frac{\mu'^2}{4} + \frac{\mu' + \xi'}{q}\right)$$

$$\text{(C.19)}\quad \Lambda = \frac{e^{-\xi}}{c^2}\left(\ddot{\mu} + \frac{3}{4}\dot{\mu}^2 - \frac{1}{2}\dot{\mu}\dot{\xi}\right) - e^{-\mu}\left(\frac{\mu'' + \xi''}{2} + \frac{\xi'^2}{4} + \frac{\mu' + \xi'}{2q}\right)$$

For the new metric (C.9), equation (C.16) reads:

$$\begin{aligned}\Lambda &= \frac{3}{c^2}H^2 - \left(\frac{1+w}{a}\right)^2\left[\frac{4w\,(w-1) + 4w^2}{(1+w)^2\,q^2} - \frac{8w}{(1+w)\,q^2}\right] \\ &= \frac{3}{c^2}H^2 + \frac{12w}{a^2q^2} = \frac{3}{c^2}H^2 + 12L\end{aligned}$$

and equation (C.17) is fulfilled identically. After a brief calculation, the terms in the first brackets of (C.18) give

$$\begin{aligned}\ddot{\mu} + \frac{3}{4}\dot{\mu}^2 - \frac{1}{2}\dot{\mu}\dot{\xi} &= \frac{2\frac{\ddot{a}}{a}\left(1-w^2\right) + \left(5w^2 - 6w + 1\right)H^2}{(1+w)^2} \\ &= \frac{2\frac{\ddot{a}}{a}(1+w)(1-w) + (1-5w)(1-w)\,H^2}{(1+w)^2} \\ &\quad \frac{1-w}{(1+w)^2}\left[2\frac{\ddot{a}}{a}(1+w) + (1-5w)\,H^2\right]\end{aligned}$$

and with (C.13) we get:

$$\frac{e^{-\xi}}{c^2}\left(\ddot{\mu} + \frac{3}{4}\dot{\mu}^2 - \frac{1}{2}\dot{\mu}\dot{\xi}\right) = \frac{2\frac{\ddot{a}}{a}(1+w) + (1-5w)\,H^2}{c^2\,(1-w)}$$

The terms in the second brackets give

$$\frac{\mu'\xi'}{2} + \frac{\mu'^2}{4} + \frac{\mu' + \xi'}{q} = -\frac{12w}{(w+1)^2\,q^2}$$

so that

$$e^{-\mu}\left(\frac{\mu'\xi'}{2} + \frac{\mu'^2}{4} + \frac{\mu' + \xi'}{q}\right) = -\frac{12w}{a^2q^2} = -12L.$$

Hence, the entire equation (C.18) reads:

$$\Lambda = \frac{2\frac{\ddot{a}}{a}(1+w) + (1-5w)\,H^2}{c^2\,(1-w)} + 12L$$

It turned out that (C.18) and (C.19) yield the same condition, but the calculations for (C.19) are more extensive. The first bracket of (C.19) coincide with the first bracket of equation (C.18). Let $f = \frac{\mu''+\xi''}{2} + \frac{\xi'^2}{4} + \frac{\mu'+\xi'}{2q}$, so that the second part of (C.19) is $fe^{-\mu}$. We have to show that $fe^{-\mu} = -12L$:

$$\begin{aligned} f &= \frac{2w\,(w-1)}{(w+1)^2\,q^2} + \frac{32w^2 - 12w^3 - 4w}{(w^2-1)^2\,q^2} + \frac{6w - 2w^2}{(w^2-1)\,q^2} \\ &= \frac{2w\,(w-1)^3 + 2w\left(16w - 6w^2 - 2\right) + 2w\,(3-w)\left(w^2-1\right)}{(w^2-1)^2\,q^2} \\ &= \frac{2w\left(12w - 6w^2 - 6\right)}{(w^2-1)^2\,q^2} = \frac{-12w\left(w^2 - 2w + 1\right)}{(w+1)^2\,(w-1)^2\,q^2} = -\frac{12w}{(w+1)^2\,q^2} \end{aligned}$$

Hence, with (C.13) follows $fe^{-\mu} = -12L$. Thus, it is proved that the empty space equations for (C.9) are:

$$\begin{aligned} \frac{3}{c^2}H^2 &= \Lambda - 12L \\ \frac{2\frac{\ddot{a}}{a}\,(1+w) + (1-5w)\,H^2}{c^2\,(1-w)} &= \Lambda - 12L \end{aligned}$$

C.6. **McVittie solution.**

McVittie's metric is given by the line element:

$$ds^2 = \left[\frac{1-\frac{r_g}{4a(t)q}}{1+\frac{r_g}{4a(t)q}}\right]^2 c^2dt^2 - a^2(t)\left[1+\frac{r_g}{4a(t)q}\right]^4 d\sigma^2 \tag{C.20}$$

We refer again to Einstein's equations for the general isotropic spacetime, see subsection C.3, and use the shortcut $u = \frac{r_g}{4a(t)q}$ (and again $H = \dot{a}/a$) in order to simplify the necessary calculations. Correspondingly, we obtain the relations[106]:

$$\partial_0 u = -\frac{r_g\dot{a}}{4a^2q} = -Hu \tag{C.21}$$

$$\partial_1 u = -\frac{r_g}{4aq^2} = -\frac{1}{q}u \tag{C.22}$$

With respect to the definition of u, the general isotropic ansatz (C.1) represents metric (C.20) if

$$e^{\xi(t,q)} = \left(\frac{1-u}{1+u}\right)^2 \quad \text{and} \quad e^{\mu(t,q)} = a^2(1+u)^4 \tag{C.23}$$

so that

$$\xi = 2\ln\left(\frac{1-u}{1+u}\right) \quad \text{and} \quad \mu = 2\ln\left[a(1+u)^2\right].$$

Derivatives of ξ and μ

The derivations of ξ and μ with respect to the coordinate x^k are given by

$$\partial_k\xi = \frac{4\partial_k u}{u^2-1}, \quad \partial_k\mu = 2\frac{\partial_k a}{a} + \frac{4\partial_k u}{1+u}$$

so that

$$\dot{\xi} = \frac{4Hu}{1-u^2}, \quad \xi' = \frac{4u}{(1-u^2)q}, \quad \dot{\mu} = 2H\frac{1-u}{1+u}, \quad \mu' = -\frac{4u}{(1+u)q}.$$

The second derivatives are

$$\ddot{\xi} = \partial_0\left[\frac{4Hu}{1-u^2}\right] = 4\frac{H\left(u^2+1\right)\partial_0 u + u\left(1-u^2\right)\partial_0 H}{\left(1-u^2\right)^2} = 4u\frac{\frac{\ddot{a}}{a}\left(1-u^2\right)-2H^2}{\left(1-u^2\right)^2}$$

$$\dot{\xi}' = \partial_1\left[\frac{4Hu}{1-u^2}\right] = 4H\frac{u^2+1}{\left(1-u^2\right)^2}\partial_1 u = -4uH\frac{u^2+1}{\left(1-u^2\right)^2 q}$$

$$\xi'' = \partial_1\left[\frac{4u}{(1-u^2)q}\right] = 4\frac{\left(u^2+1\right)q\partial_1 u - \left(1-u^2\right)u}{\left(1-u^2\right)^2 q^2} = -\frac{8u}{\left(1-u^2\right)^2 q^2}$$

[106]Remember that $\dot{H} = \frac{\ddot{a}}{a} - H^2$, see relation (C.12)

and

$$\begin{aligned}
\ddot{\mu} &= \partial_0\left[2H\frac{1-u}{1+u}\right] = \frac{2\left(1-u^2\right)\partial_0 H - 4H\partial_0 u}{(u+1)^2} \\
&= \frac{2\left[\frac{\ddot{a}}{a}\left(1-u^2\right)+H^2\left(u^2+2u-1\right)\right]}{(u+1)^2} \\
\dot{\mu}' &= \partial_1\left[2H\frac{1-u}{1+u}\right] = -4H\frac{\partial_1 u}{(u+1)^2} = \frac{4uH}{(u+1)^2 q} \\
\mu'' &= \partial_1\left[-\frac{4u}{(1+u)q}\right] = -4\frac{q\partial_1 u - u - u^2}{(u+1)^2 q^2} = 4u\frac{2+u}{(u+1)^2 q^2}.
\end{aligned}$$

C.7. **Empty-space equations for McVittie's metric.**
We refer again to (C.16), (C.17), (C.18) and (C.19) in subsection C.5, which are the empty-space equations for the general isotropic ansatz (C.1). For McVittie's metric it applies $\mu''+\frac{1}{4}\mu'^2+\frac{2}{q}\mu'=0$ and equation (C.16) yields $\frac{3H^2}{c^2}=\Lambda$. Equation (C.17) is fulfilled identically since $\dot{\mu}'=\frac{1}{2}\dot{\mu}\xi'$. The terms in the first brackets of (C.18) give

$$\begin{aligned}
\ddot{\mu}+\frac{3}{4}\dot{\mu}^2-\frac{1}{2}\dot{\mu}\dot{\xi} &= \frac{2\frac{\ddot{a}}{a}\left(1-u^2\right)+\left(5u^2-6u+1\right)H^2}{(u+1)^2} \\
&= \frac{2\frac{\ddot{a}}{a}(1+u)(1-u)+(1-5u)(1-u)H^2}{(u+1)^2} \\
&= \frac{1-u}{(u+1)^2}\left[2\frac{\ddot{a}}{a}(1+u)+(1-5u)H^2\right]
\end{aligned}$$

and those in the second brackets yield zero, $\frac{\mu'\xi'}{2}+\frac{\mu'^2}{4}+\frac{\mu'+\xi'}{q}=0$. Together with (C.23) equation (C.18) reads:

$$\frac{2\frac{\ddot{a}}{a}(1+u)+(1-5u)H^2}{c^2(1-u)}=\Lambda$$

It turned out that $\frac{\mu''+\xi''}{2}+\frac{\xi'^2}{4}+\frac{\mu'+\xi'}{2q}=0$, so equation (C.19) yields the same result. Finally, the remaining empty-space equations for McVittie's metric are:

$$\boxed{\begin{aligned}
\frac{3}{c^2}H^2 &= \Lambda \\
\frac{2\frac{\ddot{a}}{a}(1+u)+(1-5u)H^2}{c^2(1-u)} &= \Lambda
\end{aligned}}$$

Appendix D. FORTRAN, Maple and Gnuplot source codes

D.1. Isotropic coordinates for Schwarzschild-de Sitter.

We used the following FORTRAN 77 and Gnuplot scripts to transform the Schwarzschild-de Sitter metric into isotropic coordinates.

D.1.1. *Relation of the coordinates q and r.*

In subsection 5.3.1 we established a first order approximation for the isotropic $q(r)$ coordinate in the Schwarzschild-de Sitter case. Algorithm 1 was used to plot figure 5.1.

Algorithm 1 Relation between q and r (Gnuplot)

```
reset
M=2.6e45
Grav=6.67259e-14
c=2.99792458e8
Mpc=3.08568025e22
Gpc=1000*Mpc
H=71000/Mpc
OL=0.73
Lambda=3*(H**2)*OL/(c**2)
rg=2*M*Grav/(c**2)
rL=sqrt(3/Lambda)
eps=(rg/rL)**2
set xrange [0.0001:8.9]
set format x "%g Gpc"
set yrange [0:10]
set format y "%g Gpc"
set xlabel "r-axis"
set ylabel "q-axis"
f(x)=eps*(x*Gpc/(4*rg)+1/(1-x*Gpc/rg)+7/8)*sqrt(x*Gpc*((x*Gpc/rg)-1)/rg)
                                                                    /2
qk(x)=(rg/4)*exp(f(x)+(2+15*eps/16)*log(sqrt(x*Gpc/rg)
                                          +sqrt((x*Gpc/rg)-1)))/Gpc
qs(x)=(rg/4)*(sqrt(x*Gpc/rg)+sqrt((x*Gpc/rg)-1))**2/Gpc
qd(x)=2*rL/((rL/(x*Gpc))+sqrt((rL/(x*Gpc))**2-1))/Gpc
plot qk(x) title "Schwarzschild-de Sitter (first order approximation)" with lines
  ls 9, qs(x) title "Schwarzschild" with lines ls 7, qd(x) title "De Sitter" with lines
```

Algorithm 1 can be modified to plot figure 5.2:

Algorithm 2 $q\,(r)$ near r_g (Gnuplot)

```
reset
M=2.6e45
Grav=6.67259e-14
c=2.99792458e8
Mpc=3.08568025e22
pc=Mpc/1000000
H=71000/Mpc
OL=0.73
Lambda=3*(H**2)*OL/(c**2)
rg=2*M*Grav/(c**2)
rL=sqrt(3/Lambda)
eps=(rg/rL)**2
set xrange [0.125111:0.125149]
set format x "%g pc"
set xtics 0.00001
set yrange [0.03121:0.0325]
set format y "%g pc"
set xlabel "r-axis"
set ylabel "q-axis"
f(x)=eps*(x*pc/(4*rg)+1/(1-x*pc/rg)+7/8)*sqrt(x*pc*((x*pc/rg)-1)/rg)/2
qk(x)=(rg/4)*exp(f(x)+(2+15*eps/16)*log(sqrt(x*pc/rg)+sqrt((x*pc/rg)-1)))/pc
qs(x)=(rg/4)*(sqrt(x*pc/rg)+sqrt((x*pc/rg)-1))**2/pc
plot qk(x) title "Schwarzschild-de Sitter (first order approximation)" with lines
                                        ls 9, qs(x) title "Schwarzschild" with lines ls 7
```

D.1.2. ***Numerical approximation of*** g_{11}.

Algorithm 3 is based on the Euler method. This Fortran77 program was used for the numerical approximation of

$$\frac{du}{dx} = \frac{1}{\sqrt{1 - e^{-x} - \frac{\Lambda}{3} r_g^2 e^{2x}}}.$$

The start values are $x_0 = \ln \kappa$ and $u_0 = \ln \left[\frac{1}{2}\kappa - \frac{1}{4} + \frac{1}{2}\sqrt{\kappa^2 - \kappa} \right]$. κ is replaced by K in the source code. According to (5.40), it applies $B = \exp^2 (x - u)$. Algorithm 3 plots the function $f = 1 + g_{11}$, i.e. the points $P_n \left(u_n \mid 1 - B_n \right)$ into a file named *k.txt*. The physical units of the constants are: M (mass) in g, G (gravitational constant) in $\frac{\mathrm{m}^3}{\mathrm{s}^2 \mathrm{g}}$, c (speed of light) in $\frac{\mathrm{m}}{\mathrm{s}}$, Lambda (cosmological constant) in $\frac{1}{\mathrm{m}^2}$ and rg (gravitational radius) in m.

Algorithm 3 Isotropic coordinates for Schwarzschild-de Sitter (FORTRAN 77)

```
PROGRAM Kottler
INTEGER n, i
REAL*8 u, x, h, K, B
REAL*8 M, G, c, rg, Lambda, rL, eps
M=2.6d45
G=6.67d-14
c=299792458.d00
rg=2.d00*G*M/c**2.d00
Lambda=1.3d-52
rL=DSQRT(3.d00/Lambda)
eps=(Lambda*rg**2)/3.d00
n=2.27d5
h=1d-4
K=4.d00
x=DLOG(K)
u=DLOG(0.5d00*K-0.25d00+0.5d00*DSQRT(K*K-K))
OPEN (7,FILE='k.txt')
DO i=1,n
x=x+h
CONTINUE
u=u+h/DSQRT(1.d00-DEXP(-x)-eps*DEXP(2.d00*x))
B=(DEXP(x-u))**2.d00
WRITE (7,*) u, 1.d00-B
ENDDO
CLOSE (7)
END
```

In order to plot details of the transition region, we replaced the rows 12, 13, 14 in

algorithm 3 by:

```
n=1.d4
h=1d-3
K=DEXP(12.d00)
```

Figure 5.3 was plotted with the following Gnuplot scripts:

Algorithm 4 Isotropic coordinates for Schwarzschild-de Sitter (Gnuplot)

```
reset
set key top left
set xlabel "q"
set xrange [0:25.4]
set xtics ("1 pc" 2.08, "" 4.38, "" 6.68, "1 kpc" 8.99, "" 11.29, "" 13.59, "1 Mpc"
                                        15.89, "" 18.2, "" 20.5, "1 Gpc" 22.8, "" 25.11 )
set yrange [-0.6:0.6]
BS(x)=(1+exp(-x)/4)**4
BD(x)=(1/(1+exp(2*x)*1.602319341e-22))**2
plot 1-BS(x) title "Schwarzschild" with lines ls 9,
                                                1-BD(x) title "De Sitter" with lines ls 3,
                        "k.txt" title "Numerical Schwarzschild-de Sitter" with lines ls 7
```

Transition region:

Algorithm 5 Isotropic coordinates for Schwarzschild-de Sitter (Gnuplot)

```
reset
set key top left
set xlabel "q"
set xrange [13.4:18.3]
set xtics ("0.1 Mpc" 13.59, "" 14.29, "" 14.69, "" 14.98, "" 15.2, "" 15.38,"" 15.54,
            "" 15.67, "" 15.79, "1 Mpc" 15.89, "" 16.59, "" 16.99, "" 17.28, "" 17.5,
                                    "" 17.67, "" 17.84, "" 17.97, "" 18.09, "10 Mpc" 18.2)
set yrange [-0.0000015:0.0000015]
BS(x)=(1+exp(-x)/4)**4
BD(x)=(1/(1+exp(2*x)*1.602319341e-22))**2
plot 1-BS(x) title "Schwarzschild" with lines ls 9,
                                                1-BD(x) title "De Sitter" with lines ls 3,
                        "k.txt" title "Numerical Schwarzschild-de Sitter" with lines ls 7
```

D.1.3. ***Function terms for the*** g_{11} ***component.***

The following Gnuplot script was used to plot figure 5.4. It shows that both functions (5.43) and (5.44) cover the numerical graph for B in the Schwarzschild-de Sitter case.

Algorithm 6 The isotropic Schwarzschild-de Sitter g_{11} component (Gnuplot)

```
reset
set key top left
set xlabel "q"
set xrange [0:25.4]
set xtics ("1 pc" 2.08, "" 4.38, "" 6.68, "1 kpc" 8.99, "" 11.29, "" 13.59, "1 Mpc"
                                        15.89, "" 18.2, "" 20.5, "1 Gpc" 22.8, "" 25.11 )
set xrange [13.4:18.3]
set yrange [-0.0000015:0.000002]
BS(x)=(1+exp(-x)/4)**4
BD(x)=(1/(1+exp(2*x)*1.602319341e-22))**2
S(x)=BS(x)+BD(x)-1
P(x)=BS(x)*BD(x)
plot 1-BS(x) title "Schwarzschild" with lines ls 9, 1-BD(x) title "De Sitter" with
        lines ls 3, "k.txt" title "Numerical Schwarzschild-de Sitter" with lines ls 7,
                        1-S(x) title "1-S(u) Schwarzschild-de Sitter" with lines ls 8,
                        1-P(x) title "1-P(u) Schwarzschild-de Sitter" with lines ls 1
```

D.1.4. ***Function for g_{11} with respect to the r coordinate.***
Algorithm 3 had to be slightly modified to generate the data for figure 6.1. The rows 12, 13, 14 and 23 were replaced by

```
n=1.d4
h=1d-3
K=DEXP(12.d00)
⋮
WRITE (7,*) x, 1.d00-B
```

Figure 6.1 was plotted with Gnuplot script 7:

Algorithm 7 Graph of the function $1 + g_{11}(r)$ (Gnuplot)

```
reset
set key top left
set xlabel "r"
set xtics ("0.1 Mpc" 13.59, "" 14.29, "" 14.69, "" 14.98, "" 15.2, "" 15.38,"" 15.54,
           "" 15.67, "" 15.79, "1 Mpc" 15.89, "" 16.59, "" 16.99, "" 17.28, "" 17.5,
                                "" 17.67, "" 17.84, "" 17.97, "" 18.09, "10 Mpc" 18.2)
set xrange [13.4:18.3]
set yrange [-0.0000015:0.0000015]
BS(x)=(1+exp(-x)/4)**4
BD(x)=(1/(1+exp(2*x)*1.602319341e-22))**2
P(x)=BS(x)*BD(x)
plot "k.txt" title "Numerical Schwarzschild-de Sitter" with lines ls 1,
                                        1-P(x) title "Product-metric" with lines ls 7
```

D.2. **Einstein tensor for the Product-metric.**

In section 5.6 we determined the stress-energy-momentum tensor so that the Product-metric (5.45) is an exact solution of Einstein's equations including a cosmological constant. We used the Maple algorithm 8 to compute Einstein's tensor G^i_k. In our paper, Ricci's tensor is determined by definition (A.8): $R_{nk} = \sum_a R^a_{nak}$. The Maple subroutine for the Ricci tensor (The Maple-Ricci tensor is denoted by $\widetilde{R}_{nk}$ in the following) is predefined by

$$\widetilde{R}_{nk} = \sum_a R^a_{ank} = -\sum_a R^a_{nak} = -R_{nk}$$

In order to take into account the opposite sign, we changed the signature of the metric from $(1 \mid 3)$ to $(3 \mid 1)$, see rows $7, 8, 9, 10$ in algorithm 8. Hence, the final result of our Maple algorithm represents the Einstein tensor G^i_k for the metric (5.45)

$$ds^2 = \left(\frac{1-\frac{r_g}{4q}}{1+\frac{r_g}{4q}}\right)^2 \left(\frac{1-\frac{q^2}{4r_\Lambda^2}}{1+\frac{q^2}{4r_\Lambda^2}}\right)^2 c^2dt^2 - \left(1+\frac{r_g}{4q}\right)^4 \left(\frac{1}{1+\frac{q^2}{4r_\Lambda^2}}\right)^2 d\sigma^2$$

with respect to the definitions given in section A.

Algorithm 8 Einsteintensor for the Product-metric (Maple)

```
restart;
with(tensor):
coords := [t,q,theta,phi];

exi := ((1-rg/(4*q))/(1+rg/(4*q)))^2*((1-(1/12)
                                    *Lambda*q^2)/(1+(1/12)*Lambda*q^2))^2:

emu := (1+rg/(4*q))^4/(1+(1/12)*Lambda*q^2)^2:

g:= array(symmetric,sparse, 1..4, 1..4):
g[1,1]:= -c^2*exi:
g[2,2]:= emu:
g[3,3]:= emu*q^2:
g[4,4]:= emu*q^2*sin(theta)^2:
metric:=create([-1,-1], eval(g)):

tensorsGR(coords, metric, contra_metric, det_met, C1, C2, Rm, Rc, R, G, C):
GRaise := raise(contra_metric, G, 2);
```

D.2.1. ***Product-metric and stress-energy-momentum tensor.***
From Einstein's field equations we get $T_k^i = \frac{c^4}{8\pi\gamma} G_k^i$. Accordingly, the stress-energy-momentum tensor is given by the functions (5.52), (5.53) and (5.54). In order that the data has the physical unit N/m^2 we plotted $T_k^i/1000$ in figure 5.5 with Gnuplot script 9:

Algorithm 9 Stress-energy-momentum tensor for the Product-metric (Gnuplot)

```
reset
M=2.6e45
Grav=6.67259e-14
c=2.99792458e8
Mpc=3.08568025e22
pc=Mpc/1000000
H=71000/Mpc
OL=0.73
Lambda=3*(H**2)*OL/(c**2)
rg=2*M*Grav/(c**2)
rL=sqrt(3/Lambda)
konst=(c**4)*Lambda/(8*3.1415927*Grav)
set key bottom right
set xrange [0:4.9]
set xtics ("rg/4" 0.03125,1,2,3,4,5)
set yrange [-5e-10:0]
set xlabel "q - axis"
set format x "%g pc"
set ylabel "Stress–energy–momentum tensor in N/m²"

f1(x)=1+7*rg**2/(192*rL**2)+rg**2/(16*(x*pc)**2)-rg/(3*x*pc)
                  -rg*x*pc/(12*rL**2)-(x*pc)**2*(1/4+rg**2/(384*rL**2))/(rL**2)

f2(x)=1+rg**2/(64*rL**2)-rg**2/(16*(x*pc)**2)+rg/(3*x*pc)

g(x)=(1+rg/(4*x*pc))**5*(1-rg/(4*x*pc))*(1-x**2/(4*rL**2))
                                        +rg*x*pc/(12*rL**2)-(x*pc)**2/(4*rL**2)

T00(x)=konst*((1+rg/(12*x*pc)-rg*x*pc/(24*rL**2))
                                                    /((1+rg/(4*x*pc))**5)-1)/1000
T11(x)=konst*(f1(x)/g(x)-1)/1000

T22(x)=konst*(f2(x)/g(x)-1)/1000

plot T00(x) title "T00 component" with lines ls 3, T11(x) title "T11 component"
                        with lines ls 7, T22(x) title "T22 component" with lines ls 9
```

D.3. **Numerical solution of Einstein's equations.**
Einstein's equations for the general orthogonal, isotropic and spherically symmetric ansatz lead to the first order system

$$\frac{dy}{du} = z, \quad \frac{dz}{du} = -z + Ky^5 e^{2u}$$

see section 5.7. In case of $K = K(t)$, the latter system of differential equations can be solved numerically with algorithm 10. The initial conditions

$$u_0,\ y_0 = 1 + \frac{1}{4}e^{-u_0},\ z_0 = -\frac{1}{4}e^{-u_0}$$

match with the isotropic Schwarzschild solution. We started at $u_0 = \ln 4$ which corresponds to the coordinate $q_0 = r_g e^{u_0} = 4r_g$.

Fourth-order Runge–Kutta method
The fourth-order Runge–Kutta method for a first order system

$$y' = f(u, y, z) \quad z' = g(u, y, z)$$

is given by

$$\begin{aligned} y_{n+1} &= y_n + \frac{1}{6}(k_1 + 2k_2 + 2k_3 + k_4) + \mathcal{O}\left(h^5\right) \\ z_{n+1} &= z_n + \frac{1}{6}(l_1 + 2l_2 + 2l_3 + l_4) + \mathcal{O}\left(h^5\right) \end{aligned}$$

where

$$\begin{aligned} k_1 &= hf(u_n, y_n, z_n) \\ k_2 &= hf\left(u_n + \frac{1}{2}h, y_n + \frac{1}{2}k_1, z_n + \frac{1}{2}l_1\right) \\ k_3 &= hf\left(u_n + \frac{1}{2}h, y_n + \frac{1}{2}k_2, z_n + \frac{1}{2}l_2\right) \\ k_4 &= hf(u_n + h, y_n + k_3, z_n + l_3) \end{aligned}$$

and

$$\begin{aligned} l_1 &= hg(u_n, y_n, z_n) \\ l_2 &= hg\left(u_n + \frac{1}{2}h, y_n + \frac{1}{2}k_1, z_n + \frac{1}{2}l_1\right) \\ l_3 &= hg\left(u_n + \frac{1}{2}h, y_n + \frac{1}{2}k_2, z_n + \frac{1}{2}l_2\right) \\ l_4 &= hg(u_n + h, y_n + k_3, z_n + l_3) \end{aligned}$$

see for example [96]. The following algorithm 10 is based on this method.

Algorithm 10 Fourth-order Runge–Kutta method (Fortran 77)

```
PROGRAM NumEinstEQN
INTEGER n, i
REAL*8 u, y, z, h, k(4), l(4), Kt
n=2670
h=1d-2
u=DLOG(4.d00)
y=1.d00+0.25d00*DEXP(-u)
z=-0.25d00*DEXP(-u)
Kt=-4.806958022d-22
OPEN (7,FILE='dat.txt')
WRITE (7,*) u, 1.d00-y**4.d00
DO i=1,n u=u+h
CONTINUE
k(1)=h*z
l(1)=h*(-z+Kt*(y**5)*Exp(2.d00*u))
k(2)=h*(z+l(1)/2.d00)
l(2)=h*(-z-l(1)/2.d00+Kt*(y+k(1)/2.d00)**5*Exp(2.d00*u+h))
k(3)=h*(z+l(2)/2.d00)
l(3)=h*(-z-l(2)/2.d00+Kt*(y+k(2)/2.d00)**5*Exp(2.d00*u+h))
k(4)=h*(z+l(3)) l(4)=h*(-z-l(3)+Kt*(y+k(3))**5*Exp(2.d00*(u+h)))
y=y+(k(1)+2.d00*k(2)+2.d00*k(3)+k(4))/6.d00
z=z+(l(1)+2.d00*l(2)+2.d00*l(3)+l(4))/6.d00
WRITE (7,*) u, 1.d00-y**4.d00
ENDDO
CLOSE (7)
END
```

Gnuplot script 11 was used to plot the data:

Algorithm 11 Numerical solution, figure 5.6 (Gnuplot)

```
reset
set key top left
set xlabel "q"
set xrange [0:25.4]
set xtics ("1 pc" 2.08, "" 4.38, "" 6.68, "1 kpc" 8.99, "" 11.29, "" 13.59, "1 Mpc"
                                        15.89, "" 18.2, "" 20.5, "1 Gpc" 22.8, "" 25.11 )
set yrange [-0.6:0.6]
BS(x)=(1+exp(-x)/4)**4
BD(x)=(1/(1+exp(2*x)*1.602319341e-22))**2
P(x)=BS(x)*BD(x)
plot 1-P(x) title "Product-metric" with lines ls 1,
                                    "dat.txt" title "Numerical solution" with lines ls 7
```

Gnuplot script 11 can be easily modified to plot figure 5.8. The requisite numerical data can be generated with algorithm 10. We used the following script to plot figure 5.7:

Algorithm 12 Large distance behaviour (Gnuplot)

```
reset
set key top left
set xlabel "q"
set xrange [0:29.5]
set xtics ("1 pc" 2.08, "" 4.38, "" 6.68, "1 kpc" 8.99, "" 11.29, "" 13.59, "1 Mpc"
                    15.89, "" 18.2, "" 20.5, "1 Gpc" 22.8, "" 25.11, "100 Gpc" 27.4)
set yrange [-0.5:1.2]

BS(x)=(1+exp(-x)/4)**4
BD(x)=(1/(1+exp(2*x)*1.602319341e-22))**2
P(x)=BS(x)*BD(x)

plot 1-P(x) title "Product-metric" with lines ls 1,
                                "dat.txt" title "Numerical solution" with steps ls 7
                        1.1-BD(x) title "De Sitter (shifted upwards)" with lines ls 3,
                    0.9-BS(x) title "Schwarzschild (shifted downwards)" with lines ls 9
```

D.4. **Schwarzschild-de Sitter cavity in a FLRW background.**
The following Fortran77 program numerically inverts the $R > rg$ branch of function (7.21):

$$t\left(R\right)=\mp\begin{cases}\dfrac{2r_g}{c}\left[\dfrac{1}{3}\sqrt{\dfrac{R}{r_g}}^3+\sqrt{\dfrac{R}{r_g}}-\operatorname{Artanh}\left(\sqrt{\dfrac{R}{r_g}}\right)\right]+k_1, & R<r_g\\[2ex] \dfrac{2r_g}{c}\left[\dfrac{1}{3}\sqrt{\dfrac{R}{r_g}}^3+\sqrt{\dfrac{R}{r_g}}+\dfrac{1}{2}\ln\left(\dfrac{\sqrt{\frac{R}{r_g}}-1}{\sqrt{\frac{R}{r_g}}+1}\right)\right]+k_2, & R>r_g\end{cases}$$

We chose $k_2 = 0$ in algorithm 13

Algorithm 13 Inverse function for $t\left(R\right)$

```
PROGRAM invert
INTEGER n, i
REAL*8 t, R, w, h
REAL*8 M, G, c, rg, Lambda, rL
M=2.6d45
G=6.67d-14
c=299792458.d00
rg=2.d00*G*M/c**2.d00
Lambda=1.3d-52
rL=DSQRT(3.d00/Lambda)
n=1d4
h=1d2
R=2.d00*rg
OPEN (7,FILE='inv.txt')
DO i=1,n
R=R+h
CONTINUE
w=DSQRT(R/rg)
t=2*rg*((w**3)/3+w+DLOG((w-1)/(w+1))/2)/c
WRITE (7,*) t, R
ENDDO
CLOSE (7)
END
```

Algorithm 13 can be easily modified in order to get data of the inverse function for the $R < r_g$ branch.

D.4.1. ***Expansion with nonzero cosmological constant.***
Consider a spatially flat FLRW universe which contains a static Schwarzschild-de Sitter region. Subsection 7.2 is concerned with the expansion of the spherical boundary, which is determined by equation (7.27):

$$\frac{dy}{dx} = \left(1 - \frac{1}{y} - \varepsilon y^2\right)\sqrt{\frac{1}{y} + \varepsilon y^2}$$

Algorithm 14 was used to approximate (7.27). The x values are multiplied by $r_g/\left(c \cdot 365 \cdot 24 \cdot 3600\text{s}\right) \approx 0.41$, so that the time coordinate is given in years.

Algorithm 14 Schwarzschild-de Sitter cavity in FLRW (FORTRAN 77)

```
PROGRAM RadiusCavity
INTEGER n, i
REAL*8 x, y, h, L, alpha
REAL*8 M, G, c, rg, Lambda, rL, eps
M=2.6d45
G=6.67d-14
c=299792458.d00
rg=2.d00*G*M/c**2.d00
Lambda=1.3d-52
rL=DSQRT(3.d00/Lambda)
eps=(Lambda*rg**2)/3.d00
n=2.3d05
h=1.d-4
x=0.d00
y=1.001d00
OPEN (7,FILE='R.txt')
DO i=1,n
x=x+h
CONTINUE
alpha=1.d00-1.d00/y-eps*y**2.d00
L=alpha*DSQRT(1.d00-alpha)
y=y+h*L
WRITE (7,*) x*rg/(c*3.1536d07), y
ENDDO
CLOSE (7)
END
```

By modifying row 15, one can easily generate data for different start values. The data for figure 7.2 was generated with the latter algorithm.

D.4.2. ***Large scale data for the expansion of the cavity.***
In order to generate the large scale data for figure 7.3, algorithm 14 was slightly modified. Row 12, 13 and 23 were replaced by

```
n=2d05
h=1.d6
  ⋮
WRITE (7,*) x*rg/(c*3.1536d16), y*rg/3.08568025d22
```

In order to generate the $\Lambda = 0$ data, one has to change the value for "Lambda" in row 9 additionally.

The data for figure 7.3 was plot with the following Gnuplot script:

Algorithm 15 Expansion in the region $R(t) \gg r_g$ (Gnuplot)

```
reset
set key top left
set xlabel "t - axis"
set ylabel "R - axis"
set format x "%g Gyr"
set format y "%g Mpc"
set xrange [0:27]
set yrange [0:5]
set xtics (0,5,10,13.75,20,25)
  plot "RL.txt" title "Lambda" with lines ls 3, "R0.txt" title "no Lambda" with
lines ls 9
set arrow from 13.75,1 to 13.7,0
replot
```

Additionally, we double-checked our results with a Runge-Kutta-Fehlberg approximation of equation (7.26)

$$\frac{dR}{cdt} = \left[1 - \frac{r_g}{R} - \left(\frac{R}{r_\Lambda}\right)^2\right] \sqrt{\frac{r_g}{R} + \left(\frac{R}{r_\Lambda}\right)^2}$$

with the help of Maple. The Runge-Kutta-Fehlberg (rkf45) method is the default numerical method in Maple. The corresponding source code is given in the following:

Algorithm 16 Double check for the $R(t)$ solution (MAPLE)

```
restart;
Sonnenmassen := 1.3*10^12;
Msun := 2*10^33;
M := Msun*Sonnenmassen;
Mpc := 3.08568025*10^22;
Grav := 6.6738480*10^(-14);
c := 299792458; 299792458
H := 70.4*(1000/Mpc);
OL := .728;
Lambda := 3*H^2*OL/c^2;
rg := 2*M*Grav/c^2;
rL := sqrt(3/Lambda);
DGLL := diff(y(x), x) = c*(1-rg/y(x)-(y(x)/rL)^2)*sqrt(rg/y(x)+(y(x)/rL)^2);
RL := dsolve({DGLL, y(0) = 1.001*rg}, y(x), numeric);
DGLN := diff(y(x), x) = c*(1-rg/y(x))*sqrt(rg/y(x));
RN := dsolve({DGLN, y(0) = 1.001*rg}, y(x), numeric);
with(plots);
  odeplot(RL, [x, y(x)], 0 .. 10^18, color = blue, axes = boxed, labels = ["t/s",
"q/m"]);
  odeplot(RN, [x, y(x)], 0 .. 10^18, color = blue, axes = boxed, labels = ["t/s",
"q/m"]);
```

The numerical approximation with the Runge-Kutta-Fehlberg (rkf45) method confirms our previous results, see figure D.1:

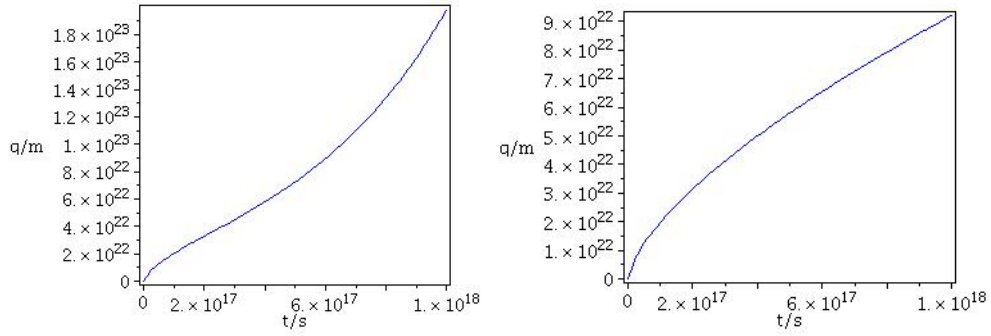

FIGURE D.1. Numerical solution of equation (7.26) in case of $\Lambda > 0$ and $\Lambda = 0$. The graphic shows the influence of the cosmological constant at large scales. For the numerical approximation of (7.26) we used again the gravitational radius $r_{LG} \approx 0.125\,\mathrm{pc}$, which corresponds to the Local Group.

D.4.3. ***The influence of the cosmological constant.***
Algorithm 17 solves the differential equation (7.29) in case of $\Lambda > 0$ and $\Lambda = 0$. The program compares the $\Lambda > 0$ solution[107] y_L and the $\Lambda = 0$ solution y_N solution, and it determines the value x_1 so that $y_L(x_1)/y_N(x_1) = 1.01$. The '1% - threshold' R_1 is defined by

$$R_1 := r_g y_L(x_1) \tag{D.1}$$

Algorithm 17 computes the '1% - threshold' R_1 for a given mass M.

Algorithm 17 Influence of the cosmological constant (MAPLE)

```
restart;
Sonnenmassen := 1.3*10^12;
Msun := 2*10^33;
M := Msun*Sonnenmassen;
Mpc := 3.08568025*10^22;
Grav := 6.6738480*10^(-14);
c := 299792458; 299792458
H := 70.4*(1000/Mpc);
OL := .728;
Lambda := 3*H^2*OL/c^2;
rg := 2*M*Grav/c^2;
rL := sqrt(3/Lambda);
ystart := 1.001*rg
DGLL := diff(y(x), x) = c*(1-rg/y(x)-(y(x)/rL)^2)*sqrt(rg/y(x)+(y(x)/rL)^2);
RL := dsolve({DGLL, y(0) = ystart}, y(x), numeric);
DGLN := diff(y(x), x) = c*(1-rg/y(x))*sqrt(rg/y(x));
RN := dsolve({DGLN, y(0) = ystart}, y(x), numeric);
x1 := 1.015*10^17;
yN := rhs(RN(x1)[2]);
yL := rhs(RL(x1)[2]);
Q := yL/yN;
while (Q<1.01) do
x1:=x1+x1/10000:
Q:=rhs(RL(x1)[2])/rhs(RN(x1)[2]):
rhs(RL(x1)[2])/Mpc;
od;
```

Algorithm 17 returns the data x_1, y_L/y_N and R_1 while $y_L/y_N < 1.01$. The '1% - threshold' R_1 is given in Mpc, but algorithm 17 can be easily modified to get the data in meters or parsec for example. Some numerical results are given in the following. Each data pair was computed with algorithm 17.

[107] where $y = R/r_g$, $x = ct/r_g$ and $\varepsilon := (r_g/r_\Lambda)^2$

Mass in $10^{12} M_{\odot}$	R_1 in Mpc
0.01	0.1304358853
0.02	0.1643389123
0.03	0.1881210923
0.04	0.2070540762
0.05	0.2230422381
0.06	0.2370177391
0.07	0.2495148589
0.08	0.2608717602
0.09	0.2713175801
0.1	0.2810155758
0.15	0.3216825223
0.2	0.3540574578
0.25	0.3813968336
0.3	0.4052946001
0.35	0.4266643645
0.4	0.4460843744
0.45	0.4639464825
0.5	0.4805298054
0.55	0.4960414061
0.6	0.5106391062
0.65	0.5244468127
0.7	0.5375634040
0.75	0.5500692776
0.8	0.5620310507
0.85	0.5735042177
0.9	0.5845358232
0.95	0.5951660477
1	0.6054295567
1.3	0.6607614908
1.5	0.6930437485
2	0.7627933516
2.5	0.8216941652
3	0.8731802402

TABLE 1. Numerical data for $R_1\,(M)$

The data of table 1 was plotted with Gnuplot to obtain figure 7.4.

D.4.4. ***Voids in the early universe.***
Algorithm 18 can be used to estimate the size of cosmic voids in the early universe. The differential equation here is

$$\frac{dR}{cdt} = -\left[1 - \frac{r_g}{R} - \left(\frac{R}{r_\Lambda}\right)^2\right]\sqrt{\frac{r_g}{R} + \left(\frac{R}{r_\Lambda}\right)^2}$$

The radius "Rvoid" of the void (in Mpc) is defined at row 10. The program calculates the mass "Mvoid" of the material, which has to be evacuated from a cosmological model with $\Omega_M = 0.273$ and $\Omega_\Lambda = 0.728$ to make the void. The start value is the radius of the void (in Mpc) today, "Rvoid" in line 10. In the last line, "yL" gives an estimation for the former radius of the void. The expansion time "age" is defined at line 18.

Algorithm 18 Voids in the early universe (MAPLE)

```
restart;
Mpc := 3.08568025*10^22;
Grav := 6.6738480*10^(-14);
c := 299792458; 299792458
H := 70.4*(1000/Mpc);
OL := 0.728;
Lambda := 3*H^2*OL/c^2;
OM := 0.273;
rho := evalf[10](3*H^2*OM/(8*Pi*Grav));
Rvoid := 10;
Mvoid := evalf[5](H^2*OM*(Rvoid*Mpc)^3/(2*Grav));
Msun := 2*10^33;
MvoidS := evalf[5](Mvoid/Msun);
rg := 2*Mvoid*Grav/c^2;
rL := sqrt(3/Lambda);
DGLL := diff(y(x), x) = -c*(1-rg/y(x)-(y(x)/rL)^2)*sqrt(rg/y(x)+(y(x)/rL)^2);
RL := dsolve({DGLL, y(0) = Rvoid*Mpc}, y(x), numeric);
age := 13.75*365*24*3600*10^9;
yL := rhs(RL(age)[2])/Mpc;
```

D.4.5. ***Influence of the cosmological constant.***
Based on the differential equation

$$\frac{dR}{cdt} = \left[1 - \frac{r_g}{R} - \left(\frac{R}{r_\Lambda}\right)^2\right] \sqrt{\frac{r_g}{R} + \left(\frac{R}{r_\Lambda}\right)^2}$$

we studied the influence of the cosmological constant in the ΛCDM Swiss-Cheese model. The current data of a galaxy, a cluster or a void (including a supermassive black hole in its center) is used to extrapolate the later size at a given point of time. Algorithm 19 approximates the later radius "yL" in the ΛCDM Swiss-Cheese model in comparison with a $\Lambda = 0$ model (radius "yN"). The last row calculates the influence of Λ in percent. The data in row 2 and 14 can be changed to study a cluster or a void.

Algorithm 19 Influence of Λ in the ΛCDM Swiss-Cheese model (MAPLE)

```
restart;
Sonnenmassen := 10^12;
Msun := 2*10^33;
M := Msun*Sonnenmassen;
Mpc := 3.08568025*10^22;
Gyr := 3600*(365*24)*10^9
Grav := 6.6738480*10^(-14);
c := 299792458; 299792458
H := 70.4*(1000/Mpc);
OL := 0.728;
Lambda := 3*H^2*OL/c^2;
rg := 2*M*Grav/c^2;
rL := sqrt(3/Lambda);
ystart := 0.05*Mpc
DGLL := diff(y(x), x) = c*(1-rg/y(x)-(y(x)/rL)^2)*sqrt(rg/y(x)+(y(x)/rL)^2);
RL := dsolve({DGLL, y(0) = ystart}, y(x), numeric);
DGLN := diff(y(x), x) = c*(1-rg/y(x))*sqrt(rg/y(x));
RN := dsolve({DGLN, y(0) = ystart}, y(x), numeric);
expansiontime := Gyr;
yL := rhs(RL(expansiontime)[2])/Mpc;
yN := rhs(RN(expansiontime)[2])/Mpc;
100*(yL/yN-1);
```

D.5. **Lemaitre Tolman Bondi solution.**
Algorithm 20 solves equation

$$\frac{dR}{d\xi} \approx \sqrt{1 + \frac{r_{LG}}{R} + \left(\frac{R}{r_\Lambda}\right)^2}$$

which is the "+" branch of (8.10) for $\mathcal{E} \equiv 1$ and $\mathcal{M} \equiv r_{LG} \approx 1.25 \cdot 10^{-10}$Gpc. We introduced the $\xi = ct$ coordinate, it is $r_\Lambda \approx 5\,\text{Gpc}$ and $c \approx 3{\cdot}10^8\text{m/s} \approx 0.3\,\text{Gpc/Gyr}$. The initial values are determined by (8.37) for $\eta = 0.1$. Algorithm 20 can also produce the $\Lambda = 0$ data if row 12 is replaced by: "L=DSQRT(1.d00+1.25d-10/R)" The comparison data, which we calculated by using a Taylor series, cf. (8.35) where

Algorithm 20 LTB solution (FORTRAN 77)

```
PROGRAM RadiusLTB
INTEGER n, i
REAL*8 x, R, h, L
n=1.d05
h=1.d-4
x=1.0422d-14
R=3.1276d-13
OPEN (7,FILE='R.txt')
DO i=1,n
x=x+h
CONTINUE
L=DSQRT(1.d00+1.25d-10/R+R**2.d00/25.d00)
R=R+h*L
WRITE (7,*) x/0.3d00, R
ENDDO
CLOSE (7)
END
```

$R_1 \approx 116\,\text{kpc}$ and $R_2 \approx 116\,\text{Mpc}$, is given in the following table.

time t in Gyr	R in Gpc
0.00003333067585	0.00001
0.0003333301961	0.0001
0.003333329816	0.001
0.03333345673	0.01
0.3360104716	0.1
1.668838060	0.5
3.316438584	1
6.505525406	2

time t in Gyr	R in Gpc
9.485351722	3
12.21607434	4
14.69449653	5
16.93782231	6
18.97130418	7
20.82132554	8
22.51228241	9
24.06552799	10

TABLE 2. Data for $R\,(t)$ in a LTB model including Λ

D.6. **Geodesic path in the new spacetime model.**
With the help of Maple we approximated the second order differential equation (9.15)

$$\ddot{q} = \frac{1}{w^2-1}\left[2H\left(w^2+1\right)\dot{q} + 2w\left(w+3\right)\frac{\dot{q}^2}{q} - \frac{a^2H}{c^2}\dot{q}^3\right] - \frac{4c^2w\left(w-1\right)}{a^2q\left(w+1\right)}$$

where[108]

$$a = \exp\left(Ht\right), \quad w = Lq^2\exp\left(2Ht\right), \quad H = c\cdot\sqrt{\frac{\Lambda}{3}-4L}$$

by the Runge Kutta Fehlberg method. The initial values at $t = 0$s are $v_0 = 1$m/s and $q_0 = 1$m. We chose $L = \Lambda/13$.

Algorithm 21 Radial geodesic equation for the new spacetime (Maple)

```
restart;
with(DEtools):

c := 3*10^8;
Lambda := 1.3*10^(-52);
L := (1/13)*Lambda;
H := sqrt((1/3)*Lambda-4*L)*c;
a := exp(H*x);
w := L*a^2*y(x)^2;

DGL := diff(y(x), x, x) = 2*H*(w^2+1)*(diff(y(x), x))/(w^2-1)
                          +2*w*(w+3)*(diff(y(x), x))^2/((w^2-1)*y(x))
                              -a^2*H*(diff(y(x), x))^3/(c^2*(w^2-1))
                                  -4*(w-1)*c^2*w/((w+1)*a^2*y(x));

DEplot(DGL, y(x), x = 1 .. 4*10^17, method = rkf45, [[y(0)=1, (D(y))(0)=1]],
                        linecolor = blue, axes = boxed, labels = ["t/s", "q/m"]);

DEplot(DGL, y(x), x = 1 .. 1.4*10^18, method = rkf45, [[y(0)=1, (D(y))(0)=1]],
                        linecolor = blue, axes = boxed, labels = ["t/s", "q/m"]);
```

[108] We chose $a_0 = 1$ in (9.2).

Symbols and abbreviations

Table of symbols and abbreviations used in this paper:

Λ	cosmological constant, $\Lambda \approx 1.3 \cdot 10^{-52}\mathrm{m}^{-2}$
c	speed of light, $c \approx 299792458\frac{\mathrm{m}}{\mathrm{s}}$
H_0	Hubble constant, $H_0 \approx 0.07\frac{1}{\mathrm{Gyr}}$
a	$a = a(t)$, cosmic scale factor
H	$H = H\,(t) := \frac{\dot{a}}{a}$
γ	constant of gravitation, $\gamma \approx 6,67259 \cdot 10^{-11}\frac{\mathrm{Nm}^2}{\mathrm{kg}^2}$
ρ_c	critical density of the universe, $\rho_c = \frac{3H_0^2}{8\pi\gamma}$
Ω_Λ	dark energy density parameter, $\Omega_\Lambda = \frac{\Lambda c^2}{3H_0^2}$
Ω_b	baryon density parameter
Ω_c	dark matter density parameter
Ω_M	$\Omega_M = \Omega_b + \Omega_c$, $\Omega_M = \frac{\rho_0}{\rho_c} = \frac{8\pi\gamma}{3H_0^2}\rho_0$, where ρ_0 is the current density
Ω_{tot}	total density parameter of the universe, $\Omega_{tot} = \Omega_\Lambda + \Omega_M$
$M_\odot$	Mass of the sun, $M_\odot \approx 2 \cdot 10^{33}\mathrm{g}$
M_{LG}	Mass of the Local Group, $M_{LG} \approx 1.3 \cdot 10^{12} M_\odot$
r_g	$r_g = \frac{2M\gamma}{c^2}$, gravitational radius (Schwarzschild radius) of a mass M
r_{LG}	Gravitational radius of the Local Group, $r_{LG} \approx 0.125\,\mathrm{pc}$
r_Λ	$r_\Lambda := \sqrt{\frac{3}{\Lambda}} \approx 5\,\mathrm{Gpc}$

References

[1] M. Abramowitz, I. A. Stegun: Handbook of mathematical functions with formulas, graphs, and mathematical tables, Dover Publications, 1965

[2] H. Aihara et al: The Eighth Data Release of the Sloan Digital Sky Survey: First Data from SDSS-III, arXiv:1101.1559v2 [astro-ph.IM], 2011

[3] Ö. Akarsu C. B. Kılınç: de Sitter expansion with anisotropic fluid in Bianchi type-I space-time, arXiv:1001.0550v2, 2010

[4] R. A. Alpher, R. C. Herman: On the Relative Abundance of the Elements, Phys. Rev. **74**, 1737-1742, 1948

[5] R. Balbinot, R. Bergamini, A. Comastri: Solution of the Einstein-Strauss problem with a Λ term, Phys. Rev. D **38**, 2415–2418, 1988

[6] J. D. Barrow, F. J. Tipler: The Anthropic Cosmological Principle, Oxford University Press, 1988

[7] Y. Baryshev, A. Chernin, P. Teerikorpi: The local Hubble flow: a manifestation of dark energy, arXiv:astro-ph/0011528v1, 2000

[8] M. Berry: Kosmologie und Gravitation, B.G.Teubner Stuttgart, 1990

[9] T Biswas, A Notari: "Swiss-Cheese" Inhomogeneous Cosmology & the Dark Energy Problem, arXiv:astro-ph/0702555, 2007

[10] G. R. Blumenthal, S. M. Faber, J. R. Primack, M. J. Rees: Formation of galaxies and large-scale structure with cold dark matter, Nature **311**, 517-525, 1984

[11] H. Bondi, T. Gold: The Steady-State theory of the expanding universe, MNRAS **108**, 252, 1948

[12] W.B. Bonnor: A generalization of the Einstein-Straus vacuole, Class. Quantum Grav. **17**, 2739 - 2748, 2000

[13] H. W. Brinkmann: On Riemann spaces conformal to Einstein spaces, PNAS **9**, 172–174, 1923

[14] I. N. Bronstein: Taschenbuch der Mathematik, B.G.Teubner Stuttgart-Leibzig, 1996

[15] L. Calder, O. Lahav: Dark Energy: back to Newton ?, arXiv:0712.2196 [astro-ph], 2008

[16] S. Capozziello, M. Funaro, C. Stornaiolo: Cosmological black holes as seeds of voids in the galaxy distribution, Astronomy and Astrophysics, v.420, p.847-851, 2004

[17] Cardano, Gerolamo (1545): Ars magna or The Rules of Algebra, Dover, 1993

[18] M. P. Carmo: Differentialgeometrie von Kurven und Flächen, Vieweg Braunschweig, 1983

[19] M. Carrera, D. Giulini: On the generalization of McVittie's model for an inhomogeneity in a cosmological spacetime, arxiv.org/pdf/0908.3101, 2009

[20] M. Carrera, D. Giulini: Influence of global cosmological expansion on local dynamics and kinematics, arXiv:0810.2712, 2009

[21] S. M. Carroll, W. H. Press, E. L. Turner: The cosmological constant, ARA&A **30**, 499-542, 1992

[22] S. Chandrasekhar: The Mathematical Theorie of Black Holes, Oxford Clarendon Press, 1983

[23] B. Chen, R. Kantowski, X. Dai: Time Delay in Swiss Cheese Gravitational Lensing, arXiv:1006.3500v1 [astro-ph.CO], 2010

[24] B. Chen, R. Kantowski, X. Dai: Gravitational Lensing Corrections in Flat LambdaCDM Cosmology, arXiv:0909.3308v2, 2010

[25] A. Chernin, P. Teerikorpi, Y. Baryshev: Why is the Hubble flow so quiet?, arXiv:astro-ph/0012021v1, 2000

[26] A. D. Chernin et al: Dark energy and the mass of the Local Group, arXiv:0902.3871v1 [astro-ph.CO], 2009

[27] A. D. Chernin et al: Dark energy domination in the Virgocentric flow, arXiv:1006.0555v1 [astro-ph.CO], 2010

[28] Yu. V. Chugreev, M. A. Mestvirishvili, K. A. Modestov: The quintessence scalar field in the relativistic theory of gravity, Theoretical and Mathematical Physics **152**, 1342-1350, 2007

[29] F. I. Cooperstock, V. Faroni, D. N. Vollick: The Influence of the Cosmological Expansion on Local Systems, The ApJ **503**, 61-66, 1998

[30] A. M. da Silva, M. Fontanini, D. C. Guariento: How the expansion of the universe determines the causal structure of McVittie spacetimes, arXiv:1212.0155 [gr-qc], 2012

[31] M. Davis, G. Efstathiou, C. S. Frenk, S. D. M. White: The evolution of large-scale structure in a universe dominated by cold dark matter, ApJ, **292**, 371-394, 1985.

[32] G. C. Debney, R. P. Kerr, A. Schild: Solutions of the Einstein and Einstein-Maxwell Equations, J. Math. Phys. **10**, 1842-1854, 1969

[33] G. Efstathiou, W. J. Sutherland, S. J. Maddox: The cosmological constant and cold dark matter, Nature **348**, 705-707, 1990

[34] A. Einstein: Erklärung der Perihelbewegung des Merkur aus der allgemeinen Relativitätstheorie, Sitzungsberichte der Königlich Preußischen Akademie der Wissenschaften (Berlin), 831-839, 1915

[35] A. Einstein: Die Grundlage der allgemeinen Relativitätstheorie, Annalen der Physik, 4. Folge, Band **49**, 1916

[36] A. Einstein: Prinzipielles zur allgemeinen Relativitätstheorie, Annalen der Physik, 4. Folge, Band **55**, 1918

[37] A. Einstein, E. G. Straus: The Influence of the Expansion of Space on the Gravitation Fields Surrounding the Individual Stars, Rev. Mod. Phys. **17**, 120-124, 1945

[38] A. Einstein: wissenschaftliche Taschenbücher - Grundzüge der Relativitätstheorie, Akad.-Verl. Berlin [u.a.], 1970

[39] A. Engel, E. Schucking: The Collected Papers of Albert Einstein, Volume 6: The Berlin Years: Writings, 1914-1917, Princeton University Press, 1997

[40] V. Faraoni, A. Jacques: Cosmological expansion and local physics, arXiv:0707.1350 [gr-qc], 2007

[41] P. J. Francis et al: The Distribution of Lyα-emitting Galaxies at z=2.38. II. Spectroscopy, ApJ **614**, 75, 2004

[42] Anna Frebel et al.: Discovery of HE 1523-0901, a Strongly r-Process Enhanced Metal-Poor Star with Detected Uranium, arXiv:astro-ph/0703414v1, 2007

[43] A. Friedman: Über die Krümmung des Raumes, Zeitschrift für Physik **10**, 377-387, 1922.

[44] G. Gamow: The Origin of Elements and the Separation of Galaxies, Phys. Rev. **74**, 505–506, 1948

[45] G. Gamow: The Evolution of the Universe, Nature **162**, 680-682, 1948

[46] P. M. Garnavich et al.: Constraints on cosmological models from Hubble Space Telescope observations of high-z supernovae, ApJ **493**, L53-57, 1998

[47] J. Garriga, A. Vilenkin: Solutions to the cosmological constant problems, Phys.Rev. D **64**, 023517, arXiv:hep-th/0011262, 2001

[48] A. Ghez, M. Morris, E. E. Becklin, T. Kremenek, A. Tanner: The Accelerations of Stars Orbiting the Milky Way's Central Black Hole, arXiv:astro-ph/0009339v1, 2000

[49] R. Gobat et al: A mature cluster with X-ray emission at z = 2.07, arXiv:1011.1837v2 [astro-ph.CO], 2010

[50] G. Goldhaber, S. Perlmutter: A study of 42 type Ia supernovae and a resulting measurement of Ω_M and Ω_Λ, Proceedings of the 3rd International Symposium on Sources and Detection of Dark Matter in the Universe (DM98), Marina del Rey, California, USA, 18-20 February 1998; Physics Reports **307**, 325-331, 1998

[51] J. R. Gott, M. Juric, D. Schlegel, F. Hoyle, M. Vogeley, M. Tegmark, N. Bahcall, J. Brinkmann: A Map of the Universe, ApJ **624**, 463-484, 2005

[52] I. S. Gradshteyn, I. M. Ryzhik: Table of Integrals, Series, and Products, Elsevier Academic Press, 2007

[53] D. Gromoll, W. Klingenberg, W. Meyer: Riemannsche Geometrie im Großen, Springer-Verlag Berlin-Heidelberg-New York, 1975

[54] A. Gromov: An Example of Exact Solution in the LTB Model, arXiv:astro-ph/9605201v1, 1996

[55] A. H. Guth: Inflationary universe: A possible solution to the horizon and flatness problems, Phys. Rev. D **23**, 347–356, 1981

[56] S. W. Hawking, G. F. R. Ellis: The large scale structure of space-time, Cambridge monographs on mathematical physiks, 1973

[57] Y. Hoffman, L. A. Martinez-Vaquero, G. Yepes, S. Gottloeber: The Local Hubble Flow: Is it a Manifestation of Dark Energy?, arXiv:0711.4989v2 [astro-ph.CO], 2008

[58] G. Hinshaw et al: Five-Year Wilkinson Microwave Anisotropy Probe (WMAP) Observations: Data Processing, Sky Maps, and Basic Results, ApJS **180**, 225–245, doi: 10.1088/0067-0049/180/2/225, 2009

[59] E. Hubble: A relation between distance and radial velocity among extra-galactic nebulae, Mount Wilson Observatory, Carnegie Institution of Washington, 1929

[60] D. Huterer, M. S. Turner: Prospects for probing the dark energy via supernova distance measurements, Phys. Rev. D **60**, 081301, arXiv:astro-ph/9808133, 1999

[61] M. Israelit, N. Rosen: Newton's laws in a cosmological model, ApJ **400**, 21-24, 1992

[62] M. Israelit, N. Rosen: A spherically symmetric mass on an FRW background, ApJ **461**, 560 - 564, 1996

[63] N. Jarosik et al: Seven-Year Wilkinson Microwave Anisotropy Probe (WMAP) Observations: Sky Maps, Systematic Errors, and Basic Results, arXiv:1001.4744v1 [astro-ph.CO], 2010

[64] J. Jost: Riemannian Geometrie and Geometric Analysis, Springer Berlin [u.a.], 2002

[65] N. Kaloper, M. Kleban D. Martin: McVittie's Legacy: Black Holes in an Expanding Universe, arXiv:1003.4777v3 [hep-th], 2010

[66] I. D. Karachentsev, O. G. Kashibadze: Total masses of the Local Group and M 81 group derived from the local Hubble flow, arXiv:astro-ph/0509207v2, 2005

[67] I. D. Karachentsev, O. G. Kashibadze: Masses of the local group and of the M81 group estimated from distortions in the local velocity field, Astrophysics **49**, 3-18, 2006

[68] W. Klingenberg: De Gruyter studies in mathematics - Riemannian Geometrie, de Gruyter Berlin, 1982

[69] F. Kottler: Über die physikalischen Grundlagen der Einsteinschen Gravitationstheorie, Annalen der Physik, 4. Folge, Band **56**, 443, 1918

[70] T. Koupelis, K. F. Kuhn: In quest of the universe, Jones & Bartlett Learning, 2007

[71] W. Kühnel: Differentialgeometrie Kurven - Flächen - Mannigfaltigkeiten, Vieweg Verlag, 2005

[72] K. Lake, M. Abdelqader: More on McVittie's Legacy: A Schwarzschild - de Sitter black and white hole embedded in an asymptotically ΛCDM cosmology, Phys. Rev. D **84**, 044045, arXiv:1106.3666 [gr-qc], 2011

[73] L. D. Landau, E. M. Lifschitz: Lehrbuch der theoretischen Physik - Klassische Feldtheorie, Verlag Harri Deutsch, Thun und Frankfurt am Main, 1997

[74] P. Landry, M. Abdelqader, K. Lake: The McVittie solution with a negative cosmological constant, arXiv:1207.6350 [gr-qc], 2012

[75] G. Lemaitre: Un Univers homogène de masse constante et de rayon croissant rendant compte de la vitesse radiale des nébuleuses extra-galactiques, Annales de la Société Scientifique de Bruxelles **47**, 49, 1927

[76] A. R. Liddle, D. H. Lyth: Inflation and Mixed Dark Matter Models, arXiv:astro-ph/9304017v1, 1993

[77] H. Martel, P. R. Shapiro, S. Weinberg: Likely values of the cosmological constant, ApJ **492**, 29-40, 1998

[78] A. de la Macorra, G. Piccinelli: General Scalar Fields as Quintessence, Phys. Rev. D **61**, 123503, arXiv:hep-ph/9909459, 2000

[79] G. C. McVittie: The mass-particle in an expanding universe, MNRAS **93**, 325-339, 1933

[80] J. Miralda-Escude: The Dark Age of the Universe, Science **300**, 1904-1909, arXiv:astro-ph/0307396v1, 2003

[81] C. W. Misner, K. S. Thorne, J. A. Wheeler: Gravitation, W.H.Freeman and company, San Francisco, 1973

[82] R. Nandra, A. N. Lasenby, M. P. Hobson: The effect of a massive object on an expanding universe, MNRAS **422**, 2931-2944, arXiv:1104.4447 [gr-qc], 2012

[83] P. D. Noerdlinger, V. Petrosian: The effect of cosmological expansion on self-gravitating ensembles of particles, ApJ **168**, 1-9, 1971

[84] S. Nojiri, S. D. Odintsov: Introduction to Modified Gravity and Gravitational Alternative for Dark Energy, International Journal of Geometric Methods in Modern Physics **4**, 115-146, arXiv:hep-th/0601213v5, 2007

[85] R. Oloff: Geometrie der Raumzeit - eine Einführung in die Relativitätstheorie, Vieweg Braunschweig [u.a.], 1999

[86] Y. Ono et al: Spectroscopic Confirmation of Three z-Dropout Galaxies at z = 6.844 - 7.213: Demographics of Lyman-Alpha Emission in z ~ 7 Galaxies, arXiv:1107.3159v2 [astro-ph.CO], 2011

[87] J. R. Oppenheimer, H. Snyder: On Continued Gravitational Contraction, Phys. Rev. **56**, 455 - 459, 1939

[88] J. P. Ostriker, P. J. Steinhardt: The observational case for a low-density Universe with a non-zero cosmological constant, Nature **377**, 600-602, 1995

[89] C. Patterson: Age of meteorites and the earth, Geochimica et Cosmochimica Acta **10**, 230–237, 1956

[90] P. J. E. Peebles: Tests of cosmological models constrained by inflation, ApJ **284**, 439-444, 1984

[91] P. J. E. Peebles: Principles of Physical Cosmology, Princeton University Press, 1993

[92] L. Pentericci et al: Spectroscopic confirmation of z˜7 LBGs: probing the earliest galaxies and the epoch of reionization, arXiv:1107.1376v1 [astro-ph.CO], 2011

[93] V. Petrosian, E. Salpeter, P. Szekeres: Quasi-Stellar Objects in Universes with Non-Zero Cosmological Constant, ApJ **147**, 1222-1226, 1967

[94] V.A. Petrov: Einstein, Hilbert and Equations of Gravitation, arXiv:gr-qc/0507136v1, 2005

[95] S. Perlmutter et al: Measurements of Ω and Λ from 42 High-Redshift Supernovae, ApJ **517**, 565-586, 1999

[96] W. H. Press: Numerical recipes: the art of scientific computing, Cambridge University Press, 2007

[97] R. H. Price, J. D. Romano: In an expanding universe, what doesn't expand?, arXiv:gr-qc/0508052v2, 2012

[98] A. G. Riess et al: Observational Evidence from Supernovae for an Accelerating Universe and a Cosmological Constant, ApJ **116**, 1009-1038, 1998

[99] H. P. Robertson: On Relativistic Cosmology, Phil. Mag. **5**, 835 - 848, 1928

[100] V. C. Rubin, W.K. Jr. Ford, N. Thonnard: The rotation curve of a galaxy shows the orbital velocity at different distances from the center of rotation and relates the orbital velocity of stars or gas to the total mass inside their orbits, ApJ **238**, 471-487, 1980

[101] S. E. Rugh, H. Zinkernagel: The Quantum Vacuum and the Cosmological Constant Problem, Studies In History and Philosophy of Modern Physics **33**, 663-705, 2002

[102] R. K. Sachs, H. Wu: General Relativity for Mathematicians, Springer New York [u.a.], 1977

[103] P. D. Sackett: The Shape of Dark Matter Halos, astro-ph/9903420, 1999

[104] P. Schneider: Extragalactic astronomy and cosmology: an introduction, Springer Verlag, 2006

[105] E. Schücking: Das Schwarzschildsche Linienelement und die Expansion des Weltalls, Zeitschrift für Physik **137**, 595-603, 1954

[106] R. U. Sexl, H. K. Urbantke: Gravitation und Kosmologie, Bibliographisches Institut Mannheim/Wien/Zürich, B.I.-Wissenschaftsverlag, 1975

[107] J. Silk: The Big Bang, W. H. Freeman and Company, 1989

[108] J. Silk, G. A. Mamon: The Current Status of Galaxy Formation, arXiv:1207.3080 [astro-ph.CO], 2012

[109] M. H. Soffel: Astronomy and astrophysics - Relativity in Astronomie, Celestial Mechanics and Geodesy, Springer Berlin [u.a.], 1989

[110] H. Stephani: Allgemeine Relativitätstheorie - eine Einführung in die Theorie des Gravitationsfeldes, Dt. Verlag der Wissenschaften, 1977

[111] C. Stornaiolo: Cosmological Black Holes, arXiv:gr-qc/0101120v2, 2002

[112] H. Stöcker: Taschenbuch der Physik, Verlag Harri Deutsch, 1998

[113] B. Temple, J. Smoller: Expanding wave solutions of the Einstein equations that induce an anomalous acceleration into the Standard Model of Cosmology, PNAS **106**, 14213-14218, doi:10.1073/pnas.0901627106, 2009

[114] B. Temple, J. Smoller: General Relativistic Self-Similar Waves that induce an Anomalous Acceleration into the Standard Model of Cosmology, arXiv:1005.3859, 2010

[115] "The Nobel Prize in Physics 2011". Nobelprize.org. 23 Dec 2011, http://www.nobelprize.org/nobel_prizes/physics/laureates/2011/

[116] J. L. Tinker et al.: Void Statistics in Large Galaxy Redshift Surveys: Does Halo Occupation of Field Galaxies Depend on Environment?, ApJ **686**, 53-71, doi:10.1086/589983, 2008

[117] R. Tolman: Effect of inhomogeneity on cosmological models, PNAS **20**, 169–176, 1934.

[118] R. B. Tully: Alignment of clusters and galaxies on scales up to 0.1c, ApJ **303**, 25-38, 1986

[119] M. Valtonen et al: Measuring Black Hole Spin in OJ287, arXiv:1001.1284v1 [astro-ph.CO], 2010

[120] R. M. Wald: General Relativity, University of Chicago Press, 1984

[121] W. Walter: Gewöhnliche Differentialgleichungen, Springer-Verlag Berlin-Heidelberg-New York, 1996

[122] S. Weinberg: The Cosmological Constant Problems, arXiv:astro-ph/0005265v1, 2000

[123] H. Weyl: Raum Zeit Materie (Vorlesungen über allgemeine Relativitätstheorie), Springer Berlin [u.a.], 1988